

Mapping the function of the NS3 protein of African horsesickness virus using RNAi and yeast two-hybrid analyses

by

Wayne Arthur Barnes

Submitted in partial fulfilment of the requirements of the degree
Master of Science
in the Faculty of Natural and Agricultural Sciences
Department of Microbiology and Plant Pathology
University of Pretoria
Pretoria

March 2011

DECLARATION

I declare that the dissertation, which I hereby submit for the degree M.Sc (Microbiology) at the University of Pretoria, is my own work and had not previously been submitted by me for a degree at this or any other tertiary institution.

Signed:

Date:

ACKNOWLEDGEMENTS

- The Lord for His grace, guidance and love and for granting me this opportunity.
- Prof. Jacques Theron, for his motivation and support. It was a great pleasure and privilege to complete this degree under your supervision.
- Dr. Christine Maritz-Olivier, for all your help, advice, protocols and motivation with regards to the yeast two hybrid assays.
- Dr. Vida van Staden, for your inputs and co-supervision.
- My parents and family for your support and encouragement.
- Lorraine, for your motivation, support, encouragement, love and believe in me.

SUMMARY

Mapping the function of the NS3 protein of African horse sickness virus using RNAi and yeast two-hybrid analyses

by

Wayne Arthur Barnes

Supervisor: Prof. J. Theron
Department of Microbiology and Plant Pathology
University of Pretoria

Co-supervisor: Dr V. Van Staden
Department of Genetics
University of Pretoria

for the degree M.Sc

African horsesickness virus (AHSV), a member of the *Orbivirus* genus within the *Reoviridae* family, has a ten-segment double-stranded (ds)RNA genome that is encapsidated within a single non-enveloped virus particle. In addition to seven structural proteins (VP1-VP7), four non-structural proteins (NS1, NS2 and NS3/NS3A) are synthesized in infected cells but their function in the viral life cycle is not yet fully understood. The non-structural protein NS3 is believed to mediate virus release from infected cells. Although it has generally been accepted that non-enveloped viruses are released from infected cells after cellular lysis, available data for Bluetongue virus (BTV), the prototype orbivirus, has indicated that NS3 may form a bridge between the virus particle and the host cell budding machinery, and that it might have some controlling role in mature virus release from infected cells. Whether AHSV NS3 has a direct role in virus egress has not been addressed directly to date. Consequently, the aims of this investigation were to determine whether NS3 of AHSV has an intrinsic activity to release virus particles from infected cells and to determine whether NS3 may engage host cell proteins to aid virus release.

To investigate whether AHSV NS3 is capable of mediating virus release, a RNA interference (RNAi)-based approach was used. Three small interfering RNAs (siRNAs) were designed that targeted different regions on AHSV-3 NS3 mRNA, *i.e.* siNS3-65 (corresponding to nucleotides 65-85), siNS3-74 (corresponding to nucleotides 74-92) and siNS3-266

(corresponding to nucleotides 266-284). Using a NS3 expression reporter plasmid and an *in vitro* model of infection, results were obtained that showed that the synthetic siRNAs, most notably siNS3-266, silenced NS3 mRNA and protein expression effectively. Moreover, silencing of NS3 gene expression with siNS3-266 resulted in a lower percentage of virus release when compared to control cells, albeit that the total virus yield was similar. These results thus provide evidence that AHSV release is enhanced by NS3. Towards defining host cell proteins that interact with the AHSV NS3 protein, a two-hybrid system was used that allows the detection of protein-protein interactions *in vivo* in yeast cells. Since AHSV infects both insect and mammalian hosts, cDNA libraries were constructed of Vero mammalian and *Culicoides* insect cell lines, and then screened for proteins interacting with the N-terminal of the AHSV-3 NS3 protein. As NS3-interacting cDNA clones, SARA was isolated from the insect cell cDNA library and L34 from the mammalian cDNA library. The SARA protein is localized to membranes and is implicated in membrane trafficking of proteins. The L34 protein is a multifunctional protein that, in addition to forming part of the 60S subunit of the ribosome, acts as an inhibitor of cyclin-dependent kinases 4 and 5, which play key regulatory roles during progression of the eukaryotic cell cycle. Moreover, L34 also regulates the synthesis of polyamines, which are involved in various cellular processes, including membrane stabilization. Although the biological significance of these interactions has yet to be investigated, the results nevertheless provide a foundation for mapping the role of NS3 in the AHSV life cycle.

TABLE OF CONTENTS

DECLARATION	i
ACKNOWLEDGEMENTS	ii
SUMMARY	iii
LIST OF ABBREVIATIONS	
LIST OF FIGURES	
LIST OF TABLES	
CHAPTER ONE	1
LITERATURE REVIEW	
1.1 GENERAL INTRODUCTION	1
1.2 AFRICAN HORSESICKNESS (AHS)	3
1.2.1 History of AHS	3
1.2.2 Susceptible species and transmission	4
1.2.3 Pathogenesis and clinical signs	4
1.2.4 Treatment and vaccination	5
1.3 AFRICAN HORSESICKNESS VIRUS (AHSV)	6
1.3.1 Classification	6
1.3.2 Virion structure	7
1.3.3 Viral genome	8
1.3.4 Viral proteins	9
1.3.4.1 Outer capsid proteins	9
1.3.4.2 Inner capsid proteins	11
1.3.4.3 Non-structural proteins	12
1.4 ORBIVIRUS REPLICATION AND MORPHOGENESIS	14
1.5 THE NON-STRUCTURAL PROTEIN NS3	16
1.5.1 Properties of NS3	17
1.5.2 NS3 and virus release	19
1.5.3 Significance of L-domain motifs in NS3	22
1.6 LYTIC-INDEPENDENT RELEASE OF NON-ENVELOPED VIRUSES	24
1.7 APPROACHES TOWARD STUDYING PROTEIN FUNCTION	26
1.7.1 RNA Interference (RNAi)	26
1.7.1.1 Mechanism of RNAi	27
1.7.1.2 RNAi as an investigative tool in mammalian cells	28

1.7.1.3	Application of RNAi to viruses with a segmented dsRNA genome	30
1.7.2	Yeast two-hybrid screening	32
1.7.2.1	Basis of the yeast two-hybrid system	33
1.7.2.2	Constraints of the yeast two-hybrid system	35
1.7.2.3	Application of yeast two-hybrid screens to viruses with a segmented dsRNA genome	37
1.8	AIMS OF THIS INVESTIGATION	38
CHAPTER TWO		40
SMALL INTERFERING RNA (siRNA)-MEDIATED SILENCING OF AHSV-3 NS3 GENE EXPRESSION IN VERO CELLS AFFECTS VIRUS RELEASE		
2.1	INTRODUCTION	40
2.2	MATERIALS AND METHODS	42
2.2.1	Bacterial strains and plasmids	42
2.2.2	Large-scale preparation of recombinant mammalian expression plasmids	42
2.2.2.1	Preparation of competent cells	42
2.2.2.2	Transformation of competent cells	43
2.2.2.3	Plasmid DNA extraction	43
2.2.3	Characterization of recombinant mammalian expression plasmids	44
2.2.3.1	Agarose gel electrophoresis	44
2.2.3.2	Restriction endonuclease digestions	44
2.2.3.3	Nucleotide sequencing and sequence analysis	44
2.2.4	Transient expression of eGFP and NS3-eGFP in Vero cells	45
2.2.4.1	Cell culture and virus	45
2.2.4.2	Transfection of Vero cell monolayers	45
2.2.4.3	Epifluorescence microscopy	46
2.2.5	RNA interference assays in Vero cells	46
2.2.5.1	Small interfering RNAs (siRNAs)	46
2.2.5.2	Co-transfection of Vero cells with siRNA and recombinant pCMV-Script® expression vectors	49
2.2.5.3	Transfection and virus challenge assays in Vero cells	49
2.2.6	Semi-quantitative real-time polymerase chain reaction (RT-PCR)	50
2.2.6.1	Primers	50
2.2.6.2	Total RNA extraction	50

2.2.6.3	cDNA synthesis	51
2.2.6.4	Control PCR reactions	51
2.2.6.5	Semi-quantitative real-time PCR	51
2.2.6.6	Data analysis	52
2.2.7	Viral plaque assay	52
2.2.8	Protein analyses	53
2.2.8.1	Preparation of cell lysates	53
2.2.8.2	SDS-polyacrylamide gel electrophoresis (SDS-PAGE)	53
2.2.8.3	Western blot analysis	54
2.3	RESULTS	54
2.3.1	Characterization of recombinant plasmids pCMV-eGFP and pCMV-NS3-eGFP	54
2.3.2	Transient expression of eGFP and NS3-eGFP in Vero cells	55
2.3.3	Silencing of NS3-eGFP protein expression by siRNAs in Vero cells	57
2.3.4	Silencing of AHSV-3 NS3 mRNA expression by siRNAs in Vero cells	58
2.3.5	Silencing of AHSV-3 NS3 protein expression in Vero cells	60
2.3.6	Effect of NS3 gene silencing on virus release	62
2.4	DISCUSSION	62
CHAPTER THREE		69
CULICOIDES AND VERO CELL PROTEINS INTERACT WITH THE NS3 PROTEIN OF AHSV-3, AS EVIDENCED BY YEAST TWO-HYBRID SCREENS		
3.1	INTRODUCTION	69
3.2	MATERIALS AND METHODS	72
3.2.1	Bacterial and yeast strains, plasmids and culture conditions	72
3.2.2	Cell cultures	72
3.2.3	DNA amplification	73
3.2.3.1	Primers	73
3.2.3.2	Polymerase chain reaction (PCR)	73
3.2.4	Purification of DNA fragments from agarose gels	74
3.2.5	Cloning of DNA fragments into plasmid vectors	74
3.2.5.1	Ligation reactions	74
3.2.5.2	Preparation of competent <i>E. coli</i> JM109 cells	75
3.2.5.3	Transformation of competent cells	75

3.2.6	Screening of transformants	75
3.2.6.1	Plasmid DNA extraction	75
3.2.6.2	Restriction endonuclease digestions	76
3.2.6.3	Nucleotide sequencing	76
3.2.7	Plasmid constructions	77
3.2.8	cDNA synthesis	78
3.2.8.1	Total RNA extraction and purification	78
3.2.8.2	cDNA synthesis	79
3.2.8.3	cDNA amplification by long distance (LD)-PCR	80
3.2.9	Construction of AD plasmid/cDNA libraries	80
3.2.9.1	Preparation of the cDNA products and pACT2 AD plasmid vector	81
3.2.9.2	Ligation of DNA fragments	81
3.2.9.3	Preparation of electrocompetent <i>E. coli</i> JM109 cells	81
3.2.9.4	Electroporation	81
3.2.10	Characterization of constructed AD plasmid/cDNA libraries	82
3.2.10.1	Determining the percentage of recombinant clones	82
3.2.10.2	Titering of AD plasmid/cDNA libraries	82
3.2.11	Large-scale plasmid isolation of Vero and KC cDNA libraries	83
3.2.12	Sequential transformation of AH109 yeast cells with the DNA-BD/bait construct and AD plasmid/cDNA libraries	83
3.2.12.1	Transformation with pGBKT7-NS3 ₁₋₁₀₈	83
3.2.12.2	Test for autonomous reporter gene activation	84
3.2.12.3	Transformation with AD plasmid/cDNA libraries	84
3.2.13	Two-hybrid screening of reporter genes	85
3.2.13.1	Nutritional marker genes	85
3.2.13.2	β -galactosidase colony-lift filter assays	86
3.2.14	Nested PCR screening of positive clones	86
3.2.15	Plasmid isolation from yeast	87
3.2.16	Rescue of AD/cDNA library plasmids and sequencing of the cDNA inserts	87
3.3	RESULTS	88
3.3.1	Construction of the recombinant bait vector pGBKT7-NS3 ₁₋₁₀₈	88
3.3.2	Construction of AD plasmid/cDNA libraries	92
3.3.3	Two-hybrid screening for protein-protein interactions	95
3.3.4	Sequencing and sequence analysis of positive AD/cDNA library inserts	97

3.3.5	Verification of NS3-host cell protein interactions	102
3.4	DISCUSSION	104
	CHAPTER FOUR	111
	CONCLUDING REMARKS	
	REFERENCES	115
	APPENDIX	141

LIST OF ABBREVIATIONS

Acc.	accession
AD	activating domain
AD/library	fusion of the AD with a library cDNA
Ade ⁻ , His ⁻ , Leu ⁻ , Trp ⁻	requires adenine (Ade), histidine (His), leucine (Leu) or tryptophan (Trp) in the medium to grow
AHS	African horse sickness
AHSV	African horse sickness virus
Amp ^r	ampicillin resistance
BD	binding domain
BHK	Baby hamster kidney
BLAST	Basic Local Alignment Search Tool
bp	base pair
BTV	Bluetongue virus
C	carboxy
ca.	approximately
Cdk	cyclin-dependent kinase
cDNA	complementary DNA
cfu	colony forming units
cm ²	cubic centimetre
CO ₂	carbon dioxide
ColE1	<i>E. coli</i> origin of replication
CPE	cytopathic effect
DO	dropout medium; dropout media are missing one or more of the nutrients required by untransformed yeast to grow
DDO	double dropout medium
ddH ₂ O	double-distilled deionized water
DEPC	diethyl pyrocarbonate
DNA	deoxyribonucleic acid
DNA-BD/bait	fusion of the DNA-BD with a bait
DNase	deoxyribonuclease
dNTP	deoxyribonucleoside-5'-triphosphate
ds	double stranded
DTT	dithiothreitol
e.g.	<i>exempli gratia</i> (for example)

EHDV	Epizootic haemorrhagic disease virus
EDTA	ethylenediaminetetra-acetic acid
eGFP	enhanced green fluorescent protein
<i>et al.</i>	<i>et alia</i> (and others)
ESCRT	endosomal sorting complex required for transport
EtOH	ethanol
FBS	foetal bovine serum
Fig.	figure
GAPDH	glyceraldehyde-3-phosphate dehydrogenase
GFP	green fluorescent protein
h	hour
<i>i.e.</i>	<i>id est</i> (that is)
IPTG	isopropyl- β -D-thiogalactopyranoside
Kan ^r	kanamycin resistance
kb	kilobase pairs
KC cells	<i>Culicoides variipennis</i> insect cells
kDa	kilodalton
<i>lacZ</i>	gene that codes for β -galactosidase
<i>lacZ'</i>	gene that codes for the α -peptide of β -galactosidase
L-domain	late assembly domain
LB	Luria-Bertani
LD-PCR	long distance-PCR
LiOAc	lithium acetate
M	molar
MEM	Minimum Essential Medium
mg	milligram
min	minute
mm	millimetre
ml	millilitre
mM	millimolar
MOI	multiplicity of infection
MOPS	3-(N-morpholino)propanesulfonic acid
M _r	molecular weight
mRNA	messenger ribonucleic acid
ms	millisecond
MVB	multivesicular body
N	amino

NaOAc	sodium acetate
NH ₄ OAc	ammonium acetate
ng	nanogram
nm	nanometer
No.	number
nt	nucleotides
OD	optical density
<i>ori</i>	origin of replication
ORF	open reading frame
pfu	plaque forming units
PAGE	polyacrylamide gel electrophoresis
PBS	phosphate-buffered saline
PCR	polymerase chain reaction
PKR	dsRNA-activated protein kinase R
pmol	picomole
PSB	protein solvent buffer
PtdIns(3)P	phosphatidylinositol-3-phosphate
QDO	quadruple dropout medium
REST	Relative Expression Software Tool
RISC	RNA-induced silencing complex
RNA	ribonucleic acid
RNAi	RNA interference
RNase	ribonuclease
rpm	revolutions per minute
RT	reverse transcription
RT-PCR	reverse transcription-PCR
s	second
SARA	smad anchor for receptor recognition
SD	Minimal Synthetic Dropout medium
S.D.	standard deviation
SDS	sodium dodecyl sulphate
shRNA	small hairpin RNA
siRNA	small interfering RNA
ss	single stranded
TDO	triple dropout medium
TE	Tris-EDTA
TEMED	N',N',N',N'-tetramethylethylenediamine

TGF- β	transforming growth factor- β
U	units
UHQ	ultra-high quality
UV	ultraviolet
V	volts
v.	version
v/v	volume per volume
VIB	viral inclusion body
w/v	weight per volume
X-Gal	5-bromo-4-chloro-3-indolyl β -D-galactopyranoside
YPDA	yeast extract-peptone-dextrose-adenine hemisulphate agar
$^{\circ}\text{C}$	degrees Celsius
μg	microgram
μl	microlitre
μm	micrometre
μM	micromolar
$2\ \mu$	yeast origin of replication
$2',5'$ -AS	$2',5'$ -oligoadenylate synthetase

LIST OF FIGURES

Fig. 1.1	Schematic representation of the BTV particle.	8
Fig. 1.2	Schematic diagram of the replication cycle of BTV.	16
Fig. 1.3	A topological model for interaction of AHSV NS3 with the cellular membrane.	18
Fig. 1.4	A model for the role of BTV NS3 in virus release.	21
Fig. 1.5	Schematic representation of how NS3 may facilitate budding of BTV from infected cells.	22
Fig. 1.6	RNAi-mediated gene silencing.	28
Fig. 1.7	A typical yeast two-hybrid library screen.	34
Fig. 2.1	Local secondary structure of the AHSV-3 NS3 (a) and NS3-eGFP (b) mRNAs, as predicted by the MFOLD software programme.	47
Fig. 2.2	Plasmid maps of the recombinant mammalian expression plasmids pCMV-eGFP and pCMV-NS3-eGFP (a), and agarose gel electrophoretic analysis of the recombinant plasmids following restriction endonuclease digestions (b).	56
Fig. 2.3	Fluorescent microscopy of eGFP and NS3-eGFP gene expression in Vero cells.	57
Fig. 2.4	Silencing of NS3-eGFP protein expression in Vero cells.	59
Fig. 2.5	Inhibition of AHSV-3 NS3 mRNA expression in Vero cells by NS3-directed siRNAs.	61
Fig. 2.6	Western blot depicting the expression of AHSV-3 NS3 in Vero cells subjected to transfection with the indicated NS3-directed siRNAs.	61
Fig. 2.7	Effect of NS3-directed siRNAs on the total infectious virus yield (a) and the percentage virus released of AHSV-3 in Vero cells.	63
Fig. 3.1	Agarose gel electrophoretic analysis of the recombinant plasmid pGBKT7-NS3 ₁₋₁₀₈ .	90
Fig. 3.2	Nucleotide and amino acid sequence alignments of the truncated NS3-N ₁₋₁₀₈ bait construct and the corresponding region of AHSV-3 NS3.	91

- Fig. 3.3 Agarose gel electrophoretic analysis of the double-stranded cDNA amplified by LD-PCR, following reverse transcription of total RNA extracted from Vero mammalian cells and KC insect cells. 93
- Fig. 3.4 PCR screening of *E. coli* JM 109 colonies, following transformation with pACT2 AD plasmid/cDNA libraries of Vero mammalian cells (a) and KC insect cells (b). 94
- Fig. 3.5 Screening of co-transformed AH109 yeast colonies for putative protein-protein interactions between a truncated NS3 protein and cDNA library proteins. 96
- Fig. 3.6 Nested PCR screening of *S. cerevisiae* strain AH109 colonies, containing the NS3₁₋₁₀₈ bait plasmid and plasmid cDNA libraries of Vero mammalian cells (a) and KC insect cells (b). 98
- Fig. 3.7 Alignment of the amino acid sequence of a 44-amino acid Vero cell protein with the full-length amino acid sequences of different L34 ribosomal proteins. 100
- Fig. 3.8 Alignment of the amino acid sequence of a 46-amino acid KC cell protein with the amino acid sequences of invertebrate SARA proteins (a) and vertebrate SARA proteins (b). 101
- Fig. 3.9 Agarose gel electrophoretic analysis of plasmids constructed for reverse two-hybrid screening. 103
- Fig. 3.10 Reverse yeast two-hybrid screening to confirm putative protein-protein interactions. 105

LIST OF TABLES

Table 1.1	BTV genome segments and their encoded proteins	10
Table 1.2	Overview of different validation methods	36
Table 2.1	AHSV-3 NS3-directed and control siRNAs used in this study	46
Table 2.2	Primers used in semi-quantitative real-time PCR	50
Table 3.1	Primers used in this study to amplify specific DNA fragments for cloning purposes and sequencing of cloned insert DNA	73
Table 3.2	Summary of BLAST-P information for Vero cell prey proteins that interacted with the AHSV-3 NS3 ₁₋₁₀₈ bait protein	100
Table 3.3	Summary of BLAST-P information for KC cell prey proteins that interacted with the AHSV-3 NS3 ₁₋₁₀₈ bait protein	101

CHAPTER ONE

LITERATURE REVIEW

1.1 GENERAL INTRODUCTON

Determining the origin of viruses has largely been complicated, not only due to their inability to form fossils, but also due to lack of ancient viral DNA and RNA. Nevertheless, since viruses are dependent on living cells (host) for their replication and survival, it can be hypothesized that viruses have existed since the evolution of living cells. However, it was only near the end of the 18th century, in 1892, that Dimitry Ivanovsky demonstrated that the sap of leaves infected with tobacco mosaic disease remained infectious, even after filtration through a Chamberland filter that was capable of retaining bacteria. This observation suggested a disease agent smaller than any known before, and was the first step in a series of observations and experiments that led to the discovery of viruses. Indeed, the term filterable agent was the name first used to describe these organisms well before the term viruses were specifically applied to them (Levy *et al.*, 1994). Today, hundreds of viruses are known and many of them are of agricultural and medical importance. Amongst these is African horsesickness virus (AHSV), the causative agent of African horsesickness (AHS). AHS is an infectious non-contagious, arthropod-borne viral disease of equids. The disease is characterized by clinical signs that develop as a consequence of damage to the circulatory and respiratory systems, thus giving rise to serious effusion and haemorrhage in various organs and tissues (Mellor and Hamblin, 2004). The mortality rate in horses is high, sometimes in excess of 90% (Coetzer and Erasmus, 1994). Consequently, based on its potential economic and international importance, AHS has been classified as a notifiable disease by the Office International des Epizootics (OIE) (Coetzer and Erasmus, 1994; Mellor and Hamblin, 2004).

Much of the pioneering research on AHS has been performed by Sir Arnold Theiler during the early 20th century. In 1900, he demonstrated the filterability of the pathogen through Berkefield and Chamberland filters, thereby indicating that the pathogen was indeed a virus. Theiler's research also indicated that there existed immunologically distinct strains of the AHS virus agent, since immunity acquired against one strain did not always protect the horse when challenged by a heterologous virus strain. In 1903, Theiler and Pitchford-Watkins

established that AHSV may be transmitted by biting insects and, in 1921, Theiler reported the first detailed descriptions of the clinical signs and lesions produced by infections with AHSV (reviewed in Coetzer and Erasmus, 1994). During the late 1960s and 1970s, several studies were undertaken aimed at characterizing the structure and morphology of AHSV (Verwoerd and Huismans, 1969; Oellerman *et al.*, 1970; Bremer, 1976; Bremer *et al.*, 1990). Consequently, AHSV has been classified as a member of the genus *Orbivirus* in the family *Reoviridae*. This family is comprised of a large number of viruses with segmented double-stranded (ds)RNA genomes and the virus particles have both an inner and outer protein capsid (Urbano and Urbano, 1994; Calisher and Mertens, 1998).

With the advent of gene cloning, genetic engineering and protein expression technologies, much progress has been made regarding structure-function relationships of different AHSV genes and encoded gene products (Vreede and Huismans, 1994; Uitenweerde *et al.*, 1995; Maree and Huismans, 1997; Van Staden *et al.*, 1995; Van Niekerk *et al.*, 2001a; de Waal and Huismans, 2005). However, the phenomenon of RNA interference (RNAi), a post-transcriptional gene silencing process in which dsRNA initiates specific cleavage of cytoplasmic mRNA (Fire *et al.*, 1998), may provide a means whereby these studies can be extended to investigate the role of individual AHSV proteins within the context of the whole virus. Moreover, studies regarding the interaction of individual AHSV proteins with cellular proteins may not only provide new insights regarding virus-host interactions, but will also improve understanding of the virus replication cycle. A potentially powerful tool for these types of investigations is the yeast two-hybrid screening system (Fields and Song, 1989), which has greatly facilitated studies regarding protein-protein interactions in various biological systems (Uetz and Hughes, 2000; Vitour *et al.*, 2004; Rual *et al.*, 2005).

In this review of the literature, aspects relating to AHSV epidemiology, structure and replication will be discussed, and emphasis will be placed on the non-structural protein NS3 and its role in virus egress. This will be followed by a discussion of RNAi and yeast two-hybrid screening, and a brief description of the aims of this investigation.

1.2 AFRICAN HORSESICKNESS (AHS)

1.2.1 History of AHS

AHS is an ancient disease and the first historical description of the disease can be found in an Arabian document (Le Kitâb El-Akouâ El Kâfiâh Wa El Chafiâh) that described an outbreak in 1327 in the Yemen. AHS was first recognized on the African continent in the 16th century. Father Monclaro, in his account of a journey of Francisco Baro in 1569 to east Africa, described a disease outbreak resembling AHS amongst horse that were imported from India and used in the exploration of central and east Africa. In 1652, the first settlers arrived in the Cape of Good Hope in southern Africa and this was soon followed, in 1657, by the introduction of horses and mules from Europe and the Far East. The first severe AHS outbreak occurred in 1719, killing 1 700 horses. Over the subsequent years, at least 10 major and several lesser outbreaks have been recorded in South Africa (Barnard, 1995; Mellor and Hamblin, 2004). The most severe outbreak of AHS occurred in 1854-1855, causing the death of 40% of the horse droves (*ca.* 70 000 horses). The frequency and severity of the outbreaks have, however, declined over the last century. This is probably due to improved surveillance and strict zoning measures, as well as vaccination of horses with polyvalent, live attenuated vaccines (Bosman *et al.*, 1995; Mellor and Hamblin, 2004).

Although AHS is believed to be endemic to sub-Saharan Africa, except for occasional outbreaks in North Africa and the Arabian Peninsula (Rafyi, 1961; Mirchamsy and Hazrati, 1973; Mellor, 1994), there have been, however, several outbreaks of the disease in the Persian Gulf, middle Eastern and southern European countries (Howell, 1960; Howell, 1963; Mellor, 1993). One of the most devastating epizootic outbreaks occurred in 1959 to 1961 in the Middle East, killing over 300 000 equines (predominantly horses, but also susceptible donkeys). The outbreak was halted by culling of susceptible equine hosts, and through combined vaccination and vector control efforts (Mellor, 1993). Of the nine AHSV serotypes, serotypes 1 to 8 are found in restricted areas of sub-Saharan Africa, while serotype 9 is more widespread. This serotype has been responsible for almost all epidemics outside Africa, the exception being the Spanish-Portuguese outbreaks during 1989 to 1990 that were due to serotype 4 (Coetzer and Erasmus, 1994).

1.2.2 Susceptible species and transmission

AHS affects primarily equine species, with horses being the most susceptible (Theiler, 1921). The mortality rate in horses may range between 70 to 95% (Coetzer and Erasmus, 1994). However, antibodies to AHSV have been detected in dogs, cattle, sheep, camels, buffalo, elephants, donkeys, mules and zebra (Van Rensburg *et al.*, 1981; Coetzer and Erasmus, 1994; Fassi-Fihri *et al.*, 1998; el Hasnaoui *et al.*, 1998). Indeed, zebra have long been considered the natural vertebrate host and reservoir of AHSV since they rarely exhibit clinical signs of infection (Barnard, 1998). Consequently, zebras are believed to play an important role in the persistence of the virus in Africa. Interestingly, donkeys in South Africa appear to be naturally resistant to AHSV (mortality rate less than 10%) and animals that become infected, rarely display clinical symptoms. Therefore, donkeys, in addition to zebras, may also act as reservoir host in South Africa (Alexander, 1948; Hamblin *et al.*, 1998).

AHS is not contagious and the virus is transmitted primarily through the bites of adult female midges, belonging to the genus *Culicoides* (du Toit, 1944; Mellor *et al.*, 1975). Although *ca.* 30 of the more than 1 500 *Culicoides* species are capable of transmitting orbiviruses, *C. imicola* is believed to be the primary vector in Europe, Africa and Asia (Mellor, 1994; Meiswinkel and Paweska, 2003). *C. botlinos*, which has a wide distribution in southern Africa, has also been identified as a potential vector of AHSV (Venter *et al.*, 2000) and is common in cooler highland areas where *C. imicola* is rare. It has also been reported that *C. variipennis*, which is dominant in the USA, but not in South Africa, can experimentally transmit AHSV (Boorman *et al.*, 1975). Moreover, in Spain, AHSV has been found in *C. obsoletus* and *C. pulicaris*, both of which are the most common *Culicoides* species in central and northern Europe (Mellor *et al.*, 1983). Epidemic outbreaks of AHS have been well correlated with climate conditions favoured by the *Culicoides* species, with early heavy rainfall, followed by warm, dry spells generally considered as optimal breeding conditions (Venter and Meiswinkel, 1994). Indeed, climate change may increase the range of the vector insect and therefore raises the possibility that AHS may spread more globally (Purse *et al.*, 2005).

1.2.3 Pathogenesis and clinical signs

During initial AHSV infection, virus multiplication takes place in regional lymph nodes and then spreads to pulmonary microvascular endothelial cells (Laegreid *et al.*, 1992). The

prominent pathological features associated with infection include oedema, effusion and haemorrhage, and thus result in the loss of endothelial cell barrier function (Coetzer and Erasmus, 1994). Following initial infection, virus is disseminated via the bloodstream through the body, which causes infection of a range of secondary organs such as the lungs, spleen, lymphoid tissues, choroid plexus, pharynx and certain endothelial cells (Coetzer and Erasmus, 1994). Pathogenesis and the severity of disease symptoms displayed by the host are influenced by a wide range of factors, amongst other, viral tropism, permissivity, host immune status and host genetic susceptibility (Laegreid *et al.*, 1993).

Four distinct clinical syndromes have been described in horses with AHS, *i.e.* the pulmonary (acute), cardiac (subacute), mixed pulmonary and cardiac (cardio-pulmonary) and fever forms (Brown and Dardiri, 1990). The fever form of the disease develops after an incubation period of 5-14 days and the affected horses develop mild to moderate fever, scleral infection and mild depression, followed by complete recovery. The cardiac form has an incubation period of 7-14 days and results in mild fever, pericardial effusion and oedema of subcutaneous and intermuscular tissue of the head, neck and chest. Approximately 35% of horses affected with this form of the disease recover, but mortality rates exceeding 50% have been reported. The mixed pulmonary and cardiac form of AHS has symptoms of both forms of the disease, and the mortality rate is *ca.* 70% with death occurring within 3-6 days after onset of fever. The pulmonary form develops rapidly (within 4-5 days) and is characterized by high fever, pulmonary oedema and plural effusion, resulting in a mortality rate often exceeding 95% (Coetzer and Erasmus, 1994).

1.2.4 Treatment and vaccination

Although there is currently no specific treatment available for AHS, great emphasis has been placed on the control of AHS incidence (House, 1998; Sanchez-Vizcaino, 2004). Since AHSV is non-contagious and can only spread via the bites of infected *Culicoides* species, control is effected through the use of insecticides and repellents to control the vector population, as well as by restricting animal movement to prevent infected animals from initiating new foci of infection, and by slaughtering of viraemic animals to prevent them acting as sources of virus for vector insects (Mellor and Hamblin, 2004).

In southern Africa, AHS is controlled by vaccination with polyvalent, live attenuated vaccines that are administered twice in the first and second year of life of susceptible animals, and annually thereafter (Taylor *et al.*, 1992). Due to concerns regarding incomplete protection as a consequence of interference between the virus serotypes (Erasmus, 1994), potential for gene segment reassortment between virulent and avirulent strains (House, 1998) and the fact that some strains of the virus in the vaccine might only be weakly immunogenic (Laegreid, 1996), research has been undertaken to develop alternate vaccines. Subunit vaccines, based on the use of baculovirus-expressed AHSV-4 VP7 (Wade-Evans *et al.*, 1997) and the outer capsid proteins VP2 and VP5 (Martinez-Torrecuadrada *et al.*, 1996; Scanlen *et al.*, 2002), have been investigated. A recombinant Venezuelan equine encephalitis virus-derived vector, expressing AHSV-4 VP2 and VP5, has also been developed but failed to induce neutralizing antibodies in horses (MacLachlan *et al.*, 2007). More recently, a modified vaccinia Ankara (MVA) strain, which is replication deficient, was used for expression of different AHSV antigens (VP2, VP7 and NS3 of AHSV-4) and presented in ponies (Chiam *et al.*, 2009). Analysis of the antibody responses indicated that only the VP2 vaccine was capable of inducing a neutralizing antibody response.

1.3 AFRICAN HORSESICKNESS VIRUS (AHSV)

1.3.1 Classification

African horsesickness virus (AHSV) is a member of the *Orbivirus* genus, one of nine genera within the family *Reoviridae*, which encompasses vertebrate, arthropod and plant pathogens (Calisher and Mertens, 1998). Viruses within this family possess segmented dsRNA genomes (10-12 segments) encapsidated within single non-enveloped virus particles with a diameter of 57-80 nm and exhibit icosahedral symmetry (Gorman, 1992; Urbano and Urbano, 1994). Orbiviruses differ from other members of the *Reoviridae* by the presence of a double-layered protein capsid (Verwoerd and Huisman, 1969; Borden *et al.*, 1971), their greater sensitivity to lipid solvents and detergents (Gorman and Taylor, 1985), loss of virus infectivity in mild acid conditions (Gorman and Taylor, 1985), and they are able to replicate in both insects and vertebrates (Gorman, 1992). To date, there are 21 recognized serogroups of orbiviruses and they can be differentiated from each other based on biochemical and immunological tests (Mertens *et al.*, 2008). Viruses within each serogroup can be classified into serotypes on the basis of antibody-mediated neutralization of viral infectivity (Knudson and Monath, 1990;

Brown *et al.*, 1991). There are presently nine recognized serotypes of AHSV (McIntosh, 1958; Howell, 1962).

1.3.2 Virion structure

The AHSV virion is non-enveloped with two concentric protein layers that enclose a dsRNA genome consisting of ten segments (Verwoerd *et al.*, 1972; Bremer *et al.*, 1990). The outer capsid is composed of the two major structural proteins VP2 and VP5, while the inner capsid is comprised mainly of the two major proteins VP3 and VP7 that enclose the three minor proteins VP1, VP4 and VP6 (Roy *et al.*, 1994).

The structure of the AHSV particle is comparable to that of BTV, of which the structure of single- and double-shelled virus particles has been determined by cryoelectron microscopy and by X-ray crystallography (Hewat *et al.*, 1992a; Prasad *et al.*, 1992; Grimes *et al.*, 1998; Stuart and Grimes, 2006). Based on these analyses, it is possible to segregate the core into two distinct layers. A thin inner layer is formed from 120 molecules of VP3, arranged as 60 dimers, to form a smooth-surfaced shell. The VP3 shell is stabilized by the outer layer of the core that comprises 260 VP7 trimers, organized into pentameric and hexameric rings that protrude 5 nm from the surface with channels between them (Prasad *et al.*, 1992; Stuart *et al.*, 1998). The core contains the dsRNA genome and the three minor proteins VP1 (10 or 12 copies), VP4 (20 or 24 copies that form dimers) and VP6 (60 or 72 copies that may form hexamers), each of which plays a significant role in genome RNA replication (Stuart and Grimes, 2006). The icosahedral and fibrillar outer capsid consists of 360 globular-shaped VP5 molecules, which are arranged in 120 trimers that are located in the channels formed by the six-membered rings of the VP7 trimers. The 180 copies of VP2 form 60 triskelion-type motifs that cover all of the VP7 trimers and protrude 4 nm above the globular VP5 proteins (Hewat *et al.*, 1992a; Stuart *et al.*, 1998). A schematic diagram of the BTV particle is presented in Fig. 1.1.

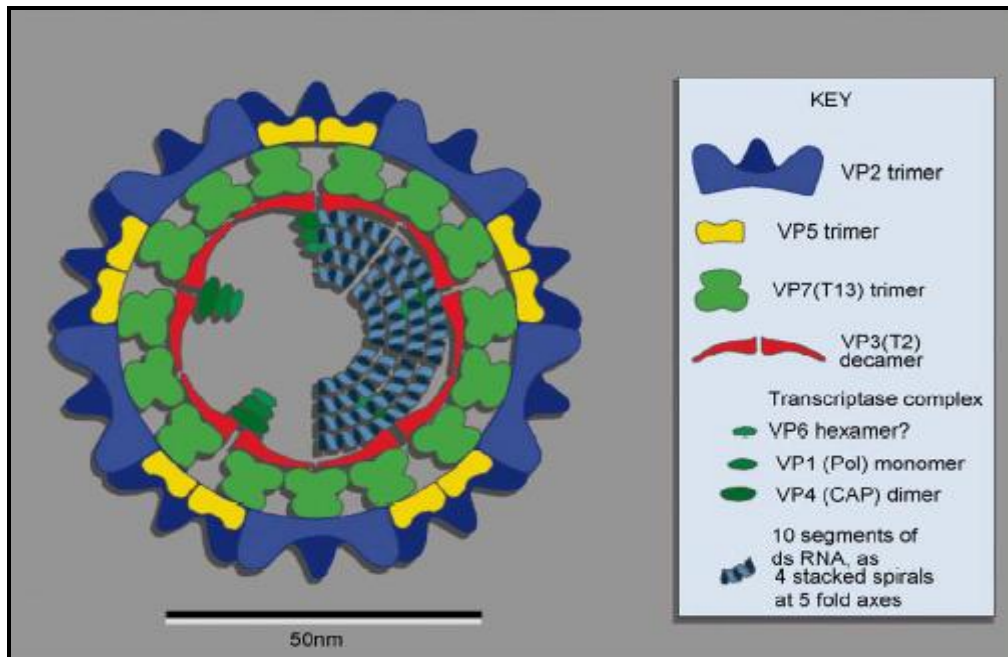


Fig. 1.1: Schematic representation of the BTV particle (Mertens, 2004). The core particle, which comprises VP3 and VP7, encloses the three minor core proteins, namely VP1, VP4 and VP6, and the ten dsRNA viral genome segments. The core is surrounded by the outer capsid composed of VP2 and VP5.

1.3.3 Viral genome

The AHSV genome consists of ten dsRNA segments, which are grouped according to size into large (L1-L3), medium (M4-M6) and small (S7-S10) genome segments (Bremer *et al.*, 1990). Each genome segment is monocistronic, except for S10, which encodes the two related non-structural proteins NS3 and NS3A (Van Staden and Huismans, 1991; Grubman and Lewis, 1992). The 5' non-coding region of the genome segments ranges in size between 12 and 35 base pairs (bp), while the 3' non-coding regions are 29 to 100 bp in length (Roy *et al.*, 1994). In contrast to BTV, the terminal hexanucleotide sequences of AHSV are not conserved through all the segments (Rao *et al.*, 1983; Roy *et al.*, 1994). Nevertheless, the 5'- and 3'-terminal sequences of each genome segment display partial inverted complementarity. This feature is thought to play a role in determining the secondary structure of the viral mRNA, which may be of importance for initiation of transcription and/or in the sorting and assembly of genome segments during virus replication (Cowley *et al.*, 1992; Mizukoshi *et al.*, 1993).

1.3.4 Viral proteins

In addition to seven structural proteins (VP1-VP7), four non-structural proteins (NS1, NS2, NS3 and NS3A) are also encoded by the viral genome. The ten orbivirus dsRNA genome segments, together with their encoded proteins and likely functions, are summarized in Table 1.1.

1.3.4.1 Outer capsid proteins

The VP2 protein, one of the two outer capsid proteins, is the most variable of the viral proteins (Potgieter *et al.*, 2003), and is the major serotype-specific antigen (Huisman and Erasmus, 1981) and viral haemagglutinin (Cowley and Gorman, 1987). Moreover, VP2 is involved in attachment of the virus to cells and has been reported to bind to sialic acid moieties of cellular receptors prior to internalization of the virus particle (Hassan and Roy, 1999; Zhang *et al.*, 2010). Neutralizing epitopes have been mapped on AHSV VP2 (Bentley *et al.*, 2000; Martinez-Torrecuadrada *et al.*, 2001) and antibodies raised in rabbits to VP2 of AHSV-4 have been reported to neutralize a virulent strain of AHSV-4 (Martinez-Torrecuadrada *et al.*, 1994). It has also been shown that vaccinia- and baculovirus-expressed AHSV VP2 can protect horses against a lethal challenge with the homologous virus serotype (Stone-Marchat *et al.*, 1996; Scanlen *et al.*, 2002).

In contrast to the VP2 protein, the role of VP5 in neutralization has not yet been clearly established. In contrast to BTV (Marshall and Roy, 1990), AHSV VP5 is able to induce neutralizing antibodies, albeit at lower levels than VP2 (Martinez-Torrecuadrada *et al.*, 1999). However, when used in conjunction with VP2, higher titers of neutralizing antibody, compared to immunization with VP2 only, have been reported (Martinez-Torrecuadrada *et al.*, 1996). Consequently, AHSV VP5 may play a supportive role to VP2 in enhancing the immune response. Recent studies on the biological activity of BTV VP5 have suggested its involvement in membrane permeabilizing activity (Hassan *et al.*, 2001). It has also been shown that VP5 has the ability to interact with host cell membranes and to induce cell-cell fusion in a manner similar to that of fusion proteins of enveloped viruses. The membrane-interacting properties occur only after VP5 has undergone a low pH-triggered activation step that may result in a fusion-competent conformation of the protein (Forzan *et al.*, 2004). However, the mechanism by which VP5 mediates membrane penetration and cell fusion is not yet known.

Table 1.1: BTV genome segments and their encoded proteins (adapted from Mertens, 2004)

Genome segment (bp)	Protein	Location	Number of amino acids	Molecular mass of proteins (Mr)	Properties	Functions
L1	VP1	Within the subcore	1305	150292	The largest protein, highly basic with a positively charged carboxyl terminus.	RNA-directed RNA polymerase responsible for RNA transcription/replication.
L2	VP2	Outer capsid	1051	122043	It forms a triskelion spike-like structure, which is found in excess in the outer layer of the core. Together with VP5 it exhibits the greatest variation in sequence between the serotypes, it determines the virus serotype and it is a neutralizing antigen, as well as a hydrophilic protein.	It possesses the viral haemagglutination and neutralization activity, is the cellular receptor protein which allows for the attachment and adsorption of the virus to the cell and is involved in the determination of virulence.
L3	VP3	Within the subcore layer	905	103269	It contains group-specific antigen determinants and it is highly conserved and hydrophobic in nature.	Controls the size and organization of the core structure.
M4	VP4	Component of the inner core	642	75826	Hydrophilic protein, which is highly conserved.	It is a methyl transferase protein that caps and methylates the mRNAs.
M6	VP5	The inner layer of the outer capsid	504	56900	It forms globular structures on the outer layer and is very variable in sequence between the serotypes.	VP5 and VP2 form the outer capsid. VP5 is involved in the permeabilization of the endosomal membrane in a pH-dependent manner during initiation of infection and it also helps determine the virus serotype.
S9	VP6	Within the subcore layer	369	38464	Hydrophilic protein with ssRNA- and dsRNA-binding ability.	May serve as a NTPase and a helicase, which unwinds the dsRNA before replication, and it binds ssRNA and dsRNA.
S7	VP7	Outer core surface	349	37916	It contains group-specific antigen determinants and is rich in hydrophobic regions.	It forms the outer core surface, which is involved in cell entry and in the high infectivity of vector insects and cells.
M5	NS1	Cytoplasm of infected cells	548	63377	Highly conserved and form tubules during replication, which consist of helically coiled ribbons of dimers.	Although the function of NS1 tubules in virus replication is unclear, it may be involved in pathogenesis.
S8	NS2	Cytoplasm of infected cells	365	41193	Only phosphorylated protein, which is largely hydrophilic and has a NTPase function.	It binds to ssRNA and may be involved in enveloping the mRNA during viral assembly and replication, and its NTPase activity might play a role in providing energy for the assortment, movement or packaging of the ssRNA that it binds.
S10	NS3 and NS3A	Cell membranes	217 206	23659 22481	NS3A is a truncated form of NS3, both proteins are glycosylated, highly variable and cytotoxic to cell.	It disrupts cell membranes allowing virus release and may be involved in determination of virulence.

1.3.4.2 Inner capsid proteins

The major core proteins, VP7 and VP3, form the outer layer of the viral core particle. Of the two proteins, VP7 is the most abundant protein in the core particle and self-assembles into trimers (Basak *et al.*, 1992), which form the outermost shell of the core. In both BTV and AHSV, VP7 has been demonstrated to be a serogroup-specific antigen (Huismans and Erasmus, 1981; Chuma *et al.*, 1992). However, in contrast to BTV, the AHSV VP7 protein forms flat hexagonal structures in the cytoplasm of both virus-infected (Burroughs *et al.*, 1994) and recombinant baculovirus-infected cells (Chuma *et al.*, 1992; Maree and Paweska, 2005). Although the functional significance of the VP7 crystalline structures is not yet known, it is thought to represent a by-product rather than an essential component of the AHSV replication cycle (Burroughs *et al.*, 1994). The crystal structure of a single domain (*i.e.* the top domain) of AHSV VP7 has been solved (Basak *et al.*, 1996) and was found to be structurally similar to that of BTV VP7 (Basak *et al.*, 1992; Grimes *et al.*, 1995). The top domain of BTV and AHSV VP7 both contain a surface-exposed RGD motif, which, in the case of BTV, has been shown to be responsible for core attachment to *Culicoides* cells (Tan *et al.*, 2001). The VP3 protein plays a major role in the structural integrity of the virus core and forms the protein scaffold on which the VP7 capsomeres are assembled (Stuart *et al.*, 1998). The BTV VP3 protein has been reported to contain group-specific antigenic determinants (Inumaru *et al.*, 1987) and is capable of interacting with ssRNA (LeBlois *et al.*, 1992). Co-expression of AHSV VP3 and VP7 genes in insect cells by means of recombinant baculoviruses has been shown to result in their spontaneous assembly into core-like particles (CLPs), which structurally resemble empty authentic AHSV cores (Maree *et al.*, 1998).

The three minor structural proteins, VP1, VP4 and VP6, are candidates for the virus-directed RNA polymerase and associated enzymes that are responsible for transcription of the ten viral mRNAs during infection. The VP1 protein is considered to be the virus replicase-transcriptase enzyme based on its size (150 kDa), location and molar ratio (estimated at 10-12 molecules per virion) in the core (Stuart *et al.*, 1998), and it possesses motifs characteristic of RNA polymerases (Roy *et al.*, 1988; Vreede and Huismans, 1998). Baculovirus-expressed BTV VP1 has been shown to exhibit detectable RNA-elongation activity in the presence of single-stranded poly(U) template and a poly(A) primer (Roy *et al.*, 1988; Urakawa *et al.*, 1989). More recently, it was reported that soluble recombinant BTV VP1 exhibited a processive replicase activity, synthesizing complete complementary RNA strands of *in vitro*-

synthesized BTV ssRNA templates (Boyce *et al.*, 2004). The 5' ends of the viral mRNA species are believed to be capped and methylated during transcription, thus resulting in stabilization of the viral mRNA synthesized during infection (Roy, 1992). The VP4 protein of BTV has been reported to demonstrate guanylyl transferase (Le Blois *et al.*, 1992) and methyltransferase type 1 and type 2 (Ramadevi *et al.*, 1998) activities. Furthermore, VP4 also binds to GTP and displays nucleoside triphosphate phosphohydrolase (NTPase) activity, which is considered to be of importance for transcription and dsRNA processing (Ramadevi and Roy, 1998). The third minor protein, VP6, is a highly basic protein with a strong affinity for both ss- and dsRNA (Roy *et al.*, 1990; Hayama and Li, 1994; de Waal and Huismans, 2005). Sequence analysis of BTV and AHSV VP6 sequences has revealed a motif common to helicases (Roy, 1992; Turnbull *et al.*, 1996). In this regard, it has been reported that purified BTV VP6, upon incubation with dsRNA in the presence of ATP, led to the unwinding of the dsRNA template (Stauber *et al.*, 1997). Thus, VP6 may be involved in the unwinding the dsRNA genome prior to the initiation of transcription or, based on its RNA-binding ability, it may be involved in the encapsidation of viral RNA.

1.3.4.3 Non-structural proteins

The NS1 protein of orbiviruses is synthesized abundantly in virus-infected cells and is readily assembled as tubular structures within the cytoplasm. These tubules are biochemically and morphologically distinct from the microtubules and neurofilaments present in normal cells (Huismans and Els, 1979). The tubular structures are formed by helically coiled ribbons of NS1 dimers, but the biophysical character of the tubules differ between BTV and AHSV. In contrast to BTV tubules that have a diameter of 52 nm and lengths of up to 1000 nm (Hewat *et al.*, 1992b), the AHSV tubules have a diameter of 23 nm and vary in length up to 4 μm (Maree and Huismans, 1997). Moreover, whereas BTV tubules exhibit a defined ladder-like appearance, AHSV tubules appear to have a fine reticular “cross-weave” appearance. No function has yet been assigned to NS1, but it has been proposed that the protein may be a major determinant of BTV pathogenesis in the vertebrate host since it augments virus-cell association that ultimately leads to lysis of the infected cell (Owens *et al.*, 2004).

The NS2 protein is the predominant component of virus inclusion bodies (VIBs) (Hyatt and Eaton, 1988; Brookes *et al.*, 1993) and expression of NS2, in the absence of other viral proteins in both insect and mammalian cells, results in the formation of inclusion bodies (IBs)

that are indistinguishable of VIBs found in virus-infected cells (Thomas *et al.*, 1990; Uitenweerde *et al.*, 1995; Modrof *et al.*, 2005). The VIBs have been shown to contain ssRNA, dsRNA, NS1, as well as complete and incomplete virus particles (Eaton *et al.*, 1988; Eaton *et al.*, 1990; Brookes *et al.*, 1993). These observations therefore have led to the recognition of VIBs as the sites in which virus assembly occurs. NS2 is also the only virus-specific protein that is phosphorylated in infected cells (Huismans *et al.*, 1987a; Devaney *et al.*, 1988). Although the significance of NS2 phosphorylation is not completely understood, a recent report has indicated that phosphorylation of BTV NS2 is important for VIB formation (Modrof *et al.*, 2005). The NS2 protein also has a strong affinity for ssRNA but not for dsRNA, suggesting that it may have a role in the recruitment and packaging of viral ssRNA prior to encapsidation (Huismans *et al.*, 1987a; Theron and Nel, 1997; Lymperopoulos *et al.*, 2003). Interestingly, BTV NS2 displays phosphohydrolase (NTPase) activity, and can bind and hydrolyse ATP and GTP to their corresponding nucleotide monophosphates (Horscroft and Roy, 2000; Taraporewala *et al.*, 2001). It has been suggested that the NTPase activity of NS2 may play a role in providing energy for the assortment, movement, packaging or condensation of bound ssRNA (Horscroft and Roy, 2000).

In contrast to NS1 and NS2, the two closely related non-structural proteins NS3 and NS3A are synthesized in low abundance in orbivirus-infected cells (Huismans, 1979; French *et al.*, 1989; Van Staden *et al.*, 1995). The segment 10 gene, encoding NS3, contains two in-phase translation initiation codons that initiate the synthesis of NS3 and NS3A, respectively (Van Staden and Huismans, 1991). The BTV NS3 protein, in contrast to that of AHSV, has been reported to be glycosylated (Wu *et al.*, 1992) and it was suggested that *N*-linked glycosylation of the NS3 protein may serve to protect it from degradation (Bansal *et al.*, 1998). Within BTV-infected cells the NS3 proteins have been observed to co-localize with BTV particles within disrupted regions of the plasma membrane, suggesting that the NS3 protein may be involved in the release of BTV from infected cells (Hyatt *et al.*, 1989; Wu *et al.*, 1992). In addition, it has been reported that baculovirus-expressed virus-like particles (VLPs) are only released in the presence of NS3 protein (Hyatt *et al.*, 1992), thus furthermore suggesting a role for NS3 proteins in virus release. Similarly, the AHSV NS3 protein is also localized to sites of AHSV release in Vero cells (Stoltz *et al.*, 1996).

1.4 ORBIVIRUS REPLICATION AND MORPHOGENESIS

Although there are considerable differences in several of the replicative processes of members of the *Reoviridae* family, the overall strategy appears to be the same. Using BTV as a model for orbivirus replication and morphogenesis (Fig. 1.2), four major events in the replication cycle of orbiviruses have been identified and are discussed below in greater detail. These events are: adsorption and penetration, uncoating and formation of replicative complexes, formation of virus tubules and virus inclusion bodies, and movement of virus to and release from the cell surface (Mertens, 2004; Roy, 2008).

BTV rapidly adsorbs to susceptible mammalian cells, with maximal adsorption occurring within 20 min (Huisman *et al.*, 1973). The binding and internalization of BTV in mammalian cells is mediated by the outer capsid protein VP2 (Huisman and Van Dijk, 1990; Hassan and Roy, 1999). Although the cellular receptors to which BTV binds have not yet been identified, it has been reported that the VP2 of BTV attaches to sialoglycoproteins of mammalian cells prior to internalization (Hassan and Roy, 1999; Zhang *et al.*, 2010).

Following adsorption, BTV is transported into the cytoplasm of the cell via receptor-mediated endocytosis that involves formation of clathrin-coated vesicles within the cell, which subsequently fuse to form endosomes (Hyatt *et al.*, 1989; Eaton *et al.*, 1990). Within the endosome, the outer capsid proteins (VP2 and VP5) are removed, presumably due to the acidic conditions within the endosome, and the transcriptionally active core particles are released into the cytoplasm of infected cells (Huisman *et al.*, 1987b). It has been suggested that VP5 may be responsible for the release of transcriptionally active cores from the endosomes, since removal of VP2 from the virions results in the exposure of N-terminal helical membrane-destabilizing domains of VP5 (Hassan *et al.*, 2001). The replication of BTV is initiated by the synthesis and extrusion of capped and methylated mRNA from transcriptionally active cores within the cytoplasm. The mRNA transcripts function not only to encode proteins, but also as templates for production of minus-strands to form the dsRNA genome segments encapsidated in the progeny virions (Mertens and Diprose, 2004). However, the mechanism by which viral mRNAs are selected and encapsidated prior to replication is not yet known.

Soon after the initiation of transcription of BTV mRNAs, granular matrix structures accumulate near the core particles (Hyatt *et al.*, 1987). These VIBs increase both in size and number as the viral infection progresses (Eaton *et al.*, 1990). Newly synthesized viral transcripts, the four subcore viral proteins (VP1, VP3, VP4 and VP6), as well as assembled cores and subcores have been identified in the VIBs and therefore appear to be the sites of orbivirus replication and early viral assembly (Hyatt and Eaton, 1988). The assembly of the BTV VP3 subcore has been reported (Kar *et al.*, 2004). VP3 was reported to have three distinct domains, *i.e.* an apical, a carapace and a dimerization domain. The dimerization domain mediates formation of VP3 dimers, which pack together in decamers to form the icosahedral structure of the VP3 layer. Although it has been reported that BTV VP3 can bind to RNA (Loudon and Roy, 1991), it was recently reported that BTV RNAs failed to associate with the VP3 decamers (Kar *et al.*, 2004). Consequently, it was suggested that assembly of the BTV core may begin with a complex formed by minor core proteins and the VP3 decamers, and that these assembly intermediates recruit the viral RNA prior to completion of the assembly of the VP3 subcore (Kar *et al.*, 2004). More recently, co-expression of the BTV structural proteins with NS2 has indicated that VP7 requires co-expression of VP3 to be recruited to the VIBs and that neither of the outer capsid proteins VP5 and VP2 have an affinity for the VIBs (Modrof *et al.*, 2005; Kar *et al.*, 2007). Therefore, it would appear that progeny core particles are first produced in the VIBs, then moved to the periphery of the VIBs where they are coated by the outer capsid proteins VP5 and VP2 (Kar *et al.*, 2007). Little is known of the mechanism whereby VP2 and VP5 are added to the developing virus particle. However, it was recently reported that VP5 associates with lipid rafts in the plasma membrane and that the core particles are transported to these sites for the final assembly of the outer capsid proteins (Bhattacharya and Roy, 2008). In addition to VIBs, NS1-rich tubules form part of the ‘insoluble’ phase of the cell and become a characteristic structure of the cell from an early stage of infection (Huisman and Els, 1979; Eaton *et al.*, 1988). It has been reported that NS1 may be a determinant of pathogenesis in the vertebrate host by leading to lysis of infected cells (Owens *et al.*, 2004).

Investigations regarding virus release from mammalian cells have demonstrated a strong correlation between the presence of NS3 and NS3A, and virus release (Hyatt *et al.*, 1989; Stoltz *et al.*, 1996). The virions may leave infected cells in one of two ways. Early after infection, when the host cell metabolism is not completely inhibited and the integrity of the host plasma membrane is maintained, progeny virions have been observed to bud through the

plasma membrane and thus acquire a transient envelope (Gould and Hyatt, 1994). Alternatively, during the latter stages of infection, when the integrity of the plasma membrane is not maintained, egress of virions can be accomplished as non-enveloped virions by extrusion through the locally disrupted plasma membrane surface (Hyatt *et al.*, 1989).

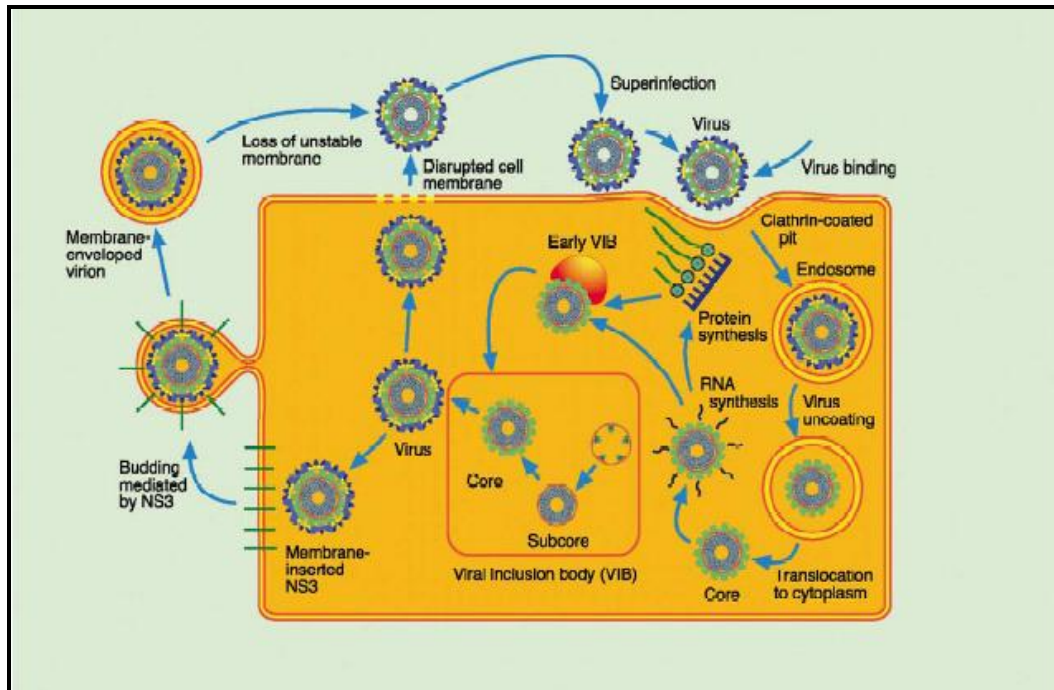


Fig. 1.2: Schematic diagram of the replication cycle of BTV (Mertens, 2004). The adsorption of the virus involves a receptor of unknown nature in the cell membrane of susceptible host cells. The viruses enter the cell via endocytosis, after which clathrin-coated vesicles, containing the virions, form and are drawn to the cell nucleus. The outer capsid proteins are removed to yield core particles in the cell cytoplasm. Transcription of the virion RNA occurs and the proteins generated by translation of the viral mRNA condense with the viral ssRNA around the parental cores to form VIBs. Structural proteins are translated and condense at the VIB periphery to form cores and subcores. The outer capsid proteins are added, after which the virions are released from the cells via lysis, budding or extrusion from the cells.

1.5 THE NON-STRUCTURAL PROTEIN NS3

Since NS3 is the focus of this study, the following sections will focus in greater detail on its properties and role in viral egress. The information on AHSV NS3 will be supplemented, where applicable, with relevant information obtained from studies on NS3 of BTV, the prototype orbivirus.

1.5.1 Properties of NS3

The AHSV NS3 and NS3A proteins are encoded by the RNA genome segment S10 from alternative start codons in the same open reading frame, and differ only with respect to ten additional amino acids present at the N-terminal end of NS3 (Van Staden and Huismans, 1991). The NS3 proteins are synthesized in smaller amounts compared to the two other non-structural proteins (NS1 and NS2) (Huismans, 1979; French *et al.*, 1989), and also in different amounts depending on the host cells. Whereas NS3 accumulates in high levels in insect cells during virus infection, low levels of protein is expressed in infected mammalian cells (Guirakhoo *et al.*, 1995; Van Staden *et al.*, 1995).

Interestingly, NS3 is not highly conserved between the different AHSV serotypes and represents the second most variable protein encoded by AHSV. Indeed, up to 37% amino acid variation across all serotypes and almost 28% amino acid variation within a single serotype has been reported (Van Niekerk *et al.*, 2001b). Comparison of the nucleotide sequences indicated that the observed variation clusters into three distinct phylogenetic groups, which have been termed clades α (serotypes 4, 5, 6 and 9), β (serotypes 3 and 7) and γ (serotypes 1, 2 and 8) (Martin *et al.*, 1998; Van Niekerk *et al.*, 2001b; Quan *et al.*, 2008). In contrast, BTV NS3 is highly conserved and shows a maximum of 7% variation (Pierce *et al.*, 1998; Balasuriya *et al.*, 2008). Despite the difference in AHSV NS3 sequence variation, a number of conserved regions have been identified that are also present in NS3 of BTV (Van Staden *et al.*, 1995; Van Niekerk *et al.*, 2003). The conserved regions comprise an initiation codon for NS3A, a proline-rich region between residues 22 and 34, a highly conserved region between residues 43 and 92, two hydrophobic domains (residues 116-137 and 154-170) predicted to form transmembrane helices necessary for stable membrane interaction, and a highly variable hydrophilic region (residues 137-154) between the latter two domains (Fig. 1.3).

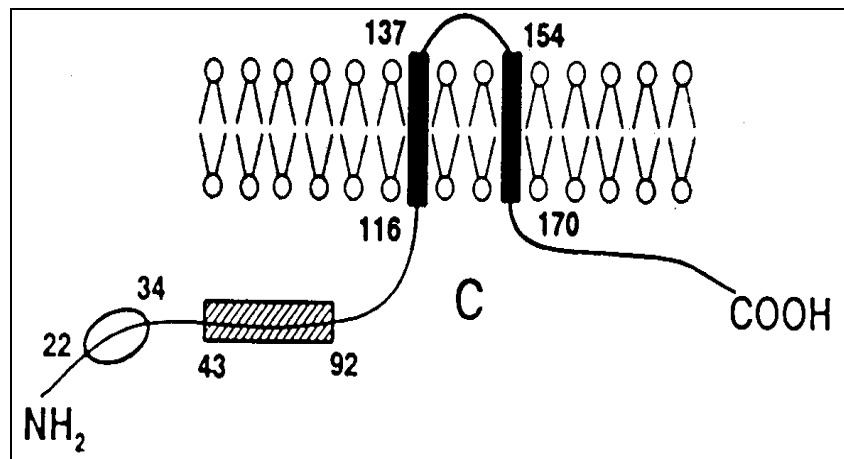


Fig. 1.3: A topological model for the interaction of AHSV NS3 with the cellular membrane (Van Staden *et al.*, 1995). The model depicts NS3 with a long N-terminal and shorter C-terminal domain, both located in the cytoplasm (C), and two transmembrane domains (black boxes) connected via a short extracellular domain. The conserved region and proline-rich region are indicated by a hatched box and oval, respectively. Numbers in the figure refer to amino acid residues in AHSV-3 NS3.

Albeit that the exact function of NS3 during AHSV replication is not fully understood, it is thought to have an analogous function to BTV NS3, which has been proposed to play a role in the release of progeny virions from infected cells (Hyatt *et al.*, 1992). This is supported by immuno-electron microscopy studies indicating the presence of NS3 at sites of membrane damage and virus exit in AHSV-infected Vero cells (Stoltz *et al.*, 1996). Moreover, AHSV NS3 expressed by a baculovirus recombinant is not only plasma membrane-associated, but also has a cytotoxic effect on the *Spodoptera frugiperda* insect cells (Van Staden *et al.*, 1995). Although the mechanism by which NS3 causes cell death is not known, it may be as a result of an alteration of the permeability of the cell membrane. In a subsequent study, it was shown that the cytotoxic effect was abrogated when mutations were introduced into either of the NS3 hydrophobic transmembrane domains, thus indicating that cytotoxicity is dependent on the membrane association of the protein (Van Niekerk *et al.*, 2001a). In this regard, it is interesting to note that BTV NS3 has been suggested to act as a viroporin based on its ability to form homo-oligomers, localization to the plasma membrane and Golgi apparatus of infected cells, and increased plasma membrane permeability (Han and Harty, 2004). It was suggested that these properties of BTV NS3 may facilitate lytic virus release through destabilization of the plasma membrane. Whether AHSV NS3 may similarly act as a viroporin-like protein remains to be determined.

The cytotoxicity of NS3, coupled with a potential role in virus release, suggests that NS3 may be a virulence determinant (Martin *et al.*, 1998; O'Hara *et al.*, 1998). Recently, the generation of reassortant viruses between different AHSV strains, with NS3 from clades α , β or γ , was described (Meiring *et al.*, 2009). Characterization of the derived reassortants, in which the S10 genome segment encoding NS3 was exchanged with or without other genome segments, indicated that exchange of the NS3 gene resulted in changes in virus release, membrane permeability and total virus yield. These results therefore indicate an important role for NS3 in these viral processes. However, differences in the cytopathic effects (CPE) and the effect on cell viability between the parental virus strains could not be ascribed to NS3 alone, and it was suggested that various viral and host factors may rather play a role (Meiring *et al.*, 2009).

1.5.2 NS3 and virus release

With the exception of the above-mentioned studies on AHSV NS3, much of the information regarding the role of NS3 in virus release has been obtained from studies conducted with BTV. As indicated previously, investigations regarding release of BTV progeny virions from mammalian cells have demonstrated a strong correlation between the presence of NS3 and virus release (Hyatt *et al.*, 1989). In addition, virions have been demonstrated to leave infected cells in two ways. Early after the infection, progeny virions have been observed to bud through the plasma membrane, acquiring a transient envelope. Alternatively, egress of virions can be accomplished by non-enveloped particles by extrusion through locally disrupted plasma membrane surfaces (Hyatt *et al.*, 1989). Although virus release is observed in mammalian cells, virions remain mainly associated with cellular components and only a minority of particles is found in the extracellular medium, presumably due to release as a consequence from CPE and lysis of infected cells (Castro *et al.*, 1989; Guirakhoo *et al.*, 1995). In contrast to mammalian cells, infection of C6/36 insect cells results in persistent infection with no CPE and the majority of progeny virions are released into the supernatant without apparent cell lysis (Homan and Yunker, 1988; Guirakhoo *et al.*, 1995). In contrast to virus release from mammalian cells, no studies aimed at unraveling the mechanisms underlying virus release from insect cells have been undertaken to date. Nevertheless, the above results indicate that the host cell environment, including differences in cellular proteins and membranes, may play an important role in viral release mechanisms.

Recent studies have provided a clearer understanding regarding BTV egress from mammalian host cells (Beaton *et al.*, 2002; Wirblich *et al.*, 2006; Celma and Roy, 2009). Using yeast two-hybrid screening, Beaton *et al.* (2002) demonstrated that the cytoplasmic C-terminal domain of NS3 is capable of interacting with the outer capsid protein VP2. Moreover, it was also reported that an amphipathic α -helix, comprising the first 13 amino acids of NS3 (and thus absent in NS3A), interacts with the calpactin light chain (p11) of the cellular annexin II complex. The annexin II complex, also termed the Calpactin complex, comprises two heavy chains (p36) and two light chains (p11) that interact to form a functional heterotetramer. This complex has been implicated in membrane-related events along the endocytic and regulated secretory pathways, including exocytosis and the trafficking of proteins out of the cell (Raynal and Pollard, 1994; Gerke, 2001). Not only does NS3 interact with p11 at the same site as p36, but the interaction between NS3 and p11 was found to be highly specific as a synthetic NS3 peptide mimicking the sequence of the p11 binding domain was shown to reduce the titre of released progeny virus from BTV-infected C6/C36 insect cells (Beaton *et al.*, 2002). Since NS3 recruits p11 in the place of p36, it was proposed that this interaction may help to either direct NS3 to sites of cellular exocytosis, or it could be part of an active extrusion process. Based on the overall findings, a model for NS3-mediated non-lytic release of BTV was proposed (Fig. 1.4). According to this model, NS3 facilitates virus egress by forming a bridge between the progeny virions and p11, thereby directing the virions to the export machinery of the host cell (Beaton *et al.*, 2002). Evidence in support of a role for NS3 in trafficking virions to the cell membrane via VP2 was recently presented by Celma and Roy (2009). Using a reverse genetics system for BTV, a mutant virus was generated that contained mutations in the C-terminal domain of NS3 resulting in the abrogation of NS3-VP2 interaction. It was subsequently reported that no budding virus particles could be observed in mammalian cells infected with the mutant virus, thus demonstrating that NS3 plays a key role in the interaction of viral particles via VP2 with cellular proteins during virus egress (Celma and Roy, 2009).

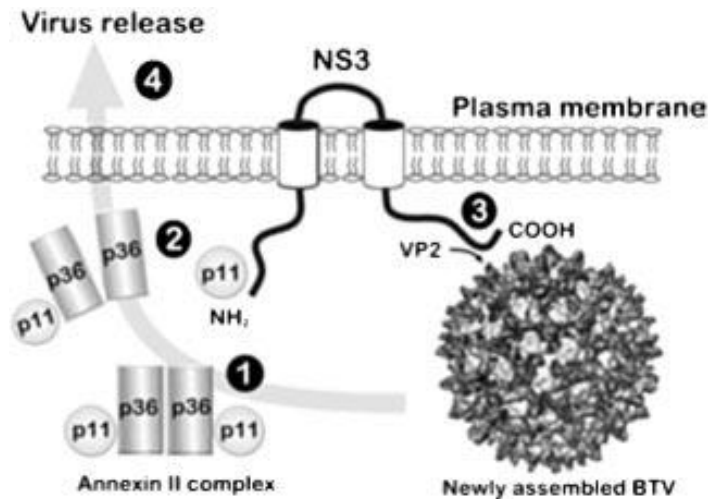


Fig. 1.4: A model for the role of BTV NS3 in virus release (Beaton *et al.*, 2002). (1) The host proteins p11 and p36 form part of the annexin II complex that is involved in cellular exocytosis. (2) NS3 interacts with p11, either alone or in a partial annexin II complex by displacement of one copy of p36 via a sequence at its N-terminal domain. (3) Progeny virions bind to NS3 via interaction between a C-terminal domain in NS3 and the outer capsid protein VP2. (4) The virions are drawn into contact with the p11/annexin II complex and engage the cellular exocytic machinery, thus resulting in non-lytic virus.

In addition to the interaction of NS3 with the p11 component of the annexin II complex, NS3 has also been shown to be capable of interacting with Tsg101 (Wirblich *et al.*, 2006). Using pull-down assays, it was shown that NS3 and NS3A of both BTV and AHSV-6 both bind *in vitro* to human Tsg101 and also to its orthologue from *Drosophila melanogaster* (Wirblich *et al.*, 2006). The Tsg101 protein forms part of the ESCRT-I complex (endosomal sorting complex required for transport), which has been implicated in the intracellular trafficking and release of various enveloped viruses (Garrus *et al.*, 2001; Martin-Serrano *et al.*, 2001; Freed, 2004; Calistri *et al.*, 2009). The interaction of BTV NS3 with Tsg101 is mediated by a conserved PSAP late assembly (L)-domain motif in NS3, and appears to play a role in viral release as silencing of Tsg101 gene expression with small interfering RNA (siRNA) reduced the release of BTV and AHSV-6 from infected HeLa cells up to 5- and 3-fold, respectively (Wirblich *et al.*, 2006). The importance of NS3-Tsg101 interaction with regards to virus release was recently confirmed by Celma and Roy (2009). Using a reverse genetics approach, a mutant virus was generated that contained site-specific mutations in the L-domain of BTV NS3, thus abrogating the interaction between NS3 and Tsg101. It was subsequently shown that in BSR cells infected with the mutant virus, virion particles remained tethered to the cell membrane, apparently arrested in the process of virus budding (Celma and Roy, 2009).

Cumulatively, these results indicate that NS3 may be capable of interacting with various different cellular proteins in order to facilitate virus budding from infected host cells. An amended model, indicating these various interactions, is presented in Fig. 1.5.

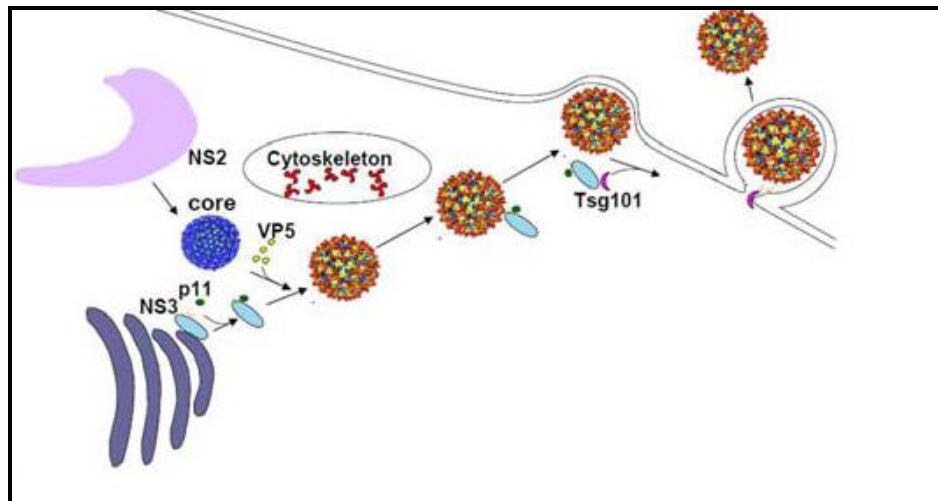


Fig. 1.5: Schematic representation of how NS3 may facilitate budding of BTM from infected cells through interaction of the cytoplasmic N-terminus of NS3 with the cellular release factors calpactin p11 and Tsg101 (via late domain motifs), while its cytoplasmic C-terminus interacts with the BTM outer capsid protein VP2 (Roy, 2008).

1.5.3 Significance of L-domain motifs in NS3

Although the presence of L-domains in BTM NS3 has been noted previously (Strack *et al.*, 2000), their functional relevance has not been investigated until recently (Wirblich *et al.*, 2006). In contrast, the L-domains of retroviruses have been studied extensively and these studies have provided valuable insights regarding their functional importance during viral budding. To enable budding at the plasma or endosomal membranes, retroviruses recruit various cellular proteins that normally function in the biogenesis of multivesicular bodies (MVBs) (Freed, 2002; Bieniasz, 2006; Calistri *et al.*, 2009). The MVBs play an important role in protein sorting and degradation, and they are formed by the budding of vesicles into the lumen of late endosomal compartments through a process that is reminiscent of budding of enveloped viruses away from the cytoplasm (Pornillos *et al.*, 2002; Raiborg *et al.*, 2003). The biogenesis of MVBs require at least four separate heteromeric protein complexes, *i.e.* ESCRT-0, -I, -II and -III, which are transiently recruited from the cytosol to the endosomal membrane where they function sequentially in the sorting of proteins into the

MVB pathway and in the formation of MVB vesicles (Katzman *et al.*, 2001; Babst *et al.*, 2002; Gruenberg and Stenmark, 2004; Babst, 2005; Hurley and Emr, 2006). Notably, in contrast to ESCRT-II, both the ESCRT-I and ESCRT-III complexes play essential roles in virus budding (Bieniasz, 2006).

Retroviruses bind to the different components of the MVB pathway by means of L-domains, which are highly conserved protein-protein interaction motifs (Gottlinger *et al.*, 1991; Xiang *et al.*, 1996; Puffer *et al.*, 1997; Yatsuda and Hunter, 1998). Three classes of motifs have been identified (P[T/S]AP, PPXY and YPXL/LXXLF) and, in each case, the integrity of these motifs appears to be essential for L-domain activity, as mutations in these motifs induce a defective assembly phenotype whereby virions and cell membranes failed to segregate. In addition to retroviruses, the PTAP and/or PPXY motifs have been reported to also facilitate budding of rhabdoviruses (Craven *et al.*, 1999), filoviruses (Harty *et al.*, 2000) and arenaviruses (Perez *et al.*, 2003). More recently, a novel L-domain motif (FPIV) was identified in paramyxoviruses that could functionally replace the PTAP motif in the Gag protein of HIV-1 (Schmitt *et al.*, 2005).

With the exception of the FPIV motif, cell binding partners have been identified for each of the identified L-domain motifs. The P(T/S)AP motif recruits the Tsg101 protein, a component of the ESCRT-I complex (Garrus *et al.*, 2001; Martin-Serrano *et al.*, 2001; Demirov *et al.*, 2002; Wirblich *et al.*, 2006). Both the YPXL and LXXLF motifs bind to AIP-1/Alix, which acts downstream of Tsg101 and appears to bridge the ESCRT-I and ESCRT-III complexes (Martin-Serrano *et al.*, 2003; Strack *et al.*, 2003). The PPXY motif is a consensus sequence for interaction with WW domains, a protein module that is present in multiple copies in HECT (homologous to E6AP C-terminus) ubiquitin ligases (Sudol *et al.*, 1996; Macias *et al.*, 2002). Thus, the PPXY motif appears to play a role in recruiting host ubiquitin ligases (Bouamr *et al.*, 2003; Blot *et al.*, 2004). Although knowledge regarding the exact targets of the ubiquitin ligases and their interactions with other components of the budding machinery is limited (Calistri *et al.*, 2009), several studies have, however, suggested that this family of ubiquitin ligases might play a role in virus budding (Harty *et al.*, 2000; Strack *et al.*, 2000; Martin-Serrano *et al.*, 2005; Usami *et al.*, 2008).

Based on the important role of L-domain motifs in the budding of enveloped viruses, it is therefore interesting to note that L-domain motifs are also present in the NS3 protein of non-

enveloped orbiviruses. Sequence analysis of the NS3 sequences of several orbiviruses (BTV, AHSV, EHDV, Chuzan virus and Broadhaven virus) indicated that all of the NS3 sequences contained the two most commonly observed L-domain motifs, PPXY and P(T/S)AP, albeit that these sequences were more variable in AHSV strains (Wirblich *et al.*, 2006). As discussed above (Section 1.5.2), the interaction of BTV NS3 with Tsg101 via the PSAP motif appears to play a role in virus release. With regards to the PPXY L-domain motif, Wirblich *et al.* (2006) reported that BTV NS3 was capable of binding to different HECT ubiquitin ligases, such as NEDD4.1, WWP1 and Itch, in *in vitro* pull-down assays. However, based on the use of a Gag protein-based VLP assay in mammalian cells, it was shown that the L-domain motifs in NS3 do not function as effectively as the L-domain motifs of other enveloped viruses (Wirblich *et al.*, 2006). It was thus concluded that the ability of NS3 to interact with different proteins of the MVB pathway via the L-domain motifs is likely to be more important in the vector insect where BTV establishes a persistent infection without causing significant CPE. In contrast, virus release from mammalian cells may rather be facilitated by the viroporin activity of BTV NS3, *i.e.* virus release by inducing membrane destabilization.

1.6 LYTIC-INDEPENDENT RELEASE OF NON-ENVELOPED VIRUSES

In contrast to enveloped viruses (Freed, 2004; Welsch *et al.*, 2007; Chen and Lamb, 2008), relatively few studies have been conducted on the mechanism by which non-enveloped viruses are released from cells. It has generally been accepted that non-enveloped viruses are released passively from infected cells after cellular lysis (Smith and Enquist, 2002). However, several recent studies have indicated that the virions of non-enveloped viruses can be released from cells, without causing cell lysis, by actively exploiting cytoskeleton filaments or membrane lipid rafts.

Poliovirus has been proposed to utilize an autophagosome-mediated exit without lysis (AWOL) pathway for the non-lytic extracellular release of progeny virions (Taylor *et al.*, 2009). In this model, double-membrane vesicles, resembling autophagosomes, that accumulate during the late stages of poliovirus infection are proposed to contain a small amount of cytosol and entrapped virus particles. These virally induced vesicles are tethered to microtubules via the non-structural protein 3A, thus rendering them immobile and thereby minimizing viral release during infection. When the microtubules are broken down under

natural circumstances, *e.g.* the end of infection or entry of the infected cell into mitosis, the vesicles are free to be transported to the plasma membrane where the virus entrapped in the vesicles can be released via fusion of the vesicles with the plasma membrane (Taylor *et al.*, 2009). In the case of the autonomous parvovirus Minute Virus of Mice (MVM), Bär *et al.* (2008) reported that the transport and release of progeny virions is guided by the cytoskeleton and mediated by virus-modified lysosomal and/or late endosomal vesicles. Specifically, vesicular egress of the virions was shown to be dependent on active gelsolin, a multifunctional protein that cleaves actin filaments. However, the exact mechanism underlying the virus egress is yet to be determined. It has also been reported that the actin cytoskeleton plays an important role in the exocytosis of progeny rotavirus virions (Gardet *et al.*, 2007). It was demonstrated that the rotavirus outermost capsid protein, VP4, binds to actin and that the movement of VP4 along the actin network results from actin treadmilling, a process in which the oriented removal of actin within microfilaments causes a treadmilling involving both actin monomers and actin-binding proteins. Blocking of actin treadmilling with jasplakinolide, a cyclic peptide that binds and stabilizes filamentous actin, resulted in a loss of polarized virus release, albeit that the total virus production was unaffected (Gardet *et al.*, 2007). It was thus concluded that although actin-based VP4 motility does not control assembly of VP4 with immature virions, actin treadmilling is essential to ensure polarized release of rotavirus. In BTV-infected cells, virus particles have been observed to be attached to vimentin in intermediate filaments (Eaton *et al.*, 1987), as well as underneath the cell membrane in association with the actin-rich cortical layer (Eaton *et al.*, 1990). Recently, it was demonstrated that the association of mature BTV particles with intermediate filaments are driven by the interaction of VP2 with vimentin (Bhattacharya *et al.*, 2007). Disruption of vimentin intermediate filament networks with colchicine resulted in an accumulation of intracellular virus particles and a reduction in the amount of virus released, thus suggesting that the VP2-vimentin association contributes to virus egress (Bhattacharya *et al.*, 2007).

In addition to the above, lipid rafts have also been implicated in the transport of viral particles to the cell surface (Chazal and Gerlier, 2003; Schmitt and Lamb, 2005). Lipid rafts are dynamic, detergent-resistant regions of the plasma membrane enriched in cholesterol, glycosphingolipids, glycosylphosphatidylinositol (GPI)-anchored proteins and some membrane proteins (Brown and London, 1998). These lipid rafts are considered to be relay stations in intracellular signaling and transport (Simons and Ikonen, 1997; Foster *et al.*, 2003). Studies aimed at understanding rotavirus assembly and release have shown that lipid rafts

purified from infected cells contained infectious rotavirus particles. It was thus suggested that lipid rafts may provide a means for targeting of the mature virions to the cell membrane in a pathway that bypasses the Golgi apparatus, the classic exocytosis pathway (Sapin *et al.*, 2002; Cuadras *et al.*, 2003; Chwetzoff and Trugnan, 2006). In a subsequent study, Cuadras *et al.* (2006) reported that silencing of VP4 gene expression substantially reduced the association of rotavirus particles with lipid rafts, indicating that VP4 plays a direct role in the association of virions with lipid rafts. In this regard, it has recently been reported that the BTV outer capsid protein VP5 is capable of interacting with lipid rafts via a WHYL motif in the VP5 sequence (Bhattacharya and Roy, 2008). Moreover, it was also shown that NS3 directly interacts with VP5, as well as with lipid rafts in virus-infected cells. The importance of these interactions with regards to virus egress was not investigated. However, based on the ability of NS3 to bind to both VP2 (Beaton *et al.*, 2002) and VP5, it was suggested that lipid rafts may provide a scaffold for virus assembly and that NS3 might serve to keep the two outer capsid proteins in position for the final assembly of the virus cores (Bhattacharya and Roy, 2008). Intriguingly, the VP5 sequences of AHSV strains do not possess a WHYL motif and it is therefore unclear as to whether AHSV can likewise associate with lipid rafts.

1.7 APPROACHES TOWARD STUDYING PROTEIN FUNCTION

Although it is thought that the AHSV NS3 protein may act in a manner similar to NS3 of BTV to mediate virus release, experimental evidence for this supposition is lacking. Based on the preceding sections, two approaches that may provide potentially valuable insights into the function of viral proteins comprise gene silencing and protein-protein interaction studies. Consequently, these technologies will be addressed in greater detail in the following sections.

1.7.1 RNA Interference (RNAi)

In the past, targeted inhibition of mammalian gene expression has been achieved primarily by approaches such as homologous recombination (Vasquez *et al.*, 2005; Sorrell and Kolb, 2005), antisense oligonucleotides (Scanlon *et al.*, 2005), ribozymes (Robishaw *et al.*, 2004) and intrabodies (Owens *et al.*, 2004; Visintin *et al.*, 2004). However, over the last decade, RNA interference (RNAi) has emerged as the primary means whereby specific genes in mammalian systems can be suppressed or silenced. RNAi, a process by which dsRNA directs sequence-specific degradation of a cognate mRNA, was first discovered in the nematode

Caenorhabditis elegans (Fire *et al.*, 1998; Montgomery *et al.*, 1998). It has since become clear that RNAi is an evolutionary conserved gene silencing system and has been described for protozoa, insects and mammals (Agrawal *et al.*, 2003). Because of its apparent universal applicability and high specificity, RNAi has become a powerful tool for analyzing gene function in diverse groups of organisms, including viruses, and it has been proposed that RNAi may provide a therapeutic approach for controlling viral infections (Ketzinel-Gilad *et al.*, 2006; Stram and Kuzntzova, 2006; Kanzaki *et al.*, 2008; Csorba *et al.*, 2009).

1.7.1.1 Mechanism of RNAi

Biochemical and genetic analyses have provided a mechanistic understanding of RNAi-mediated gene silencing (Meister and Tuschl, 2004; Tomari and Zamore, 2005; Jinek and Doudna, 2009). In the first step, referred to as the RNAi initiating step, long dsRNA is typically cleaved into discrete 21-nucleotide (nt) RNA fragments, termed small interfering RNA (siRNA), by the RNase III-like enzyme Dicer (Bernstein *et al.*, 2001). Dicers are 200-kDa multidomain proteins and have a single dsRNA processing centre that contains two RNA cleavage sites (Provost *et al.*, 2002). Cleavage of the dsRNA at two nearby phosphodiester bonds on opposite RNA strands thus results in siRNA duplexes that are typically 21-nt in length, have 5' phosphate and 3' hydroxyl groups and 2-nt overhangs at the 3'-termini (Zhang *et al.*, 2004). In the second step, referred to as the effector step of RNAi, the siRNAs are assembled into a RNA-induced silencing complex (RISC), which subsequently guides the sequence-specific recognition of the target mRNA (Hong *et al.*, 2008; Hutvagner and Simard, 2008). Every RISC contains a member of the Argonaute protein family, which is characterized by the presence of a PAZ domain and a PIWI domain (Cerutti *et al.*, 2000; Carmell *et al.*, 2002). It is thought that interaction between the PAZ domain and 2-nt 3' overhangs of the siRNA duplexes allows for transfer of siRNAs into RISC (Lingel *et al.*, 2004). Moreover, based on the similarity of the PIWI domain with RNase H (Song *et al.*, 2004), it has been proposed that the Argonaute proteins may act as the catalytic subunit, termed Slicer, that is responsible for hydrolysis of the target mRNA (Liu *et al.*, 2004; Parker *et al.*, 2005; Ma *et al.*, 2005). A two-step mechanistic model for RNAi-mediated gene silencing is presented in Fig. 1.6.

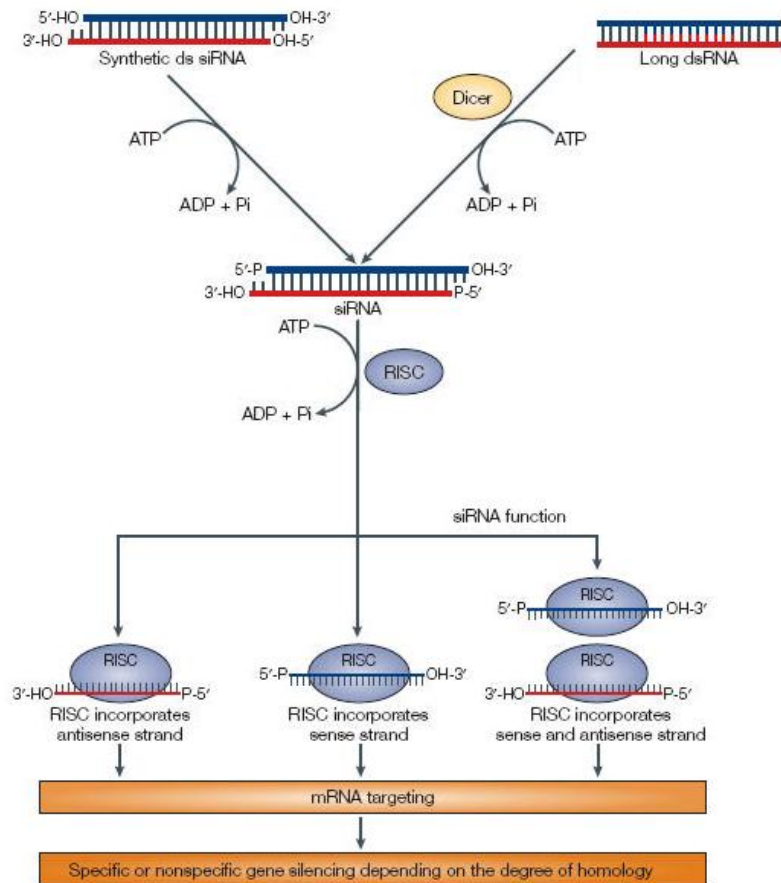


Fig. 1.6: RNAi-mediated gene silencing (Mittal, 2004). The processing of long dsRNA by Dicer leads to the formation of siRNAs, which consists of 21-nt RNA duplexes with symmetric 2-nt 3' overhangs and 5' phosphate groups. Exogenously provided synthetic siRNAs are converted into active functional siRNAs by an endogenous kinase that provides 5' phosphate groups in the presence of ATP. siRNAs associate with cellular proteins to form an RNA-induced silencing complex (RISC), which contains a helicase that unwinds the duplex siRNA in an ATP-dependant reaction. In an ideal situation, the antisense strand guides the RISC to the target mRNA for endonucleolytic cleavage. In theory, each of the siRNA strands can be incorporated into RISC and direct RNAi. The antisense strand of a siRNA can direct the cleavage of a corresponding sense RNA target, whereas the sense strand of a siRNA can direct the cleavage of an antisense target.

1.7.1.2 RNAi as an investigative tool in mammalian cells

Despite its utility in diverse organisms, it was initially difficult to detect potent and specific RNAi by dsRNA longer than 30 bp in commonly used mammalian cell culture systems (McManus and Sharpe, 2002; Agrawal *et al.*, 2003). This was largely due to the fact that introduction of the dsRNA into the cytoplasm of mammalian cells triggered an interferon (IFN) response, which results in a systemic, non-specific shutdown of protein synthesis (Manche *et al.*, 1992; Stark *et al.*, 1998). These sequence non-specific effects, however, have

been resolved when it was reported that in mammalian cells RNAi can be triggered by introducing synthetic 21- to 23-nt siRNA duplexes, rather than a long dsRNA, into the cells (Caplen *et al.*, 2001; Elbashir *et al.*, 2001a). The siRNAs avoid provoking the interferon response by virtue of their small size and are incorporated directly into the RNAi pathway by mimicking the products of the Dicer enzyme, which catalyzes the initiation step of RNAi (Fig. 1.6). In addition to the use of chemically synthesized siRNAs, various vector-based RNAi approaches, including plasmid DNA vectors (Brummelkamp *et al.*, 2002; Cheng and Chang, 2007; Wu *et al.*, 2009) and viral vectors such as adenoviruses, retroviruses and lentiviruses (Wadhwa *et al.*, 2004; Manjunath *et al.*, 2009), have been reported that allow for the production of short hairpin RNAs (shRNAs) that can be converted by Dicer into functional siRNAs. Only siRNAs will be discussed in greater detail in the following sections, as the application of siRNA to mediate gene silencing is closely aligned with the aims of this investigation.

- ***siRNA design***

At present, it is not possible to predict with complete certainty the degree of gene silencing a particular siRNA will produce and the design of an effective siRNA is still an empirical process. In addition to a number of general guidelines and recommendations (Elbashir *et al.*, 2001a; Mittal, 2004; Shao *et al.*, 2007), several siRNA design algorithms (Reynolds *et al.*, 2004; Ui-Tei *et al.*, 2004; Shah *et al.*, 2007; Naito *et al.*, 2009) have also been developed that may increase the probability of producing an effective siRNA. These guidelines and algorithms are, however, only predictive and do not guarantee a gene silencing effect. Nevertheless, the two most important factors influencing siRNA efficiency appears to be the structural characteristics of the siRNA and the target site within the gene.

To achieve efficient siRNA-mediated gene silencing, it has been suggested to select 19-nt long sequences in the coding region flanked by AA at the 5'-end and TT at the 3'-end. Furthermore, a G+C content of 30-80% was reported to be advantageous for the internal stability of the siRNA (Elbashir *et al.*, 2001b; 2001c; Chan *et al.*, 2009), whilst the 5' and 3' untranslated regions (UTRs) should be avoided since associated regulatory proteins may compromise RNAi (Mittal, 2004). Based on the analysis of effective siRNAs, it has been reported that they have a reduced thermodynamic stability at the 5'-end of the antisense strand relative to the 3'-end within the RNA duplex (Khvorova *et al.*, 2003; Schwarz *et al.*, 2003).

This asymmetry allows for the unwinding of dsRNA from the one end preferentially and is thought to increase the likelihood of incorporating the antisense strand, corresponding to the target mRNA transcript, into RISC and thereby minimizing off-target effects caused by the sense strand (Jackson *et al.*, 2003; Ding *et al.*, 2007).

Several siRNAs synthesized against different regions of the same target mRNA have been reported to silence gene expression to differing extents (Holen *et al.*, 2002; Bohula *et al.*, 2003; Stassen *et al.*, 2007), suggesting that accessibility of the target sequence on the mRNA should also be taken into account when designing siRNAs for gene silencing. Several reports have suggested that the low effectivity of siRNAs may be ascribed to the non-accessibility of the targeted mRNA regions for cleavage, which may be caused either by higher order RNA structures (Bohula *et al.*, 2003; Kretschmer-Kazemi Far and Sczakiel, 2003) or by protein coverage (Elbashir *et al.*, 2001a; Holen *et al.*, 2002). Consequently, it has been advised that at least three different siRNA duplexes targeting the same mRNA should be tested independently for a reproducible phenotype (Mittal, 2004).

- ***Synthesis of siRNAs***

RNAi-based gene silencing experiments are typically performed with chemically synthesized siRNAs (Elbashir *et al.*, 2001a; Caplen *et al.*, 2001). Despite being able to obtain siRNAs of high purity, uniform composition and large amounts, chemical synthesis of siRNAs is expensive. An alternative cost-effective and rapid method for siRNA synthesis is based on cleavage of long dsRNA (100-200 bp), which is prepared by *in vitro* transcription, with either Dicer or RNase III to generate a pool of siRNAs suitable for gene silencing (Yang *et al.*, 2002; Myers *et al.*, 2003; Xuan *et al.*, 2006). This approach virtually guarantees that one or more of the siRNAs in the pool will have siRNA gene silencing activity, and therefore abrogates the need to screen and identify individual effective siRNAs. However, there may be several potential limitations to this approach. In addition to the presence of unprocessed or partially processed long dsRNA that can activate the interferon response and result in non-specific translation inhibition, there is also the potential for increased off-target effects. Moreover, competition from less effective siRNAs in a pool may also reduce the overall efficacy compared to the use of a single very effective siRNA.

- ***Detection of the targeted gene silencing effect***

Establishing RNAi as a means to silence expression of a target gene in mammalian cells also requires methods whereby the level of targeted mRNA and presence of the encoded protein can be monitored. For validation of the gene silencing effect, standard molecular biology techniques are frequently used. Methods for quantification of the target mRNA level include Northern blot hybridization, quantitative reverse transcriptase (RT)-PCR or real-time PCR, whereas immunodetection methods are used to quantitate the level of protein and can be performed on either whole-cells (*e.g.* flow cytometry) or cell lysates (*e.g.* Western blot analysis, immunoprecipitation and enzyme-linked immunosorbent assays) (Sandy *et al.*, 2005; Ho *et al.*, 2006; Tilesi *et al.*, 2006). In contrast to methods based on cell lysates, which provide information regarding the average silencing effect for a cell population, methods based on whole-cells provide information about the nature of the silencing effect, *i.e.* the percentage of the cell population that shows the gene silencing phenotype and to what extent (Ho *et al.*, 2006).

1.7.1.3 Application of RNAi to viruses with a segmented dsRNA genome

Since the initial report by Elbashir *et al.* (2001a), whom identified RNAi activity in mammalian cells, numerous publications have subsequently described the use of RNAi to inhibit viruses from diverse virus families. However, despite its impact in probing gene function, there have been only a few studies exploring the potential for RNAi approaches to members of the *Reoviridae* family and these have focused mostly on rotaviruses. RNAi has been used to study *in vivo* the role of both structural proteins (Déctor *et al.*, 2002; Zambrano *et al.*, 2007) and non-structural proteins (Campagna *et al.*, 2005; López *et al.*, 2005; Cuadras *et al.*, 2006; Montero *et al.*, 2006), and more recently to study the importance of different heat shock proteins (Broquet *et al.*, 2007; Dutta *et al.*, 2009) and endosomal chaperones (Maruri-Avidal *et al.*, 2008) on the morphogenesis of rotavirus infectious particles. Although RNAi has also been applied to reoviruses with the aim of understanding the function of reovirus proteins associated with the formation of viral inclusions (Kobayashi *et al.*, 2006; Carvalho *et al.*, 2006; Kobayashi *et al.*, 2009), there is a paucity of RNAi-based studies undertaken on orbiviruses.

With the exception of a study performed by Wirblich *et al.* (2006) illustrating the importance of the cellular Tsg101 protein in BTV release (Section 1.5.2), only one other study has reported the use of RNAi to silence orbivirus gene expression. Specifically, siRNAs were used to silence expression of the VP7 gene of AHSV, which encodes for a structural protein required for stable capsid assembly. It was shown that synthetic VP7-directed siRNAs silenced effectively both VP7 protein and mRNA expression, and decreased production of infectious virus particles as was evidenced by a reduction in the progeny virion titres when compared to control cells (Stassen *et al.*, 2007). These studies therefore indicate that RNAi can be an important genetic tool for the study of AHSV and for the analysis of specific viral genes important for AHSV physiology.

1.7.2 Yeast two-hybrid screening

All biological processes depend on interactions formed between proteins and consequently, the characterization of a protein's interactions may contribute to elucidating the functions of the protein. Numerous technologies have been developed to study protein-protein interactions, from biochemical approaches such as co-purification, co-immunoprecipitation and affinity purification, to molecular genetic approaches such as the yeast two-hybrid system (Young, 1998; Uetz and Hughes, 2000; Brückner *et al.*, 2009). Compared to biochemical screens, the yeast two-hybrid system is able to detect interactions *in vivo* in a true cellular environment (Fields and Song, 1989; Rossi *et al.*, 1997; Arndt *et al.*, 2000). Not only is the system therefore more sensitive than many biochemical screens, but also is more suited to the detection of weak or transient interactions (Causier and Davies, 2002). Moreover, yeast two-hybrid technology is relatively inexpensive since it does not rely on the use of antibodies and costly procedures such as protein purification. Its relative methodical simplicity has furthermore aided in the yeast two-hybrid system having become one of the most popular screening methods for protein-protein interactions (Brückner *et al.*, 2009). To a greater extent, the popularity of the yeast two-hybrid system stems from its use to determine whether two known proteins interact with each other and to elucidate the function of a protein by identifying well-characterized interacting partners (Fields and Song, 1989; Chien *et al.*, 1991). Subsequent modifications of the yeast two-hybrid system have allowed for the detection of ternary protein complex formation (Egea-Cortines *et al.*, 1999), as well as for the dissection of amino acid residues involved in particular protein-protein interactions (Cress *et al.*, 1994; Franke *et al.*, 1994).

1.7.2.1 Basis of the yeast two-hybrid system

The first yeast two-hybrid systems were based on the modular nature of many eukaryotic transcription factors. Eukaryotic transcription factors can be physically divided into two distinct domains, namely an N-terminal DNA-binding domain (DNA-BD) and a C-terminal transcription activating domain (AD). These domains are independently non-functional as a transcription factor but, when in very close proximity to one another, can reconstitute transcription activity (Keegan *et al.*, 1986). This phenomenon has been exploited in the yeast two-hybrid system through the generation of independent fusion proteins incorporating these separate domains (*i.e.* one fusion protein incorporates the DNA-binding domain and the other the transcription activating domain). Interaction of such polypeptide fusions generates a functional transcription factor that then recruits RNA polymerase II, leading to transcription of a reporter gene that had previously been engineered into the genome of the yeast host. The most commonly used yeast two-hybrid system is the GAL4 system in which the DNA-binding and transcription activation domains of the yeast GAL4 proteins are used (Fields and Song, 1989). Typically, nutritional markers (*e.g.* the ability of yeast to grow on medium lacking histidine) and enzymatic reporters (*e.g.* the expression of β -galactosidase) are used in tandem for the analysis. Thus, yeast bearing appropriate reporter genes can be transfected with plasmid-based cDNA constructs encoding a library of independent fusions (the “prey”) with the transcription activation domain of the transcriptional factor GAL4. The fusion proteins encoded by these constructs will not in isolation be able to activate transcription of the reporter genes because, although each one includes a transcription activation domain, none possess a DNA-binding domain. However, if a second plasmid, encoding a fusion between a protein of interest (the “bait”) and the DNA-binding domain of GAL4, is introduced into the same yeast cell, expression of the reporter gene may occur. It therefore follows that such expression is dependent upon an interaction between the bait and the prey. Isolation of yeast clones in which a functional interaction has occurred, permits the isolation of the plasmid DNA encoding the GAL4 transcription activation domain. Consequently, the interacting prey protein can be identified following sequence analysis and database searching (Luban and Goff, 1995; Toby and Golemis, 2001; Causier and Davies, 2002). A flow diagram, depicting a typical yeast two-hybrid screen, is provided graphically in Fig. 1.7.

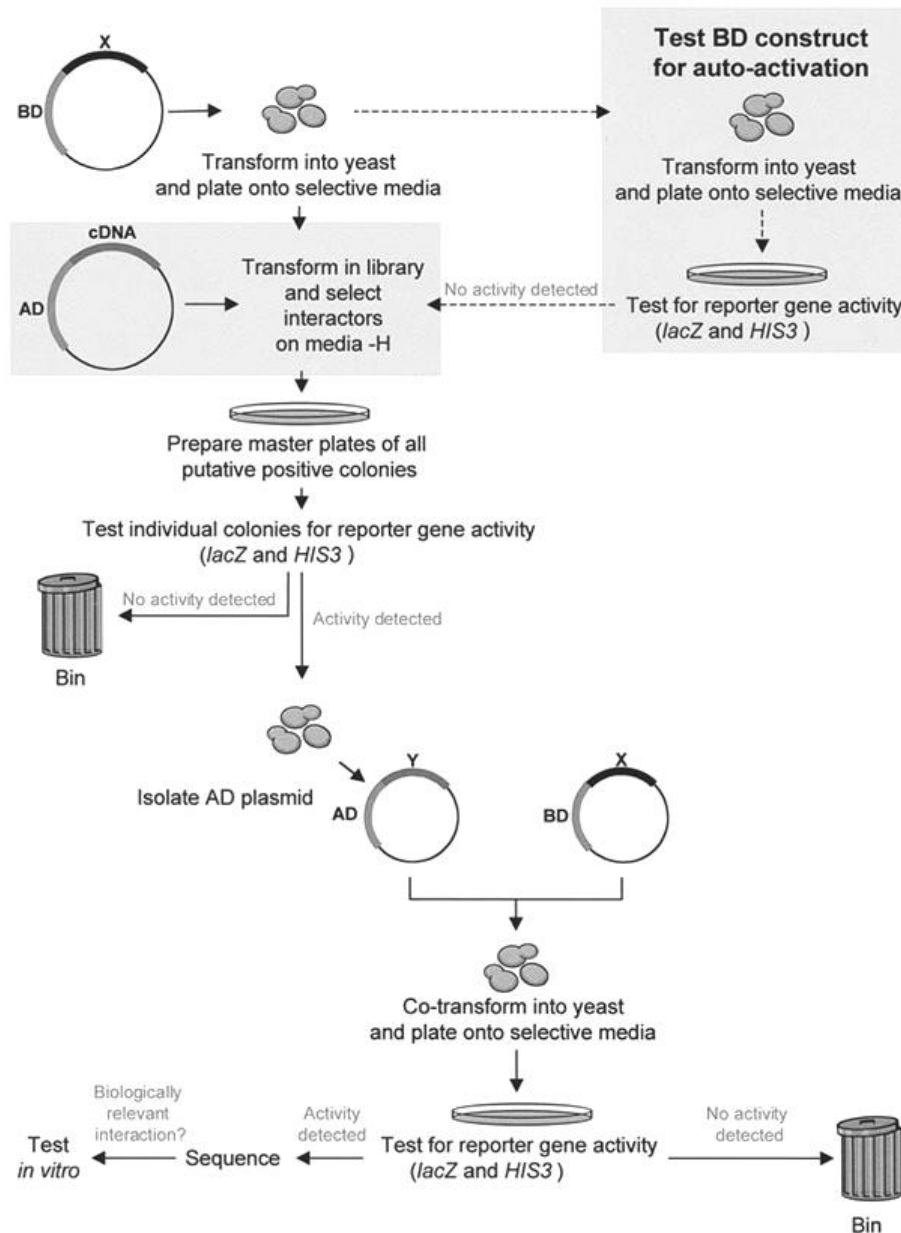


Fig. 1.7: A typical yeast two-hybrid library screen (Causier and Davies, 2002). The diagram describes a typical yeast two-hybrid library screen using the GAL4 protein system with *lacZ* and *HIS3* reporter genes. The first step is to transform the appropriate yeast strain with the construct encoding the test protein (X) fused in-frame with the GAL4 DNA-binding domain (BD). After verifying that the BD-X fusion protein does not auto-activate transcription of the reporter genes, the yeast cells can be transformed with the GAL4 activation domain (AD)-cDNA fusion library. Following selection of transformants on medium lacking histidine, the putative positives for a protein-protein interaction are transferred to a fresh plate lacking histidine to generate a master plate. From the master plate, yeast can be plated for β -galactosidase assays and onto medium lacking histidine to confirm reporter gene activity. The activation domain plasmid can be rescued from yeast cells demonstrating both reporter gene activities. The AD plasmid can be transformed back into yeast cells harbouring the BD-X construct, and re-assayed for reporter gene activity. If the interaction is detected, the activation domain plasmid can then be extracted from yeast cells and the cloned cDNA can be sequenced in order to identify the interacting protein.

1.7.2.2 Constraints of the yeast two-hybrid system

Although the yeast two-hybrid system offers many advantages over biochemical methods, *e.g.* cost, convenience and sensitivity, it still has associated limitations. Most notably, both false negative and false positive results are often generated in yeast two-hybrid library screens.

False negatives in the yeast two-hybrid system refer to protein-protein interactions that cannot be detected due to the inherent limitations of the screening method. The yeast two-hybrid system requires translocation of the interacting proteins into the nucleus and is therefore not suitable for membrane-associated proteins or integral membrane proteins. This is due to the fact that the activation domain of a transcription factor, when fused to a membrane protein, will be retained in the nuclear membrane and is thus rendered unavailable for reconstitution of a functional transcription factor in the nucleus (Xia *et al.*, 2006). Likewise, proteins that harbour strong signals for localization to other subcellular compartments may also generate a high rate of false negatives since the nucleus is not the natural environment for most of these proteins (Toby and Golemis, 2001). Moreover, interaction with proteins that are not stably expressed or are toxic to yeast cells may also not be detected in a yeast two-hybrid screen (Causier and Davies, 2002).

False positives in the yeast two-hybrid system refer to physical interactions detected during the screening in yeast that are not reproducible in an independent system. A major source of false positives is caused by the activation of transcription of the reporter gene through direct interaction between the prey component of the transcription activation domain fusion and the upstream activating sequences in the reporter gene construct (Rual *et al.*, 2005). A second source of false positives is due to auto-activators, which may represent up to 10% of the baits (protein fused to the DNA-binding domain). Such auto-inducers may either emerge during the course of the screen by spontaneous mutations (Rual *et al.*, 2005) or it may be that the bait protein may possess a transcription activation domain that may activate reporter gene expression (Fashena *et al.*, 2000). To avoid the latter, it has been recommended that the DNA-binding domain fusion proteins be tested for auto-activation of the reporter genes prior to testing for protein-protein interactions (Causier and Davies, 2002; Vidalain *et al.*, 2005). False positives may also be due to an irrelevant interaction between a prey peptide fragment and the bait protein, whilst some proteins appear to be inherently “sticky” and thus show unspecific interactions (Colas and Brent, 1998; Serebriiskii *et al.*, 2000). In this case, the

identified preys can be tested for interaction with unrelated baits. Preys interacting with other than the screening bait should thus be classified as false positives. In addition, the use of two or more reporter genes may also contribute to eliminating a large number of false positives. Selection of two active reporters requires a more solid transcriptional activation and thus provides a more stringent assay for protein-protein interactions. However, this approach can concomitantly penalize detection of weak and transient interactions (Luo *et al.*, 1996; Vidalain *et al.*, 2005).

By taking the above into account, it thus follows that yeast two-hybrid screens are merely capable of providing an overview of the potential protein-protein interactions. It is therefore important that interactions that have been identified in yeast two-hybrid screens are confirmed by at least one alternative, non-yeast-based assay. A description of different validation methods that can be used is provided in Table 1.2. It has been recommended that more than one method must be used to validate an identified protein-protein interaction, and these methods should preferentially consist of an *in vitro* biochemical method and *in vivo/in situ* method (Table 1.2). Whereas the *in vitro* biochemical methods allow for the study of physical protein-protein interactions, the *in vivo/in situ* methods allow insight into possible co-expression and co-localization of the two proteins involved, but generally do not provide conclusive evidence for direct interaction (Lalonde *et al.*, 2008; Brückner *et al.*, 2009).

Table 1.2: Overview of different validation methods (adapted from Brückner *et al.*, 2009)

Method	Type	Description
Pull-down assay	<i>in vitro</i>	Tagged bait (mostly expressed in <i>E. coli</i>) is immobilized on a resin and subsequently “pulls down” the target protein (prey) from lysates (of eukaryotic cells or of <i>E. coli</i> expressing proteins of interest). After washing steps, the prey is detected by SDS-PAGE and/or Western blot.
Co-immunoprecipitation	<i>in vitro</i>	A specific antibody is used to precipitate the bait from cell lysates (see above). After washing steps, the co-immunoprecipitated prey is detected as above.
Surface plasmon resonance	<i>in vitro</i>	Bait immobilized on the surface of a sensor chip is probed by injection of prey onto the surface. Protein interaction is detected online via a change in refractive index at the sensor surface. The protein is eluted and analyzed by mass spectroscopy.
Immunohistochemistry, immunocytochemistry	<i>in situ</i>	Proteins in fixed cells or tissue sections are detected with fluorescently tagged antibodies and using confocal or fluorescent microscopy. Allows for visualization of co-expression of proteins of interest in the same cell and potential subcellular co-localization.

Fluorescent detection in live cells	<i>in vivo</i>	Proteins in living cells are detected with fluorescently tagged antibodies as above (using permeabilized cells) or after expression of fluorescently tagged protein variants. Allows for visualization of co-localization of proteins of interest.
Fluorescence resonance energy transfer (FRET)	<i>in vivo</i>	Bait and prey are fused to two different fluorescent tags with overlapping emission/excitation spectra. If both proteins are in close proximity, excitation of the first fluorophore (donor) leads to energy transfer to the second fluorophore (acceptor). Acceptor fluorescence can be observed <i>in vitro</i> (fluorometer) or in living cells (confocal microscopy).
Bioluminescence resonance energy transfer (BRET)	<i>in vivo</i>	Similar to FRET, but with bait fused to bioluminescent luciferase, thus avoiding the external excitation step susceptible to generate background. Detection is as above with FRET.

1.7.2.3 Application of yeast two-hybrid screens to viruses with a segmented dsRNA genome

The yeast two-hybrid system has been used extensively to investigate interactions between different rotavirus non-structural proteins (Poncet *et al.*, 1997; González *et al.*, 1998; Torres-Vega *et al.*, 2000; Eichwald *et al.*, 2007), as well as to identify novel cellular proteins interacting with rotavirus proteins. By employing NSP1 as bait in a yeast two hybrid system, Graff *et al.* (2002) identified interferon regulatory factor 3 (IRF-3) as an NSP1 interactor and suggested that the role of NSP1 may therefore be to inhibit activation of IRF-3 and thus to diminish the cellular interferon response. Screening of a monkey kidney CV1 cell cDNA library for proteins interacting with NSP3 led to the isolation of a partial cDNA that displayed homology with a human eukaryotic initiation factor (eIF4GI). It was subsequently proposed that the interaction between NSP3 and eIF4GI leads to the enhancement of translation of rotavirus mRNAs and the concomitant impairment of translation of cellular mRNAs (Piron *et al.*, 1998). These studies were more recently extended by Vitour *et al.* (2004). Using a similar approach, a novel cellular protein was identified that interact with NSP3. The protein, designated RoXaN (rotavirus X protein associated with NSP3), was shown to interact with the dimerization domain of NSP3 and to form a ternary complex with eIF4GI during rotavirus infection, thus implicating RoXaN in translational regulation. Using yeast two-hybrid screening, NSP4 has been reported to bind to the extracellular matrix proteins laminin- β 3 and fibronectin (Boshuizen *et al.*, 2004), as well as to caveolin-1, which is a major structural protein of caveolae (Parr *et al.*, 2006). Interestingly, caveolae are a subset of lipid raft plasma membrane microdomains (Anderson, 1998; Parton *et al.*, 2006) that have been implicated in non-lytic virus release virus (Section 1.6). Utilizing reverse yeast two-hybrid analyses, Mir *et*

al. (2007) mapped the binding site of NSP4 to caveolin-1 to amino acid residues at both the N- and C-termini of caveolin-1. However, the biological significance of the interaction is yet to be determined. In addition to rotaviruses, the yeast two-hybrid system has also been used to investigate interactions between the reovirus non-structural proteins σ NS and μ NS (Becker *et al.*, 2003). It was shown that these proteins are the minimal viral components required to form inclusions, which then recruit other reovirus proteins and RNA to initiate viral genome replication.

In the case of orbiviruses, the interaction between BTV NS3 and p11, and between NS3 and VP2 was identified using a yeast two-hybrid screening approach and a commercially available HeLa cDNA library (Beaton *et al.*, 2002). The biological significance of these respective interactions has been discussed previously (Section 1.5.2). In a similar yeast two-hybrid screen, the non-structural protein NS1 was noted to interact with SUMO-1, a cellular protein responsible for induction of post-translational modification of proteins involved in intracellular trafficking. Although this protein interaction was not confirmed in an independent assay, it was recently hypothesized that NS1 may play a role in trafficking of immature or mature virus particles through its interaction with SUMO-1 (Roy, 2008). In the case of AHSV, Beylveld (2007) used the yeast two-hybrid system to investigate interactions between the NS3 N-terminal domain and a commercially available *Drosophila melanogaster* cDNA library. Putative interactions between the truncated NS3 protein and the cellular proteins ubiquitin and Hsp70 were identified. However, these interactions have yet to be validated and their biological relevance established.

1.8 AIMS OF THIS INVESTIGATION

From the review of the literature, it is evident that many aspects regarding orbivirus replication, morphogenesis and release still need to be elucidated. In contrast to other vertebrate-infecting members of the *Reoviridae* family, unravelling of the orbivirus replication cycle is complicated by their ability to replicate in both the vertebrate host and vector insect. Moreover, the effect of orbivirus replication in these distinct host types is markedly different. For BTV, replication of the virus in insect cells results in persistent infection with no CPE, whilst infection of mammalian cells results in cell death (Guirakhoo *et al.*, 1995). This implies that there may be different mechanisms that traffic progeny virions

out of the infected cells. Indeed, virus particles may either bud through the cell membrane or move through local disruptions of the plasma membrane (Hyatt *et al.*, 1989; Han and Harty, 2004). Recent evidence has implicated the non-structural protein NS3 in virus release (Beaton *et al.*, 2002; Wirblich *et al.*, 2006; Celma and Roy, 2009; Meiring *et al.*, 2009). For BTV, the data indicate that NS3 uses host cell proteins and acts as an intermediate to facilitate release of progeny virions across the cell membrane. Whether the same holds true for NS3 of AHSV has yet to be determined. Mapping the role of AHSV NS3 in the virus replication cycle can benefit significantly through the use of RNAi technology. RNAi represents a potentially powerful tool to generate loss-of-function phenotypes that can facilitate investigations regarding virus gene function in the context of virus-infected cells (Stassen *et al.*, 2007). In addition, yeast two-hybrid screening analyses may allow for the identification of cellular proteins capable of interacting with NS3 and contribute to the release of progeny virions from the host cells (Beaton *et al.*, 2002). Information gained from these types of studies should therefore advance our understanding of the mechanisms used by AHSV to escape from susceptible host cells. Towards the long-term goal of mapping the role of NS3 in the AHSV replication cycle and virus-cell interactions, the specific aims of this investigation were as follows:

- To determine whether NS3 is responsible for AHSV egress from mammalian host cells by making use of an RNAi-based approach.
- To determine whether NS3 interacts with cellular proteins representative of the cellular export machinery in mammalian and insect cells by making use of yeast two-hybrid screening analyses.

CHAPTER TWO

SMALL INTERFERING RNA (siRNA)-MEDIATED SILENCING OF AHSV-3 NS3 GENE EXPRESSION IN VERO CELLS AFFECTS VIRUS RELEASE

2.1 INTRODUCTION

African horsesickness virus (AHSV), a member of the *Orbivirus* genus within the *Reoviridae* family, encodes four non-structural proteins (NS1, NS2, NS3/3A) of which the function in virus replication is not yet fully understood. Of these, NS3 is a membrane-associated protein (Van Staden *et al.*, 1995) that has been proposed to be involved in virus release due to its localization at sites of membrane damage and virus exit (Stoltz *et al.*, 1996). Based on the use of AHSV reassortant viruses, NS3 was more recently implicated as a determinant in controlling the percentage of virus released from cells (Meiring *et al.*, 2009). It can be envisaged that a clearer understanding of the biological role of NS3 may be obtained by observing phenotypic consequences resulting from its inactivation. In this regard, RNA interference (RNAi) can provide an investigative tool that may greatly facilitate studies aimed at generating such loss-of-function phenotypes (López *et al.*, 2005; Kobayashi *et al.*, 2006; Wirblich *et al.*, 2006; Stassen *et al.*, 2007).

RNA interference (RNAi) is a conserved gene silencing mechanism that recognizes double stranded (ds)RNA as a signal to trigger the sequence-specific degradation of homologous mRNA (Fire *et al.*, 1998). As a result of biochemical and genetic studies in several experimental systems, the mechanisms underlying RNAi have begun to unfold. These suggest the existence of conserved machinery for dsRNA-induced gene silencing, which proceeds via a multistep mechanism. Initially, long dsRNA molecules are recognized and cleaved into 21-nt small interfering RNA duplexes (siRNAs) by the action of an endogenous dsRNA-specific endonuclease, Dicer, a member of the RNase III family. Subsequently, the siRNAs are incorporated into the RNA-induced silencing complex (RISC), which identifies substrates through their homology to siRNAs and target these cognate mRNAs for destruction (Meister and Tuschl, 2004; Hutvagner and Simard, 2008; Jinek and Doudna, 2009).

RNAi is commonly achieved by introducing chemically synthesized siRNA into cells or, alternatively, by short hairpin RNA (shRNA) that is expressed intracellularly from plasmid

and viral vectors (Wadhwa *et al.*, 2004; Cheng and Chang, 2007; Manjunath *et al.*, 2009; Moore *et al.*, 2010). Despite the availability of a number of guidelines and recommendations (Mittal, 2004; Shao *et al.*, 2007), as well as design algorithms and programmes (Ui-Tei *et al.*, 2004; Reynolds *et al.*, 2004; Naito *et al.*, 2009), it is still not possible to predict with complete certainty the degree of gene silencing a particular siRNA will produce. Consequently, it is generally recommended that the silencing capability of several (at least three) candidate siRNAs be evaluated (Mittal, 2004). Moreover, since assays with infectious viruses are time-consuming and labour-intensive, a simple method for the evaluation of active siRNAs is required. A number of assay methods have been used to evaluate gene silencing in mammalian cells. These include methods aimed at detecting endogenous mRNA levels of silenced genes such as Northern blot analysis or quantitative reverse transcriptase-PCR (qRT-PCR) (Sandy *et al.*, 2005). However, these methods are expensive to perform and not suited to rapid screening of several different candidate siRNAs. Consequently, detection of down-regulation of the endogenous protein levels has become the preferred method for this purpose (Sandy *et al.*, 2005). In addition to performing Western blot analysis with protein-specific antibodies, other approaches have relied on cloning of the target gene's coding sequence in-frame with fluorescent (*e.g.* green fluorescent protein [eGFP]) and enzymatic (*e.g.* luciferase) reporters (Yokota *et al.*, 2003; Liu *et al.*, 2006; Stassen *et al.*, 2007). Upon transcription, these constructs provide a chimeric mRNA and efficient targeting of the gene of interest leads to degradation of the mRNA, and therefore no reporter product is produced. Because fluorescence is easy to visualize under a fluorescent microscope and can be quantified by fluorometry or flow cytometry, the eGFP gene has become a popular reporter whereby RNAi can be studied (Sandy *et al.*, 2005).

The characterization of AHSV NS3 function has been confined to the study of NS3 expressed in bacterial and eukaryotic expression systems (Van Staden *et al.*, 1995; Stoltz *et al.*, 1996; Van Niekerk *et al.*, 2001a), and more recently by studying reassortant viruses between different AHSV serotypes (Meiring *et al.*, 2009). These investigations have suggested a role for NS3 in virus release, membrane permeability and pathogenesis. The segmented nature of the AHSV genome, however, makes it amenable to analysis by RNAi. RNAi technology may be well suited to silence expression of individual AHSV genes without affecting the expression of others, thus allowing for characterization of the function of proteins in the context of the whole virus (Stassen *et al.*, 2007). Consequently, the primary aims of this part of the study were to develop an RNAi assay whereby expression of the NS3 gene of AHSV-3

could be silenced by siRNAs in Vero mammalian cells, and to determine the effect of NS3 gene silencing on virus release from these mammalian cells.

2.2 MATERIALS AND METHODS

2.2.1 Bacterial strains and plasmids

The *Escherichia coli* DH5 α strains were routinely cultured in LB broth (1% [w/v] tryptone; 1% [w/v] NaCl; 0.5% [w/v] yeast extract; pH 7.4) (Sambrook *et al.*, 1989) at 37°C with shaking at 200 rpm, and maintained at 4°C on LB agar (LB broth containing 1.2% [w/v] bacteriological agar) or at -70°C as glycerol cultures. For plasmid DNA selection and maintenance in *E. coli*, the medium was amended with 50 μ g/ml of kanamycin (Roche Diagnostics). The recombinant mammalian expression vector pCMV-eGFP, which contains a full-length copy of the enhanced green fluorescent protein (eGFP) gene, was obtained from Mrs. L. Stassen (Department of Microbiology and Plant Pathology, University of Pretoria). The recombinant mammalian expression vector pCMV-NS3-eGFP, harbouring a cDNA copy of the AHSV-3 NS3 gene fused in-frame to the eGFP reporter gene, was obtained from Dr. V. Van Staden (Department of Genetics, University of Pretoria).

2.2.2 Large-scale preparation of recombinant mammalian expression plasmids

2.2.2.1 Preparation of competent cells

Competent *E. coli* DH5 α cells were prepared and transformed according to the method of Sambrook *et al.* (1989). A single colony of a freshly streaked *E. coli* DH5 α culture was inoculated into 20 ml of LB broth and incubated overnight at 37°C with shaking. An aliquot (1 ml) of the overnight culture was then used to inoculate 100 ml of pre-warmed (37°C) LB broth in a 250-ml Erlenmeyer flask. The culture was incubated at 37°C with shaking until an OD₆₀₀ of 0.94 was reached. Cells from 30 ml of the culture were harvested by centrifugation at 5000 rpm for 10 min at 4°C. The supernatant was discarded and the pellet suspended in 10 ml of an ice-cold solution comprising 80 mM CaCl₂ and 50 mM MgCl₂. Following incubation on ice for 10 min, the cells were centrifuged at 5000 rpm for 10 min at 4°C, and then suspended in 5 ml of ice-cold 100 mM CaCl₂. Glycerol (1.5 ml) was added and aliquots of 200 μ l were pipetted into 1.5-ml Eppendorf tubes, snap-frozen in liquid nitrogen and stored at -70°C until needed.

2.2.2.2 Transformation of competent cells

Competent cells (200 μ l) were allowed to thaw on ice and mixed with 0.5 μ l (200 ng) of recombinant plasmid DNA. Following incubation on ice for 30 min, the tubes were heat-shocked at 42°C for 90 s. The tubes were then immediately chilled on ice for 2 min, after which 800 μ l of pre-warmed LB broth was added and the tubes were incubated at 37°C for 1 h with shaking. The transformation mixtures were plated in volumes of 100 μ l onto LB agar supplemented with 50 μ g/ml kanamycin. The agar plates were incubated overnight at 37°C. A positive control (5 ng of pGEM 3Zf⁺ plasmid DNA) and negative control (competent cells only) were also included to determine the competency of the *E. coli* DH5 α cells and to test for contamination, respectively.

2.2.2.3 Plasmid DNA extraction

Plasmid DNA was isolated using the alkaline lysis-method (Birnboim and Doly, 1979). A single bacterial colony was inoculated into a 500-ml Erlenmeyer flask containing 250 ml of LB broth supplemented with 50 μ g/ml kanamycin. The culture was incubated overnight at 37°C with shaking. Cells from 50 ml of the culture were harvested by centrifugation at 5000 rpm for 15 min in an Eppendorf 5804R centrifuge. The cell pellet was suspended in 4 ml of ice-cold Solution 1 (50 mM glucose; 25 mM Tris; 10 mM EDTA; pH 8.0) and incubated on ice for 30 min. Following incubation, 8 ml of freshly prepared Solution 2 (0.2 M NaOH; 1% [w/v] SDS) was added and the tubes incubated on ice for 5 min. Following addition of 6 ml of ice-cold Solution 3 (3 M NaOAc; pH 4.8), the tubes were incubated on ice for 1 h. The cell lysates were centrifuged at 10 000 rpm for 15 min, and the plasmid DNA-containing supernatant was recovered and filtered through Whatman[®] filter paper. The plasmid DNA was precipitated by addition of 2.5 volumes of 96% EtOH and incubation overnight at -20°C. The precipitated plasmid DNA was collected by centrifugation at 10 000 rpm for 15 min, suspended in 6 ml of UHQ water and 2.5 ml of ice-cold 7.5 M NH₄OAc was added. After incubation on ice for at least 30 min, the high-molecular-weight RNA precipitate was removed by centrifugation at 10 000 rpm for 10 min. The plasmid DNA was subsequently recovered from the supernatant by ethanol precipitation, as described above. The DNA pellet was rinsed with 70% EtOH, vacuum-dried and suspended in 80 μ l of 1 \times TE buffer (10 mM Tris-HCl; 1 mM EDTA; pH 8.0). Alternatively, to obtain highly pure plasmid DNA that could be used for cell transfections, the recombinant plasmid DNA was extracted with the QIAfilter Plasmid Midi kit (Qiagen) according to the manufacturer's instructions. The

plasmid DNA was analyzed by gel electrophoresis on a 1% (w/v) agarose gel, and its concentration was determined with a Nanodrop[®] ND-1000 spectrophotometer (Thermo Fischer Scientific Inc.).

2.2.3 Characterization of recombinant mammalian expression plasmids

2.2.3.1 Agarose gel electrophoresis

DNA was analyzed by agarose gel electrophoresis (Sambrook *et al.*, 1989). A horizontal 1% (w/v) agarose gel was cast and electrophoresed at 100 V in 1 × TAE buffer (40 mM Tris-HCl; 20 mM NaOAc; 1 mM EDTA; pH 8.5). To allow visualization of the DNA when viewed on a UV transilluminator, the gel was supplemented with 0.5 µg/ml ethidium bromide. The size of DNA fragments was determined according to their migration pattern in an agarose gel compared to that of a DNA molecular weight marker (GeneRuler[™] 1 kb and GeneRuler[™] 100 bp DNA Ladders; Fermentas).

2.2.3.2 Restriction endonuclease digestions

Restriction endonuclease digestion of plasmid DNA was performed in Eppendorf tubes and contained the appropriate concentration of salt (using the 10× buffer supplied by the manufacturer) for the specific enzyme and 5 U of enzyme per µg of plasmid DNA. The reaction volumes were typically 15 µl and incubation was at 37°C for 1 h. The restriction enzymes were supplied by Roche Diagnostics. The digestion products were analyzed on a 1% (w/v) agarose gel in the presence of an appropriate DNA molecular weight marker.

2.2.3.3 Nucleotide sequencing and sequence analysis

The nucleotide sequence of cloned insert DNA was determined by automated sequencing with the ABI PRISM[®] BigDye[™] Terminator v.3.1 Cycle Sequencing Ready Reaction kit (Applied Biosystems) according to the manufacturer's instructions. The reaction mixtures (10 µl) contained 250 ng of purified plasmid DNA, 2 µl of BigDye[™] Termination Mix, 1 × sequencing buffer and 3.2 pmol of either the T3 (5'-AATTAACCCTCACTAAAGGG-3') or T7 (5'-GTAATACGACTCACTATAGGGC-3') sequencing primer. Cycle sequencing reactions were performed in a Perkin-Elmer GeneAmp[®] 2700 thermal cycler with 25 of the following cycles: denaturation at 96°C for 10 s, primer annealing at 50°C for 15 s, and elongation at 60°C for 4 min. The extension products were precipitated by addition of 1 µl of 3 M NaOAc (pH 4.6) and 25 µl of absolute EtOH. The tubes were incubated for 15 min at

room temperature in the dark, centrifuged at 15 000 rpm for 30 min and the supernatant carefully aspirated. The extension products were resolved on an ABI PRISM[®] Model 3130 automated sequencer (Applied Biosystems).

The nucleotide sequences obtained were analyzed with the BioEdit v.7.0.4.1 (Hall, 1999) software package. The nucleotide and deduced amino acid sequences were compared against the entries in the GenBank database with respectively the BLAST-N and BLAST-P programmes (Altschul *et al.*, 1997), available on the National Centre for Biotechnology Information web page (<http://www.ncbi.nlm.nih.gov/BLAST>). Pair-wise alignments were performed with ClustalW included in the BioEdit software package.

2.2.4 Transient expression of eGFP and NS3-eGFP in Vero cells

2.2.4.1 Cell culture and virus

Vero cells (ATCC CCL-81) were propagated and maintained as monolayers in 75-cm² tissue culture flasks, and cultured in Minimal Essential Medium (MEM) supplemented with 5% fetal bovine serum (FBS) and antibiotics (1 × penicillin, streptomycin, fungizone) (Highveld Biological). The flasks were incubated at 37°C in a humidified incubator with a constant supply of 5% CO₂. African horsesickness virus serotype 3 (AHSV-3), used in viral challenge assays, was kindly provided by Mr. F. Wege (Department of Genetics, University of Pretoria). AHSV-3 was propagated in confluent BHK-21 (ATCC CCL-10) monolayers.

2.2.4.2 Transfection of Vero cell monolayers

The day before transfection, Vero cells were trypsinized, diluted with fresh medium and seeded in 6-well tissue culture dishes (Nunc) to reach 75% confluency within 24 h of incubation at 37°C in the presence of 5% CO₂. The cells were subsequently transfected with pCMV-eGFP or pCMV-NS3-eGFP. For each transfection, 4 µg of purified plasmid DNA and 10 µl of Lipofectamine[™] 2000 reagent were each diluted in 250 µl of MEM medium lacking serum and antibiotics. Following incubation at room temperature for 5 min, the two solutions were mixed and incubated at room temperature for 20 min to allow DNA-lipofectamine complexes to form. Prior to transfection, the medium was aspirated from the cell monolayers and the cells were rinsed three times with 2 ml of serum- and antibiotic-free MEM medium. The cells were subsequently overlaid with the DNA-lipofectamine complexes. Following addition of 1.5 ml of MEM medium supplemented with 5% (v/v) FBS, the tissue culture

dishes were incubated for 24 h at 37°C in a CO₂ incubator. As a control, mock-transfected cells were also included.

2.2.4.3 Epifluorescence microscopy

The transfected Vero cell monolayers were observed at 24 h post-transfection for the expression of eGFP and NS3-eGFP on a Zeiss Axiovert 200 fluorescent microscope fitted with the no. 10 Zeiss filter set (excitation at 450-490 nm; emission at 515-565 nm). The images of different microscope fields were captured with a Nikon DXM1200 digital camera.

2.2.5 RNA interference assays in Vero cells

2.2.5.1 Small interfering RNAs (siRNAs)

siRNAs targeting three different regions on the AHSV-3 NS3 mRNA were designed with Silencer[™] design software (Ambion). The siRNA sequences were subjected to a BLAST-N search against entries in the GenBank database to ensure lack of sequence homology to sequences other than the intended target gene. The accessibility of the target sites was also evaluated by RNA secondary structure analysis of the NS3 and NS3-eGFP mRNA, using MFOLD v.3.1 software (Zuker, 2003) (Fig. 2.1). A negative control siRNA, designated universal negative siRNA (UN-siRNA), was obtained from Qiagen and reportedly lacks homology to any known viral and cellular genes. The siRNAs were supplied as lyophilized, desalted duplexes and were suspended in RNase-free buffer (100 mM KOAc; 30 mM HEPES-KOH; 2 mM MgOAc; pH 7.4) at a concentration of 20 µM prior to storage at -20°C. The siRNAs used in this study are shown in Table 2.1.

Table 2.1: AHSV-3 NS3-directed and control siRNAs used in this study

siRNA	siRNA sequences (5'-3')	G+C contents	Coding region targeted (nt)
siNS3-65	Sense: AAUCAGAGAGCAAUUGUACtt Antisense: GUACAAUUGCUCUCUGAUUtc	33% 38%	65-85
siNS3-74	Sense: GCAAUUGUACCGUAUGUUCtt Antisense: GAACAUACGGUACAAUUGCtc	38% 43%	74-92
siNS3-266	Sense: GAACCGAUACGUCAAAUAAtt Antisense: UUAUUUGACGUAUCGGUUCtg	33% 38%	266-284
UN-siRNA	Sense: UUCUCCGAACGUGUCACGUtt Antisense: ACGUGACACGUUCGGAGAAtt	47% 47%	No homology

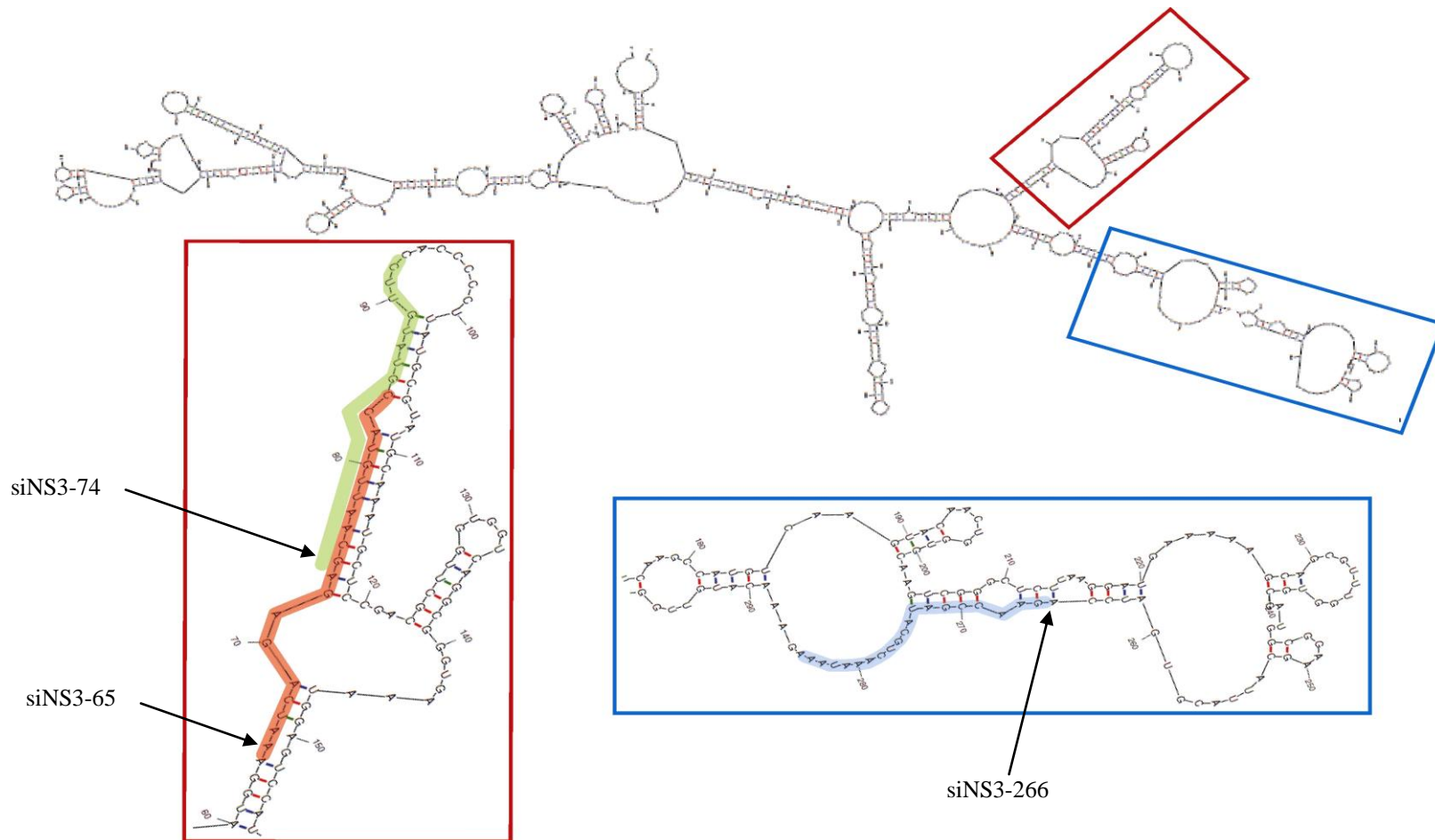


Fig. 2.1a: Local secondary structure of AHSV-3 NS3 mRNA, as predicted by the MFOLD software programme (Zuker, 2003). The regions targeted by the NS3-directed siRNAs are enlarged, and are indicated in orange (siNS3-65), green (siNS3-74) and blue (siNS3-266).

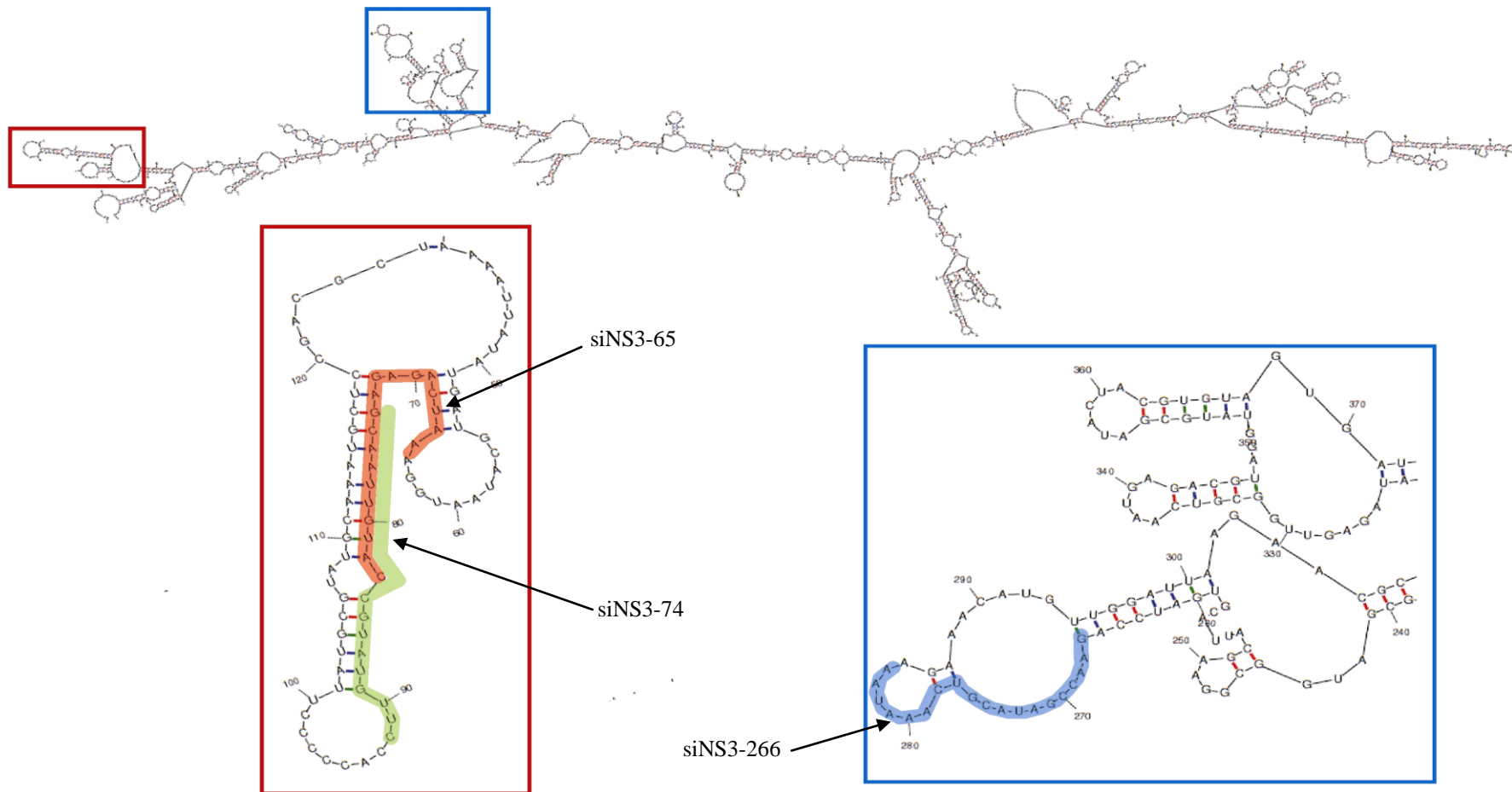


Fig. 2.1b: Local secondary structure of AHSV-3 NS3-eGFP mRNA, as predicted by the MFOLD software programme (Zuker, 2003). The regions targeted by the NS3-directed siRNAs are enlarged, and are indicated in orange (siNS3-65), green (siNS3-74) and blue (siNS3-266).

2.2.5.2 Co-transfection of Vero cells with siRNA and recombinant pCMV-Script® expression vectors

Vero cells were seeded in 6-well tissue culture dishes to reach 75% confluency within 24 h of incubation at 37°C in the presence of 5% CO₂. Subsequently, pCMV-eGFP or pCMV-NS3-eGFP plasmid DNA was each co-transfected with the respective siRNAs into Vero cells using Lipofectamine™ 2000 reagent (Invitrogen). Briefly, 4 µg of purified plasmid DNA and 10 µl of Lipofectamine™ 2000 reagent were separately diluted in 250 µl of MEM medium without serum and antibiotics, incubated at room temperature for 5 min and then mixed to allow the formation of DNA-lipofectamine complexes. Likewise, 25 µM of the siRNA and 10 µl of Lipofectamine™ 2000 reagent were each diluted in 250 µl of MEM medium without serum and antibiotics and, following incubation at room temperature for 5 min, were mixed to allow the formation of RNA-lipofectamine complexes. After incubation at room temperature for 20 min, the two solutions were mixed and then used to overlay the Vero cell monolayers. The cell monolayers were prepared for transfection as described above. The tissue culture dishes were incubated for 24 h at 37°C in a CO₂ incubator, and then examined by epifluorescence microscopy. As a control, mock-transfected cells were also included.

2.2.5.3 Transfection and virus challenge assays in Vero cells

The day before transfection, cells were seeded in 6-well tissue culture dishes to reach 75% confluency within 24 h of incubation at 37°C in the presence of 5% CO₂. The Vero cells were then transfected with the respective siRNAs using Lipofectamine™ 2000 according to the procedures described by Wirblich *et al.* (2006), with the following modifications. Briefly, 10 µl of Lipofectamine™ 2000 reagent was diluted in 250 µl of MEM medium (without serum and antibiotics) and, following incubation at room temperature for 5 min, was added to 250 µl of antibiotic- and serum-free MEM medium containing 25 µM of the appropriate siRNA. The mixture was then incubated at room temperature for 20 min to allow the formation of RNA-lipofectamine complexes. The cell monolayers were rinsed three times with 2 ml of MEM medium (without serum and antibiotics) and then overlaid with the RNA-lipofectamine complexes. Following addition of 1.5 ml of antibiotic-free MEM medium containing 5% (v/v) FBS, the tissue culture dishes were incubated for 12 h at 37°C in a CO₂ incubator. Following incubation, the cell monolayers were washed twice with MEM medium (lacking serum and antibiotics) and then transfected for a second time with the respective siRNAs, as described above, and incubated for a further 12 h. The transfected cells were then infected

with AHSV-3 at a multiplicity of infection (MOI) of 1 pfu/cell. After 1 h of infection, the virus inoculum was removed and 2 ml of MEM medium containing 5% (v/v) FBS was added to the cells. At 24 h post-infection, the cell monolayers were either processed for RNA isolation or used in viral plaque assays as described below.

2.2.6 Semi-quantitative real-time polymerase chain reaction (RT-PCR)

2.2.6.1 Primers

Primers used for relative quantification of specific mRNA transcripts by real-time PCR were designed based on the nucleotide sequence for the AHSV-3 NS3 gene (as determined in this study) and a cellular gene encoding glyceraldehyde-3-phosphate dehydrogenase (GAPDH; GenBank Acc. no. U10983). The primers were designed with DNAMAN v.4.13 (Lynnon Biosoft), and optimal primer pairs were analyzed and identified with PerlPrimer v.1.1.6 (Marshall, 2004). Each of the primers was subjected to a BLAST-N analysis to verify target sequence specificity. The primers, indicated in Table 2.2, were obtained from Inqaba Biotechnical Industries.

Table 2.2: Primers used in semi-quantitative real-time PCR

Primer	Nucleotide sequence	T _m (°C)	Annealing position
NS3-sense	5'-TCAATGAGACGTAGGTATGCG-3'	56	335
NS3-antisense	5'-TCTTCGACAGCCAACCATC-3'		
GAPDH-F	5'-GCATGGCCTTCCGTGTTCTAC-3'	57	653
GAPDH-R	5'-CCTGCTTCACCACCTTCTTGATGTC-3'		

2.2.6.2 Total RNA extraction

Total RNA was extracted from Vero cells with the Aurum™ Total RNA extraction kit (BioRad) according to the manufacturer's instructions. Briefly, the culture medium was removed and the cells were rinsed once with 1 × PBS (137 mM NaCl; 2.7 mM KCl; 4.3 mM Na₂HPO₄; 1.4 mM KH₂PO₄; pH 7.4). The cell monolayers were suspended in 350 µl of the supplied lysis solution and lysed by vigorous pipetting before being transferred to an Eppendorf tube. After addition of an equal volume of 70% EtOH, the cell lysate was centrifuged through an RNA-binding column at 15 000 rpm for 30 s. The column was rinsed

with wash solution, treated for 15 min at room temperature with RNase-free DNase I to remove contaminating chromosomal DNA, and the RNA was then eluted from the column using the supplied elution buffer.

2.2.6.3 cDNA synthesis

The isolated RNA was reverse transcribed with the QuantiTect[®] Reverse Transcription kit (Qiagen) according to the manufacturer's instructions. Prior to reverse transcription, the RNA preparations (5 µl) were each incubated at 42°C for 2 min with 2 µl of 1 × Genomic DNA Wipeout buffer (supplied in the kit) to eliminate any traces of contaminating genomic DNA. For reverse transcription of the RNA, 4 µl of 5 × Quantiscript[®] RT buffer, 1 µl of Quantiscript[®] Reverse Transcriptase and 1 µl of a RT primer mix (containing a mixture of oligo-dT and random primers) were added to the RNA preparation in a final volume of 20 µl. The reaction mixtures were then incubated at 42°C for 30 min, after which the enzyme was inactivated by heating to 95°C for 3 min. The cDNA was stored at -20°C until required.

2.2.6.4 Control PCR reactions

To confirm the absence of contaminating DNA in the RNA preparations and to determine the amplification specificity of the designed primers (Table 2.2), conventional PCR reactions were performed. The RNA and cDNA samples were diluted in nuclease-free water as serial 10-fold dilutions and used as template in the PCR reactions. The PCR reaction mixtures contained 2 µl of the appropriate dilution of RNA or cDNA, 10 pmol of each the gene-specific sense and antisense primer, 200 µM of each dNTP, 0.6 U of *Taq* DNA polymerase (Southern Cross Biotechnology), 2.5 µl of the supplied reaction buffer, 1.5 mM MgCl₂ and UHQ water to a final volume of 25 µl. Reactions mixtures lacking template were also included as controls. Thermal cycling was performed in a Eppendorf Mastercycler[®] thermal cycler with the following cycling parameters: initial denaturation at 94°C for 2 min, followed by 30 cycles of denaturation at 94°C for 30 s, primer annealing at 56°C for 30 s and extension at 72°C for 30 s. The reaction mixtures were analyzed by agarose gel electrophoresis on a 2% (w/v) agarose gel in the presence of an appropriate DNA molecular weight marker.

2.2.6.5 Semi-quantitative real-time PCR

Semi-quantitative real-time PCR was performed using the QuantiTect[™] SYBR[®] Green PCR kit (Qiagen) and the LightCycler[®]480 system (Roche Diagnostics). Each reaction mixture (10

μl) contained 1 μl of the 10⁻¹ dilution of cDNA, 10 pmol of each of the gene-specific sense and antisense primer and 5 μl of 2 × QuantiTect™ SYBR® Green PCR master mix (containing HotStarTaq® DNA polymerase, dNTP mixture inclusive of dUTP, SYBR® Green I, ROX passive reference dye and 5 mM MgCl₂). The reaction mixtures were incubated at 95°C for 15 min to activate the HotStarTaq® DNA polymerase enzyme and then subjected to 45 cycles of denaturation at 94°C for 15 s, primer annealing at 60°C for 20 s and primer extension at 72°C for 30 s. Non-template negative controls with the respective primer sets were also included. To confirm specific amplification, the amplicons were analyzed by agarose gel electrophoresis in the presence of a DNA molecular weight marker, and melt-curve analysis of the amplicons was performed with the LightCycler® software (Roche Diagnostics) according to the manufacturer's protocol.

2.2.6.6 Data analysis

Data were analyzed with the Relative Expression Software Tool (REST®) (Pfaffl *et al.*, 2002), where the relative expression of target (NS3) normalized to an endogenous reference (GAPDH) in a sample (NS3 siRNA-treated, AHSV-3 infected cells) relative to an experimental control (UN-siRNA-treated, AHSV-3 infected cells), is given by $R = (E_{\text{target}})^{\Delta CP_{\text{target}} (\text{control} - \text{sample})} / (E_{\text{ref}})^{\Delta CP_{\text{ref}} (\text{control} - \text{sample})}$. In this formula, R represents the expression ratio of the target gene, E is the PCR efficiency, ΔCP is the crossing point difference of an unknown sample versus a control sample, and ref represents a reference gene. For Crossing Point (CP) determination, the Second Derivate Maximum Method was used, which is included in the LightCycler® software.

2.2.7 Viral plaque assay

Extracellular virus titers were determined by collecting the supernatant of siRNA-treated, virus infected cells. For determination of intracellular (cell-associated) virus titres, cells were removed from the wells by addition of 1 ml of 2 mM Tris (pH 8) and transferred to Eppendorf tubes. The tubes were vortexed and the cells lysed by passage through a 22G needle. To determine the viral titers, plaque assays were performed on CER cells, a BHK derivative, according to the method described by Oellerman (1970). The cells were infected with serial 10-fold dilutions of virus in 2 mM Tris buffer and following adsorption of the virus to the cells for 30 min at room temperature, the cells were overlaid with 4 ml of a sterile solution containing 2.4% agarose and Earle's saline, which was diluted in Earle's medium without

serum to 0.4%. The tissue culture dishes were incubated at 37°C for 72 h in a CO₂ incubator. Following incubation, the monolayers were flooded with Neutral Red (0.05% [w/v] in 0.5 M phosphate buffer; pH 6.5) and the plaques were counted after incubation at 37°C for 1-2 h. Total virus yield was calculated as the sum of released and cell-associated virus, and virus release was expressed as the percentage released virus versus total virus (Meiring *et al.*, 2009).

2.2.8 Protein analyses

2.2.8.1 Preparation of cell lysates

Virus-infected Vero cell monolayers were rinsed once with 1 × PBS and trypsinized by the addition of Trypsin Versene. Following incubation at 37°C for 5 min, the cells were transferred to an Eppendorf tube, collected by centrifugation at 3000 rpm for 10 min and rinsed once with 1 × PBS. The cells were suspended in 20 µl of 1 × PBS and an equal volume of 2 × PSB buffer (0.125 M Tris-HCl [pH 6.8]; 4% [w/v] SDS; 20% [v/v] glycerol; 10% [v/v] 2-mercaptoethanol; 0.002% [w/v] bromophenol blue) was added to each sample. The samples were heated for 5 min in boiling water prior to SDS-PAGE analysis.

2.2.8.2 SDS-polyacrylamide gel electrophoresis (SDS-PAGE)

Proteins were resolved by electrophoresis in a discontinuous gel system, as described by Laemmli (1970). The 5% stacking gel (5% [w/v] acrylamide; 0.17% [w/v] bis-acrylamide; 125 mM Tris-HCl [pH 6.8]; 0.1% [w/v] SDS) and the 12% separating gel (12% [w/v] acrylamide; 0.34% [w/v] bis-acrylamide; 0.375 mM Tris-HCl [pH 8.8]; 0.1% [w/v] SDS) were each polymerized by addition of 0.08% (w/v) ammonium persulphate and 10 µl of TEMED. Electrophoresis was performed in a Hoefer Mighty Small™ electrophoresis unit at 100 V for 3 h in 1 × TGS buffer (25 mM Tris; 192 mM glycine; 0.1% [w/v] SDS; pH 8.3). Following electrophoresis, the gels were stained for 30 min with 0.125% (w/v) Coomassie brilliant blue (prepared in 50% [v/v] methanol; 10% [w/v] acetic acid), and then destained in a solution containing 25% (v/v) methanol and 10% (v/v) glacial acetic acid until the proteins were visible. The sizes of the resolved proteins were estimated by comparison to reference molecular mass proteins (Pre-stained Protein Molecular Weight Marker; Fermentas).

2.2.8.3 Western blot analysis

Western blot analysis was performed by transferring the separated proteins on an unstained SDS-polyacrylamide gel to a Hybond™-C⁺ membrane (Amersham Pharmacia Biotech AB). The nitrocellulose membrane, cut to the same size as the gel, was equilibrated in transfer buffer (25 mM Tris; 186 mM glycine) for 20 min prior to gel transfer. The proteins were electroblotted onto the membrane for 90 min at 28 V with a Mighty Small™ Transphor blotting apparatus (Hoefer). After transfer, the membrane was washed once in 1 × PBS for 5 min, and non-specific binding sites were blocked by incubation for 30 min in blocking solution (1% [w/v] fat-free milk powder in 1 × PBS). The membrane was then incubated overnight at room temperature with slight agitation in an anti-AHSV-3 antiserum (diluted 1:100 in blocking solution). Following incubation, the unbound antibodies were removed by washing the membrane three times for 5 min each in wash buffer (0.05% [v/v] Tween-20 in 1 × PBS). The secondary antibody, Protein A conjugated to horseradish peroxidase and diluted 1:100 in blocking solution, was added to the membrane and incubated for 2 h at room temperature. The membrane was washed three times for 5 min each in wash buffer, and once for 5 min in 1 × PBS. To detect immunoreactive proteins, the membrane was immersed in freshly prepared enzyme substrate solution (60 mg 4-chloro-1-naphtol in 20 ml methanol and 60 µl hydrogen peroxide in 100 ml 1 × PBS, mixed just prior to use). Once the bands became visible, the membrane was rinsed with dH₂O and air-dried.

2.3 RESULTS

2.3.1 Characterization of recombinant plasmids pCMV-eGFP and pCMV-NS3-eGFP

Prior to determining the importance of AHSV-3 NS3 in virus release by making use of an RNAi-based approach, it was first necessary to develop and optimize a protocol for siRNA-mediated NS3 gene silencing. To facilitate rapid evaluation of different NS3-directed siRNAs to silence NS3 gene expression in mammalian (Vero) cells, a reporter plasmid, designated pCMV-NS3-eGFP, was used. This reporter plasmid comprises of a NS3-eGFP chimeric gene cloned into the pCMV-Script® mammalian expression vector. The chimeric gene was constructed by making use of a strategy whereby the eGFP reporter gene was fused in-frame to the C-terminus of the NS3 gene, thus ensuring that transcription of the NS3 gene would need to occur in order to obtain a fluorescently tagged NS3 protein (Fig. 2.2a). Prior to using the pCMV-NS3-eGFP reporter plasmid and pCMV-eGFP control plasmid in RNAi

assays, large-scale plasmid extractions were performed and the recombinant plasmids were characterized by restriction endonuclease digestions using agarose gel electrophoresis, as well as by nucleotide sequencing of the cloned insert DNA.

Digestion of purified pCMV-eGFP plasmid DNA with both *EcoRI* and *HindIII* excised a 720-bp DNA fragment, which is in agreement with the size of the eGFP gene (Fig. 2.2b, lane 7). Digestion of the purified pCMV-NS3-eGFP plasmid DNA with both *BamHI* and *HindIII* yielded two DNA fragments of 4.3 kb and 1.5 kb, which is in agreement with the expected size of the pCMV-Script[®] vector DNA and the NS3-eGFP chimeric gene, respectively (Fig. 2.2b, lane 3). Subsequent digestion of the recombinant plasmid DNA with *EcoRI* and either *HindIII* or *BamHI* excised DNA fragments corresponding in size with the eGFP gene (720 bp) and the NS3 gene (758 bp), thus confirming that the vector harbours a chimeric NS3-eGFP gene (Fig. 2.2b, lanes 4 and 5, respectively).

As a final confirmation regarding the integrity of the cloned insert DNA, the nucleotide sequence of the eGFP and NS3-eGFP genes was determined. No nucleotide differences were observed between the sequences of these genes and those reported previously for eGFP (Stassen, 2006) and AHSV-3 NS3 (van Staden and Huismans, 1991). The deduced amino acid sequence of the NS3-eGFP protein also confirmed that the reading frame of the chimeric protein was maintained (results not shown).

2.3.2 Transient expression of eGFP and NS3-eGFP in Vero cells

Although the pCMV-Script[®] vector has been designed to allow protein expression in a wide variety of mammalian cell lines (Stratagene), members of our research group have used the vector to express cloned insert DNAs in BHK-21 cells only. Thus, to determine whether the NS3-eGFP chimeric gene can indeed be expressed in Vero cells, cell monolayers were mock-transfected and transfected with the recombinant mammalian expression plasmids pCMV-eGFP and pCMV-NS3-eGFP. Prior to transfection, the recombinant plasmids were purified with a commercial kit, since impurities in the plasmid DNA preparation may influence transfection efficiencies.

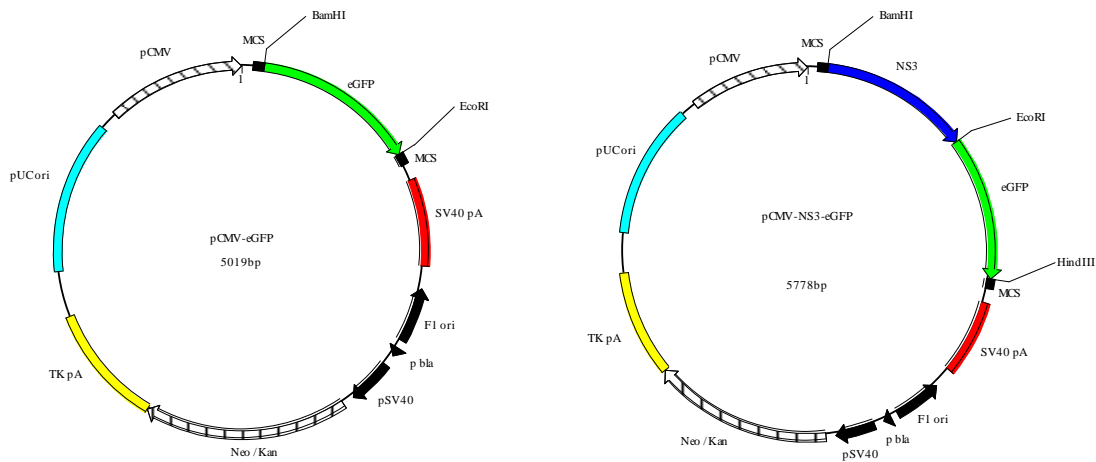


Fig. 2.2a: Plasmid maps of the recombinant mammalian expression plasmids pCMV-eGFP, harbouring the eGFP reporter gene, and pCMV-NS3-eGFP, harbouring a chimeric NS3-eGFP gene. The eGFP gene is indicated in green and the AHSV-3 NS3 gene in blue.

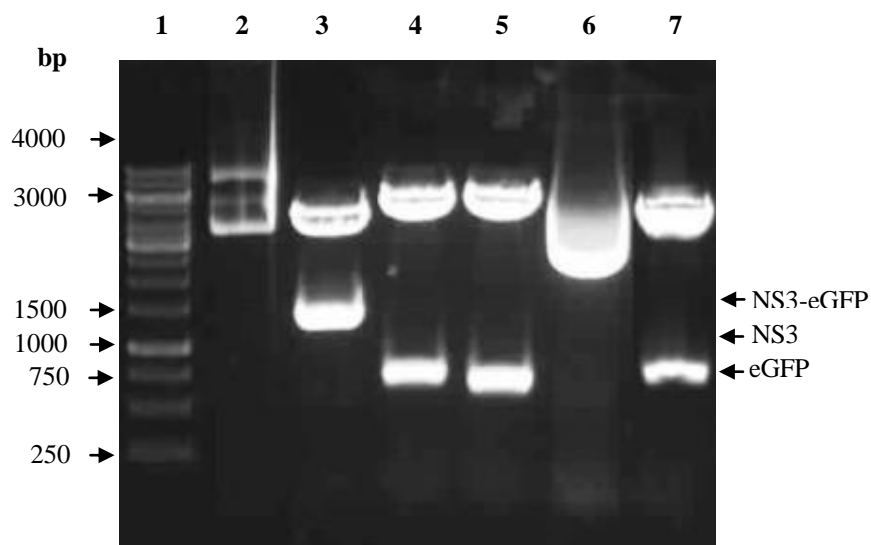


Fig. 2.2b: Agarose gel electrophoretic analysis of the recombinant plasmids pCMV-NS3-eGFP and pCMV-eGFP, following restriction endonuclease digestions. Lane 1: DNA molecular weight marker; Lane 2: uncut pCMV-NS3-eGFP plasmid DNA; Lane 3: pCMV-NS3-eGFP digested with both *Bam*HI and *Hind*III; Lane 4: pCMV-NS3-eGFP digested with both *Eco*RI and *Hind*III; Lane 5: pCMV-NS3-eGFP digested with both *Eco*RI and *Bam*HI; Lane 6: uncut pCMV-eGFP plasmid DNA; Lane 7: pCMV-eGFP digested with both *Eco*RI and *Hind*III. The sizes of the DNA molecular weight marker, GeneRuler™ 1 kb DNA Ladder (Fermentas), are indicated to the left of the figure in base pairs.

Examination of the cell monolayers by fluorescent microscopy at 24 h post-transfection (Fig. 2.3) indicated that whereas Vero cells transfected with pCMV-eGFP and pCMV-NS3-eGFP fluoresced brightly, no fluorescence was observed in mock-transfected cells. To confirm expression of the NS3-eGFP protein, cell lysates were prepared and analyzed by SDS-PAGE. No uniquely expressed protein could be observed in the Coomassie-stained SDS-polyacrylamide gel when compared to mock-transfected cells (not shown). This is most likely due to the low levels of transient gene expression, which is often the case when using mammalian expression systems (Yin *et al.*, 2007). Nevertheless, it should be noted that the NS3-eGFP protein has previously been expressed in *Spodoptera frugiperda* insect cells with a baculovirus recombinant and it was shown that the synthesized chimeric protein reacted with an anti-NS3 antibody (Miss T.L. Hatherell, Department of Genetics). Therefore, the fluorescence observed in Vero cells transfected with pCMV-NS3-eGFP provides strong evidence for the successful expression of the NS3-eGFP protein in Vero cells.

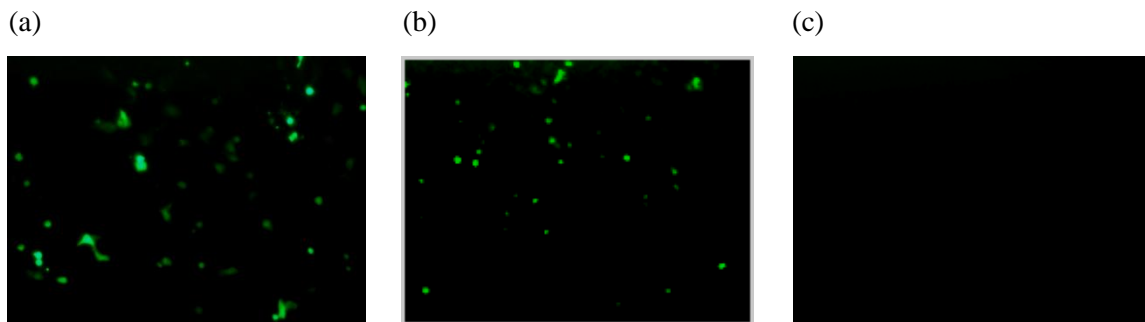


Fig. 2.3: Fluorescent microscopy of eGFP and NS3-eGFP gene expression in Vero cells. Vero cells transfected with pCMV-eGFP (a) and pCMV-NS3-eGFP (b) were analyzed for protein expression 24 h post-transfection with a Zeiss Axiovert fluorescent microscope. Mock-transfected cells (c) were included as a control. Magnification, 10 \times .

2.3.3 Silencing of NS3-eGFP protein expression by siRNAs in Vero cells

Towards developing an RNAi strategy whereby AHSV-3 NS3 expression could be silenced in Vero cells, siRNAs directed to three different sites on the AHSV-3 NS3 mRNA were designed and chemically synthesized. The siRNAs were designated siNS3-65, siNS3-74 and siNS3-266, respectively. To determine whether these NS3-directed siRNAs could efficiently reduce expression of NS3 in Vero cells, the cells were co-transfected with pCMV-NS3-eGFP in the absence or presence of the different siRNAs, and NS3-eGFP expression was assessed at 24 h post-transfection by fluorescent microscopy. Since the AHSV-3 NS3 coding region was

fused in-frame with that of the eGFP gene, siRNA-mediated cleavage of the chimeric mRNA would lead to reduced expression of the reporter and thus provide a means whereby the efficiency of gene silencing can be analyzed qualitatively at the protein level by fluorescent microscopy.

Fluorescent microscopy revealed that although the control siRNA had no apparent effect on NS3-eGFP protein expression, expression of the fusion protein appeared to be only slightly diminished in cells co-transfected with siNS3-65 or siNS3-74. In contrast, siNS3-266 appeared to silence NS3-eGFP expression efficiently since the fluorescence was reduced to near background levels (Fig. 2.4, Panel a). To show specificity of the siRNA targeting, Vero cells were also transfected with pCMV-eGFP in a parallel series of experiments. The results showed that the eGFP protein was highly expressed in cells transfected with the plasmid in the presence of co-transfected NS3-directed siRNAs and the control siRNA (Fig. 2.4, Panel b). Generally, Vero cells expressing NS3-eGFP appeared morphologically different to those expressing eGFP (compare Figs. 2.3 and 2.4), possibly due to the cytotoxicity associated with the NS3 protein. It was therefore not possible to accurately quantify silencing of NS3-eGFP expression by fluorometry, despite several attempts. Nevertheless, these results indicate that NS3-eGFP expression can in principle be inhibited by siRNAs directed against the NS3 mRNA, and that siNS3-266 was the most efficacious in silencing NS3-eGFP gene expression.

2.3.4 Silencing of AHSV-3 NS3 mRNA expression by siRNAs in Vero cells

Since RNAi functions by silencing gene expression at a post-transcriptional level, the effect of the different siRNAs on NS3 mRNA expression in AHSV-3 infected Vero cells was subsequently examined. To investigate, Vero cell monolayers were transfected twice over a 24-h period with the NS3-directed siRNAs or a control non-silencing siRNA (UN-siRNA), followed by infection with AHSV-3. At 24 h post-infection, total RNA was isolated from the cells and subjected to reverse transcription followed by semi-quantitative real-time PCR. In this study, GAPDH was used as endogenous reference gene for data normalization and for calculation of fold changes in NS3 transcripts with the REST[®] software programme (Pfaffl *et al.*, 2002).

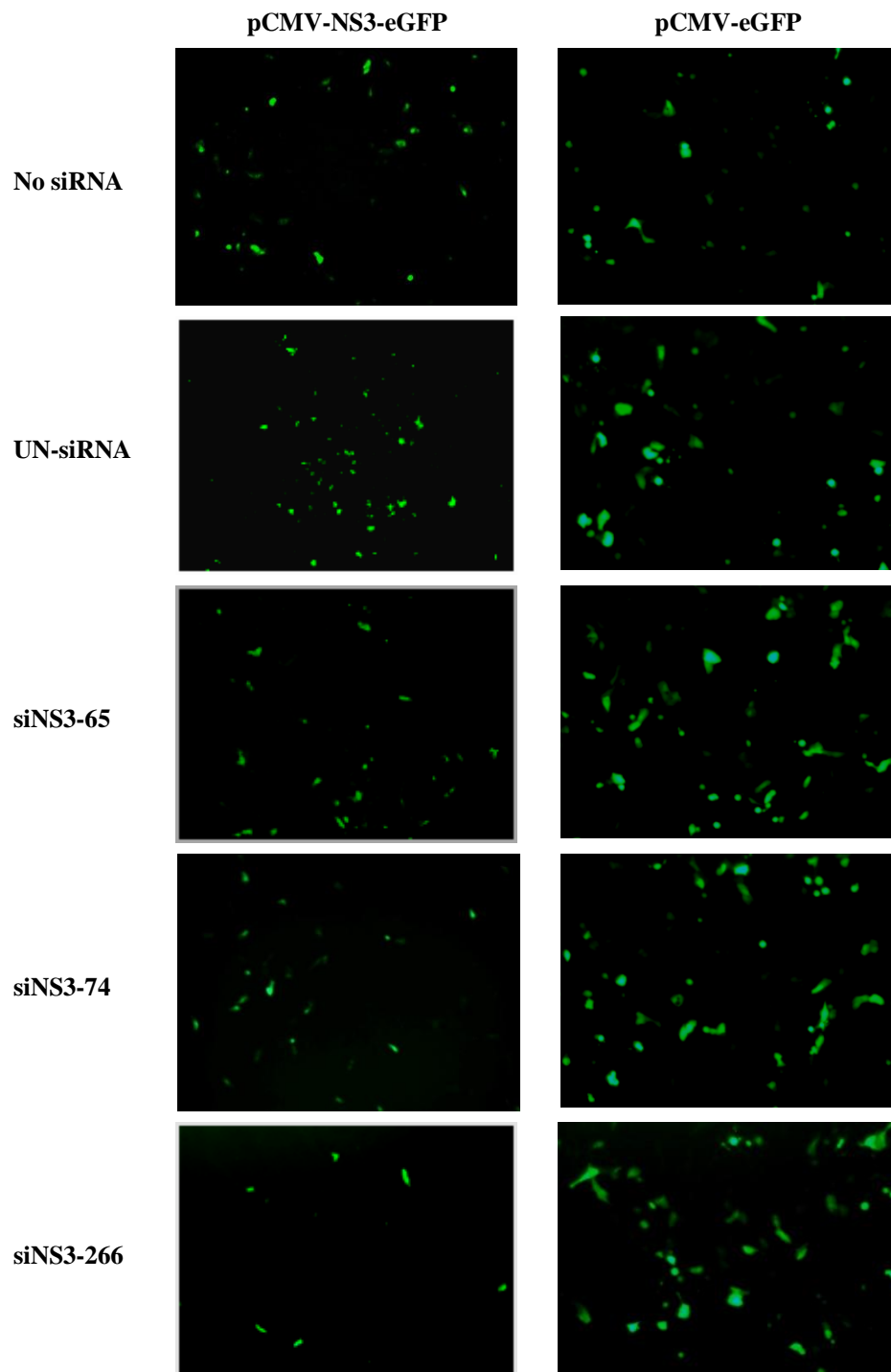


Fig. 2.4: Silencing of NS3-eGFP protein expression in Vero cells. Fluorescent micrographs of cells transfected with pCMV-NS3-eGFP and pCMV-eGFP, and co-transfected with different NS3-directed siRNAs (siNS3-65, siNS3-74 and siNS3-266), as well as a control siRNA (UN-siRNA). At 24 h post-transfection, representative fields were photographed. Magnification, 10 \times .

The data, presented in Fig. 2.5, indicated that the different NS3-directed siRNAs differed in their ability to reduce NS3 mRNA expression in the AHSV-3 infected Vero cells. In Vero cells transfected with either siNS3-65 or siNS3-74, only a slight reduction (0.5-fold) in NS3 mRNA transcripts could be observed. In contrast, NS3 mRNA expression was reduced significantly in Vero cells transfected with siNS3-266. The results indicated that this siRNA induced a 31.3-fold reduction in NS3 transcripts as compared with cells transfected with the control UN-siRNA. These results not only correlate with those presented above (Fig. 2.4), but also suggest that the observed silencing of NS3-eGFP protein expression was indeed due to degradation of the NS3 mRNA.

The possibility of DNA contamination in the RNA preparations used above was eliminated by performing DNase I treatments and verified by subjecting the samples to PCR amplification, using *Taq* DNA polymerase and the gene-specific primer pairs (Table 2.2). No amplicons were obtained from control reaction mixtures lacking template or from the RNA preparations that were subsequently used for cDNA synthesis. In addition, the amplification specificity of the real-time PCR was verified by agarose gel electrophoresis and a single amplicon of the expected length for each target was obtained (150 bp for NS3; 104 bp for GAPDH) (results not shown).

2.3.5 Silencing of AHSV-3 NS3 protein expression in Vero cells

To investigate whether the reduction in NS3 mRNA correlated with a down-regulation in NS3 protein in siRNA-treated AHSV-3 infected Vero cells, a Western blot was performed. For this purpose, whole-cell lysates were prepared from Vero cells that had been transfected with the NS3-directed siRNAs and then infected with AHSV-3, as described above. The proteins were resolved by SDS-PAGE and the unstained SDS-polyacrylamide gel was subsequently subjected to immunoblotting using an anti-AHSV-3 antiserum.

Analysis of the Western blot indicated that the NS3-directed siRNAs reduced the amount of detectable NS3 protein in the treated Vero cells as compared to AHSV-3 infected cells (Fig. 2.6). Although not quantitative, it did, however, appear that expression of NS3 was reduced to a greater extent in AHSV-3 infected cells treated with siNS3-266, and to a lesser extent in cells treated with siNS3-65 or siNS3-74. Notably, NS3 expression was reduced to a similar extent in Vero cells treated with the latter two NS3-directed siRNAs. These results were consistent with the data obtained at the mRNA level by semi-quantitative real-time PCR assays.

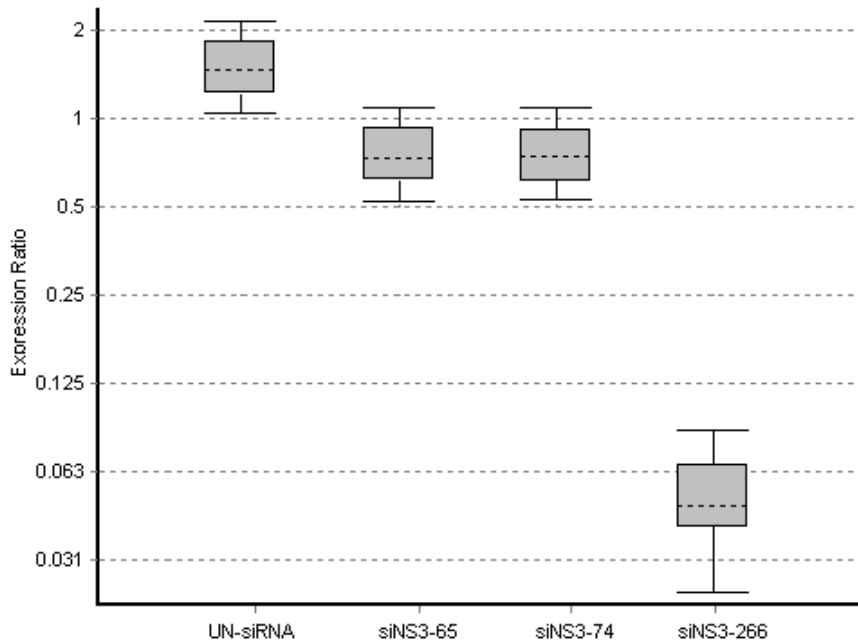


Fig. 2.5: Inhibition of AHSV-3 NS3 mRNA expression in Vero cells by NS3-directed siRNAs. At 24 h post-infection, the ratio of NS3 mRNA transcripts in infected cells transfected with NS3-directed siRNAs (siNS3-65, siNS3-74 or siNS3-266) to that in infected cells transfected with a control non-silencing siRNA (UN-siRNA) was quantified by real-time PCR using the GAPDH gene as endogenous control. In the figure, boxes represent the interquartile range and the dotted line represents the median gene expression. Whiskers represent the minimum and maximum observations. Data are shown as the means \pm S.D. of six replicates.

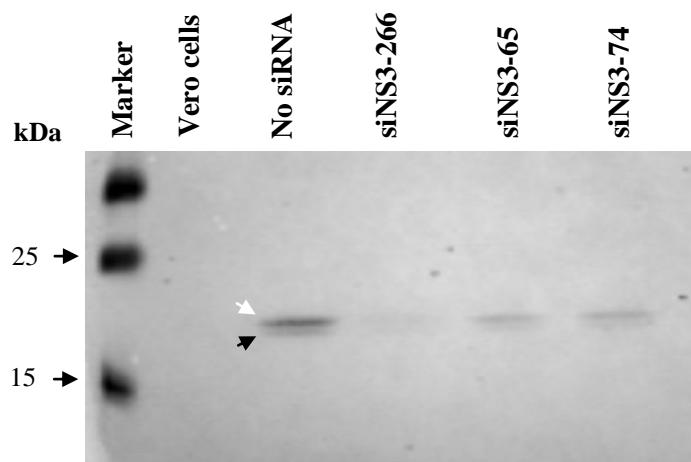


Fig. 2.6: Western blot depicting the expression of AHSV-3 NS3 in Vero cells subjected to transfection with the indicated NS3-directed siRNAs. Western blot analysis was performed with whole-cell lysates prepared at 24 h post-infection, and the membrane was incubated with anti-AHSV-3 antiserum. The molecular weight markers (kDa) are indicated to the left of the blot. Vero cells and untreated AHSV-3 infected cells (No siRNA) were included as controls. In the figure, NS3 and NS3A are indicated with white and black arrows, respectively.

2.3.6 Effect of NS3 gene silencing on virus release

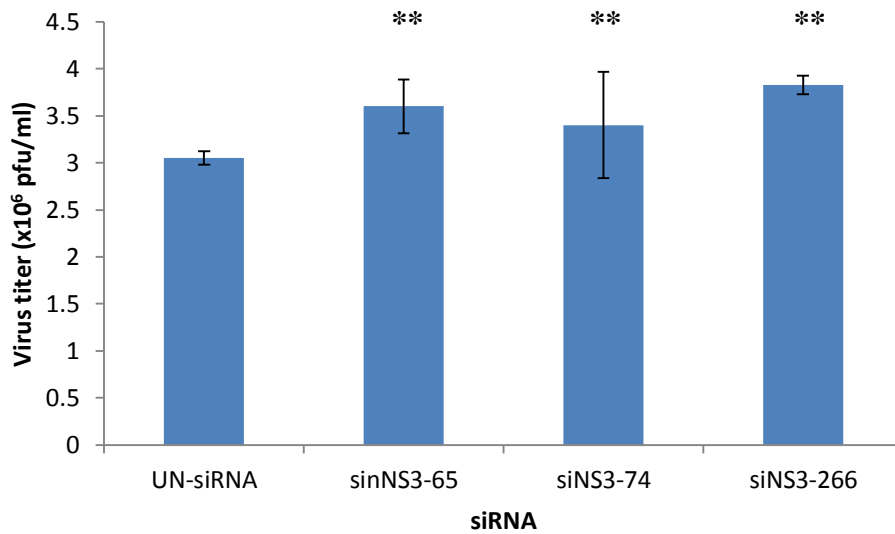
To evaluate the effect of NS3 gene silencing on virus release, the levels of infectious virus present both intracellularly (cell-associated) and in the culture medium from Vero cells that had been transfected with the NS3-directed siRNAs or control non-silencing siRNA, and then infected with AHSV-3, was subsequently determined. The respective titres, as determined at 24 h post-infection, were combined to represent the total virus yield, whilst virus release was calculated by expressing the titres obtained from the culture medium as a percentage of the total titre.

Vero cells that had been treated with the control non-silencing siRNA and with the NS3-directed siRNAs prior to infection with AHSV-3 all produced similar levels of total progeny virus, ranging between $3\text{-}3.8 \times 10^6$ pfu/ml (Fig. 2.7a). These results therefore indicate that virus replication occurred in the cells during the 24-h culture period and that transfection of the cells with the NS3-directed siRNAs did not non-specifically interfere with virus replication as compared to cells transfected with the non-silencing control siRNA. Although the viruses were predominantly cell-associated, a significantly lower percentage (28%) of AHSV-3 virions was released from the virus-infected cells that had been transfected with siNS3-266 (Fig. 2.7b). In contrast, 45% and 43% of the AHSV-3 virions were released from Vero cells that had been treated with siNS3-74 and siNS3-65, respectively. The levels of virus release from these siRNA-treated Vero cells were similar to that of cells treated with the control non-silencing UN-siRNA (49%). Taking into consideration the greater ability of siNS3-266 to suppress NS3 gene expression, as evidenced in two independent assays (Figs. 2.5 and 2.6), these results thus indicate that silencing of NS3 expression reduces virus release from the infected cells.

2.4 DISCUSSION

The orbivirus non-structural proteins are thought to play key roles in virus replication, and elucidation of their mechanisms of action has therefore been an active area of research. Amongst the non-structural proteins, the BTV NS3 protein has recently been implicated in virus release from infected cells (Beaton *et al.*, 2002; Han and Harty, 2004; Wirblich *et al.*, 2006; Celma and Roy, 2009). In contrast to BTV NS3, much less is known regarding the role of AHSV NS3 in this process (Stoltz *et al.*, 1996; Meiring *et al.*, 2009). A major constraint in

(a)



(b)

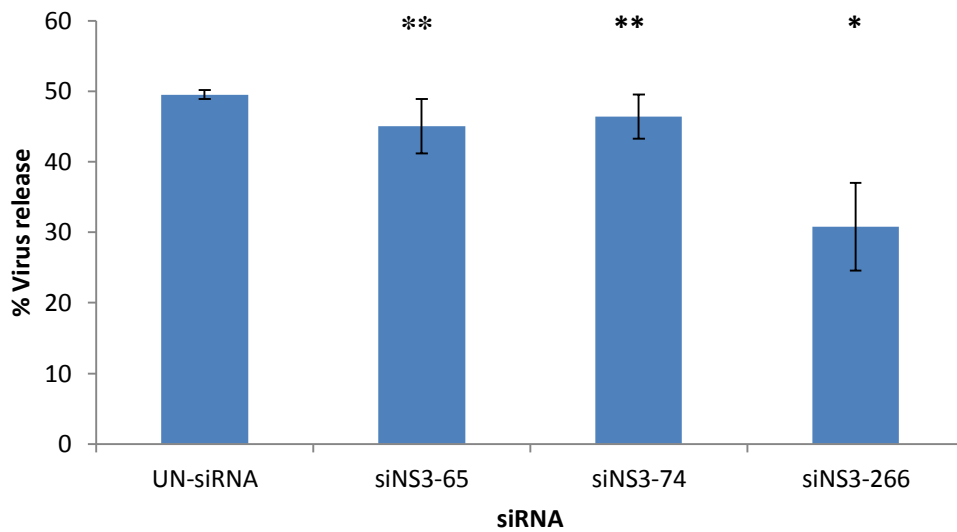


Fig. 2.7: Effect of NS3-directed siRNAs on the total infectious virus yield (a) and the percentage virus released of AHSV-3 in Vero cells. The cells were transfected with the indicated NS3-directed siRNAs and control UN-siRNA prior to infection with AHSV-3, and at 24 post-infection the cell-associated and released virus was titrated. Values indicate the means \pm S.D. of two independent experiments. Values were compared to that obtained for control non-silencing UN-siRNA treated cells by the *t*-test, where * indicates a statistically significant difference ($p < 0.01$), and ** indicates no statistically significant difference ($p > 0.05$).

these types of studies has been the lack of a reverse genetics system for AHSV that would allow for genetic manipulation of the viral genome in order to study protein function in greater detail. Therefore, in this study, an RNAi-based approach was adopted to investigate the involvement of NS3 in AHSV release. It was reasoned that if NS3 does indeed play a role in virus release, then silencing of its expression should interfere with the process of virus release, leading to a reduction in the amount of released virion particles.

Despite RNAi having become a powerful and widely used approach for the analysis of viral gene function (Arias *et al.*, 2004; Dykxhoorn and Lieberman, 2005; Wirblich *et al.*, 2006), there were initially several impediments to the use of this approach in mammalian cells. Most notably, mammalian cells harbour a potent antiviral response that is triggered by the presence of dsRNA viral replication intermediates. Key components of this response are the dsRNA-activated protein kinase R (PKR), which results in a generalized inhibition of translation, and 2',5'-oligoadenylate synthetase (2',5'-AS), the product of which is an essential co-factor for the non-specific ribonuclease RNase L (Stark *et al.*, 1998; Sledz *et al.*, 2003). The ultimate outcome of this set of responses is cell death via apoptosis. To avoid these antiviral effects, synthetic 21-nt siRNAs with 2-nt 3'overhangs were used in this investigation. Not only do the siRNAs avoid provoking the PKR response by virtue of their small size, but they are also incorporated directly into the RNAi pathway by mimicking the products of the Dicer enzyme (Elbashir *et al.*, 2001a; Caplen *et al.*, 2001). Moreover, Vero mammalian cells were used for all experiments since they lack interferon genes due to spontaneous gene deletions (Desmyter *et al.*, 1968; Mosca and Pitha, 1986; Ge *et al.*, 2003). This strategy therefore made it possible to attribute the gene silencing effects observed to NS3 gene silencing and loss of NS3 function by RNAi, and not to the antiviral effects of the interferon response.

The goal with most RNAi protocols is to effectively reduce protein levels in cells and to study the functional consequences of their removal. The key challenge for achieving effective gene silencing is primarily dependant on the effectiveness and specificity of the RNAi effector molecule. However, only a limited number of siRNAs is capable of inducing highly effective and sequence-specific gene silencing (Elbashir *et al.*, 2001a; Reynolds *et al.*, 2004; Naito *et al.*, 2009). In addition, the efficiency of siRNA-induced gene silencing can only be experimentally measured based on inhibition of the target gene expression. Therefore, it is important to use a robust and comparative validating system for determining the efficiency of different siRNAs. Although various different target gene-reporter based siRNA validation

systems have been described, they typically rely on the use of luciferase, epitope tags or eGFP as the reporter gene (Yokota *et al.*, 2003; Wu *et al.*, 2004; Liu *et al.*, 2006; Lantermann *et al.*, 2007). In contrast to the other reporters, which require an enzyme substrate or antibodies to detect the reporter protein, the fluorescence from eGFP does not require additional co-factors, substrates or other gene products (Chalfie *et al.*, 1994). Moreover, the eGFP reporter protein contains chromatophore mutations that make the protein 35-times brighter than wild-type GFP and has been codon-optimized for high expression in mammalian cells (Chiu *et al.*, 1996; Cormack *et al.*, 1996). Like wild-type GFP, eGFP fluorescence is stable, species-independent and can be monitored by fluorescence microscopy, flow cytometry and fluorometry (Zhang *et al.*, 1996; Stassen *et al.*, 2007). Consequently, eGFP was specifically chosen as reporter gene in this study since the ability of the NS3-directed siRNAs to silence its target gene can be analyzed readily by a visual decrease in the number of green fluorescent cells when viewed under a fluorescent microscope and quantitatively by fluorometry (Stassen *et al.*, 2007).

One caveat of siRNA design is that not all RNA duplexes will cleave their target with efficiency and much effort has gone toward identifying a set of rules for selecting an effective siRNA target site within a gene (Elbashir *et al.*, 2001a; Caplen *et al.*, 2001; Reynolds *et al.*, 2004; Ui-Tei *et al.*, 2004; Wang *et al.*, 2009). Despite these developments, there are presently no reliable methods to select effective siRNA sequences without empirical testing. Consequently, in this study, three 21-nt target sequences from different regions in the coding region of the AHSV-3 NS3 gene were selected. Towards identifying a functional siRNA that can efficiently inhibit AHSV-3 NS3 gene expression, a previously constructed pCMV-NS3-eGFP reporter plasmid was co-transfected with the respective NS3-directed siRNAs into Vero cells. The results indicated that NS3-eGFP expression was reduced in these cells compared to cells transfected with the reporter plasmid only, albeit to differing extents (Fig. 2.4). Since the hallmark of RNAi is the degradation of targeted mRNA transcripts, the potential of the NS3-directed siRNAs to down-regulate the levels of NS3 transcripts and protein in AHSV-3 infected Vero cells was also investigated. The results indicated that of the three NS3-directed siRNAs used, siNS3-266 interfered significantly with NS3 mRNA and protein expression. In contrast, the effect of siNS3-65 and siNS3-74 were comparable, albeit much less efficient compared to the results obtained with siNS3-266 (Figs. 2.5 and 2.6).

The above results indicated that the different NS3-directed siRNAs differed in their efficacy to silence NS3 gene expression. It is unlikely that the observed difference in silencing efficiency between the three NS3-directed siRNAs is due to differences in transfection efficiency since, in three independent experiments, siNS3-266 consistently suppressed NS3 gene expression more efficiently than did either siNS3-65 or siNS3-74. These results are in agreement with several previous reports, indicating that siRNAs targeted to different sites on the same mRNA differ in their silencing efficiency (Holen *et al.*, 2002; Harborth *et al.*, 2003; Vickers *et al.*, 2003; Scherer *et al.*, 2004; Lambeth *et al.*, 2007; Patel *et al.*, 2009). At present, there is still a lack of clear understanding of the mechanisms that determine gene silencing efficiency of a given siRNA. Nevertheless, a number of hypotheses have been proposed in the literature, including the thermodynamic properties of the siRNA that play a role in its stability, as well as strand bias in duplex unwinding and retention by RISC (Khvorova *et al.*, 2003; Schwartz *et al.*, 2003; Lu and Matthews, 2008), binding of viral and/or cellular proteins on the mRNA that may cause positional effects (Holen *et al.*, 2002; Miyagishi and Taira, 2005), and the local secondary and tertiary structure of the targeted mRNA that may affect the accessibility of the siRNA (Bohula *et al.*, 2003; Kretschner-Kazemi Far and Sczakiel, 2003; Vickers *et al.*, 2003; Luo and Chang, 2004; Gredell *et al.*, 2008). Indeed, several reports have argued that local secondary structures in the target mRNAs may restrict the accessibility of RISC and attenuate or even abolish RNAi efficiency (Heale *et al.*, 2005; Schubert *et al.*, 2005; Overhof *et al.*, 2005; Tafer *et al.*, 2008). Despite the respective NS3-directed siRNAs targeting accessible sites on NS3 mRNA (Fig. 2.1a), as predicted with the MFOLD software programme (Zuker, 2003); it is difficult to accurately model the complex secondary structure of mRNA (Kawasaki *et al.*, 2003). Moreover, the relevance of such predictions is also uncertain since the method does not take into account either tertiary structure or RNA-protein interactions. Although these models should therefore be viewed as merely predictive, it is nevertheless tempting to speculate that the target site of siNS3-65 and siNS3-74 were both less accessible for interaction with the corresponding RISC/siRNA complex due to local structural constraints, thus resulting in less effective binding and consequently, less efficient degradation of the target mRNA.

Although previous studies have suggested a role for AHSV NS3 in virus release, these were based primarily on observations made by electron microscopy analyses of AHSV-infected mammalian cells (Stoltz *et al.*, 1996) and through the study of reassortant viruses in which the NS3 gene was exchanged with mostly other gene segments (Meiring *et al.*, 2009). Thus,

having successfully established and validated an RNAi-based gene silencing assay for NS3 of AHSV-3, it was next investigated whether suppression of NS3 gene expression influences the release of progeny virions from infected cells. For this purpose, Vero cells were transfected with the NS3-directed siRNAs and then infected with AHSV-3. At 24 h post-infection, culture supernatants and cells were harvested, and the extracellular and cell-associated virus titres determined by plaque assays. Although the largest proportion of virus remained cell-associated, as typically observed with orbiviruses (Eaton *et al.*, 1990; Guirakhoo *et al.*, 1995; Meiring *et al.*, 2009), differences were nevertheless noted in the percentage virus released. Compared to cells that had been treated with a control non-silencing siRNA, a significantly lower percentage of viruses were released from Vero cells that had been treated with siNS3-266. In agreement with their less efficacious silencing profile, siNS3-65 and siNS3-74 had a less remarkable effect on virus release and the results were in agreement with those obtained for the control transfected cells (Fig. 2.7). Notably, the total virus titres were similar in all cases, indicating that the siRNAs had little or no effect on virus replication and infectivity.

The above results indicate that AHSV-3 NS3 does indeed mediate release of progeny virions from infected cells. However, the mechanism by which NS3 facilitates virus release is not yet clear. It has been reported that AHSV and BTV can be released from infected cells either by budding through the plasma membrane or by extrusion through locally disrupted membranes (Hyatt *et al.*, 1989; Stoltz *et al.*, 1996). Budding of BTV particles appears to result from interactions between NS3 and components of the vacuolar sorting pathway (Beaton *et al.*, 2002; Wirblich *et al.*, 2006), whilst the viroporin activity of BTV NS3 may facilitate lytic virus release by mediating membrane permeabilization (Han and Harty, 2004). Moreover, it has been suggested that the non-structural protein NS1, in conjunction with NS3, may also be involved in virus release (Owens *et al.*, 2004; Meiring *et al.*, 2009). This is based on observations that inhibition of BTV NS1 led to a shift from lytic release of virus particles to budding from the plasma membrane in BTV-infected mammalian BSR cells (Owens *et al.*, 2004). Specifically, it was proposed that when NS3 protein levels are low relative to NS1 protein levels, progeny viruses accumulate within the cytoplasm of the cell and are eventually released through either lysis or cell death. However, when NS1 is inhibited, the residual NS3 protein levels may be sufficient to promote a shift from lytic release to budding. Although this explanation may potentially account for the lower level of virus release from Vero cells treated with siNS3-266 (in which AHSV-3 NS3 expression was significantly suppressed), further studies are required to test this hypothesis.

In conclusion, the results obtained in this part of the study supported previous findings that siRNAs can induce potent gene silencing of heterologous genes in mammalian cells. Specifically, it was demonstrated that expression of AHSV-3 NS3 is silenced effectively in Vero cells, albeit that siRNAs targeting different regions on the NS3 mRNA differed in their gene silencing efficacy. Moreover, the developed RNAi assay allowed for a preliminary investigation into NS3 function in virus-infected Vero cells. The results are the first to provide direct experimental evidence that virus release is indeed enhanced by AHSV NS3. However, whether this is a function of NS3 alone or due to interactions between NS3 and components of the cellular export machinery, as in the case of BTV NS3, remains to be investigated. The details of these studies are provided in the following Chapter.

CHAPTER THREE

***CULICOIDES* AND VERO CELL PROTEINS INTERACT WITH THE NS3 PROTEIN OF AHSV-3, AS EVIDENCED BY YEAST TWO-HYBRID SCREENS**

3.1 INTRODUCTION

The genus *Orbivirus* of the family *Reoviridae* comprises a number of important animal pathogens such as African horsesickness virus (AHSV) and Bluetongue virus (BTV). In contrast to other members of the *Reoviridae* family, the orbiviruses are transmitted by insect *Culicoides* spp. to vertebrate hosts, and have the ability to replicate in both insect and mammalian hosts (Gorman, 1992; Calisher and Mertens, 1998). One of the major morphological differences observed during infection of insect and mammalian cells in culture are that virus appears to preferentially bud from the plasma membrane of insect cells, thus leaving the cells intact. In contrast, in mammalian cell culture, a high proportion of virus remains cell-associated, leading to eventual cell lysis (Homan and Yunker, 1988; Castro *et al.*, 1989; Hyatt *et al.*, 1989; Guirakhoo *et al.*, 1995). It therefore appears that orbiviruses may make use of different mechanisms in order to be released from infected cells.

The non-structural protein NS3 is the only membrane-associated protein encoded by orbiviruses (Hyatt *et al.*, 1991; Wu *et al.*, 1992; Van Staden *et al.*, 1995), thus making it a likely candidate for aiding virus release from infected cells. Indeed, a strong correlation between the presence of NS3 and virus release has been noted in AHSV- and BTV-infected mammalian cells (Hyatt *et al.*, 1991; Stoltz *et al.*, 1996). Furthermore, BTV virus-like particles (VLPs) are released from *Spodoptera frugiperda* insect cells by co-expression with NS3, and NS3 protein can be found localized at the membrane site where VLP egress occurs (Hyatt *et al.*, 1992). It has also been reported that NS3 of AHSV and BTV exhibits cytotoxicity when expressed in mammalian or *S. frugiperda* cells (French *et al.*, 1989; Van Staden *et al.*, 1995). This cytotoxicity was subsequently shown to be dependent on membrane association of the protein, which is mediated by two transmembrane domains (Van Niekerk *et al.*, 2001a; Han and Harty, 2004). The above studies provide compelling evidence that NS3 may facilitate virus release by inducing membrane permeabilization, thereby causing

local disruption of the plasma membrane and allowing virus particles to be extruded through a membrane pore.

In addition to lytic virus release, it has also been observed that orbiviruses can leave infected mammalian cells by budding at the cell membrane prior to cell lysis (Hyatt *et al.*, 1989; Stoltz *et al.*, 1996). This phenomenon has also been reported for other non-enveloped viruses such as rotavirus (Jourdan *et al.*, 1991), parvovirus (Bär *et al.*, 2008) and poliovirus (Tucker *et al.*, 1993; Taylor *et al.*, 2009). Recent studies have shown that the NS3 protein of BTV interacts with the p11 subunit of the heterotetrameric annexin II complex, as well as with the VP2 outer capsid protein of BTV (Beaton *et al.*, 2002). Since annexin II is involved in cellular exocytosis, it has been proposed that the interactions between p11, NS3 and VP2 provide a mechanism by which progeny viruses exploit the exocytotic pathway for non-lytic virus release. In addition to its interaction with p11, BTV NS3 is also capable of interacting with Tsg101, a cellular protein component of the ESCRT-I complex, through a late (L) domain motif present in NS3 (Wirblich *et al.*, 2006). Several studies have reported that recruitment of proteins of the ESCRT-I and ESCRT-III complexes through L-domains is important for budding of enveloped viruses (Pornillos *et al.*, 2002; Freed, 2004; Bieniasz, 2006; Calistri *et al.*, 2009). This data therefore suggests that NS3-Tsg101 interaction is important for budding of the BTV virions from the plasma membrane. Although not yet investigated, it can be envisaged that the above non-lytic virus egress pathways may be particularly important during infection of insect vectors such as *Culicoides* spp., since orbiviruses establish persistent infection in insect cells without apparent cytopathic effects (Guirakhoo *et al.*, 1995).

Based on the above, it follows that different protein-protein interactions between BTV NS3 and cellular proteins are important during BTV egress. However, no similar information is available for AHSV NS3. It can be envisaged that considerable assistance in the elucidation of the functions of AHSV NS3 can be obtained by investigating the protein's interactions with other proteins. Towards this end, the yeast two-hybrid system (Fields and Song, 1989; Chien *et al.*, 1991) has been used widely for the identification of protein interaction (González *et al.*, 1998; Beaton *et al.*, 2002; Becker *et al.*, 2003; Mir *et al.*, 2007). This system is based on the fact that many eukaryotic transcription factors, including GAL4 of yeast, have discrete and separable DNA-binding and activation domains (Keegan *et al.*, 1986). Consequently, protein-protein interactions can be investigated by fusing one test protein to the DNA-binding domain (DNA-BD) of the yeast GAL4 transcription factor, and a random library of potential protein

partners to the GAL4 activation domain (AD). Following expression in a suitable yeast strain, the interactions can be detected by assaying for expression of a GAL4-responsive reporter gene. Despite its usefulness, the yeast two-hybrid system has several associated problems. False positives are often generated due to proteins that are capable of independently recognizing and binding to activation sequences upstream of the reporter gene (Fashena *et al.*, 2000; Rual *et al.*, 2005). In addition, proteins that are cytotoxic or contain strong hydrophobic domains may prove problematic in the system (Causier and Davies, 2002; Xia *et al.*, 2006). The latter is especially noteworthy, as the NS3 protein of both AHSV and BTV is cytotoxic and localizes to membranes via its hydrophobic transmembrane domains (Van Niekerk *et al.*, 2001a; Han and Harty, 2004). These problems, however, can be circumvented by making use of a truncated version of the NS3 protein that lacks the hydrophobic domains. Moreover, several commercial yeast two-hybrid systems have become available that utilize different yeast strains containing a number of reporter genes that are under the control of distinct upstream activating sequences (UAS). Genes such as *TRP1*, *LEU2*, *HIS3* and *ADE2* are frequently used as reporter genes, in conjunction with *lacZ*, to provide a more stringent assay for protein-protein interactions (Toby and Golemis, 2001; Vidalain *et al.*, 2005). The use of more than one reporter gene reduces the incidence of false positives, because any independently binding protein would need to bind to all of the different recognition sequences in order to activate the respective reporter genes.

In contrast to BTV, the mechanisms underlying the release of AHSV from infected cells and the role of NS3 in this process has not yet been investigated in any great detail. In the previous Chapter, it was shown that silencing of AHSV NS3 expression affected virus egress and a reduction in virus release from mammalian cells was evident. Thus, to gain further insights into the role that the AHSV NS3 protein plays in virus egress, the aim of this part of the study was to identify host cell proteins that interact with NS3 by using a yeast two-hybrid system. For this purpose, a truncated NS3 protein, lacking the hydrophobic transmembrane domains, was generated and used to screen cDNA libraries of Vero mammalian cells and *Culicoides variipennis* (KC) insect vector cells for cellular proteins interacting with NS3.

3.2 MATERIALS AND METHODS

3.2.1 Bacterial and yeast strains, plasmids and culture conditions

The *Escherichia coli* JM109 and *E. coli* KC8 strains were cultured in LB broth (1% [w/v] tryptone; 1% [w/v] NaCl; 0.5% [w/v] yeast extract; pH 7.4) (Sambrook *et al.*, 1989) at 37°C with shaking at 200 rpm, and maintained at 4°C on LB agar (LB broth containing 1.2% [w/v] bacteriological agar) or at -70°C as glycerol cultures. For plasmid DNA selection and maintenance in the *E. coli* strains, the following concentrations of antibiotics were used: 50 µg/ml for ampicillin and 50 µg/ml for kanamycin. The antibiotics were obtained from Roche Diagnostics. *Saccharomyces cerevisiae* strain AH109 (**genotype:** *MATatrp1-901 leu2-3,112 ura3-52 his3-200 gal4Δgal80Δ LYS2::GAL1_{UAS}-GAL1_{TATA}-HIS3MEL1 GAL2_{UAS}-GAL2_{TATA}-ADE2, URA3::MEL1_{UAS}-MEL1_{TATA}-lacZ*), used in yeast two-hybrid screens, was obtained from Dr. C. Maritz-Olivier (Department of Genetics, University of Pretoria). The non-transformed AH109 yeast strain was maintained on YPDA agar (1% [w/v] yeast extract; 2% [w/v] peptone; 2% [w/v] dextrose; 0.003% [w/v] adenine hemisulphate; 2% [w/v] bacteriological agar). Transformed AH109 yeast strains were plated onto standard (SD) or dropout (DO) agar (0.67% [w/v] yeast nitrogen base without amino acids; 100 ml of the appropriate 10× dropout solution; 2% [w/v] bacteriological agar) (Clontech Laboratories, Inc.). The pGEM[®]-T Easy cloning vector system was obtained from Promega, whilst recombinant plasmid pCMV-NS3-eGFP, harbouring a cDNA copy of the AHSV-3 NS3 gene fused in-frame to the eGFP reporter gene, was obtained from Dr. V. Van Staden (Department of Genetics, University of Pretoria). The DNA-BD plasmid vector pGBKT7 (*GAL4*₍₁₋₁₄₇₎DNA-BD, *ColE1 ori*, 2µ *ori*, Kan^r, *TRP1*) and the AD plasmid vector pACT2 (*GAL4*₍₇₆₈₋₈₈₁₎AD, *ColE1 ori*, 2µ *ori*, Amp^r, *LEU2*), for use in yeast two-hybrid screens, were obtained from Dr. C. Maritz-Olivier. Plasmid maps of the respective vectors are provided in the Appendix to this dissertation.

3.2.2 Cell cultures

Vero cells (ATCC CCL-81) were propagated and maintained as monolayers in 75-cm² tissue culture flasks, and cultured in Minimal Essential Medium (MEM) (Highveld Biological) supplemented with 5% (v/v) foetal bovine serum (FBS) and antibiotics (1 × penicillin, streptomycin, fungizone). The flasks were incubated at 37°C in a humidified incubator with a constant supply of 5% (v/v) CO₂. KC (embryonic *Culicoides variipennis*) cells were propagated at 27°C in modified Schneider's *Drosophila* medium (Highveld Biological)

supplemented with 10% (v/v) FBS and the appropriate antibiotics (1 × penicillin, streptomycin, fungizone).

3.2.3 DNA amplification

3.2.3.1 Primers

The primers used in PCR to amplify different DNA fragments for cloning purposes are indicated in Table 3.1. The primers were designed with PerlPrimer v.1.1.6 (Marshall, 2004). To facilitate cloning of the amplicons, unique restriction endonuclease recognition sites were incorporated at the 5' terminus of the respective primers. The primers were obtained from Integrated DNA Technologies or Inqaba Biotechnical Industries.

Table 3.1: Primers used in this study to amplify specific DNA fragments for cloning purposes and sequencing of cloned insert DNA

Primer	Nucleotide sequence
PCR amplification *:	
NS3-Nterm-Forward	5' - ggatcc aaTTATCCCTTGTCATGAGTCTAGC - 3'; <i>Bam</i> HI site incorporated
NS3-Nterm-Reverse	5' - GCctg cagTAACATTGACGCCAACTCTA - 3'; <i>Pst</i> I site incorporated
NS3-N-Xho	5' - GCctg cagTTACATTGACGCCAACTCTA - 3'; <i>Xho</i> I site incorporated
SARA-Forward	5' - GCggatcc AGGCCTGGAGTCAACACAAT - 3'; <i>Bam</i> HI site incorporated
SARA-Reverse	5' - GCctg cagCACCGTTTAATGTGGGATATCACT - 3'; <i>Pst</i> I site incorporated
L34-Forward	5' - GCGCGCggatcc AGGTGGTCATATGGCC - 3'; <i>Bam</i> HI site incorporated
L34-Reverse	5' - GCGCGCctg cagACTCTGTGCTTGTGC - 3'; <i>Pst</i> I site incorporated
Nucleotide sequencing:	
T7	5' - GTAATACGACTCACTATAGGGC - 3'
T3	5' - AATTAACCCTCACTAAAGGG - 3'
3' DNA-BD	5' - ATCATAATCATAGAAATTCGCC - 3'
pACT2 Forward	5' - TTCGATGATGAAGATACCCACCAAACCC - 3'
pACT2 Reverse	5' - GTGAACTTGCGGGGTTTTTCAGTATCTACGAT - 3'

* In primer sequences, the restriction endonuclease sites are indicated in bold lower case letters. In primer NS3-Nterm-Reverse, an introduced stop codon is indicated in italics.

3.2.3.2 Polymerase chain reaction (PCR)

The PCR reaction mixtures (50 µl) contained 50 ng of plasmid DNA as template, 1 × PCR buffer (50 mM KCl; 10 mM Tris-HCl [pH 9.0]; 0.1% [v/v] TritonX-100), 1.5 mM MgCl₂, 200 µM of each dNTP, 10 pmol of each the appropriate forward and reverse primer (Table 3.1), and 2 U of SuperTherm *Taq* DNA polymerase (Whitehead Scientific). The tubes were

placed in a Perkin-Elmer GeneAmp[®] 2700 thermal cycler. Following initial denaturation of 2 min at 94°C, the samples were subjected to 25 cycles of denaturation for 30 s at 94°C, primer annealing for 30 s at 62°C (NS3-Nterm Forward and Reverse primers), 65°C (SARA Forward and Reverse primers) or 68°C (L34 Forward and Reverse primers) and elongation for 1 min at 72°C. After the last cycle, a final elongation step was performed at 72°C for 5 min to complete synthesis of all DNA strands. For control purposes, reaction mixtures containing all reagents except template DNA were included. Aliquots of the PCR reaction mixtures were analyzed by electrophoresis on a 1% (w/v) agarose gel in the presence of an appropriate DNA molecular weight marker (GeneRuler[™] 100 bp; Fermentas), as described previously (Section 2.2.3.1).

3.2.4 Purification of DNA fragments from agarose gels

DNA fragments were purified from agarose gel slices with the NucleoSpin[®] Extract II kit (Mackerey-Nagel) according to the manufacturer's instructions. Briefly, the agarose gel slice was transferred into a pre-weighed clean 1.5-ml Eppendorf tube and 200 µl of buffer NT was added per 100 mg of agarose. The agarose was melted by incubation at 50°C for at least 3 min, centrifuged through a DNA-binding column at 13 000 rpm for 1 min and washed with 600 µl of buffer NT3. Following brief centrifugation to remove residual buffer, the DNA was eluted from the column with 10 µl of the supplied elution buffer. An aliquot of the sample was analyzed by electrophoresis on a 1% (w/v) agarose gel to assess the purity and concentration of the DNA.

3.2.5 Cloning of DNA fragments into plasmid vectors

3.2.5.1 Ligation reactions

For cloning of PCR amplicons, the pGEM[®]-T Easy vector system (Promega) was used. The ligation reaction mixtures contained 5 µl of a 2 × Rapid ligation buffer, 50 ng of pGEM[®]-T Easy vector DNA, 150 ng of purified amplicon, 1 µl of T4 DNA ligase (3 U/µl) and UHQ water to a final volume of 10 µl. Ligation of specific DNA fragments and vector DNA (pGBKT7 or pACT2) was performed in a 30-µl reaction volume that contained 1 × DNA ligase buffer (2 mM Tris-HCl; 0.1 mM EDTA; 0.5 mM DTT; 6 mM KCl; 5% [v/v] glycerol; pH 7.5) and 1 µl of T4 DNA ligase (1 U/µl; Roche Diagnostics). The ratio of insert to vector was typically in excess of 3:1. All of the ligation reactions were incubated overnight at 16°C.

3.2.5.2 Preparation of competent *E. coli* JM109 cells

Competent *E. coli* JM109 cells were prepared according to the method described by Sambrook *et al.* (1989). A single colony of a freshly streaked *E. coli* JM109 culture was inoculated into 20 ml of LB broth and incubated overnight at 37°C. Following incubation, 1 ml of the overnight culture was inoculated into 100 ml of pre-warmed (37°C) sterile LB broth and incubated at 37°C until an OD₆₀₀ of 0.94 was reached. The cells from 30 ml of the culture were harvested by centrifugation at 5000 rpm for 10 min at 4°C. The cell pellet was suspended in 10 ml of an ice-cold solution comprising 80 mM CaCl₂ and 50 mM MgCl₂, incubated on ice for 10 min and then pelleted as above. The cell pellet was suspended in 5 ml of ice-cold 100 mM CaCl₂. Following the addition of 1.5 ml of glycerol, the cells were pipetted in aliquots of 200 µl into 1.5-ml Eppendorf tubes, snap-frozen in liquid nitrogen and stored at -70°C until needed.

3.2.5.3 Transformation of competent cells

After allowing the competent *E. coli* JM109 cells to thaw on ice, the cells were transformed by the heat shock-method, as described by Sambrook *et al.* (1989). The competent *E. coli* JM109 cells (200 µl) and the ligation reaction mixture were mixed, and incubated on ice for 30 min. The tubes were then incubated at 42°C for 90 s and immediately placed on ice for 2 min. Subsequently, 800 µl of pre-warmed (37°C) LB broth was added and the cells were incubated at 37°C for 1 h with shaking. A positive control (5 ng of pGEM 3Zf⁺ plasmid DNA) and negative control (competent cells only) were included to determine the competency of the *E. coli* JM109 cells and to test for contamination, respectively. The transformation mixtures were plated in volumes of 100-200 µl onto LB agar supplemented with the appropriate antibiotic. In instances where DNA fragments were cloned into pGEM[®]-T Easy vector DNA, the cells were plated together with 10 µl of 100 mM IPTG and 50 µl of 2% (w/v) X-Gal to identify recombinant clones, based on insertional inactivation of the *lacZ'* marker gene. All agar plates were incubated overnight at 37°C.

3.2.6 Screening of transformants

3.2.6.1 Plasmid DNA extraction

Plasmid DNA was isolated using the alkaline lysis-method (Birnboim and Doly, 1979), as described by Sambrook *et al.* (1989). For small-scale plasmid extractions, a single colony was inoculated into 5 ml of LB broth, containing the appropriate antibiotic, and incubated

overnight at 37°C. The cells from 3 ml of the overnight cultures were harvested by centrifugation at 15 000 rpm for 1 min and the cell pellets were suspended in 100 µl of ice-cold Solution I (50 mM glucose; 25 mM Tris; 10 mM EDTA; pH 8.0), followed by incubation at room temperature for 5 min and 1 min on ice. The resultant spheroplasts were lysed by addition of 200 µl of freshly prepared Solution II (0.2 M NaOH; 1% [w/v] SDS) and incubated on ice for 5 min, after which the bacterial chromosomal DNA, protein-SDS complexes and high-molecular-weight RNA were precipitated by addition of 150 µl of ice-cold Solution III (3 M NaOAc; pH 4.8). After incubation on ice for 10 min and centrifugation at 15 000 rpm for 15 min, the plasmid DNA was precipitated from the recovered supernatants by addition of 2.5 volumes of 96% EtOH and incubation on ice for 30 min. The precipitated plasmid DNA was collected by centrifugation at 15 000 rpm for 15 min, rinsed with 70% EtOH, vacuum-dried and then suspended in 20 µl of 1 × TE buffer (10 mM Tris-HCl; 1 mM EDTA; pH 8.0). To remove contaminating RNA, extracted plasmid DNA was incubated with 1 µl of RNase A (10 mg/ml) at 37°C for 30 min.

3.2.6.2 Restriction endonuclease digestions

Approximately 1 µg of plasmid DNA was digested with 5 U of restriction enzyme in the appropriate concentration of salt, using the 10× buffer supplied by the manufacturer. The final reaction volumes were typically 20 µl and incubation was at 37°C for 1 h. All restriction enzymes were supplied by Roche Diagnostics or Fermentas. The digestion products were analyzed on a 1% (w/v) agarose gel in the presence of an appropriate DNA molecular weight marker.

3.2.6.3 Nucleotide sequencing

Nucleotide sequencing of cloned insert DNA was performed with the ABI PRISM[®] BigDye[™] Terminator v.3.1 Cycle Sequencing Ready Reaction kit (Applied Biosystems) according to the manufacturer's instructions. The T3 and T7 primers (pGEM[®]-T Easy), T7 and 3' DNA-BD primers (pGBKT7), and pACT2 Forward and Reverse primers (pACT2) were used as sequencing primers (Table 3.1). Each sequencing reaction contained 1 × sequencing buffer, 2 µl of BigDye[™] Termination Mix, 3.2 pmol of sequencing primer, 250 ng of plasmid DNA and UHQ water to a final volume of 10 µl. Cycle sequencing reactions were performed in a Perkin-Elmer GeneAmp[®] 2700 thermal cycler with 25 of the following cycles: denaturation at 96°C for 10 s, primer annealing at 50°C for 15 s, and elongation at 60°C for 4 min. The

extension products were precipitated by addition of 1 µl of 3 M NaOAc (pH 4.6) and 25 µl of absolute EtOH. The tubes were incubated for 15 min at room temperature in the dark, centrifuged at 15 000 rpm for 30 min and the supernatant carefully aspirated. The extension products were resolved on an ABI PRISM[®] Model 3130 automated sequencer (Applied Biosystems). The nucleotide sequences obtained were analyzed with the BioEdit v.7.0.4.1 (Hall, 1999) software package. The nucleotide and deduced amino acid sequences were compared against the entries in the GenBank database with respectively the BLAST-N and BLAST-P programmes (Altschul *et al.*, 1997), available on the National Centre for Biotechnology Information web page (<http://www.ncbi.nlm.nih.gov/BLAST>).

3.2.7 Plasmid constructions

All molecular cloning techniques used in the construction of the respective recombinant plasmids were performed according to the procedures described in the preceding sections. All plasmid constructs were confirmed by restriction endonuclease digestion and by nucleotide sequencing.

- **pGBKT7-NS3₁₋₁₀₈**

Towards construction of the recombinant bait vector pGBKT7-NS3₁₋₁₀₈, a truncated NS3 gene comprising only of the N-terminal region of the AHSV-3 NS3 gene (amino acid residues 1-108; 324 nt) was PCR-amplified using plasmid pCMV-NS3-eGFP as template DNA, together with primers NS3-Nterm-Forward and NS3-Nterm-Reverse (Table 3.1). The amplicon was cloned into pGEM[®]-T Easy to generate pGEM-NS3-N-terminal. The insert DNA was subsequently recovered by digestion with both *Bam*HI and *Pst*I, and cloned into the identical sites of the pGBKT7 DNA-BD plasmid vector.

- **pGBKT7-SARA**

Primers SARA-Forward and SARA-Reverse (Table 3.1) were used with plasmid pACT2-SARA as template DNA to generate a 189-bp amplicon, which was cloned into pGEM[®]-T Easy to generate pGEM-SARA. To construct the recombinant bait vector pGBKT7-SARA, the insert DNA was excised from plasmid pGEM-SARA by digestion with both *Bam*HI and *Pst*I, and then cloned into the pGBKT7 DNA-BD plasmid vector that had been prepared in an identical manner.

- **pGBKT7-L34**

Primers L34-Forward and L34-Reverse (Table 3.1) were used with plasmid pACT2-L34 as template DNA to generate a 127-bp amplicon, which was cloned into pGEM[®]-T Easy to generate pGEM-L34. To construct the recombinant bait vector pGBKT7-L34, the insert DNA was excised from plasmid pGEM-L34 by digestion with both *Bam*HI and *Pst*I, and then cloned into the pGBKT7 DNA-BD plasmid vector that had been prepared in an identical manner.

- **pACT2-NS3₁₋₁₀₈**

The truncated NS3 gene, comprising only of the N-terminal region of AHSV-3 NS3, was obtained by PCR amplification using pGBKT7-NS3₁₋₁₀₈ as template DNA, together with primers NS3-Nterm-Foward and NS3-N-Xho (Table 3.1). Following PCR, the amplicon was cloned into pGEM[®]-T Easy to generate pGEM-NS3-Nterm-2. To construct the recombinant prey vector pACT2-NS3₁₋₁₀₈, the truncated NS3 gene was recovered by digestion with both *Bam*HI and *Xho*I and then cloned into the identical sites of the pACT2 AD plasmid vector.

3.2.8 cDNA synthesis

3.2.8.1 Total RNA extraction and purification

Vero mammalian cells and KC insect cells were seeded in 6-well tissue culture dishes, and total RNA was extracted from the respective cell monolayers at 24, 36 and 48 h post-incubation. Total RNA was extracted with Trizol[®] Reagent (Invitrogen) according to the manufacturer's instructions. The culture medium in each well was aspirated and replaced with 1 ml of the Trizol[®] Reagent. The cells were lysed by vigorous pipetting and then transferred into a 2-ml Eppendorf tube. Following incubation at room temperature for 5 min, 200 µl of chloroform was added and the contents were mixed by shaking the tubes for 15 s. The homogenized samples were incubated at room temperature for 2 min, followed by centrifugation at 12 000 rpm for 15 min. The RNA was precipitated from the recovered aqueous phase by addition of 500 µl of isopropanol and incubation at room temperature for 10 min. The precipitated RNA was collected by centrifugation at 13 000 rpm for 10 min, washed with 75% EtOH, air-dried for 5 min and suspended in 50 µl of DEPC-treated water. The RNA samples were purified with the Nucleospin[®] RNA II Purification kit (Macherey-Nagel) according to the manufacturer's instructions. Briefly, an equal volume of RNase-free water (50 µl) was added to each RNA sample and 600 µl of lysis-binding buffer was then added.

Following centrifugation through a RNA-binding column at 12 000 rpm for 30 s, 350 μ l of membrane desalting buffer was added to the column and centrifuged at 12 000 rpm for 1 min. To remove contaminating DNA, the column was treated at room temperature for 15 min with the supplied RNase-free DNase I. Following incubation, the column was washed once with buffer RA2 and twice with buffer RA3 (12 000 rpm for 30 s). The RNA was then eluted from the column in 60 μ l of RNase-free water. For each cell line, the purified RNA samples extracted at the different time intervals were pooled and an aliquot of each was analyzed by denaturing electrophoresis on a 1% (w/v) agarose gel that was prepared in 40 mM MOPS, 10 mM NaOAc, 1 mM EDTA and 18% (v/v) formamide in DEPC-treated ddH₂O (Sambrook *et al.*, 1989). The concentration and purity of the RNA was determined with a Nanodrop[®] ND-1000 spectrophotometer (Thermo Fischer Scientific, Inc.). The samples were stored at -70°C until required.

3.2.8.2 cDNA synthesis

The total RNA was reverse transcribed with the SuperScript[™] III First-strand synthesis system for RT-PCR (Invitrogen) and SMART[™] primers (Clontech Laboratories, Inc.). The primers were designed to contain the recognition sequence of *Sfi*I (5'-GGCCNNNN↓NGGCC-3') in order to facilitate subsequent cloning procedures (please refer to the Appendix for a description of the SMART[™] technology). The reaction mixture (64 μ l) contained 1 μ g of total RNA (DNase-treated) and 12 pmol of each the CDS III/3' PCR primer (5' - ATTCTAG**aggcctccatggcc**GACATG(T)₃₀NN - 3') and SMART IV[™] primer (5' - AAGCAGTGGTATCAACGCAGAGT**ggccatggaggcc**GGG - 3'), both of which contain a *Sfi*I site (bold). After denaturation of the RNA by incubating at 65°C for 5 min, the samples were placed on ice for 5 min and the following reagents were added in the indicated order: 20 μ l of 5 \times First-strand buffer, 2 μ l of 100 mM DTT, 10 μ l of a 10 mM dNTP solution, 2.5 μ l of RNaseOUT[™] inhibitor (40 U/ μ l), 2.5 μ l of SuperScript[™] III reverse transcriptase (200 U/ μ l) and 5 μ l of RNase-free water. The RNA was reverse transcribed at 42°C for 90 min and the enzyme was then inactivated by heating to 85°C for 5 min. The first-strand cDNA was purified with the Nucleospin[®] Extract II kit (Macherey-Nagel) according to the manufacturer's instructions. Briefly, 3 volumes of buffer NT2 were added to each reaction mixture, mixed and then centrifuged through a DNA-binding column at 12 000 rpm for 1 min. The column was washed three times with buffer NT3, and the single-stranded (ss) cDNA was eluted in 80 μ l of UHQ water.

3.2.8.3 cDNA amplification by long distance (LD)-PCR

Double-stranded (ds) cDNA was synthesized by long distance-PCR according to the protocol provided in the Super SMART™ PCR cDNA Synthesis kit User Manual (Clontech Laboratories, Inc.). Each reaction mixture contained 30 µl of the first-strand cDNA as template, 1 × ExTaq buffer, 1.5 mM MgCl₂, 1 mM of each dNTP, 12 pmol of each the 5' PCR primer (5' - AAGCAGTGGTATCAACGCAGAGT - 3') and 3' PCR primer (5' - ATTCTAGAGggcctccatggccGACATG - 3') and UHQ water to a final volume of 100 µl. The tubes were placed in a Perkin-Elmer GeneAmp® 2700 thermal cycler and following incubation at 95°C for 1 min, 10 U of TaKaRa ExTaq (5 U/µl) (Takara Bio, Inc.) was added and incubation was continued at 80°C for 1 min. The thermocycling was subsequently performed at 95°C for 15 s (denaturation); 65°C for 30 s (primer annealing) and 68°C for 6 min (elongation). After 28 cycles, 75 µl of the reaction mixture was removed and stored at 4°C. To determine the optimal number of cycles required to ensure that the ds cDNA remains in the exponential phase of amplification, the remaining 25 µl of the reaction mixture was subjected to further thermocycling and 5-µl aliquots were removed after 28, 30, 32 and 34 cycles of amplification. The aliquots were analyzed by electrophoresis on a 1 % (w/v) agarose gel in the presence of an appropriate DNA molecular weight marker. Subsequently, the remaining 75 µl of the reaction mixture was returned to the thermal cycler and subjected to 4 additional cycles of amplification (*i.e.* 32 cycles in total). The ds cDNA was purified with the NucleoSpin® II extract kit (Mackerey-Nagel), as described above, and eluted in 50 µl of the supplied elution buffer. The concentration and purity of the cDNA was determined on the Nanodrop® ND-1000 spectrophotometer (Thermo Fisher Scientific, Inc.).

3.2.9 Construction of AD plasmid/cDNA libraries

3.2.9.1 Preparation of the cDNA products and pACT2 AD plasmid vector

The cDNA derived from Vero mammalian cells (1.3 µg) and KC insect cells (1.2 µg), respectively, as well as the pACT2 AD plasmid vector (2 µg) were digested with 12 U of *Sfi*I (TaKaRa Bio, Inc.) at 50°C for 3 h. The digestion products were purified with the NucleoSpin® II extract kit (Mackerey-Nagel). To prevent self-ligation of the digested pACT2 AD plasmid vector, the vector DNA was dephosphorylated by addition of 10 U of Shrimp alkaline phosphatase (10 U/µl; Fermentas), 4 µl of 10 × reaction buffer (0.1 M Tris-HCl; 0.1 M MgCl₂; 1 mg/ml BSA) and UHQ water to a final volume of 40 µl. Following incubation at

37°C for 2 h, the reaction mixture was heated to 70°C for 20 min in order to inactivate the phosphatase enzyme and then purified with the NucleoSpin[®] II extract kit (Mackerey-Nagel).

3.2.9.2 Ligation of DNA fragments

The digested cDNA products and dephosphorylated pACT2 AD plasmid vector were ligated overnight at 16°C in a final volume of 20 µl, which contained 2 µl of a 10 × DNA ligase buffer and 1 µl of T4 DNA ligase (100 U/µl; TaKaRa Bio, Inc.). The ratio of insert to vector DNA was 5:1. Following incubation, the ligation reactions were precipitated by addition of 3 volumes of absolute EtOH, 2 µl of tRNA (10 mg/ml; Sigma-Aldrich) and 3 M NaOAc (pH 5) to a final concentration of 0.3 M. The DNA was collected by centrifugation at 13 000 rpm for 30 min at 4°C, rinsed with 70% EtOH, vacuum-dried and suspended in 15 µl of UHQ water.

3.2.9.3 Preparation of electrocompetent *E. coli* JM109 cells

Electrocompetent *E. coli* JM109 cells were prepared according to the method of Dr. C. Maritz-Oliver, Department Genetics, University of Pretoria (personal communication). A 2-L Erlenmeyer flask containing 500 ml of LB broth was inoculated with 5 ml from an overnight *E. coli* JM109 culture and incubated at 37°C with shaking. Once the culture had reached an OD₆₀₀ of 0.5, the flask was incubated on ice for 20 min to inhibit further bacterial growth. The culture was divided into two equal volumes and the cells were harvested by centrifugation at 5000 rpm for 10 min at 4°C. Each cell pellet was suspended in 10 ml of ice-cold UHQ water and a further 240 ml of ice-cold UHQ water was then added. After mixing the suspensions gently, the cells were harvested as described above. Each cell pellet was washed twice more with the same procedure. After the third wash, the cell pellets were each suspended in 10 ml of ice-cold 10% glycerol. The cell suspensions were then pooled, incubated on ice for 1 h and the cells harvested by centrifugation at 5000 rpm for 10 min at 4°C. The cell pellet was finally suspended in 500 µl of ice-cold 10% glycerol. The cells were divided into aliquots of 90 µl and stored at -70°C.

3.2.9.4 Electroporation

For electroporation, the cells (90 µl) were thawed on ice and then mixed with the ligation reaction mixture (15 µl). The cells were transferred into a pre-chilled 0.1-cm inter-electrode gap electroporation cuvette (BioRad) and exposed to a single electrical pulse with a BioRad Gene Pulser[™] set at 2 000 V for 4 ms. Immediately following the electrical discharge, the

contents of the cuvette was transferred into a 1.5-ml Eppendorf tube and 800 µl of LB broth was added. Following incubation at 30°C for 1 h, aliquots of 50 µl of the electroporated cells were plated onto LB agar containing ampicillin in 150-mm diameter Petri dishes (Sterilin). The agar plates were incubated overnight at 37°C. Following incubation, 5 ml of LB-broth was added to each plate and the bacterial growth was scraped from the surface of the agar with a sterile hockey stick. The bacterial growth was suspended in 500 ml of LB broth containing 25% (v/v) glycerol in a 1-L Erlenmeyer flask. Aliquots (1 ml) of the respective plasmid cDNA libraries were pipetted into 1.5-ml Eppendorf tubes and stored at -70°C. The percentage of clones containing insert DNA and the titre of each plasmid cDNA library was determined, as described below, prior to using the respective cDNA libraries in the yeast two-hybrid screen.

3.2.10 Characterization of constructed AD plasmid/cDNA libraries

3.2.10.1 Determining the percentage of recombinant clones

To determine the percentage of recombinant clones in the plasmid cDNA libraries derived from Vero and KC cells, fifteen colonies of each cDNA library were selected randomly and subjected to colony PCR reactions. Each PCR reaction (25 µl) contained a single bacterial colony as source of template DNA, 1 × PCR buffer (50 mM KCl; 10 mM Tris-HCl [pH 9.0]; 0.1% [v/v] TritonX-100), 1.5 mM MgCl₂, 200 µM of each dNTP, 10 pmol of each the pACT2 Nested Forward (5'- TGTATGGCTTACCCATACGATGTTCC - 3') and pACT2 Nested Reverse primer (5'- GGGTTTTTTCAGTATCTACGATTCATAG- 3') and 2 U of SuperTherm *Taq* DNA polymerase (Whitehead Scientific). The tubes were placed in a Perkin-Elmer GeneAmp[®] 2700 thermal cycler. Following incubation at 94°C for 2 min, the samples were subjected to 30 cycles of denaturation at 94°C for 30 s, primer annealing at 55°C for 1 min and elongation at 72°C for 1 min. After the last cycle, a final elongation step was performed at 72°C for 2 min to complete synthesis of all DNA strands. For control purposes, reaction mixtures containing all reagents except template DNA were included. Aliquots of the PCR reaction mixtures were analyzed by agarose gel electrophoresis in the presence of an appropriate DNA molecular weight marker.

3.2.10.2 Titering of AD plasmid/cDNA libraries

The titres of the AD plasmid/cDNA libraries derived from Vero and KC cells were determined according to the procedures described in the Matchmaker[™] GAL4 Two-Hybrid

System 3 User Manual (Clontech Laboratories, Inc.). For this purpose, two dilutions of each AD plasmid/cDNA library were prepared in LB broth, *i.e.* a 10^{-3} (Dilution A) and a 10^{-6} (Dilution B) dilution. Subsequently, 1 μl from Dilution A was added to 50 μl of LB broth, mixed and the entire mixture was plated onto LB agar containing ampicillin. Two aliquots (50 μl and 100 μl) of Dilution B were also plated onto LB agar containing ampicillin. The agar plates were incubated overnight at 37°C, and the titre (cfu/ml) was calculated as follows:

- Dilution A: No. colonies $\times 10^3 \times 10^3 = \text{cfu/ml}$
- Dilution B: (No. colonies / plating volume) $\times 10^3 \times 10^3 \times 10^3 = \text{cfu/ml}$

3.2.11 Large-scale plasmid isolation of Vero and KC cDNA libraries

To obtain sufficient amounts of the plasmid cDNA libraries for large-scale yeast transformation, the plasmid DNA was isolated with the NucleoBond™ PC1000 kit (Macherey-Nagel) according to the manufacturer's instructions. An aliquot of the cDNA library (250 μl) was inoculated into a 2-L Erlenmeyer flask containing 500 ml of LB broth supplemented with ampicillin, and cultured at 30°C until an OD_{600} of 0.6 was reached. The cells were harvested by centrifugation at 5000 rpm for 15 min at 4°C, suspended in 4 ml of buffer S1 and then lysed by the sequential addition of buffers S2 and S3. The cell lysate was clarified by filtration through a NucleoBond® folded filter and the flow-through was then loaded onto a NucleoBond® AX 100 column. The column was washed twice with buffer N3 and the plasmid DNA was then eluted with 5 ml of the supplied elution buffer. During elution, 1-ml fractions were collected and the plasmid DNA in each fraction was precipitated immediately by addition of 800 μl of isopropanol. The precipitated plasmid DNA was collected by centrifugation at 15 000 rpm for 30 min at 4°C, washed with 70% EtOH and vacuum-dried. The pelleted DNA was suspended in 50 μl of UHQ water and then pooled. The integrity of the plasmid DNA was verified by agarose gel electrophoresis and its concentration was determined with a Nanodrop® ND-1000 spectrophotometer (Thermo Fischer Scientific, Inc.).

3.2.12 Sequential transformation of AH109 yeast cells with the DNA-BD/bait construct and AD plasmid/cDNA libraries

3.2.12.1 Transformation with pGBKT7-NS3₁₋₁₀₈

The DNA-BD/bait construct, pGBKT7-NS3₁₋₁₀₈, was introduced into *S. cerevisiae* AH109 yeast cells by making use of a mini-scale transformation method (Dr. C. Maritz-Olivier, personal communication). The AH109 yeast strain was streaked onto YPDA agar and

incubated for a maximum of 72 h at 30°C. A single yeast colony was then inoculated into 1 ml of UHQ water in a 2-ml Eppendorf tube, vortexed and the cells harvested by centrifugation at 13 000 rpm for 30 s. To make the yeast cell walls porous (competent), the cell pellet was suspended in 1 ml of 100 mM LiOAc (pH 7.5) and incubated at 30°C for 5 min without shaking. Following incubation, the cells were harvested by centrifugation (13 000 rpm for 30 s) and then transformed by adding the following reagents, in the indicated order, to the cell pellet: 240 µl of 50% (w/v) PEG-4000, 36 µl of 1 M LiOAc (pH 7.5), 25 µl of heat-denatured salmon sperm DNA (2 mg/ml; Sigma-Aldrich) and 500 ng of plasmid DNA in 50 µl of UHQ water. The transformation mixture was vortexed for 2 min and then incubated at 42°C for 20 min in a water bath. The cells were harvested by centrifugation, suspended in 250 µl of UHQ water and plated onto Minimal Synthetic Dropout (SD) agar that lacked tryptophan (SD/-Trp). The agar plates were incubated at 30°C until colonies were visible (2-5 days). The transformed yeast strain was first evaluated to verify that the DNA-DB/bait construct did not autonomously activate reporter gene expression prior to transforming it with the AD plasmid/cDNA libraries derived from Vero and KC cells.

3.2.12.2 Test for autonomous reporter gene activation

To test for transcriptional activation of reporter genes, the transformed AH109 yeast strains were plated onto SD/-Trp, SD/-His/-Trp (DDO, Double dropout) and SD/-His/-Trp/-Leu (TDO, Triple dropout) agar. The agar plates were incubated at 30°C for 2-5 days and inspected daily for growth. No growth was observed on the DDO and TDO media, indicating a lack of autonomous reporter gene activation. To confirm that the bait construct did not activate the *lacZ* reporter gene, a colony lift assay for activation of the *lacZ* reporter gene expression was also performed (refer to Section 3.2.13.2).

3.2.12.3 Transformation with AD plasmid/cDNA libraries

AH109 yeast cells, containing the bait construct pGBKT7-NS3₁₋₁₀₈, was subsequently used for library-scale transformations. These transformations were performed according to the 5 × TRAFCO transformation protocol (<http://to.trends.com>). The transformed yeast strain was inoculated into 12.5 ml of SD/-Trp medium and incubated overnight at 30°C with shaking. The cell titre was determined with a Nanodrop spectrophotometer at OD₆₆₀ and the volume of the cell suspension required to yield 1.25×10^8 cells in 25 ml of YPDA broth was calculated. This volume of the culture (25 ml) was transferred into a 50-ml Greiner tube (Greiner Bio

One) and the cells were harvested by centrifugation at 3000 rpm for 5 min. The cell pellet was suspended in 25 ml of pre-warmed (30°C) YPDA broth and transferred into a sterile 100-ml Erlenmeyer flask. The culture was incubated at 30°C with shaking for 3 to 4 h, until a cell titre of 2×10^7 cells/ml was obtained ($OD_{660} = 1.040$). The cells were then harvested by centrifugation, as described above, and washed once with 12.5 ml of UHQ water. The cell pellet was suspended in 180 μ l of 100 mM LiOAc (pH 7.5) and incubated at 30°C for 15 min without shaking. The cells were harvested by centrifugation and the following reagents, in the indicated order, were added to the cell pellet: 1.2 ml of 50% (w/v) PEG-4000, 180 μ l of 1 M LiOAc (pH 7.5), 250 μ l of heat-denatured salmon sperm DNA (2 mg/ml; Sigma-Aldrich), 15 μ g of the AD plasmid/cDNA library (derived from either Vero or KC cells) and 240 μ l of UHQ water. The cell pellet was vortexed until totally suspended, after which the transformation mixture was incubated at 30°C for 30 min. Subsequently, the mixture was incubated at 42°C for 15 min in a water bath and mixed by inversion for 15 s after every 5 min. The cells were harvested (3000 rpm, 5 min) and suspended gently in 5 ml of UHQ water. The transformation mixture was then plated in aliquots of 500 μ l onto SD/-Trp/-Leu agar. The agar plates were incubated at 30°C until co-transformed colonies were visible (2-5 days). To collect colonies that grew on the agar, the agar surface was flooded with 1 ml of SD/-Trp/-Leu broth containing 25% (v/v) glycerol and the growth was scraped from the surface of the agar. The suspension was pipetted in aliquots of 1 ml into 1.5-ml Eppendorf tubes and stored at -70°C.

3.2.13 Two-hybrid screening of reporter genes

3.2.13.1 Nutritional marker genes

Co-transformed AH109 yeast colonies were screened for protein-protein interactions on selective media with increasing stringency. An aliquot (1 ml) of the stored co-transformed yeast cells was thawed on ice, after which the cells were harvested by centrifugation at 3000 rpm for 2 min and suspended in 1 ml of UHQ water. Serial 10-fold dilutions were prepared in SD/-Trp/-Leu broth and the 10^{-1} , 10^{-2} and 10^{-3} dilutions were plated onto SD/-Trp/-Leu/-His agar. The agar plates were incubated at 30°C until colonies were visible (2-5 days). Colonies that grew on the agar were subsequently inoculated onto the same selective agar medium for use as master plates, as well as onto SD/-Trp/-Leu/-His/-Ade (QDO; Quadruple dropout) agar for further selection. All agar plates were incubated overnight at 30°C.

3.2.13.2 β -galactosidase colony-lift filter assays

The QDO-positive yeast colonies were inoculated in duplicate onto QDO agar plates. The agar plates were incubated for 2-4 days at 37°C until the colonies were *ca.* 1-3 mm in diameter. One of the agar plates was stored at 4°C and the duplicate was used to screen for activation of the *lacZ* reporter gene, as described in the Matchmaker™ GAL4 Two-Hybrid System 3 User Manual (Clontech Laboratories, Inc.). A sterile dry Whatman No.1 filter paper, cut to the shape and size of the Petri dish, was placed onto the agar surface and the orientation of the filter paper on the agar surface marked. The filter paper was gently and evenly pressed down onto the agar surface in order to allow for transfer of the yeast colonies to the filter paper. The filter paper was subsequently removed and transferred, with the colonies facing up, into liquid nitrogen. The filter paper was completely submerged in the liquid nitrogen for 10 s, removed and then allowed to thaw at room temperature. This freeze-thaw procedure was repeated three times in order to ensure lysis of the yeast cells. Finally, the filter paper was placed onto a second piece of filter paper, which had been pre-soaked in 100 ml of Z buffer (16.1 g/l Na₂HPO₄·7H₂O; 5.5 g/l NaH₂PO₄; 0.75 g/l KCl; 0.46 g/l MgSO₄·7H₂O; pH 7) containing 167 µl of an X-Gal solution (20 mg/ml). The filter paper was incubated at room temperature and examined periodically for the appearance of blue colonies. Yeast AH109 colonies transformed with a β -galactosidase positive control plasmid (pCL1) or co-transformed with control plasmids capable of two-hybrid interaction (pVA3 and pTD1) were also included in the assays. Colonies with a blue phenotype within 8 h of incubation were identified on the master plate and selected for further screening by nested PCR.

2.3.14 Nested PCR screening of positive clones

Yeast colonies that grew on the QDO agar were selected and screened by nested PCR to confirm the presence of insert cDNA and to determine the size of the cloned insert cDNA. The reaction mixtures used in the first PCR step contained *ca.* 1 µl of cells, 1 × KAPA *Taq* ReadyMix (KAPA Biotechnologies), 15 pmol of each the pACT2 Forward and Reverse primer (Table 3.1) and UHQ water to a final volume of 20 µl. The tubes were placed in a Perkin-Elmer GeneAmp® 2700 thermal cycler. Following incubation at 94°C for 7 min to lyse the yeast cells, the samples were subjected to 30 cycles of denaturation (94°C, 30 s), primer annealing (60°C, 30 s) and elongation (72°C, 2 min). The second nested PCR step was performed in a final volume of 20 µl by using 1 µl of the first PCR product as the template, 1 × KAPA *Taq* ReadyMix (KAPA Biotechnologies), and 12 pmol of each the pACT2 Nested

Forward primer (5' - TGTATGGCTTACCCATACGATGTTCC - 3') and pACT2 Nested Reverse primer (5' - GGGTTTTTCAGTATCTACGATTCATAG - 3'). The thermocycling programme was the same as above, except that primer annealing was performed at 55°C. The PCR reaction mixtures were analyzed by electrophoresis on a 1% (w/v) agarose gel in the presence of an appropriate DNA molecular weight marker.

2.3.15 Plasmid isolation from yeast

Plasmid DNA was isolated from QDO- and *lacZ*-positive colonies according to the method of Dr. C. Maritz-Olivier (personal communication). The yeast colonies were cultured overnight at 30°C in 1 ml of TDO broth before adding 4 ml of YPDA medium and growing the cultures for a further 4 h. The cells were harvested by centrifugation at 3000 rpm for 5 min and then suspended in 200 µl of “Smash-and-Grab” buffer (1% [w/v] SDS; 2% [v/v] TritonX-100; 100 mM NaCl; 10 mM Tris-HCl; 1 mM EDTA; pH 8). Subsequently, 200 µl of phenol:chloroform:isoamyl alcohol (25:24:1), as well as glass beads (425-600 µm; Sigma-Aldrich) were added and the mixture was vortexed vigorously for 3 min to lyse the yeast cells. Following centrifugation at 13 000 rpm for 5 min, the DNA-containing aqueous layer was recovered and the plasmid DNA was precipitated by addition of 0.5 volumes of 7.5 M NH₄OAc (pH 5) and 2 volumes of absolute EtOH. The precipitated plasmid DNA was collected by centrifugation at 13 000 rpm for 30 min, washed with 70% EtOH, vacuum-dried and suspended in 20 µl of UHQ water.

2.3.16 Rescue of AD/cDNA library plasmids and sequencing of the cDNA inserts

To rescue the AD/cDNA library plasmids, electrocompetent *E. coli* KC8 cells were prepared and transformed by electroporation with the extracted plasmid DNA (Section 3.2.15). The transformation mixtures were plated onto M9 minimal agar supplemented with ampicillin but lacking leucine. Following incubation of the agar plates at 37°C for 72 h, single colonies were inoculated into 1 ml of LB broth containing ampicillin and incubated overnight at 37°C. Plasmid DNA was extracted and the presence of cloned insert DNA was verified by performing PCR assays with the pACT2 Forward and Reverse primers, as described previously (Section 3.2.14). The identity of the cloned cDNA was determined by automated nucleotide sequencing procedures with the ABI-PRISM[®] BigDye[™] Terminator Cycle Sequencing Ready Reaction kit v.3.1 (Applied Biosystems), and the pACT2 Forward or Reverse primer as the sequencing primer (Table 3.1). The nucleotide and deduced amino acid

sequences were compared against entries in the GenBank database by using the BLAST-N and BLAST-P programmes, respectively (Altschul *et al.*, 1997). Multiple sequence alignments were performed with ClustalW included in the BioEdit v.7.0.4.1 (Hall, 1999) software package.

3.3 RESULTS

3.3.1 Construction of the recombinant bait vector pGBKT7-NS3₁₋₁₀₈

Towards identifying cellular proteins that may interact with the NS3 protein of AHSV-3, a yeast two-hybrid screening approach was employed. Notably, the structure of the NS3 protein comprises a long N-terminal and a short C-terminal cytoplasmic tail that are connected by two hydrophobic transmembrane domains and a short extracellular domain (Van Staden *et al.*, 1995; Van Niekerk *et al.*, 2003). Previous studies have implicated both hydrophobic domains (amino acid residues 111-137 and 154-170) within the NS3 protein as being important for membrane insertion (Van Niekerk *et al.*, 2001a). Thus, the hydrophobic domains could possibly interfere with the yeast two-hybrid system since the fusion proteins have to localize in the nucleus of the yeast cell where activation of the reporter genes occurs. Moreover, in the case of BTV NS3, it has been reported that the outer capsid protein VP2 binds to the C-terminal of NS3 (Beaton *et al.*, 2002; Celma and Roy, 2009), whereas different host cell proteins assisting in virus egress bind to the N-terminal of NS3 (Beaton *et al.*, 2002; Wirblich *et al.*, 2006). Based on these considerations, a bait expression plasmid was thus constructed in which the N-terminal region of AHSV-3 NS3, spanning amino acid residues 1-108 (NS3₁₋₁₀₈), was cloned into the DNA-BD plasmid vector pGBKT7.

By making use of plasmid pCMV-NS3-eGFP as template DNA, PCR amplification was performed with primers NS3-Nterm-Forward (containing a *Bam*HI site) and NS3-Nterm-Reverse (containing a *Pst*I site), as described under Materials and Methods (Section 3.2.7). The NS3-Nterm-Reverse primer was furthermore designed to incorporate a TAA stop codon at the 3'-end of the PCR-amplified truncated NS3 gene in order to terminate translation without the inclusion of additional vector-derived sequences. An aliquot of the reaction mixture was analyzed by agarose gel electrophoresis and a single discreet amplicon of the expected size (324 bp) was observed (Fig. 3.1, lane 2). In contrast, no amplification products were observed in the negative control in which template DNA was omitted.

The amplicon was gel-purified and ligated into pGEM[®]-T Easy vector DNA. Following transformation of competent *E. coli* JM019 cells, recombinant transformants with a Lac⁻ phenotype were selected from X-gal - containing indicator plates and cultured in LB broth supplemented with ampicillin. The extracted plasmid DNA was analyzed by agarose gel electrophoresis. Plasmid DNA migrating slower than the parental pGEM[®]-T Easy vector DNA were selected and analyzed for the presence of a cloned insert DNA by using restriction endonucleases of which the recognition sites had been incorporated during the design of the primers. The putative recombinant plasmid DNA was therefore digested with both *Bam*HI and *Pst*I. Following agarose gel electrophoresis, restriction fragments of *ca.* 3 kb and 324 bp, respectively, were observed, which is in agreement with the expected size of the pGEM[®]-T Easy vector (3 kb) and insert DNA (324 bp) (Fig. 3.1, lane 7). A recombinant clone, designated pGEM-NS3-N-terminal, was selected and the integrity of the cloned insert DNA was verified by nucleotide sequencing prior to it being used in further DNA manipulations. To construct the recombinant bait plasmid, the insert DNA was recovered from pGEM-NS3-N-terminal by digestion with both *Bam*HI and *Pst*I, and cloned into similarly prepared pGBKT7 vector DNA. A recombinant plasmid from which an insert of the expected size was excised by digestion with both *Bam*HI and *Pst*I (Fig. 3.1, lane 10) was designated pGBKT7-NS3₁₋₁₀₈.

Prior to using pGBKT7-NS3₁₋₁₀₈ in two-hybrid screens, the nucleotide sequence of the cloned insert DNA was determined in order to confirm that the truncated NS3 bait was cloned in the correct reading frame, *i.e.* the reading frame of GAL4 DNA-BD which forms the N-terminal part of the fusion protein. The results indicated that excepting for the introduction of the stop codon at the 3'-end of the NS3 gene to terminate translation of the DNA-BD - NS3 fusion protein, no other differences were observed between the sequence of the cloned truncated NS3 gene and that of the AHSV-3 NS3 gene determined previously (GenBank Acc. No. D12479.1). In addition, analysis of the deduced amino acid sequence confirmed that the open reading frame of the DNA-BD - NS3 fusion protein was indeed maintained and that the cloning strategy therefore did not create any unintended in-frame stop codons (Fig. 3.2).

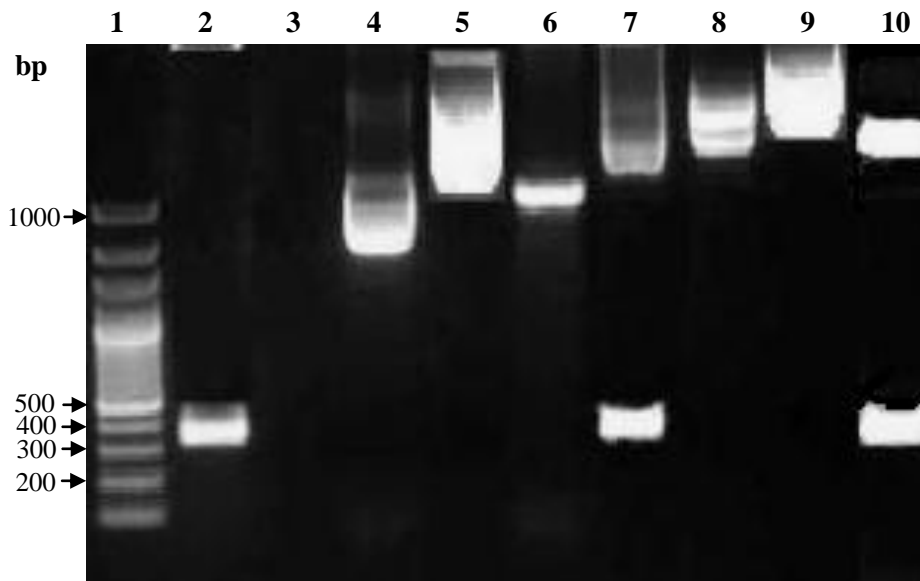


Fig. 3.1: Agarose gel electrophoretic analysis of the recombinant plasmid pGBKT7-NS3₁₋₁₀₈. Lane 1, DNA molecular weight marker; lane 2, amplicon obtained by PCR amplification using pCMV-NS3-eGFP plasmid DNA as template and primers NS3-Nterm-Forward and NS3-Nterm-Reverse; lane 3, negative control PCR reaction mixture lacking template DNA; lane 4, uncut parental pGEM[®]-T Easy vector DNA; lane 5, uncut recombinant plasmid pGEM-NS3-N-terminal; lane 6, pGEM[®]-T Easy vector DNA linearized with *Pst*I (vector lacks *Bam*HI site); lane 7, recombinant plasmid pGEM-NS3-N-terminal digested with both *Bam*HI and *Pst*I; lane 8, uncut parental pGBKT7 vector DNA; lane 9, uncut recombinant plasmid pGBKT7-NS3₁₋₁₀₈; lane 10, recombinant plasmid pGBKT7-NS3₁₋₁₀₈ digested with both *Bam*HI and *Pst*I. The sizes of the DNA molecular weight marker, GeneRuler™ 100 bp DNA Ladder Plus (Fermentas), are indicated to the left of the figure.

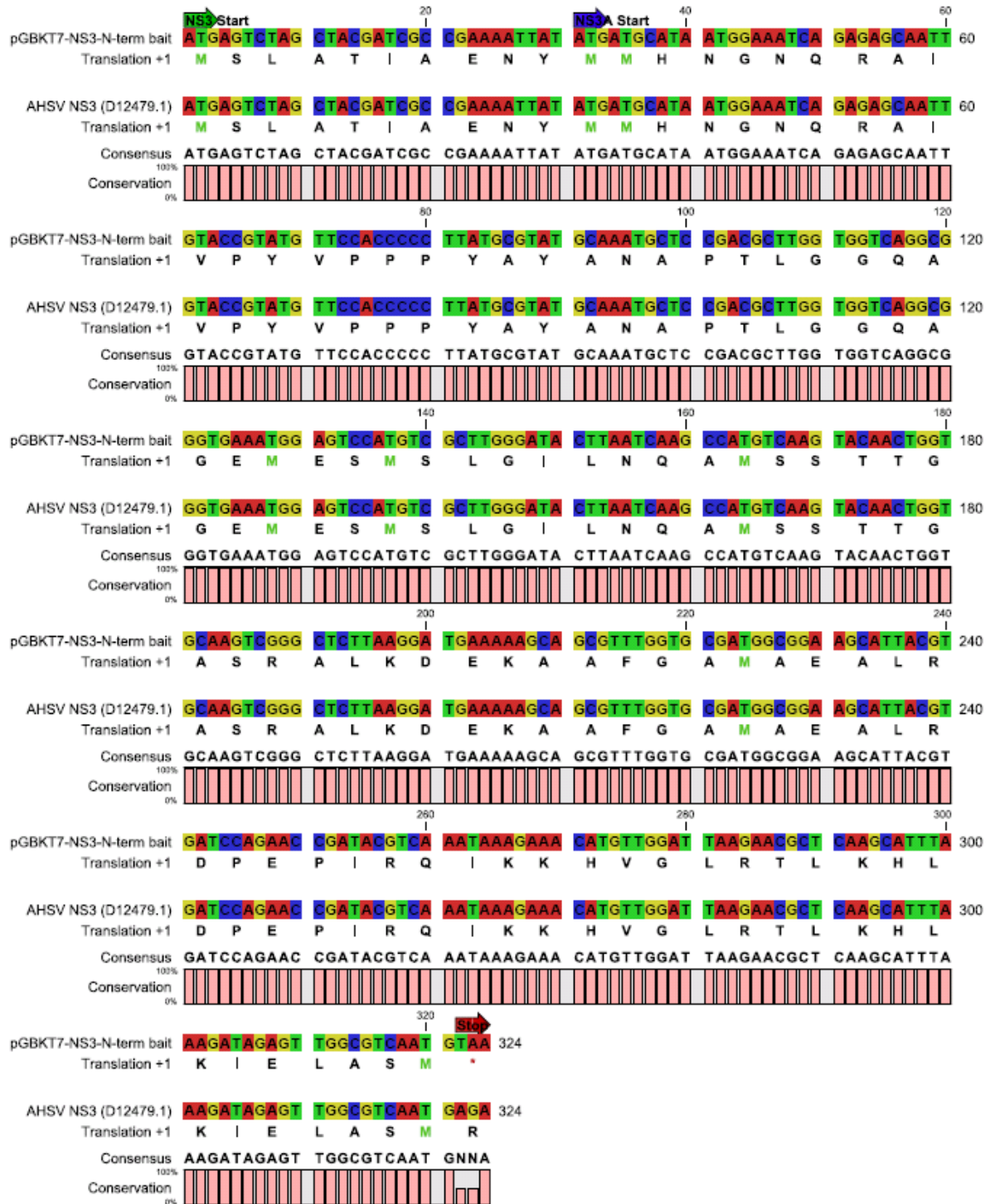


Fig. 3.2: Nucleotide and amino acid sequence alignments of the truncated NS3-N₁₋₁₀₈ bait construct and the corresponding region of AHSV-3 NS3 (GenBank Acc. No. D12479.1). The initiation codons for NS3 and NS3A are indicated with arrows. The stop codon that was introduced during PCR amplification of the truncated NS3 gene is indicated with a red asterisk.

3.3.2 Construction of AD plasmid/cDNA libraries

Although orbiviruses are predominantly released from infected mammalian cells after cell lysis, it has been noted that virus egress may also occur by budding from the plasma membrane during the early stages of infection. In vector insect cells, release is non-lytic and the virus particles leave the infected cells by budding at the plasma membrane (Hyatt *et al.*, 1989; Guirakhoo *et al.*, 1995; Stoltz *et al.*, 1996). Since orbivirus egress has only been studied in mammalian cell culture, it is therefore not known whether the same or different mechanisms underlie the egress observed from infected mammalian and vector insect cells. Based on the role that cellular proteins play in assisting budding of especially non-enveloped viruses (Welsch *et al.*, 2007; Chen and Lamb, 2008) and the involvement of NS3 in virus release (Hyatt *et al.*, 1991; Hyatt *et al.*, 1992; Stoltz *et al.*, 1996), yeast two-hybrid screens have been used previously to identify cellular proteins interacting with NS3 of BTV (Beaton *et al.*, 2002) and AHSV (Beyleveld, 2007). However, these screens have relied on the use of non-host cell cDNA libraries, *i.e.* a commercially available HeLa and *Drosophila melanogaster* cDNA library, respectively. Therefore, in this study, cDNA libraries were constructed from Vero mammalian cells and KC (*Culicoides variipennis*) insect cells. The Vero cell line is susceptible to AHSV infection (Stoltz *et al.*, 1996; Chapter 2, this dissertation), whereas *C. variipennis* has been shown to experimentally transmit AHSV (Boorman *et al.*, 1975).

For cDNA library construction, total RNA was isolated from Vero and KC cell monolayers at 12-h intervals from 24 h to 48 h post-incubation, and the RNA samples of each cell line were pooled in order to obtain representative RNA populations. The respective total RNA samples were reverse transcribed and the cDNA amplified by long-distance (LD)-PCR. The optimal number of thermal cycles was determined, as described under Materials and Methods (Section 3.2.8.3), in order to limit the generation of non-specific PCR products. The respective cDNA samples were subsequently digested with *Sfi*I, of which the recognition site had been incorporated in the primers used for cDNA synthesis. Analysis of aliquots of the digested cDNA samples indicated a smear ranging from less than 250 bp to *ca.* 3 kb (Fig. 3.3). The digested cDNA was subsequently cloned into the *Sfi*I site of the pACT2 AD plasmid vector, which had been treated with phosphatase to remove the 5' phosphate groups and thus prevent self-ligation of the vector DNA. Following electroporation of *E. coli* JM 109 cells with the respective ligation reaction mixtures, the number of independent clones was determined by

PCR amplification of the insert cDNA directly from randomly selected transformed cells. For this purpose, primers were used that anneal to regions flanking the multiple cloning site of the pACT2 vector.

The results that were obtained following colony PCR of *E. coli* JM109 cells transformed with the Vero cell cDNA library (Fig. 3.4a) and the KC cell cDNA library (Fig. 3.4b) indicated that the size of the insert cDNAs in both of these plasmid cDNA libraries ranged between 150 bp and 400 bp. These were considered to represent cloned cDNA inserts since their sizes were greater than that of the 101-bp multiple cloning site of non-recombinant pACT2, amplified in control PCR reactions (Figs. 3.4a and 3.4b, lanes 2). The Vero and KC cell cDNA libraries were subsequently amplified and the titre of the respective libraries was determined. For both the Vero cell cDNA library (6.2×10^8 cfu/ml) and the KC cell cDNA library (7.2×10^8 cfu/ml), the titres were in agreement with that proposed for plasmid cDNA libraries (10^8 cfu/ml) to render them suitable for use in two-hybrid screens (Clontech Laboratories, Inc.).

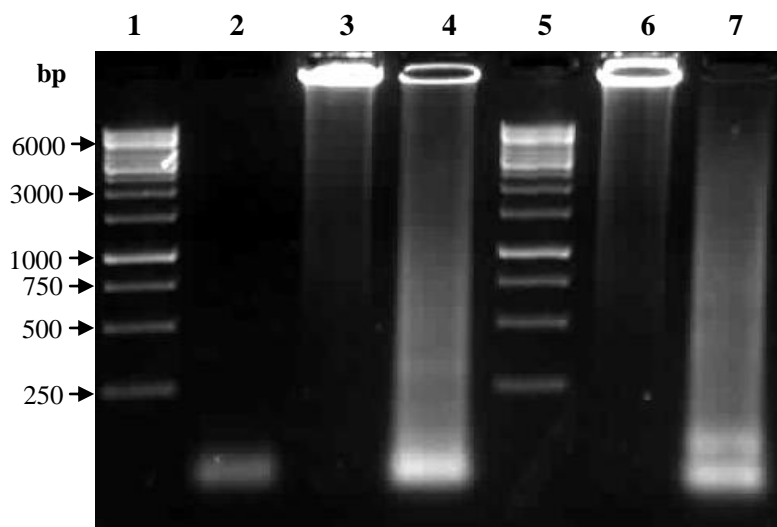
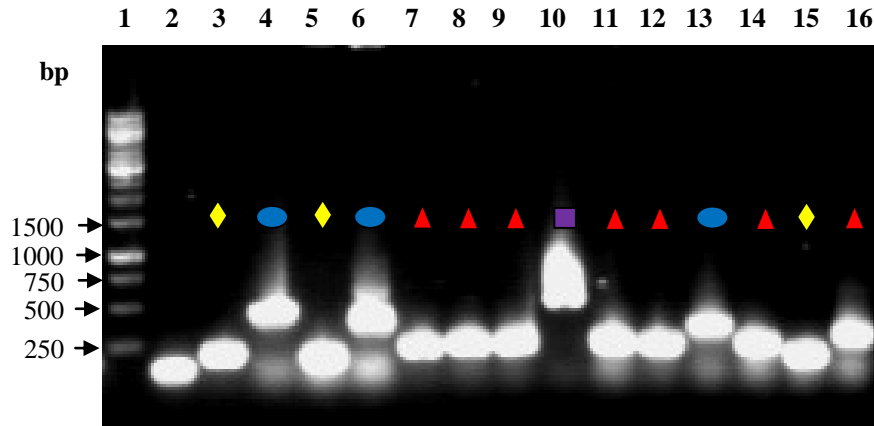


Fig. 3.3: Agarose gel electrophoretic analysis of the double-stranded cDNA amplified by LD-PCR, following reverse transcription of total RNA extracted from Vero mammalian cells and KC insect cells. Lanes 1 and 5, DNA molecular weight marker; lane 2, negative PCR reaction mixture lacking template; lane 3, undigested LD-PCR amplified cDNA from KC insect cells; lane 4, *Sfi*I-digested cDNA from KC insect cells; lane 6, undigested LD-PCR amplified cDNA from Vero mammalian cells; lane 7, *Sfi*I-digested cDNA from Vero mammalian cells. The sizes of the DNA molecular weight marker, GeneRuler™ 1 kb DNA Ladder Plus (Fermentas), are indicated to the left of the figure.

(a)



(b)

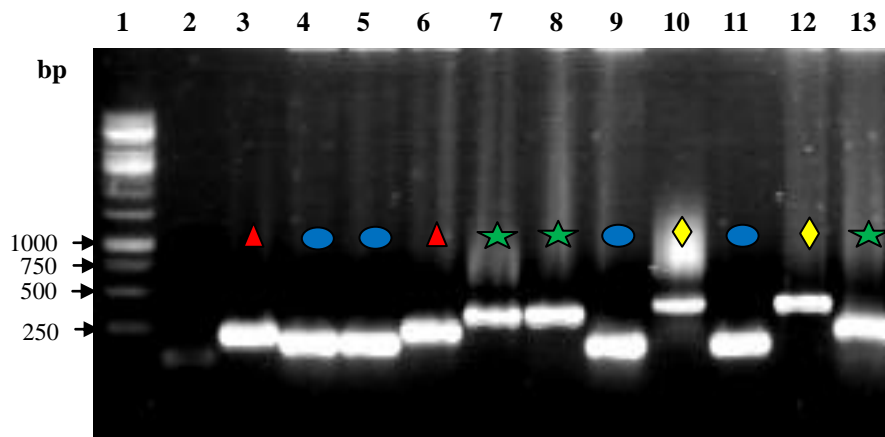


Fig. 3.4: PCR screening of *E. coli* JM 109 colonies, following transformation with pACT2 AD plasmid/cDNA libraries of Vero mammalian cells (a) and KC insect cells (b). Colony PCR was performed with the pACT2 Nested Forward and pACT2 Nested Reverse primers that anneal to sites flanking the multiple cloning site of the pACT2 vector. As a control, the primers were also used in a PCR reaction with non-recombinant pACT2 as the template DNA (lanes 2). Each of the subsequent lanes indicates the PCR amplicon that was obtained from randomly selected individual colonies. The sizes of the DNA molecular weight marker (lanes 1), GeneRuler™ 1 kb DNA Ladder Plus (Fermentas), are indicated to the left of the figures. Coloured symbols in the respective figures indicate clones containing similarly sized cDNA inserts.

3.3.3 Two-hybrid screening for protein-protein interactions

To detect interaction of AHSV-3 NS3 with cellular proteins *in vivo* in yeast cells, *S. cerevisiae* strain AH109 was used for transformations. This yeast strain contains *trp⁻* and *leu⁻* as selection markers, as well as the reporter genes *HIS3*, *ADE2* and *MEL1* (or *lacZ*) downstream of heterologous GAL4-responsive promoter elements. As a result of making use of multiple different reporter genes, two major classes of false positives are eliminated, *i.e.* those that interact directly with the sequences flanking the GAL4 binding site and those that interact with transcription factors bound to specific TATA boxes (Clontech Laboratories, Inc.).

The AH109 yeast strain was thus sequentially transformed with the pGBKT7-NS3₁₋₁₀₈ bait plasmid and with either the pACT2 AD/Vero or pACT2 AD/KC cell cDNA libraries by the lithium acetate method. Transformation with the plasmid cDNA libraries was only performed once it had been established that transformation of the AH109 yeast strain with the recombinant bait plasmid did not activate the reporter genes, as described under Materials and Methods (Section 3.2.12.2). The co-transformed AH109 cells were subsequently plated onto synthetic dropout medium lacking tryptophan and leucine (Trp⁻ Leu⁻) to select for yeast cells containing both the bait and cDNA library plasmids, as well as to determine the co-transformation efficiency. In the case of yeast cells co-transformed with the truncated NS3 bait and Vero cell cDNA library, the co-transformation efficiency was calculated at 4.6×10^4 cfu/ μ g and the number of clones screened (cfu/ μ g \times amount of library plasmid used) was thus 6.9×10^5 . In the case of yeast cells co-transformed with the truncated NS3 bait and KC cell cDNA library, the co-transformation efficiency was calculated at 5×10^4 cfu/ μ g and the number of clones screened was 7.5×10^5 .

The co-transformants were subsequently plated onto dropout medium lacking tryptophan, leucine and histidine (Trp⁻ Leu⁻ His⁻), followed by plating onto dropout medium lacking tryptophan, leucine, histidine and adenine (Trp⁻ Leu⁻ His⁻ Ade⁻) to enable stringent selection of interacting clones. Co-transformants that grew on the latter medium were also assayed for β -galactosidase expression by colony-lift filter assays, using X-gal as the chromogenic substrate. Typical results that were obtained during two-hybrid screening are indicated in Fig. 3.5.

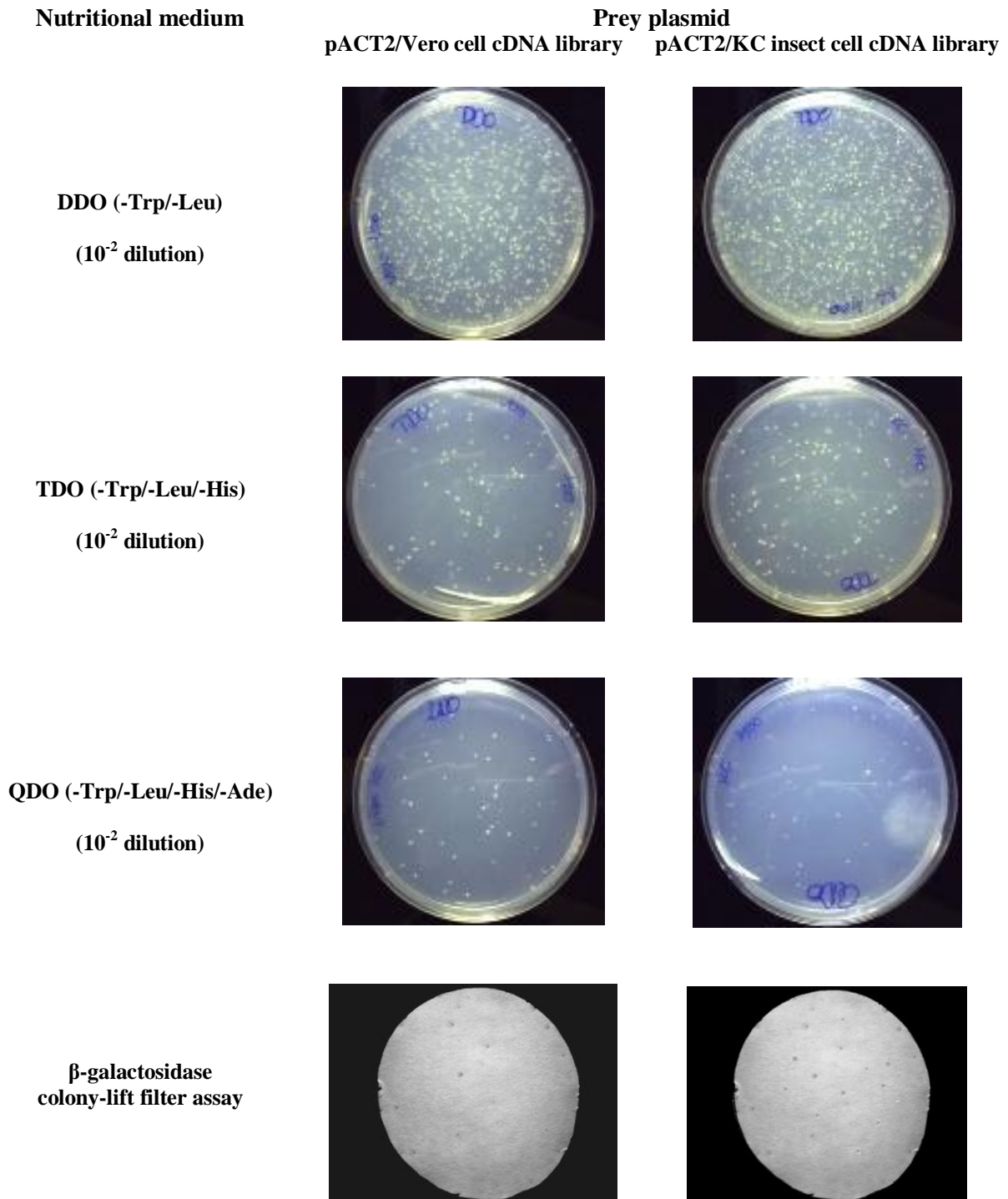


Fig. 3.5: Screening of co-transformed AH109 yeast colonies for putative protein-protein interactions between a truncated NS3 protein and cDNA library proteins. The yeast cells were co-transformed with the bait plasmid pGBKT7-NS3₁₋₁₀₈ and either the Vero mammalian or KC insect cell cDNA library. The co-transformed yeast colonies were plated onto increasingly stringent selection media (DDO, TDO and QDO), after which individual yeast colonies from the QDO agar plates were transferred to filter paper and assayed for β -galactosidase activity. The blue colonies are positive for β -galactosidase activity.

In total, 70 of 100 co-transformants of the truncated NS3 and Vero cell cDNA library, and 90 of 100 co-transformants of the truncated NS3 and KC cell cDNA library screened were able to activate transcription of the reporter genes. To eliminate duplicates, the respective pACT2 AD/cDNA library inserts were subsequently amplified by nested PCR with primer pairs that anneal to sites flanking the multiple cloning site of pACT2. Since yeast colonies were used as source of template DNA in the first round of PCR, this approach not only facilitated the rapid screening of a large number of yeast colonies, but the use of nested primers in the second PCR step also prevented amplification of spurious products originating from the high concentration of chromosomal DNA present in the samples. Following agarose gel electrophoresis, the results obtained for QDO- and *lacZ*-positive yeast clones containing the Vero cell cDNA library as prey led to the identification of two unique clones of which the size of the insert cDNA was *ca.* 300 and 400 bp, respectively (Fig. 3.6a). Similarly, only a single clone was identified following screening of the QDO- and *lacZ*-positive yeast clones containing the KC cell cDNA library as prey. All of these clones contained a cDNA insert of *ca.* 250 bp (Fig. 3.6b).

3.3.4 Sequencing and sequence analysis of positive AD/cDNA library inserts

After screening for reporter gene activation and nested PCR to eliminate duplicates, yeast clones were selected that appeared to encode AD fusion proteins capable of interacting with the NS3₁₋₁₀₈ bait protein. However, since it is possible that insert cDNAs of the same size may differ in nucleotide sequence and thus in their encoded products, a number of clones with similar insert size were also included in the analyses. Therefore, ten yeast clones co-transformed with the Vero cell cDNA library and nine yeast clones co-transformed with the KC cell cDNA library were selected for further characterization. These yeast clones, however, contained both the pGBKT7-NS3₁₋₁₀₈/bait and pACT2 AD/cDNA library plasmids, and thus necessitated that the pACT2 AD/cDNA library plasmids be rescued in order to allow for sequencing of the cloned insert cDNA. Consequently, both plasmid DNAs were isolated from the interacting yeast clones and then electroporated into *E. coli* KC8 cells, which carry a *leuB* mutation that can be complemented by *LEU2* from yeast. Thus, KC8 cells can be used to rescue pACT2 cDNA library plasmids (which carry *LEU2* and are amp^r) from yeast co-transformants that also contain a pGBKT7-NS3₁₋₁₀₈ bait plasmid (which carry *TRP1* and are kan^r). The yeast clones were therefore grown on minimal medium containing ampicillin and lacking leucine to only select for pACT2 AD/cDNA library plasmids. The plasmid DNA was

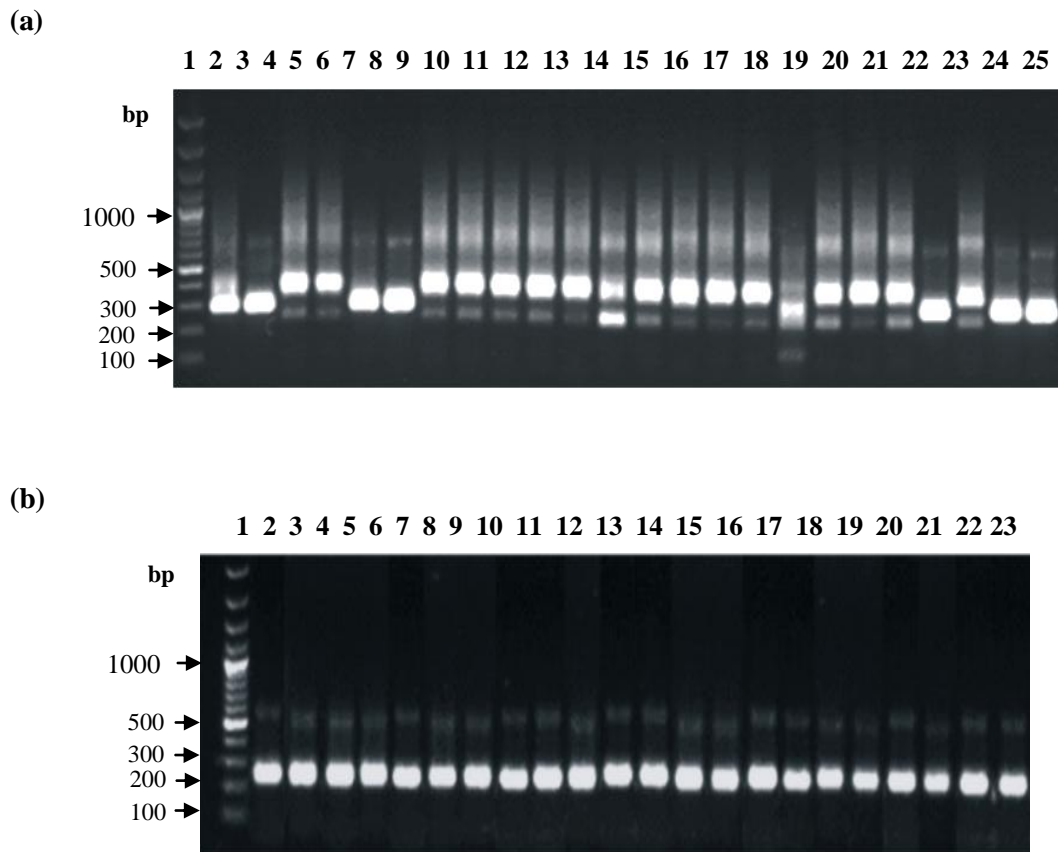


Fig. 3.6: Nested PCR screening of *S. cerevisiae* strain AH109 colonies, containing the NS3₁₋₁₀₈ bait plasmid and plasmid cDNA libraries of Vero mammalian cells (a) and KC insect cells (b). Representative results are shown for co-transformed yeast colonies that tested QDO- and *lacZ*-positive during two-hybrid screening. Nested PCR was performed with primer pairs that anneal to different sites flanking the multiple cloning site of the pACT2 vector. The sizes of the DNA molecular weight marker (lanes 1), GeneRuler™ 100 bp DNA Ladder Plus (Fermentas), are indicated to the left of the figures. Each of the subsequent lanes indicates the PCR amplicon that was obtained from different positive colonies.

subsequently extracted and subjected to nested PCR, as described above, to confirm the presence and size of the insert DNA (results not shown). The insert cDNA in the positive pACT2 AD/cDNA library plasmids were sequenced and the presence of an open reading frame fused to the GAL4 AD sequence was verified prior to comparing the sequences to those in the GenBank database by BLAST-N and BLAST-P analyses.

Of the ten independent yeast clones selected following two-hybrid screening of the Vero cell cDNA library, two of the cDNA clones encoded a 27-amino acid protein that displayed sequence identity to putative proteins of unknown function. The other eight cDNA clones encoded an identical 44-amino acid protein. A BLAST-P search of this amino acid sequence revealed 100% sequence identity to the ribosomal protein L34 of *Xenopus laevis*, and significant levels of sequence identity (92 to 97%) were found with the L34 protein from various different vertebrates (mammals) (Table 3.2). A multiple alignment of the amino acid sequences of the different L34 proteins (Fig. 3.7) revealed a high level of overall homology among all of the proteins. The ribosomal protein L34 is located in the cytoplasm of cells and is not only a component of the 60S subunit of eukaryotic ribosomes, but has also been implicated in the regulation of cyclin-dependent kinases 4 and 5 (Moorthamer and Chaudhuri, 1999) and polyamine biosynthesis (Panagiotidis *et al.*, 1995).

Similar to above, two different cDNA clones were isolated repeatedly from the nine independent yeast clones selected following two-hybrid screening of the KC cell cDNA library. One cDNA clone was isolated from four yeast clones and encoded a 25-amino acid protein that displayed sequence identity (64 to 70%) to the uracil-xanthine permease enzyme of different proteobacteria. It should be noted that despite this apparent high level of sequence identity, the expect (E) value was high (0.83 to 4.4) and thus suggested that the match was not significant. The other cDNA clone, isolated from five yeast clones, encoded a 46-amino acid protein that was identified as SARA (Smad anchor for receptor activation). This sequence, which mapped to the C-terminal of SARA proteins from both vertebrate (mammals) and invertebrate (insect) species, showed higher sequence identity (55 to 76%) with the SARA protein of invertebrates compared to that of vertebrates (44 to 46% sequence identity) (Table 3.3). An alignment of this NS3₁₋₁₀₈ - interacting sequence with the respective SARA proteins is shown in Fig. 3.8. SARA is a FYVE domain-containing membrane scaffold protein and is implicated in transforming growth factor- β (TGF- β) signalling (Tsukazaki *et al.*, 1998; Itoh *et al.*, 2002).

Table 3.2: Summary of BLAST-P information for Vero cell prey proteins that interacted with the AHSV-3 NS3₁₋₁₀₈ bait protein

NS3 ₁₋₁₀₈ interacting amino acid sequence			
QDQACFPYRGAENRCESVEGTSTESKS			
Vero prey clone no.	BLAST-P result	GenBank Acc. No.	Sequence identity
3, 26	rCG62942 - <i>Rattus norvegicus</i> (Norwegian rat)	EDL78697.1	92%
	rCG28883 - <i>Rattus norvegicus</i>	EDL82203.1	92%
NS3 ₁₋₁₀₈ interacting amino acid sequence			
GGRAYGGSMCAKCVDRDIKRAFLIEEQKIVVKVLKAQAQSQKAK			
Vero prey clone no.	BLAST-P result	GenBank Acc. No.	Sequence identity
10, 20, 35, 41, 43, 45, 48, 51	Rpl34 protein - <i>Xenopus laevis</i> (African clawed frog)	AAH99259.1	100%
	ribosomal protein L34 - <i>Rattus rattus</i> (black rat)	CAA32574.1	97%
	ribosomal protein L34 - <i>Lama pacos</i> (llama)	ABD90466.1	97%
	60S ribosomal protein L34-like <i>Callithrix jacchus</i> (marmoset)	XP_002759051.1	97%
	60S ribosomal protein L34-like - <i>Macaca mulatta</i> (rhesus monkey)	XP_001089444.1	97%
	ribosomal protein L34 - <i>Bos taurus</i> (feral cattle)	AAI03315.1	97%
	ribosomal protein L34 - <i>Homo sapiens</i> (human)	NP_000986.2	97%
	60S ribosomal protein L34 - <i>Mus musculus</i> (house mouse)	NP_001005859.1	97%
	similar to ribosomal protein L34 - <i>Equus caballus</i> (Camargue horse)	XP_001490058.1	95%
	similar to ribosomal protein L34 - <i>Pan troglodytes</i> (chimpanzee)	XP_512977.1	92%

Vero prey	-----	
<i>X. laevis</i>	MAPRLTYRRRLSYNTTSNKTRLSRTPGNRIVVLYTKKVGKAPKSACGICPGLRLGIRAVR	60
<i>R. rattus</i>	MVQRLTYRRRLSYNTASNKTRLSRTPGNRIVVLYTKKVGKAPKSACGVLPGRLRGVRAVR	60
<i>L. pacos</i>	MVQRLTYRRRLSYNTASNKTRLSRTPGQDRLPLHQEGRESTYIRMWRVPRQTARGPCCE	60
<i>C. jacchus</i>	MVQRLTYRRRLTYNTASNKTRLSRTPGNRIVVLYTKKVGKAPKSACGVCPRLRGVRVAVR	60
<i>M. mulatta</i>	MVQRLTYRRRLSYNTASNKTRLSQTPGNIIVVLYTKKVGKAPKSACGVCPRLRGVRVAVR	60
<i>B. taurus</i>	----LTYRRRLSYNTASNKTRLSRTPGNRIVVLYTKKVGKAPKSACGVCPRLRGVRVAVR	56
<i>H. sapiens</i>	MVQRLTYRRRLSYNTASNKTRLSRTPGNRIVVLYTKKVGKAPKSACGVCPRLRGVRVAVR	60
<i>M. musculus</i>	MVQRLTYRRRLSYNTASNKTRLSRTPGNRIVVLYTKKVGKAPKSACGVCPRLRGVRVAVR	60
<i>E. caballus</i>	MVQRLTYRHRLSYNTASNKTRLSRTPGNRIVVLYTKKVGKAPKSACGVCPRLQGVRAVR	60
<i>P. troglodytes</i>	MVQRLTYQCRLSYNTASNKTRLPRTPGNRIVVLYTKKVGKAPRSASGMCPGLRGVRAVR	60
Vero prey	-----GGRAYGGSMCAKCVDRDIKRAFLIEEQKIVVKVLKAQAQSQKAK	44
<i>X. laevis</i>	PKVLMRLSKTKKHVGRAYGGSMCAKCVDRDIKRAFLIEEQKIVVKVLKAQAQSQKAK	117
<i>R. rattus</i>	PKVLMRLSKTKKHVSRA YGGSMCAKCVDRDIKRAFLIEEQKIVVKVLKAQAQSQKAK	117
<i>L. pacos</i>	TQVLMRLSKTKKHVSRA YGGSMCAKCVDRDIKRAFLIEEQKIVVKVLKAQAQSQKAK	117
<i>C. jacchus</i>	PKVLMRLSKTKKHVSRA YGGSMCAKCVDRDIKRAFLIEEQKIVVKVLKAQAQSQKAK	117
<i>M. mulatta</i>	PKVLMRLSKTKKHVSRA YGGSMCAKCVDRDIKRAFLIEEQKIVVKVLKAQAQSQKAK	117
<i>B. taurus</i>	PKVLMRLSKTKKHVSRA YGGSMCAKCVDRDIKRAFLIEEQKIVVKVLKAQAQSQKAK	113
<i>H. sapiens</i>	PKVLMRLSKTKKHVSRA YGGSMCAKCVDRDIKRAFLIEEQKIVVKVLKAQAQSQKAK	117
<i>M. musculus</i>	PKVLMRLSKTQKHVSRA YGGSMCAKCVDRDIKRAFLIEEQKIVVKVLKAQAQSQKAK	117
<i>E. caballus</i>	PKVLMRLSKTKKHVSRA YGGSMCAKCVDRDIKRAFLIEEQKIVVKVLKAQAQSQKAK	117
<i>P. troglodytes</i>	PKVLRKLSKRKKHVSRA YGGSMCAKCVDRGRIKRAFLIEEQKIVVKVLKAQVQSHKAK	117
	.*****.***:*****.*.:**	

Fig. 3.7: Alignment of the amino acid sequence of a 44-amino acid Vero cell protein with the full-length amino acid sequences of different L34 ribosomal proteins. The numbers indicate the multiple alignment positions from the N terminus of each protein. The alignment was maximized by introducing gaps, which are indicated by dashes. Identical (*), highly similar (:), and similar (.) amino acids are indicated in only the overlapping sequence (highlighted in yellow). The sequences were obtained from the GenBank accession numbers indicated in Table 3.2.

Table 3.3: Summary of BLAST-P information for KC cell prey proteins that interacted with the AHSV-3 NS3₁₋₁₀₈ bait protein

NS3 ₁₋₁₀₈ interacting amino acid sequence			
GEVVAVIGVDLVGVSIVLTRIQQDQ			
KC prey clone no.	BLAST-P result	GenBank Acc. No.	Sequence identity
6, 23, 26, 43	uracil-xanthine permease - <i>Variovorax paradoxus</i> S110	YP_002941997.1	70%
	uracil-xanthine permease - <i>Acidovorax ebreus</i> TPSY	YP_002551557.1	64%
	uracil-xanthine permease - <i>Rhodferax ferrireducens</i> T118	YP_521362.1	64%
NS3 ₁₋₁₀₈ interacting amino acid sequence			
SQHNKLAPLYMNALDNELVPTLHRQAGNLHIDTPIILELIFHILDK			
KC prey clone no.	BLAST-P result	GenBank Acc. No.	Sequence identity
2, 10, 22, 25, 35	smad anchor for receptor activation - <i>Aedes aegypti</i> (mosquito)	XP_001659765.1	76%
	smad anchor for receptor activation - <i>Culex quinquefasciatus</i> (Southern house mosquito)	XP_001845691.1	73%
	smad anchor for receptor activation - <i>Drosophila melanogaster</i> (fruit fly)	AAF64468.1	57%
	zinc finger protein FYVE domain-containing protein, putative - <i>Pediculus humanus corporis</i> (body louse)	XP_002428675.1	56%
	similar to Smad anchor for receptor activation - <i>Apis mellifera</i> (honey bee)	XP_396901.2	55%
	zinc finger, FYVE domain-containing 9 isoform 2 - <i>Bos taurus</i> (feral cattle)	XP_869045.2	46%
	similar to zinc finger FYVE domain-containing protein 9 - <i>Equus caballus</i> (Camargue horse)	XP_001493880.2	46%
	Smad anchor for receptor activation - <i>Homo sapiens</i> (human)	AAC99462.1	44%
	zinc finger, FYVE domain-containing 9 - <i>Pan troglodytes</i> (chimpanzee)	XP_001144371.1	44%

(a)

KC prey	1	SQHNKLAPLYMNALDNELVPTLHRQAGNLHIDTPIILELIFHILDK	46
<i>A. aegypti</i>	1376	SQYNKLGPLYMNALDNELVPTLHRQAGNLHIDTPIILELIFHILDK	1421
<i>C. quinquefasciatus</i>	1277	SQYSKLGPLYMNALDNELVPTLHRQAGNLHIDTPIILELIFHILDK	1322
<i>D. melanogaster</i>	1300	ARGSKLPPLYMNALDNELVPTLHRQAGNLHIDTPIILELIFHILDK	1343
<i>P. corporis</i>	724	SNGEKLAPIYMNALDNELVPTLHRQAGNLHIDTPIILELIFHILDK	767
<i>A. mellifera</i>	1183	SEGMLPPIYMNALDNELVPTLHRQAGNLHIDTPIILELIFHILDK	1266
		:. ** *::*:**.*: .*: :: : : : **::**:::	

(b)

KC prey	1	SQHNKLAPLYMNALDNELVPTLHRQAGNLHIDTPIILELIFHILDK	46
<i>B. taurus</i>	1434	SNGQPLPSQYMNLDLSALVPVIHGGACQLSEG-PIVMELIFYILEN	1478
<i>E. caballus</i>	1338	SNGQPLPSQYMNLDLSALVPVIHGGACQLNEG-PIVMELIFYILEN	1382
<i>H. sapiens</i>	1287	SNGQPLPSQYMNLDLSALVPVIHGGACQLSEG-PVVMELIFYILEN	1331
<i>P. troglodytes</i>	1379	SNGQPLPSQYMNLDLSALVPVIHGGACQLSEG-PVVMELIFYILEN	1423
		*: : *.. *** ** .***:* * :* . *::**::**:::	

Fig. 3.8: Alignment of the amino acid sequence of a 46-amino acid KC cell protein with the amino acid sequences of invertebrate SARA proteins (a) and vertebrate SARA proteins (b). The numbers indicate the multiple alignment positions from the N terminus of each protein. The alignment was maximized by introducing gaps, which are indicated by dashes. Identical (*), highly similar (:), and similar (.) amino acids are also indicated. The sequences were obtained from the GenBank accession numbers indicated in Table 3.3.

3.3.5 Verification of NS3-host cell protein interactions

Despite its strength as a means to investigate protein-protein interactions, a major weakness of the yeast two-hybrid system is the possibility of a high number of false positive identifications (Serebriiskii *et al.*, 2000; Deane *et al.*, 2002; Rual *et al.*, 2005). Thus, to confirm the putative interactions detected in the above screens, additional yeast two-hybrid assays were performed. For this purpose, clone 35 of the derived Vero cell cDNA library and clone 10 of the KC cell cDNA library were selected and designated pACT2-L34 and pACT2-SARA, respectively.

- **Re-testing of phenotypes**

As an initial test, the purified rescued prey plasmid cDNAs (pACT2-L34 and pACT2-SARA) were re-transformed into fresh AH109, together with the pGBKT7-NS3₁₋₁₀₈ bait plasmid, and then re-screened for protein-protein interaction by making use of the same procedures described previously. The results indicated that each of the two preys identified during the course of this study tested positive for interaction with the NS3₁₋₁₀₈ bait, but tested negative for interaction with the un-fused GAL4 DNA-BD domain (Fig. 3.9).

- **Reverse yeast two-hybrid screens**

To further confirm the putative interactions, the library insert cDNA was also transferred from the pACT2 AD to the pGBKT7 DNA-BD vector and *vice versa*, and the two-hybrid assays were repeated. Thus, to construct the desired pGBKT7 DNA-BD plasmids, both the SARA and L34 cDNA inserts were PCR-amplified, using the recombinant pACT2 AD/cDNA library constructs as template DNA and the appropriate primers (Section 3.2.7 and Table 3.1), to generate amplicons of 189 and 127 bp, respectively. The amplicons were cloned into pGEM[®]-T Easy vector DNA and then characterized by nucleotide sequencing to confirm their integrity. The respective insert DNAs were subsequently recovered and cloned directionally into the *Bam*HI and *Pst*I sites of pGBKT7 to generate pGBKT7-SARA and pGBKT7-L34, respectively. Restriction of the derived recombinant bait plasmids with both *Bam*HI and *Pst*I resulted in the excision of DNA fragments of the expected sizes (Fig. 3.10, lanes 3 and 5, respectively). The cloned insert DNAs were also characterized by nucleotide sequencing, the results of which indicated the absence of any mismatches and confirmed that the open reading frame of the DNA-BD - SARA and DNA-BD - L34 fusion proteins were maintained (results not shown).

Since pACT2 lacks a *Pst*I site in its multiple cloning site, it was not possible to simply excise and reclone the truncated NS3₁₋₁₀₈ insert DNA from pGBKT7 into the pACT2 vector. Therefore, the truncated NS3 gene was obtained by PCR amplification. Using a similar cloning strategy as above, the truncated NS3 gene was PCR-amplified using the recombinant pGBKT7-NS3₁₋₁₀₈ construct as template DNA, together with primers NS3-Nterm-Forward and NS3-N-Xho (Table 3.1). Following PCR, the 324-bp amplicon was cloned into pGEM[®]-T Easy vector DNA. The integrity of the cloned insert DNA was verified by nucleotide sequencing prior to cloning the truncated NS3 gene into the *Bam*HI and *Xho*I sites of pACT2 AD to generate pACT2-NS3₁₋₁₀₈. To confirm successful cloning of the insert DNA, the derived recombinant plasmid was digested with both *Bam*HI and *Xho*I and yielded expected bands corresponding to 8 kb (pACT2 vector) and 324 bp (insert DNA) (Fig. 3.10, lane 7). Moreover, nucleotide sequencing confirmed that the truncated NS3₁₋₁₀₈ gene was cloned in-frame with the AD of the pACT2 vector.

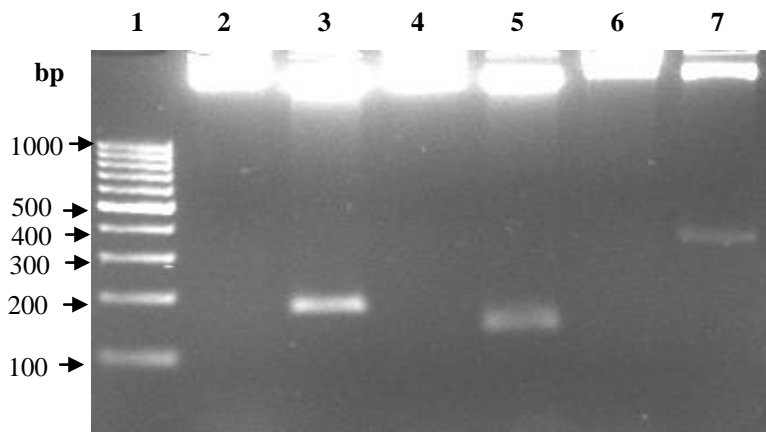


Fig. 3.9: Agarose gel electrophoretic analysis of plasmids constructed for reverse two-hybrid screening. Lane 1, DNA molecular weight marker; lane 2, uncut recombinant plasmid pGBKT7-SARA; lane 3, recombinant plasmid pGBKT7-SARA digested with both *Bam*HI and *Pst*I; lane 4, uncut recombinant plasmid pGBKT7-L34; lane 5, recombinant plasmid pGBKT7-L34 digested with both *Bam*HI and *Pst*I; lane 6, uncut recombinant plasmid pACT2-NS3₁₋₁₀₈; lane 7, recombinant plasmid pACT2-NS3 digested with both *Bam*HI and *Xho*I. The sizes of the DNA molecular weight marker, GeneRuler[™] 100 bp DNA Ladder (Fermentas), are indicated to the left of the figure.

Once the integrity of the respective vector constructs had been verified, the AH109 yeast strain was transformed sequentially with the vectors in pairwise combinations. As described previously, interaction of the candidate protein pairs was determined by the induction of three reporter genes, *HIS3*, *ADE2* and *lacZ*, based on growth on selective media and β -galactosidase colony-lift filter assays. The results indicated that activation of the respective reporter genes occurred only when NS3₁₋₁₀₈ and SARA fusion proteins were expressed together. In contrast, β -galactosidase activity was not detected when the NS3₁₋₁₀₈ and L34 fusion proteins were expressed together (Fig. 3.9). From these results it could therefore be concluded that SARA is capable of interacting with NS3 and that this interaction appears to be specific.

3.4 DISCUSSION

Host cell proteins may play an important role in mediating virus release from infected host cells. A wide variety of enveloped viruses recruit host proteins specifically to assist in the release of progeny virions from infected cells through budding (Bieniasz, 2006; Calistri *et al.*, 2009). In contrast, relatively little is known about the contributions of host proteins to egress of non-enveloped viruses such as the orbiviruses. Although the NS3 protein of BTV (Hyatt *et al.*, 1991; Hyatt *et al.*, 1992; Celma and Roy, 2009) and AHSV (Stoltz *et al.*, 1996; Meiring *et al.*, 2009) has been implicated in virus release, only two cellular partners of NS3 have been identified to date. The NS3 protein of BTV has been shown to interact with the cellular proteins p11 and Tsg101, and these interactions were shown to indeed assist in the egress of virus particles from infected cells (Beaton *et al.*, 2002; Wirblich *et al.*, 2006). Towards defining host cell proteins that interact with the AHSV NS3 protein, a yeast two-hybrid screening strategy was employed in this study. To this end, a Vero mammalian cell and KC insect cell cDNA library was constructed, and then screened using a truncated AHSV-3 NS3 protein (NS3₁₋₁₀₈) as bait. The respective screens identified L34 and SARA as NS3-interacting proteins. Of these, the interaction between NS3 and SARA appeared to be specific, as was evidenced by results obtained in pairwise reverse yeast two-hybrid screening assays.

In this study, the two-hybrid screens that were performed initially yielded only two NS3-interacting proteins. Several factors may account for these results. The approach adopted in








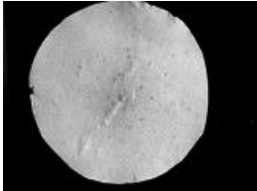
Reverse yeast two-hybrid screens		Nutritional (QDO) medium	β -galactosidase assay
Bait construct	Prey construct		
pGBKT7	pACT2		No β -galactosidase activity
pGBKT7	pACT2-NS3 ₁₋₁₀₈		No β -galactosidase activity
pGBKT7- NS3 ₁₋₁₀₈	pACT2		No β -galactosidase activity
pGBKT7	pACT2-L34		No β -galactosidase activity
pGBKT7-L34	pACT2-NS3 ₁₋₁₀₈		No β -galactosidase activity
pGBKT7	pACT2-SARA		No β -galactosidase activity
pGBKT7-SARA	pACT2-NS3 ₁₋₁₀₈		

Fig. 3.10: Reverse yeast two-hybrid screening to confirm putative protein-protein interactions. The bait vector (pGBKT7), containing either L34 or SARA as insert DNA, was respectively co-transformed into AH109 yeast cells with the prey vector (pACT2), containing NS3₁₋₁₀₈ as insert DNA. Co-transformation of pGBKT7 with either pACT2-SARA or pACT2-L34, as well as co-transformation of pGBKT7 and pACT2 was included as controls. Colony-lift filter assays for β -galactosidase activity were performed and the blue colonies are positive for β -galactosidase activity.

this study to prepare the respective plasmid cDNA libraries involved digestion of both the cDNA products and pACT2 AD vector with a single restriction endonuclease (*Sfi*I). Since non-directional plasmid cDNA libraries were therefore prepared, it can be expected that only one sixth of the cDNA products would be cloned in the correct open reading frame and this would necessitate that more than 10^6 clones be studied if a good representation is to be obtained (Sobhanifar, 2003). In this study, however, only 10^5 clones were screened, which are 10-fold less than recommended. In addition to the lack of an exhaustive screen, high-stringency selection procedures were employed to identify interaction clones. Although this approach purportedly virtually eliminates false positive interactions, it is, however, possible that low-affinity protein interactions may not have been detected in the respective two-hybrid screens. Moreover, a major drawback of testing protein-protein interactions in yeast is that interactions may depend on certain post-translational modifications (*e.g.* phosphorylation, glycosylation or disulfide bond formation), which may not occur properly or at all in the yeast strain (Fields and Sterngrandz, 1994). Furthermore, in the yeast two-hybrid system used in this study, the GAL4 DNA-BD domain was fused to the N-terminal end of the AHSV-3 NS3₁₋₁₀₈ bait protein. It has been reported that in some cases, where interactions occur at the N-terminal of the bait protein, the presence of the GAL4 DNA-BD domain may cause steric hindrance or altered protein conformation that impede interaction, thus causing false negatives (Causier and Davies, 2002; Brückner *et al.*, 2009). It should be noted that despite the identification of only a limited number of cellular partners for the AHSV-3 NS3 protein, these results are in agreement with results reported previously for similar studies undertaken on orbiviruses. In the case of BTV, 1.2×10^7 transformants of a commercial HeLa cDNA library were screened and only one NS3-interacting protein was identified (Beaton *et al.*, 2002). Likewise, screening of a commercial *D. melanogaster* cDNA library, of which the titre of the amplified library was greater than 10^9 cfu/ml, led to the identification of only two cellular proteins that putatively interact with AHSV NS3 (Beyleveld, 2007).

Two-hybrid screening, using NS3₁₋₁₀₈ as bait and a plasmid cDNA library derived from Vero mammalian cells as prey, resulted in the frequent isolation of a cDNA clone encoding an open reading frame with amino acid sequence identity to the ribosomal protein L34. The L34 protein, which is a constituent of the large (60S) subunit of the eukaryotic ribosome, is greatly conserved from prokaryotes to eukaryotes. The high conservativeness of L34 suggests that it might have been subjected to a strong selective pressure during evolution and therefore has a significant biological role (Vaccaro, 2003; Liu *et al.*, 2005). The L34 protein has been

reported to interact with cyclin-dependent kinases 4 (Cdk4) and 5 (Cdk5) (Moorthamer and Chaudhuri, 1999; Regenberg *et al.*, 2006). They form part of the cyclin-dependent kinase family and play key regulatory roles during progression of the eukaryotic cell cycle (Hanley-Hyde, 1992), contribute to cellular differentiation (Philpott *et al.*, 1997) and are implicated in apoptosis (Ahuja *et al.*, 1997; Lee *et al.*, 2000). In addition, L34 has also been reported to regulate polyamine biosynthesis by inhibiting ornithine decarboxylase, which is a key enzyme in the polyamine biosynthesis pathway (Panagiotidis *et al.*, 1995). Polyamines are low-molecular-weight aliphatic polycations found in the cells of all living organisms. Their positive charge enables polyamines to bind to macromolecules such as DNA, RNA and proteins. Consequently, polyamines are thought to play important roles in a number of cellular processes such as regulation of replication, transcription and translation (Igarashi *et al.*, 1988), as well as in the regulation of cell proliferation, modulation of cell signaling and membrane stabilization (Alm and Oredsson, 2009; Igarashi and Kashiwagi, 2010). Despite growth on QDO selective medium, no β -galactosidase activity was detected when NS3₁₋₁₀₈ and L34 were co-expressed in a reverse yeast two-hybrid screen. It may, however, be interesting to perform other protein-protein interaction assays before the NS3-L34 interaction is conclusively ruled out. Although it is unlikely that the L34 protein plays a role during virus release from infected cells, it is tempting to speculate that interaction of NS3 with L34 may modulate the metabolic activities of infected cells and, as such, could contribute to pathogenesis.

SARA, identified as the NS3₁₋₁₀₈ - interacting protein in a two-hybrid screen with the KC insect cell cDNA library, is a soluble cytoplasmic FYVE domain-containing protein and is found in both insect (Bennet and Alphey, 2002; Bökel *et al.*, 2006) and mammalian (Tsukazaki *et al.*, 1998; Hayes *et al.*, 2003; Szymkiewicz *et al.*, 2004) cells. The FYVE (Fab1, YOTB, Vac1p and EEA1) domain, of which the name has been derived from the first four proteins identified to harbour this motif (Stenmark *et al.*, 1996), is a zinc finger-like motif of 60-80 amino acid residues that binds to the membrane lipid phosphatidylinositol-3-phosphate (PtdIns(3)P) with high specificity (Burd and Emr, 1998; Gaullier *et al.*, 1998; Itoh *et al.*, 2002; Blatner *et al.*, 2004). PtdIns(3)P is highly enriched in limited (outer) membranes of the early endosomes (Panopoulou *et al.*, 2002; Gillooly *et al.*, 2003; Bökel *et al.*, 2006), and it has thus been suggested that proteins containing FYVE domains contribute to the trafficking of proteins associated with them to these locations (Downes *et al.*, 2005; Vicinanaza *et al.*, 2009). In addition to facilitating membrane localization of proteins, FYVE

domain-containing proteins have also been implicated in regulating the cytoskeleton and signal transduction (Gillooly *et al.*, 2001). Indeed, SARA is proposed to mediate TGF- β signaling in mammalian cells by recruiting the signal transducer proteins Smad2 and Smad3, thereby enabling these proteins to interact with the TGF- β receptor on the early endosomal membrane and initiate signal transduction (Tsukazaki *et al.*, 1998; Itoh *et al.*, 2002). TGF- β is a multifunctional cytokine involved during regulation of cell proliferation, differentiation, apoptosis and development (Roberts and Spora, 1993; Massagué, 2000). In *Drosophila* cells, SARA has been implicated in decapentaplegic (Dpp) signal transduction, which is an insect homologue of TGF- β (Entchev *et al.*, 2000; Bennet and Alpey, 2002).

In addition to SARA, two other FYVE domain-containing proteins are also localized to early endosomes. The EEA1 protein (early endosomal antigen 1) regulates endosome fusion (Jahn *et al.*, 2003), whilst Hrs (hepatocyte growth factor-regulated tyrosine substrate) has been shown to bind multiple proteins, including the signal transducing adaptor molecules Smad2 (Miura *et al.*, 2000) and STAM (Asao *et al.*, 1997; Bache *et al.*, 2004). Binding of Smad2 suggests that Hrs co-operates with SARA to stimulate TGF- β expression (Miura *et al.*, 2000), whereas the Hrs-STAM complex is known to mediate sorting of proteins for lysosomal degradation (Raiborg *et al.*, 2002; Raiborg *et al.*, 2007). In addition, Hrs also facilitates recruitment of the ESCRT protein complexes to the surface of early endosomal membranes via its interaction with the Tsg101 and HCRPI/Vps37 components of the ESCRT-I complex (Katzmann *et al.*, 2003; Stuchell *et al.*, 2004; Eastman *et al.*, 2005). This is subsequently followed by recruitment of the ESCRT-II and ESCRT-III complexes in a series of events that ultimately results in the inward budding of the limiting membrane to form intraluminal vesicles of multivesicular bodies (MVBs) (Katzmann *et al.*, 2002; Gruenberg and Stenmark, 2004; Hurley and Emr, 2006). Consequently, Hrs appears to play the role of a scaffold protein that sets the stage for a chain of multiple interactions that takes place at the endosomal membrane (Raiborg and Stenmark, 2002; Katzmann *et al.*, 2003).

Vesicle budding into the MVB and viral budding at the plasma membrane are considered to be topologically equivalent and it has been proposed that the same cellular machinery, could, in principle, catalyze both these processes (Pornillos *et al.*, 2002; Calistri *et al.*, 2009). Because NS3 of BTV and AHSV carries a late domain motif (PSAP and ASAP, respectively) and binds to mammalian Tsg101, as well as its insect orthologue, it has been proposed that NS3 may recruit the ESCRT machinery to facilitate virion particle budding and release

(Wirblich *et al.*, 2006). Indeed, depletion of Tsg101 by siRNA was shown to reduce virus release from BTV- and AHSV-infected mammalian cells. The localization of SARA to Hrs-enriched endosomes in both mammalian (Raiborg *et al.*, 2001; Sachse *et al.*, 2002) and insect (Bökel *et al.*, 2006) cells may therefore be of interest given the reported relationship between Tsg101 and NS3. Moreover, it was recently reported that Hrs, in addition to a PSAP late domain motif, contains multiple independent Tsg101 binding sites (Bouamr *et al.*, 2007). It is therefore tempting to speculate that the early endosomes may be enriched with Tsg101 and, following transport of NS3 to these sites via its association with SARA, it may be more readily accessible for interaction with NS3.

It is also important to note that although early work suggested that endocytosis is required for the SARA-TGF- β receptor-Smad complex to form (Tsukazaki *et al.*, 1998), several subsequent reports have indicated that this complex can occur independent of receptor internalization (Lu *et al.*, 2002; Penheiter *et al.*, 2002; Di Guglielmo *et al.*, 2003). Consequently, two distinct signaling pathways have emerged in which SARA is proposed to facilitate interaction of Smad2 and Smad3 with the TGF- β receptor at both the early endosome and plasma membrane (Massagué *et al.*, 2005; Knoblich *et al.*, 2006; Sorkin and von Zastrow, 2009). The latter is furthermore supported by immunofluorescent profiles that have demonstrated that SARA and the TGF- β receptors co-localize at the plasma membrane (Stenmark and Aasland, 1999; Penheiter *et al.*, 2002). Thus, in an alternative pathway, it could be that NS3 bound to SARA is transported directly to areas in the plasma membrane where the TGF- β receptors reside. Considering the close proximity of early endosomes to the periphery of both *Drosophila* insect cells (Bökel *et al.*, 2006) and mammalian cells (Katzmann *et al.*, 2002), it may be that NS3 could still be able to recruit Tsg101 and the rest of the ESCRT machinery from these sites.

In conclusion, yeast two-hybrid screening assays resulted in the identification of SARA as an NS3₁₋₁₀₈ - interacting protein and the interaction with this cellular protein appeared to be specific as was evidenced in a pairwise reverse two-hybrid assay. SARA is a membrane anchor protein and could conceivably play a role in NS3 trafficking *in vivo*. It is possible that SARA acts by localizing NS3 to the endosomal and/or plasma membranes, whereafter Tsg101 and the ESCRT machinery may be recruited to aid in virus budding and release. Although the mechanisms underlying these protein-protein interactions require further

investigation, the findings nevertheless support the notion that AHSV requires access to multiple cellular proteins in order to facilitate processes such virus trafficking and release.

CHAPTER FOUR

CONCLUDING REMARKS

Although much progress has been made regarding the structure-function relationship of different African horsesickness virus (AHSV) genes and encoded gene products (Vreede and Huismans, 1994; Uitenweerde *et al.*, 1995; Maree and Huismans, 1997; Van Staden *et al.*, 1995; Van Niekerk *et al.*, 2001a; de Waal and Huismans, 2005), knowledge of the molecular biology of AHSV and the role of each protein in the virus life cycle is still lacking. Amongst the AHSV-encoded proteins, the non-structural protein NS3 has been implicated in virus release from infected cells (Stoltz *et al.*, 1996; Meiring *et al.*, 2009), but the exact role of NS3 in this process remains to be clarified. In the case of the closely related Bluetongue virus (BTV), evidence has been presented indicating that NS3 is functionally involved in virus egress by forming a bridge between the outer capsid protein VP2 and the cellular export machinery (Beaton *et al.*, 2002; Wirblich *et al.*, 2006; Celma and Roy, 2009). No similar information, however, is available for AHSV NS3. Consequently, the aims of this investigation were essentially to determine the involvement of NS3 in virus release and to identify cellular proteins capable of interacting with NS3. Details of the results obtained in the course of achieving these aims have been discussed in the individual chapters. The new information that has evolved during this investigation will be briefly summarized and suggestions regarding future research will be made.

An RNA interference (RNAi)-based approach was used in this investigation to determine whether AHSV NS3 indeed mediates virus egress from infected cells. RNAi is an evolutionary conserved cellular pathway that induces degradation of target mRNA in a sequence-specific manner, leading to post-transcriptional silencing of gene expression (Fire *et al.*, 1998; Elbashir *et al.*, 2002a). Consequently, it has become a powerful research tool whereby loss-of-function phenotypes can be generated and thereby allowing virus gene function to be determined (López *et al.*, 2005; Carvalho *et al.*, 2006; Cuadras *et al.*, 2006; Zambrano *et al.*, 2007; Kobayashi *et al.*, 2009). By making use of an *in vitro* model of infection, results were obtained during the course of this investigation indicating that the synthetic siRNA siNS3-266, corresponding to nucleotides 266-289 of the AHSV-3 NS3 gene, silenced NS3 protein and mRNA expression efficaciously in Vero mammalian cells.

Moreover, compared to control cells, Vero cells that had been treated with siNS3-266 prior to virus infection displayed a significant reduction in the percentage of released virus, albeit that the virus titres were similar in both instances (Chapter 2).

Although the above results are the first to provide direct experimental proof for the involvement of NS3 in AHSV release from infected cells, the exact mechanism whereby progeny virions are released remains to be investigated, as well as the involvement of other viral or cellular proteins in this process. In this regard, it is interesting to note that previous reports have suggested a role for the non-structural protein NS1, in conjunction with NS3, in virus release from infected cells (Owens *et al.*, 2004; Meiring *et al.*, 2009). Specifically, Owens *et al.* (2004) suggested that the level of NS1 protein relative to the level of NS3 protein in infected cells may dictate whether the progeny virions are released through budding (low level of NS1 relative to that of NS3) or cell lysis (high level of NS1 relative to that of NS3). The relationship between these two viral proteins and its effect on the mode of virus release may in future be investigated by siRNA-mediated gene silencing of the NS3 and NS1 genes, as well as silencing of both viral genes. Comparative analysis of the intracellular and extracellular titres, together with immuno-electron microscopy of the infected cells, may provide novel insights regarding the interplay of these two viral proteins and the mechanism of virus release.

In the case of BTV NS3, it has been shown that the C-terminal domain of NS3 interacts with VP2, the outermost protein of the fully assembled virus particle (Beaton *et al.*, 2002), whilst the N-terminus of NS3 can interact with the cellular proteins p11 (Beaton *et al.*, 2002) or Tsg101 (Wirblich *et al.*, 2006) to assist virus release from infected cells. These results therefore suggest that NS3 forms a bridging molecule that draws the assembled virus into contact with the cellular export machinery or facilitates virus release through hijacking of the ESCRT machinery, respectively. As such, the results provide compelling evidence for the involvement of host cellular proteins to aid in BTV release. To investigate whether AHSV NS3 recruits cellular proteins that may aid in budding and release of virus particles from infected cells, yeast two-hybrid screenings were performed. For this purpose, the N-terminus of the NS3 protein was used as bait and plasmid cDNA libraries derived from Vero mammalian cells and *Culicoides variipennis* (KC) insect cells were used as prey. Two NS3₁₋₁₀₈ - interacting proteins were identified, *i.e.* L34 from Vero cells and SARA from KC cells. These interactions were furthermore investigated by pairwise reverse yeast two-hybrid

screening assays, the results of which indicated that the NS3₁₋₁₀₈ - SARA interaction appears to be specific (Chapter 3). The ribosomal protein L34 is not linked to the cellular export pathway, but it has been implicated in growth regulation through inhibition of cyclin kinase-dependent kinase activity (Moorthamer and Chaudhuri, 1999; Regenber *et al.*, 2006), and in polyamine synthesis (Panagiotidis *et al.*, 1995). The significance of the NS3-L34 interaction is not clear, since activation of the *lacZ* reporter gene could not be observed in a reverse yeast two-hybrid screen. The finding that the AHSV NS3 protein interacts with SARA may have some significance. SARA is an evolutionary conserved protein that has been suggested to serve as a membrane scaffold protein in the TGF- β signaling pathway (Massagué *et al.*, 2005; Sorkin and von Zastrow, 2009). Notably, SARA has been shown to co-localize with the TGF- β receptors at the plasma membrane and early endosomes (Stenmark and Aasland, 1999; Penheiter *et al.*, 2002). Early endosomes are enriched with the Hrs protein (Raiborg *et al.*, 2001; Bökel *et al.*, 2006), which possesses multiple independent binding sites for Tsg101 (Bouamr *et al.*, 2007). Consequently, trafficking of NS3 to the early endosomes may thus provide a means whereby NS3 has an increased likelihood of binding to Tsg101 through its late domain motif. Alternatively, SARA may allow for targeting of the NS3 protein directly to the plasma membrane through the association of SARA with TGF- β receptors located at the plasma membrane.

Considering that no membrane-targeting signals has as yet been reported for orbivirus NS3 proteins, the finding that NS3 binds to SARA suggests a role for SARA in targeting NS3 to cellular membranes. However, further experiments are required to determine its involvement, if any, in virus egress. Since yeast two-hybrid screens are only capable of providing an overview of potential protein-protein interactions (Fields and Song, 1989; Brückner *et al.*, 2009), it would be important to validate the NS3-SARA interaction using a second independent assay. For this purpose, appropriately designed pull-down assays may be used and confirmation that such an interaction occurs within AHSV-infected cells may be assessed *in vivo* by co-localization assays using confocal laser scanning microscopy. A combination of deletion mapping and site-directed mutagenesis may furthermore aid in mapping the precise SARA-binding motif in NS3. To determine the biological importance of the interaction between NS3 and SARA, RNAi assays, similar to those described and used in this investigation (Chapter 2), together with determination of virus titers in treated and untreated cells, can be used to determine the effect of SARA depletion on AHSV release.

In addition to the above studies, it may also be useful to investigate the importance of the AHSV NS3 late domain motifs in greater detail. In this regard, it has been reported that the PTAP motif of BTV NS3 is capable of binding to Tsg101 (Wirblich *et al.*, 2006), but no functional studies have been undertaken to determine the functional importance of a second PPXY late domain motif in virus budding. This motif has been reported to play a role in recruiting host ubiquitin ligases (Bouamr *et al.*, 2003; Blot *et al.*, 2004; Martin-Serrano *et al.*, 2005) and it was shown that cellular ubiquitination machinery is important for the budding of several enveloped viruses (Patnaik *et al.*, 2000; Gottwein *et al.*, 2003; Licata *et al.*, 2003). Interestingly, it has been reported that the late domain motifs in BTV NS3 do not function as effectively as the late domains of HIV-1 and Ebola virus in facilitating the release of mini-Gag virus-like particles (Wirblich *et al.*, 2006). Therefore, it may be possible that other budding mechanisms may also be exploited by orbiviruses. A novel ESCRT-independent budding mechanism, which is controlled by RAb11 family interacting proteins (Rab11-FIPS), has recently been described as being important for budding of the enveloped Respiratory syncytial virus (RSV) from infected mammalian cells (Utley *et al.*, 2008). Considering the parallels between the release pathways of orbiviruses and those involved in release of enveloped viruses (*e.g.* Tsg101 and the MVB pathway), it may thus be of interest to investigate the possible importance of this newly described budding mechanism in AHSV egress.

In summary, the results of this investigation indicated that NS3 of AHSV is capable of mediating virus release from infected mammalian cells. Furthermore, it was shown that NS3 interacts with host cell proteins, albeit that the biological relevance of these interactions and their contribution to virus release, if any, remains to be determined. It can be envisaged that the continued study of NS3 and its interaction with cellular proteins may provide valuable insights into the mechanisms used by AHSV to facilitate virus egress.

REFERENCES

- Agrawal, N., Dasaradhi, P.V.N., Mohmmmed, A., Malhotra, P., Bhatnagar, R.K. and Mukherjee, S.K. (2003). RNA interference: Biology, mechanism and applications. *Microbiol. Mol. Biol. Rev.* 67, 657-685.
- Ahuja, H.S., Zhu, Y. and Zakeri, Z. (1997). Association of cyclin-dependent kinase 5 and its activator p35 with apoptotic cell death. *Dev. Genet.* 21, 258-267.
- Alexander, R.A. (1948). The 1944 epizzotic of horsesickness in the Middle East. *Onderstepoort J. Vet. Sci. Anim. Indus.* 2, 375-391.
- Alm, K. and Oredsson, S. (2009). Cells and polyamines do it cyclically. *Essays Biochem.* 46, 63-76.
- Altschul, S.F., Madden, T.L., Schaffer, A.A., Zhang, J., Zhang, Z., Miller, W. and Lipman, D.J. (1997). Gapped BLAST and PSI-BLAST: A new generation of protein database search programs. *Nucl. Acids Res.* 25, 3389-3402.
- Anderson, R.G.W. (1998). The caveolae membrane system. *Annu. Rev. Biochem.* 67, 199-225.
- Arias, C.F., Déctor, M.A., Segovia, L., López, T., Camacho, M., Isa, P., Espinosa, R. and López, S. (2004). RNA silencing of rotavirus gene expression. *Virus Res.* 102, 43-51.
- Arndt, K.M., Pelletier, J.N., Müller, K.M., Alber, T., Michnick, S.W. and Plückthun, A. (2000). A heterodimeric coiled-coil peptide pair selected *in vivo* from a designed library-versus-library ensemble. *J. Mol. Biol.* 295, 627-639.
- Asao, H., Sasaki, Y., Arita, T., Tanaka, N., Endo, K., Kasai, H., Takeshita, T., Endo, Y., Fujita, T. and Sugamura, K. (1997). Hrs is associated with STAM, a signal-transducing adaptor molecule. Its suppressive effect on cytokine-induced cell growth. *J. Biol. Chem.* 272, 32785-32791.
- Babst, M. (2005). A protein's final ESCRT. *Traffic* 6, 2-9.
- Babst, M., Katzmann, D.J., Snyder, W.B., Wendland, B. and Emr, S.D. (2002). Endosome-associated complex, ESCRT-II, recruits transport machinery for protein sorting at the multivesicular body. *Dev. Cell* 3, 283-289.
- Bache, K.G., Raiborg, C., Mehlum, A. and Stenmark, H. (2004). STAM and Hrs are subunits of a multivalent ubiquitin-binding complex on early endosomes. *J. Biol. Chem.* 278, 12513-12521.
- Balasuriya, U.B., Nadler, S.A., Wilson, W.C., Pritchard, L.I., Smythe, A.B., Savini, G., Monaco, F., De Santis, P., Zhang, N., Tabachnick, W.J. and Maclachlan, N.J. (2008). The NS3 proteins of global strains of bluetongue virus evolve into regional topotypes through negative (purifying) selection. *Vet. Microbiol.* 126, 91-100.
- Bansal, O.B., Stokes, A., Bansal, A., Bishop, D. and Roy, P. (1998). Membrane organization of bluetongue virus nonstructural glycoprotein NS3. *J. Virol.* 72, 3362-3369.
- Bär, S., Daeffler, L., Rommelaere, J. and Nüesch, J.P.F. (2008). Vesicular egress of non-enveloped lytic parvoviruses depends on gelsolin functioning. *Plos Pathog.* 4, e1000126.

- Barnard, B.J., Bengis, R.G., Keet, D.F. and Dekker, E.H. (1995). Epidemiology of African horsesickness virus, antibodies in free-living elephants *Loxodonta africans* and their response to experimental infection. *Onderstepoort J. Vet. Res.* 62, 271-275.
- Barnard, J.H. (1998). Epidemiology of African horse sickness and the role of the zebra in South Africa. *Arch. Virol. (Suppl.)* 14, 13-19.
- Basak, A.K., Gouet, P., Grimes, J., Roy, P. and Stuart, D. (1996). Crystal structure of the top domain of African horse sickness virus VP7: Comparison with Bluetongue virus VP7. *J. Virol.* 70, 3797-3806.
- Basak, A.K., Stuart, D.I. and Roy, P. (1992). Preliminary crystallographic study of bluetongue virus capsid protein, VP7. *J. Mol. Biol.* 228, 687-689.
- Beaton, A.R., Rodriguez, J., Reddy, Y.K. and Roy, P. (2002). The membrane trafficking protein calpactin forms a complex with bluetongue virus protein NS3 and mediates virus release. *Proc. Natl. Acad. Sci. USA* 99, 13154-13159.
- Becker, M.M., Peters, T.R. and Dermody, T.S. (2003). Reovirus σ NS and μ NS proteins form cytoplasmic inclusion structures in the absence of viral infection. *J. Virol.* 77, 5948-5963.
- Bennett, D. and Alphey, L. (2002). PP1 binds Sara and negatively regulates Dpp signaling in *Drosophila melanogaster*. *Nature Genet.* 31, 419-423.
- Bentley, L., Fehrsen, J., Jordaan, F., Huismans, H. and du Plessis, D.H. (2000). Identification of antigenic regions on VP2 of African horsesickness virus serotype 3 by using phage-displayed epitope libraries. *J. Gen. Virol.* 81, 993-1000.
- Bernstein, E., Caudy, A.A., Hammond, S.M. and Hannon, G.J. (2001). Role for a bidentate ribonuclease in the initiation step of RNA interference. *Nature* 409, 363-366.
- Beylvelde, M. (2007). Interaction of nonstructural protein NS3 of African horsesickness virus with viral and cellular proteins. MSc dissertation, University of Pretoria.
- Bhattacharya, B. and Roy, P. (2008). Bluetongue virus outer capsid protein VP5 interacts with membrane lipid rafts via a SNARE domain. *J. Virol.* 82, 10600-10612.
- Bhattacharya, B., Noad, R.J. and Roy, P. (2007). Interaction between Bluetongue virus outer capsid protein VP2 and vimentin is necessary for virus egress. *Virol. J.* 15; 4:7.
- Bieniasz, P.D. (2006). Late budding domains and host proteins in enveloped virus release. *Virol.* 344, 55-63.
- Birnboim, H.C. and Doly, J. (1979). A rapid alkaline extraction procedure for screening recombinant plasmid DNA. *Nucl. Acids Res.* 7, 1513-1523.
- Blatner, N.R., Stahelin, R.V., Diraviyam, K., Hawkins, P.T., Hong, W., Murray, D. and Cho, W. (2004). The molecular basis of the differential subcellular localization of FYVE domains. *J. Biol. Chem.* 279, 53818-53827.
- Blot, V., Perugi, F., Gay, B., Prevost, M.C., Briant, L., Tangy, F., Abriel, H., Staub, O., Dokhelar, M.C. and Pique, C. (2004). Nedd4.1-mediated ubiquitination and subsequent recruitment of Tsg101 ensure HTLV-1 Gag trafficking towards the multivesicular body pathway prior to virus budding. *J. Cell Sci.* 117, 2357-2367.

- Bohula, E.A., Salisbury, A.J., Sohail, M., Playford, M.P., Riedemann, J., Southern, E.M. and Macaulay, V.M. (2003). The efficacy of small interfering RNAs targeted to the type 1 insulin-like growth factor receptor (IGF1R) is influenced by secondary structure in the IGF1R transcript. *J. Biol. Chem.* 278, 15991-15997.
- Bökel, C., Schwabedissen, A., Entchev, E., Renaud, O. and González-Gaitán, M. (2006). Sara endosomes and the maintenance of Dpp signaling levels across mitosis. *Science* 314, 1135-1139.
- Boorman, J., Mellor, P.S., Penn, M. and Jennings, M. (1975). The growth of African horse sickness virus in embryonated hen eggs and the transmission of the virus by *Culicoides variipennis* Coquillett (dipteran: Ceratopogonidae). *Arch. Virol.* 47, 343-349.
- Borden, E.C., Shope, R.E. and Murphy, F.A. (1971). Physicochemical and morphological relationships of some arthropod-borne viruses to bluetongue virus - a new taxonomic group. Electron microscopic studies. *J. Gen. Virol.* 13, 273-283.
- Boshuizen, J.A., Rossen, J.W., Sitaram, C.K., Kimenai, F.F., Simons-Oosterhuis, Y., Laffeber, C., Büller, H.A. and Einerhand, A.W. (2004). Rotavirus enterotoxin NSP4 binds to the extracellular matrix proteins laminin- β 3 and fibronectin. *J. Virol.* 78, 10045-10053.
- Bosman, P., Bruckner, G.K. and Faul, A. (1995). African horse sickness surveillance systems and regionalisation/zoning: The case of South Africa. *Rev. Sci. Tech.* 14, 645-653.
- Bouamr, F., Houck-Loomis, B.R., De Los Santos, M., Casaday, R.J., Johnson, M.C. and Goff, S.P. (2007). The C-terminal portion of the Hrs protein interacts with Tsg101 and interferes with human immunodeficiency virus type 1 Gag particle production. *J. Virol.* 81, 2909-2922.
- Bouamr, F., Melillo, J.A., Wang, M.Q., Nagashima, K., de Los Santos, M., Rein, A. and Goff, S.P. (2003). PPPYEPTAP motif is the late domain of human T-cell leukemia virus type 1 Gag and mediates its functional interaction with cellular proteins Nedd4 and Tsg101. *J. Virol.* 77, 11882-11895.
- Boyce, M., Wehrfritz, J., Noad, R. and Roy, P. (2004). Purified recombinant Bluetongue virus VP1 exhibits RNA replicase activity. *J. Virol.* 78, 3994-4002.
- Bremer, C.W. (1976). A gel electrophoretic study of the protein and nucleic acid components of African horsesickness virus. *Onderstepoort J. Vet. Res.* 43, 193-199.
- Bremer, C.W., Huismans, H. and van Dijk, A.A. (1990). Characterization and cloning of the African horsesickness virus genome. *J. Gen. Virol.* 71, 793-799.
- Brookes, S.M., Hyatt, A.D. and Eaton, B.T. (1993). Characterization of virus inclusion bodies in bluetongue virus-infected cells. *J. Gen. Virol.* 74, 525-530.
- Broquet, A.H., Lenoir, C., Gardet, A., Sapin, C., Chwetzoff, S., Jouniaux, A.M., López, S., Trugnan, G., Bachelet, M. and Thomas, G. (2007). Hsp70 negatively controls rotavirus protein bioavailability in Caco-2 cells infected by the rotavirus RF strain. *J. Virol.* 81, 1297-1304.
- Brown, C.C. and Dardiri, A.H. (1990). African horsesickness: A continuing menace. *J. Am. Vet. Med. Assoc.* 196, 2019-2021.
- Brown, D.A. and London, E. (1998). Functions of lipid rafts in biological membranes. *Annu. Rev. Cell Dev. Biol.* 14, 111-136.

- Brown, S.E., Morrison, H.G., Karabatsos, N. and Knudson, D.L. (1991). Genetic relatedness of two new Orbivirus serogroups: Orungo and Lebombo. *J. Gen. Virol.* 72, 1065-1072.
- Brückner, A., Polge, C., Lentze, N., Auerbach, D. and Schlattner, U. (2009). Yeast two-hybrid, a powerful tool for systems biology. *Int. J. Mol. Sci.* 10, 2763-2788.
- Brummelkamp, T.R., Bernards, R. and Agami, R. (2002). A system for stable expression of short interfering RNAs in mammalian cells. *Science* 296, 550-553.
- Burd, C.G. and Emr, S.D. (1998). Phosphatidylinositol(3)-phosphate signaling mediated by specific binding to RING FYVE domains. *Mol. Cell* 2, 157-162.
- Burger, L. (2006). Silencing African horsesickness virus VP7 protein expression *in vitro* by RNA interference. M.Sc Dissertation, Department of Microbiology and Plant Pathology, Faculty of Biological and Agricultural Sciences, University of Pretoria, South Africa.
- Burroughs, J.N., O'Hara, R.S., Smale, C.J., Hamblin, C., Walton, A., Armstrong, R. and Mertens, P.P.C. (1994). Purification and properties of virus particles, infectious subviral particles, cores and VP7 crystals of African horsesickness virus serotype 9. *J. Gen. Virol.* 75, 1849-1857.
- Calisher, C.H. and Mertens, P.P.C. (1998). Taxonomy of African horse sickness viruses. *Arch. Virol. (Suppl.)* 14, 3-11.
- Calistri, A., Salata, C., Parolin, C. and Palu, G. (2009). Role of multivesicular bodies and their components in the egress of enveloped RNA viruses. *Rev. Med. Virol.* 19, 31-45.
- Campagna, M., Eichwald, C., Vascotto, F. and Burrone, O.R. (2005). RNA interference of rotavirus segment 11 mRNA reveals the essential role of NSP5 in the virus replicative cycle. *J. Gen. Virol.* 86, 1481-1487.
- Caplen, N.J., Parrish, S., Imani, F., Fire, A. and Morgan, R.A. (2001). Specific inhibition of gene expression by small double-stranded RNAs in invertebrate and vertebrate systems. *Proc. Natl. Acad. Sci. USA* 98, 9742-9747.
- Carmell, M.A., Xuan, Z., Zhang, M.Q. and Hannon, G.J. (2002). The Argonaute family: Tentacles that reach into RNAi, developmental control, stem-cell maintenance, and tumorigenesis. *Genes Dev.* 16, 2733-2742.
- Carvalho, J., Arnold, M.M. and Nibert, M.L. (2007). Silencing and complementation of reovirus core protein $\mu 2$: Functional correlations with $\mu 2$ -microtubule association and differences between virus- and plasmid-derived $\mu 2$. *Virol.* 364, 301-316.
- Castro, A.E., Montague, S.R., Dotson, J.F., Jessup, D.A. and DeForge, J.R. (1989). Susceptibility of a fetal tongue cell line derived from bighorn sheep to five serotypes of bluetongue virus and its potential for the isolation of viruses. *J. Vet. Diagn. Invest.* 1, 247-253.
- Causier, B. and Davies, B. (2002). Analysing protein-protein interactions with the yeast two-hybrid system. *Plant Mol. Biol.* 50, 855-870.
- Celma, C.C. and Roy, P. (2009). A viral nonstructural protein regulates bluetongue virus trafficking and release. *J. Virol.* 83, 6806-6816.
- Cerutti, L., Mian, N. and Bateman, A. (2000). Domains in gene silencing and cell differentiation proteins: The novel PAZ domain and redefinition of the Piwi domain. *Trends Biochem. Sci.* 25, 481-482.

- Chalfie, M., Tu, Y., Euskirchen, G., Ward, W.W. and Prasher, D.C. (1994). Green fluorescent protein as a marker for gene expression. *Science* 263, 802-805.
- Chan, C.Y., Carmack, C.S., Long, D.D., Maliyekkel, A., Shao, Y., Roninson, I.B. and Ding, Y. (2009). A structural interpretation of the effect of GC-content on efficiency of RNA interference. *BMC Bioinformatics* 10 Suppl 1, S33.
- Chazal, N. and Gerlier, D. (2003). Virus entry, assembly, budding, and membrane rafts. *Microbiol. Mol. Biol. Rev.* 67, 226-237.
- Chen, B.J. and Lamb, R.A. (2008). Mechanisms for enveloped virus budding: Can some viruses do without an ESCRT? *Virology* 372, 221-232.
- Cheng, T.L. and Chang, W.T. (2007). Construction of simple and efficient DNA vector-based short hairpin RNA expression systems for specific gene silencing in mammalian cells. *Methods Mol. Biol.* 408, 223-241.
- Chiam, R., Sharp, E., Maan, S., Rao, S., Mertens, P., Blacklaws, B., Davis-Poynter, N., Wood, J. and Castillo-Olivares, J. (2009). Induction of Antibody Responses to African Horse Sickness Virus (AHSV) in Ponies after Vaccination with Recombinant Modified Vaccinia Ankara (MVA). *PLoS One* 4, e5997.
- Chien, C.T., Bartel, P.L., Sternglanz, R. and Fields, S. (1991). The two-hybrid system: a method to identify and clone genes for proteins that interact with a protein of interest. *Proc. Natl. Acad. Sci. USA* 88, 9578-9582.
- Chiu, W.L., Niwa, Y., Zeng, W., Hirano, T., Kobayashi, H. and Sheen, J. (1996). Engineered GFP as a vital reporter in plants. *Curr. Biol.* 6, 325-330.
- Chuma, T., Le Blois, H., Sanchez-Vizcaino, J.M., Diaz-Laviada, M. and Roy, P. (1992). Expression of the major core antigen VP7 of African horsesickness virus by a recombinant baculovirus and its use as a group-specific diagnostic reagent. *J. Gen. Virol.* 73, 925-931.
- Chwetzoff, S. and Trugnan, G. (2006). Rotavirus assembly: An alternative model that utilizes an atypical trafficking pathway. *Curr. Top. Microbiol. Immunol.* 309, 245-261.
- Coetzer, J.A.W. and Erasmus, B.J. (1994). African horse sickness. In: Infectious diseases of livestock with special reference to southern Africa, Vol 1. J.A.W. Coetzer, G.R. Thomson and R.C. Tustin (Eds.), pp. 460-475. Oxford University Press, Cape Town.
- Colas, P. and Brent, R. (1998). The impact of two-hybrid and related methods on biotechnology. *Trends Biotechnol.* 16, 355-363.
- Cormack, B.P., Valdivia, R. and Falkow, S. (1996). FACS optimized mutants of the green fluorescent protein (GFP). *Gene* 173, 33-38.
- Cowley, J.A. and Gorman, B.M. (1987). Genetic reassortants for identification of the genome segment coding for the bluetongue virus hemagglutinin. *J. Virol.* 61, 2304-2306.
- Cowley, J.A., Walker, P.J. and Gorman, B.M. (1992). Recognition sites in assembly of bluetongue viruses. In: Bluetongue, African horse sickness and related orbiviruses. Proceedings of the Second International Symposium. T.E. Walton and B.I. Osborn (Eds.), pp. 423-432. CRC Press, London.

- Craven, R.C., Harty, R.N., Paragas, J., Palese, P. and Wills, J.W. (1999). Late domain function identified in the vesicular stomatitis virus M protein by use of rhabdovirus-retrovirus chimeras. *J. Virol.* 73, 3359-3365.
- Cress, W.D. and Nevins, J.R. (1994). Interacting domains of EZF1, DPl, and the adenovirus E4 protein. *J. Virol.* 68, 4213-4219.
- Csorba, T., Pantaleo, V. and Burgyán, J. (2009). RNA silencing: An antiviral mechanism. *Adv. Virus Res.* 75, 35-71.
- Cuadras, M.A. and Greenberg, H.B. (2003). Rotavirus infectious particles use lipid rafts during replication for transport to the cell surface *in vitro* and *in vivo*. *Viol.* 313, 308-321.
- Cuadras, M.A., Bordier, B.B., Zambrano, J.L., Ludert, J.E. and Greenberg, H.B. (2006). Dissecting rotavirus particle-raft interaction with small interfering RNAs: Insights into rotavirus transit through the secretory pathway. *J. Virol.* 80, 3935-3946.
- de Waal, P.J. and Huismans, H. (2005). Characterization of the nucleic acid binding activity of inner core protein VP6 of African horse sickness virus. *Arch. Virol.* 150, 2037-2050.
- Deane, C., Salwiński, Ł., Xenarios, I. and Eisenberg, D. (2002). Protein interactions: Two methods for assessment of the reliability of high throughput observations. *Mol. Cell. Proteomics* 1, 349-356.
- Déctor, M.A., Romero, P., Lopez, S. and Arias, C.F. (2002). Rotavirus gene silencing by small interfering RNAs. *EMBO Rep.* 3, 1175-1180.
- Demirov, D.G., Ono, A., Orenstein, J.M. and Freed, E.O. (2002). Overexpression of the N-terminal domain of TSG101 inhibits HIV-1 budding by blocking late domain function. *Proc. Natl. Acad. Sci. USA* 99, 955-960.
- Desmyter, J., Melnick, J.L. and Rawls, W.E. (1968). Defectiveness of interferon production and of rubella virus interference in a line of African green monkey kidney cells (Vero). *J. Virol.* 2, 955-961.
- Devany, M.A., Kendall, J., Grubman, M.J. (1988). Characterization of a non-structural phosphoprotein of two orbiviruses. *Virus Res.* 11, 151-164.
- Di Guglielmo, G.M., Le Roy, C., Goodfellow, A.F. and Wrana, J.L. (2003). Distinct endocytic pathways regulate TGF- β receptor signalling and turnover. *Nature Cell. Biol.* 5, 410-421.
- Ding, H., Liao, G., Wang, H. and Zhou, Y. (2007). Asymmetrically designed siRNAs and shRNAs enhance the strand specificity and efficacy in RNAi. *J. RNAi Gene Silencing* 4, 269-280.
- Downes, C.P., Gray, A. and Lucocq, J.M. (2005). Probing phosphoinositide functions in signaling and membrane trafficking. *Trends Cell. Biol.* 15, 259-268.
- Du Toit, R.M. (1944). The transmission of bluetongue and horse sickness by *Culicoides*. *Onderstepoort J. Vet. Sci. Anim. Ind.* 19, 7-16.
- Dutta, D., Bagchi, P., Chatterjee, A., Nayak, M.K., Mukherjee, A., Chattopadhyay, S., Nagashima, S., Kobayashi, N., Komoto, S., Taniguchi, K. and Chawla-Sarkar, M. (2009). The molecular chaperone heat shock protein-90 positively regulates rotavirus infection. *Viol.* 391, 325-333.
- Dykxhoorn, D.M. and Lieberman, J. (2005). The silent revolution: RNA interference as basic biology, research tool, and therapeutic. *Annu. Rev. Med.* 56, 401-423.

- Dykxhoorn, D.M., Novina, C.D. and Sharp, P.A. (2003). Killing the messenger: short RNAs that silence gene expression. *Nat. Rev. Mol. Cell Biol.* 4, 457-467.
- Eastman, S.W., Martin-Serrano, J., Chung, W., Zang, T. and Bieniasz, P.D. (2005). Identification of human VPS37C, a component of endosomal sorting complex required for transport-I important for viral budding. *J. Biol. Chem.* 280, 628-636.
- Eaton, B.T., Hyatt, A.D. and Brookes, S.M. (1990). The replication of bluetongue virus. *Curr. Top. Microbiol. Immunol.* 162, 89-118.
- Eaton, B.T., Hyatt, A.D. and White, J.R. (1987). Association of bluetongue virus with the cytoskeleton. *Viol.* 157, 107-116.
- Eaton, B.T., Hyatt, A.D. and White, J.R. (1988). Localization of the nonstructural protein NS1 in bluetongue virus-infected cells and its presence in virus particles. *Viol.* 163, 527-537.
- Egea-Cortines, M., Saedler, H. and Sommer, H. (1999). Ternary complex formation between the MADS-box proteins SQUAMOSA, DEFICIENS and GLOBOSA is involved in the control of floral architecture in *Antirrhinum majus*. *EMBO J.* 18, 5370-5379.
- Eichwald, C., Rodriguez, J.F. and Burrone, O.R. (2004). Characterization of rotavirus NSP2/NSP5 interactions and the dynamics of viroplasm formation. *J. Gen. Virol.* 85, 625-634.
- El Hasnaoui, H., El Harrak, M., Zientara, S., Laviada, M. and Hamblin, C. (1998). Serological and virological responses in mules and donkeys following inoculation with African horse sickness virus serotype 4. *Arch. Virol.* 14, 29-36.
- Elbashir, S.M., Harborth, J., Lendeckel, W., Yalcin, A., Weber, K. and Tuschl, T. (2001a). Duplexes of 21-nucleotide RNAs mediate RNA interference in cultured mammalian cells. *Nature* 411, 494-498.
- Elbashir, S.M., Lendeckel, W. and Tuschl, T. (2001b). RNA interference is mediated by 21 and 22-nucleotide RNAs. *Genes Dev.* 15, 188-200.
- Elbashir, S.M., Martinez, J., Patkaniowska, A., Lendeckel, W. and Tuschl, T. (2001c). Functional anatomy of siRNAs for mediating efficient RNAi in *Drosophila melanogaster* embryo lysate. *EMBO J.* 20, 6877-6888.
- Entchev, E.V., Schwabedissen, A. and Gonzalez-Gaitan, M. (2000). Gradient formation of the TGF- β homolog Dpp. *Cell* 103, 981-991.
- Erasmus, B.J. (1994). African horse sickness vaccine information. Circular to veterinary surgeons in practice in South Africa. Onderstepoort Biological Products, Department of Agriculture, Republic of South Africa.
- Fashena, S.J., Serebriiskii, I. and Golemis, E.A. (2000). The continued evolution of two-hybrid screening approaches in yeast: How to outwit different preys with different baits. *Gene* 250, 1-14.
- Fassi-Fihri, O., El Harrak, M. and Fassi-Fehri, M.M. (1998). Clinical, virological and immune responses of normal and immunosuppressed donkeys (*Equus asinus africanus*) after inoculation with African horse sickness virus. *Arch. Virol.* 14, 49-56.
- Fields, S. and Sternglanz, R. (1994). The two hybrid system: An assay for protein-protein interactions. *Trends Genet.* 10, 286-292.

- Fields, S.J. and Song, O. (1989). A novel genetic system to detect protein-protein interactions. *Nature* 340, 245-246.
- Fire, A., Xu, S., Montgomery, M.K., Kostas, S.A., Driver, S. and Mello, C.C. (1998). Potent and specific genetic interference by double-stranded RNA in *Caenorhabditis elegans*. *Nature* 391, 806-811.
- Forzan, M., Wirblich, C. and Roy, P. (2004). A capsid protein of nonenveloped bluetongue virus exhibits membrane fusion activity. *Proc. Natl. Acad. Sci. USA* 101, 2100-2105.
- Foster, L.J., De Hoog, C.L. and Mann, M. (2003). Unbiased quantitative proteomics of lipid rafts reveals high specificity for signaling factors. *Proc. Natl. Acad. Sci. USA* 100, 5813-5818.
- Franke, E., Yuan, H.E.H., Bossolt, K.L., Gaff, S.P. and Luban, J. (1994). Specificity and sequence requirements for interactions between various retroviral Gag proteins. *J. Virol.* 68, 5300-5305.
- Freed, E.O. (2002). Viral late domains. *J. Virol.* 76, 4679-4687.
- Freed, E.O. (2004). Mechanisms of enveloped virus release. *Virus Res.* 106, 85-96.
- French, T.J., Inumaru, S. and Roy, P. (1989). Expression of two related nonstructural proteins of bluetongue virus (BTV) type 10 in insect cells by a recombinant baculovirus: Production of polyclonal ascitic fluid and characterization of the gene product in BTV-infected BHK cells. *J. Virol.* 63, 3270-3278.
- Gardet, A., Breton, M., Trugnan, G. and Chwetzoff, S. (2007). Role of actin in polarized release of Rotavirus. *J. Virol.* 81, 4892-4894.
- Garrus, J.E., von Schwedler, U.K., Pornillos, O.W., Morham, S.G., Zavitz, K.H., Wang, H.E., Wettstein, D.A., Stray, K.M., Cote, M., Rich, R.L., Myszka, D.G. and Sundquist, W.I. (2001). Tsg101 and the vacuolar protein sorting pathway are essential for HIV-1 budding. *Cell* 107, 55-65.
- Gaullier, J-M., Simonsen, A., D'Arrigo, A., Bremnes, B. and Stenmark, H. (1998). FYVE fingers bind PtdIns(3)P. *Nature* 394, 433-434.
- Ge, Q., McManus, M.T., Nguyen, T., Shen, C.H., Sharp, P.A., Eisen, H.N. and Chen, J. (2003). RNA interference of influenza virus production by directly targeting mRNA for degradation and indirectly inhibiting all viral RNA transcription. *Proc. Natl. Acad. Sci. USA* 100, 2718-2723.
- Gerke, V. (2001). Annexins and membrane organisation in the endocytic pathway. *Cell Mol. Biol. Lett.* 6, 204.
- Gillooly, D.J., Raiborg, C. and Stenmark, H. (2003). Phosphatidylinositol 3-phosphate is found in microdomains of early endosomes. *Histochem. Cell Biol.* 120, 445-453.
- Gillooly, D.J., Simonsen, A. and Stenmark, H. (2001). Cellular functions of phosphatidylinositol 3-phosphate and FYVE domain proteins. *Biochem. J.* 355, 249-258.
- González, R.A., Torres-Vega, M.A., López, S. and Arias, C.F. (1998). *In vivo* interactions among rotavirus nonstructural proteins. *Arch. Virol.* 143, 981-996.
- Gorman, B.M. (1992). An overview of the orbivirus. In: Bluetongue, African horse sickness and related orbiviruses. Proceedings of the Second International Symposium. T.E. Walton and B.I. Osburn (Eds.), pp. 335-347. CRC Press, London.

- Gorman, B.M. and Taylor, J. (1985). Orbiviruses. In: Field's Virology. B.N. Fields and D.M. Knipe (Eds.), pp. 275-278. Raven Press, New York.
- Gorman, B.M., Taylor, J., Brown, K. and Meltzer, A.J. (1977). Laboratory studies of orbiviruses. Structure and genetics of orbiviruses. *Annu. Rep. Qld. Inst. Med. Res.* 32, 15.
- Gottlinger, H.G., Dorfman, T., Sodroski, J.G. and Haseltine, W.A. (1991). Effect of mutations affecting the p6 Gag protein on human immunodeficiency virus particle release. *Proc. Natl. Acad. Sci. USA* 88, 3195-3199.
- Gottwein, E., Bodem, J., Muller, B., Schmechel, A., Zentgraf, H. and Krausslich, H.G. (2003). The Mason-Pfizer monkey virus PPPY and PSAP motifs both contribute to virus release. *J. Virol.* 77, 9474-9485.
- Gould, A.R. and Hyatt, A.D. (1994). The orbivirus genus, diversity, structure, replication and phylogenetic relationships. *Comp. Immunol. Microbiol. Infect. Dis.* 17, 163-188.
- Graff, J.W., Mitzel, D.N., Weisend, C.M., Flenniken, M.L. and Hardy, M.E. (2002). Interferon regulatory factor 3 is a cellular partner of rotavirus NSP1. *J. Virol.* 76, 9545-9550.
- Gredell, J.A., Berger, A.K. and Walton, S.P. (2008). Impact of target mRNA structure on siRNA silencing efficiency: A large-scale study. *Biotechnol. Bioeng.* 100, 744-755.
- Grimes, J., Basak, A., Roy, P. and Stuart, D.I. (1995). The crystal structure of bluetongue virus VP7: Implications for virus assembly. *Nature* 373, 167-170.
- Grimes, J.M., Burroughs, J.N., Gouet, P., Diprose, J.M., Malby, R., Zientara, S., Mertens, P.P. and Stuart, D.I. (1998). The atomic structure of the bluetongue virus core. *Nature* 395, 470-478.
- Grubman, M.J. and Lewis, S.A. (1992). Identification and characterization of the structural and non-structural proteins of African horse sickness virus and determination of the genome coding assignments. *Viol.* 186, 444-451.
- Gruenberg, J. and Stenmark, H. (2004). The biogenesis of multivesicular endosomes. *Nature Rev. Mol. Cell. Biol.* 5, 317-323.
- Guirakhoo, F., Catalan, J.A. and Monath, T.P. (1995). Adaptation of bluetongue virus in mosquito cells results in overexpression of NS3 proteins and release of virus particles. *Arch. Virol.* 140, 967-974.
- Hall, T.A. (1999). BioEdit: A user-friendly biological sequence alignment editor and analysis program for Windows 95/98/NT. *Nucleic Acids Symp. Ser.* 41, 95-98.
- Hamblin, G., Salt, J.S., Mellor, P.S., Graham, S.D., Smith, P.R. and Wohlsein, P. (1998). Donkeys as reservoirs of African horse sickness virus. *Arch. Virol.* 14, 37-47.
- Han, Z. and Harty, R.N. (2004). The NS3 protein of bluetongue virus exhibits viroporin-like properties. *J. Biol. Chem.* 279, 43092-43097.
- Hanley-Hyde, J. (1992). Cyclins in the cell cycle: An overview. *Curr. Top. Microbiol. Immunol.* 182, 461-466.
- Harborth, J., Elbashir, S.M., Vandeburgh, K., Manninga, H., Scaringe, S.A., Weber, K. and Tuschl, T. (2003). Sequence, chemical, and structural variation of small interfering RNAs and short hairpin RNAs and the effect on mammalian gene silencing. *Antisense Nucleic Acid Drug Dev.* 13, 83-105.

- Harty, R.N., Paragas, J., Sudol, M. and Palese, P. (1999). A proline-rich motif within the matrix protein of vesicular stomatitis virus and rabies virus interacts with WW domains of cellular proteins: Implications for viral budding. *J. Virol.* 73, 2921-2929.
- Hassan, S.H., Wirblich, C., Forzan, M. and Roy, P. (2001). Expression and functional characterization of bluetongue virus VP5 protein: Role in cellular permeabilization. *J. Virol.* 75, 8356-8367.
- Hassan, S.S. and Roy, P. (1999). Expression and functional characterization of bluetongue virus VP2 protein: Role in cell entry. *J. Virol.* 73, 9832-9842.
- Hayama, E. and Li, J.K. (1994). Mapping and characterization of antigenic epitopes and the nucleic acid-binding domains of VP6 protein of bluetongue viruses. *J. Virol.* 68, 3604-3611.
- Hayes, S., Chawla, A. and Corvera, S. (2002). TGF- β receptor internalization into EEA1-enriched early endosomes: role in signaling to Smad2. *J. Cell Biol.* 158, 1239-1249.
- Heale, B.S., Soifer, H.S., Bowers, C. and Rossi, J.J. (2005). siRNA target site secondary structure predictions using local stable substructures. *Nucl. Acids Res.* 33, e30.
- Hewat, E.A., Booth, T.F. and Roy, P. (1992a). Structure of bluetongue virus particles by cryoelectron microscopy. *J. Struct. Biol.* 109, 61-69.
- Hewat, E.A., Booth, T.F., Wade, R.H. and Roy, P. (1992b). 3-D reconstruction of bluetongue virus tubules using cryoelectron microscopy. *J. Struct. Biol.* 108, 35-48.
- Ho, H.Y., Cheng, M.L., Wang, Y.H. and Chiu, D.T. (2006). Flow cytometry for assessment of the efficacy of siRNA. *Cytometry A* 69, 1054-1061.
- Holen, T., Amarzguioui, M., Wilger, M.T., Babaie, E. and Prydz, H. (2002). Positional effects of short interfering RNAs targeting the human coagulation trigger tissue factor. *Nucl. Acids Res.* 30, 1757-1766.
- Homan, E.J. and Yunker, C.E. (1988). Growth of bluetongue and epizootic hemorrhagic disease of deer viruses in poikilothermic cell systems. *Vet. Microbiol.* 16, 15-24.
- Hong, J., Wei, N., Chalk, A., Wang, J., Song, Y., Yi, F., Qiao, R.P., Sonnhammer, E.L., Wahlestedt, C., Liang, Z. and Du, Q. (2008). Focusing on RISC assembly in mammalian cells. *Biochem. Biophys. Res. Commun.* 368, 703-708.
- Horscroft, N. and Roy, P. (2000). NTP-binding and phosphohydrolase activity associated with purified bluetongue virus non-structural protein NS2. *J. Gen. Virol.* 81, 1961-1965.
- House, J.A. (1998). Future international management of African horse sickness vaccines. *Arch. Virol.* 14, 297-304.
- Howell, P. (1963). African horse sickness. In: Emerging diseases of animals. FAO Agricultural Studies No. 61, pp. 71-108. FAO, Rome.
- Howell, P.G. (1960). The 1960 epizootic in the Middle East and SW Asia. *J. S. Afr. Vet. Med. Assoc.* 31, 329-334.
- Howell, P.G. (1962). The isolation and identification of further antigenic types of African horse sickness virus. *Onderstepoort J. Vet. Res.* 29, 139-149.
- Huisman, H. (1979). Protein synthesis in bluetongue virus-infected cells. *Virol.* 92, 385-396.

- Huismans, H. and Els, H.J. (1979). Characterization of tubules associated with the replication of three different orbiviruses. *Viol.* 92, 397-406.
- Huismans, H. and Erasmus, B.J. (1981). Identification of the serotype-specific and group-specific antigens of bluetongue virus. *Onderstepoort J. Vet. Res.* 48, 1-8.
- Huismans, H. and van Dijk, A.A. (1990). Bluetongue virus structural components. *Curr. Top. Microbiol. Immunol.* 162, 21-37.
- Huismans, H. and Verwoerd, D.W. (1973). Control of transcription during expression of the bluetongue virus genome. *Viol.* 52, 81-88.
- Huismans, H., van Dijk, A.A. and Bauskin, A.R. (1987a). *In vitro* phosphorylation and purification of a nonstructural protein of bluetongue virus with affinity for single-stranded RNA. *J. Virol.* 61, 3589-3595.
- Huismans, H., van Dijk, A.A. and Els, H.J. (1987b). Uncoating of parental bluetongue virus to core and subcore particles in infected L cells. *Viol.* 157, 180-188.
- Hurley, J.H. and Emr, S.D. (2006). The ESCRT complexes: Structure and mechanism of a membrane-trafficking network. *Annu. Rev. Biophys. Biomol. Struct.* 35, 277-298.
- Hutvagner, G. and Simard, M.J. (2008). Argonaute proteins: Key players in RNA silencing. *Nature Rev. Mol. Cell Biol.* 9, 22-32.
- Hyatt, A.D. and Eaton, B.T. (1988). Ultrastructural distribution of the major capsid proteins within bluetongue virus and infected cell. *J. Gen. Virol.* 68, 805-815.
- Hyatt, A.D., Eaton, B.T. and Brookes, S.M. (1989). The release of bluetongue virus from infected cells and their superinfection by progeny virus. *Viol.* 173, 21-34.
- Hyatt, A.D., Eaton, B.T. and Lunt, R. (1987). The grid-cell culture technique: The direct examination of virus-infected cells and progeny virus. *J. Microsc.* 145, 97-106.
- Hyatt, A.D., Gould, A.R., Coupar, B. and Eaton, B.T. (1991). Localization of the non-structural protein NS3 in bluetongue virus-infected cells. *J. Gen. Virol.* 72, 2263-2267.
- Hyatt, A.D., Zhao, Y. and Roy, P. (1992). Release of bluetongue virus-like particles from insect cells is mediated by BTV nonstructural protein NS3/NS3A. *Viol.* 193, 592-603.
- Igarashi, K. and Kashiwagi, K. (2010). Modulation of cellular function by polyamines. *Int. J. Biochem. Cell Biol.* 42, 39-51.
- Igarashi, K., Ito, K., Sakai, Y., Ogasawara, T. and Kashiwagi, K. (1988). Regulation of protein synthesis by polyamines. *Adv. Exp. Med. Biol.* 250, 315-330.
- Inumaru, S., Ghiasi, H. and Roy, P. (1987). Expression of bluetongue virus group-specific antigen VP3 in insect cells by a baculovirus vector, its use for the detection of bluetongue virus antibodies. *J. Gen. Virol.* 687, 1627-1635.
- Itoh, F., Divecha, N., Brocks, L., Oomen, L., Janssen, H., Calafat, J., Itoh, S. and Dijke Pt, P. (2002). The FYVE domain in Smad anchor for receptor activation (SARA) is sufficient for localization of SARA in early endosomes and regulates TGF- β /Smad signalling. *Genes Cells* 7, 321-331.

- Jackson, A.L., Bartz, S.R., Schelter, J., Kobayashi, S.V., Burchard, J., Mao, M., Li, B., Cavet, G. and Linsley, P.S. (2003). Expression profiling reveals off-target gene regulation by RNAi. *Nature Biotechnol.* 21, 635-637.
- Jahn, R., Lang, T. and Sudhof, T.C. (2003). Membrane fusion. *Cell* 112, 519-533.
- Jinek, M. and Doudna, J.A. (2009). A three-dimensional view of the molecular machinery of RNA interference. *Nature* 457, 405-412.
- Jourdan, N., Maurice, M., Delautier, D., Quero, A.M., Servin, L. and Trugnan, G. (1997). Rotavirus is released from the apical surface of cultured human intestinal cells through non-conventional vesicular transport that bypasses the Golgi apparatus. *J. Virol.* 71, 8268-8278.
- Kanzaki, L.I., Ornelas, S.S. and Argañaraz, E.R. (2008). RNA interference and HIV-1 infection. *Rev. Med. Virol.* 18, 5-18.
- Kar, A.K., Bishnupriya, B. and Roy, P. (2007). Bluetongue virus RNA binding protein NS2 is a modulator of viral replication and assembly. *BMC Mol. Biol.* 8: 1.
- Kar, A.K., Ghosh, M. and Roy, P. (2004). Mapping the assembly pathway of Bluetongue virus scaffolding protein VP3. *Virol.* 324, 387-399.
- Katzmann, D.J., Babst, M. and Emr, S.D. (2001). Ubiquitin-dependent sorting into the multivesicular body pathway requires the function of a conserved endosomal protein sorting complex, ESCRT-I. *Cell* 106,145-155.
- Katzmann, D.J., Odorizzi, G. and Emr, S.D. (2002). Receptor downregulation and multivesicular body sorting. *Nature Rev. Mol. Cell. Biol.* 3, 893-905.
- Katzmann, D.J., Stefan, C.J., Babst, M. and Emr, S.D. (2003). Vps27 recruits ESCRT machinery to endosomes during MVB sorting. *J. Cell Biol.* 162, 413-423.
- Kawasaki, H., Suyama, E., Lyo, M. and Taira, K. (2003). siRNAs generated by recombinant human Dicer induce specific and significant but target site-independent gene silencing in human cells. *Nucl. Acids Res.* 31, 981-987.
- Keegan, L., Gill, G. and Ptashne, M. (1986). Separation of DNA binding from the transcription-activating function of a eukaryotic regulatory protein. *Science* 231, 699-704.
- Ketzinel-Gilad, M., Shaul, Y. and Galun, E. (2006). RNA interference for antiviral therapy. *J. Gene Med.* 8, 933-950.
- Khvorova, A., Reynolds, A. and Jayasena, S.D. (2003). Functional siRNAs and miRNAs exhibit strand bias. *Cell* 115, 209-216.
- Knoblich, J.A. (2006). Cell biology. Sara splits the signal. *Science* 314, 1094-1096.
- Knudson, D.L. and Monath, T.P. (1990). Orbiviruses. In: Field's Virology. B.N. Fields and D.M. Knipe (Eds.), pp. 1405-1433. Raven Press, New York.
- Kobayashi, T., Chappell, J.D., Danthi, P. and Dermody, T.S. (2006). Gene-specific inhibition of reovirus replication by RNA interference. *J. Virol.* 80, 9053-9063.
- Kobayashi, T., Ooms, L.S., Chappell, J.D. and Dermody, T.S. (2009). Identification of functional domains in reovirus replication proteins μ NS and μ 2. *J. Virol.* 83, 2892-2906.

- Kretschmer-Kazemi Far, R. and Sczakiel, G. (2003). The activity of siRNA in mammalian cells is related to structural target accessibility: A comparison with antisense oligonucleotides. *Nucl. Acids Res.* 31, 4417-4424.
- Laegreid, W.W. (1996). African horse sickness. In: Virus infections of vertebrates. M.J. Studdert (Ed.), pp. 101-123. Elsevier, New York.
- Laegreid, W.W., Burrage, T.G., Stone-Marschat, M., Skowronek, A. (1992). Electron microscopic evidence for endothelial infection by African horsesickness virus. *Vet. Pathol.* 29, 554-556.
- Laegreid, W.W., Skowronek, A., Stone-Marschat, M. and Burrage, T.G. (1993). Characterization of virulence variants of African horse sickness virus. *Virology* 195, 836-839.
- Laemmli, U.K. (1970). Cleavage of structural proteins during the assembly of the head of bacteriophage T4. *Nature* 227, 680-685.
- Lalonde, S., Ehrhardt, D.W., Loqué, D., Chen, J., Rhee, S.Y. and Frommer, W.B. (2008). Molecular and cellular approaches for the detection of protein-protein interactions: latest techniques and current limitations. *Plant J.* 53, 610-635.
- Lambeth, L.S., Moore, R.J., Muralitharan, M.S. and Doran, T.J. (2007). Suppression of bovine viral diarrhoea virus replication by small interfering RNA and short hairpin RNA-mediated RNA interference. *Vet. Microbiol.* 119, 132-143.
- Lantermann, M., Schwantes, A., Sliva, K., Sutter, G. and Schnierle, B.S. (2007). Vaccinia virus double-stranded RNA-binding protein E3 does not interfere with siRNA-mediated gene silencing in mammalian cells. *Virus Res.* 126, 1-8.
- LeBlois, H., French, T., Mertens, P.P.C., Burroughs, J.N. and Roy, P. (1992). The expressed VP4 protein of bluetongue virus binds GTP and is the candidate guanylyl transferase of the virus. *Virology* 189, 757-761.
- Lee, M-S., Kwon, Y.T., Li, M., Peng, J., Friedlander, R.M. and Tsai, L.H. (2000). Neurotoxicity induces cleavage of p35 to p25 by calpain. *Nature* 405,360-364.
- Levy, H., Fraenkel-Conrat, H. and Owens, R.A. (1994). Virology. Third edition, pp. 1-7. Prentice Hall, Upper Saddle River, New Jersey.
- Licata, J.M., Simpson-Holley, M., Wright, N.T., Han, Z., Paragas, J. and Harty, R.N. (2003). Overlapping motifs (PTAP and PPEY) within the Ebola virus VP40 protein function independently as late budding domains: Involvement of host proteins TSG101 and VPS-4. *J. Virol.* 77, 1812-1819.
- Lingel, A., Simon, B., Izaurralde, E. and Sattler, M. (2004). Nucleic acid 3'-end recognition by the Argonaute2 PAZ domain. *Struct. Mol. Biol.* 11, 576-577.
- Liu, J., Carmell, M.A., Fabiola, V.R., Marsden, C.G., Thomson, J.M., Song, J.J., Hammond, S.M., Joshua-Tor, L. and Hannon, G.J. (2004). Argonaute2 is the catalytic engine of mammalian RNAi. *Science* 305, 1437-1441.
- Liu, L.N., Zhang, S.C., Liu, Z.H., Li, H.Y., Liu, M., Wang, Y.J. and Ma, L.F. (2005). Ribosomal proteins L34 and S29 of amphioxus *Branchiostoma belcheritsingtauense*: cDNA cloning and gene copy number. *Acta Biochim. Pol.* 52, 857-862.

- Liu, X., Cao, S., Zhou, R., Xu, G., Xiao, S., Yang, Y., Sun, M., Li, Y. and Chen, H. (2006). Inhibition of Japanese encephalitis virus NS1 protein expression in cell by small interfering RNAs. *Virus Genes* 33, 69-75.
- López, T., Rojas, M., Ayala-Bretón, C., López, S. and Arias, C.F. (2005). Reduced expression of the rotavirus NSP5 gene has a pleiotropic effect on virus replication. *J. Gen. Virol.* 86, 1609-1617.
- Loudon, P.T. and Roy, P. (1992). Interaction of nucleic acids with core-like and subcore-like particles of bluetongue virus. *Viol.* 191, 231-236.
- Lu, Z., Murray, J.T., Luo, W., Li, H., Wu, X., Xu, H., Backer, J.M. and Chen, Y.G. (2002). Transforming growth factor β activates Smad2 in the absence of receptor endocytosis. *J. Biol. Chem.* 277, 29363-29368.
- Lu, Z.J. and Mathews, D.H. (2007). Efficient siRNA selection using hybridization thermodynamics. *Nucl. Acids Res.* 36, 640-647.
- Luban, J. and Goff, S.P. (1995). The yeast two-hybrid system for studying protein-protein interactions. *Curr. Opin. Biotechnol.* 6, 59-64.
- Luo, K.Q. and Chang, D.C. (2004). The gene-silencing efficiency of siRNA is strongly dependent on the local structure of mRNA at the targeted region. *Biochem. Biophys. Res. Commun.* 318, 303-310.
- Luo, Y., Vijaychander, S., Stile, J. and Zhu, L. (1996). Cloning and analysis of DNA-binding proteins by yeast one-hybrid and one-two-hybrid systems. *Biotechniques* 20, 564-568.
- Lymperopoulos, K., Wirbilich, C., Bierley, I. and Roy, P. (2003). Sequence specificity in the interaction of Bluetongue virus non-structural protein 2 (NS2) with viral RNA. *J. Biol. Chem.* 278, 31722-31730.
- Ma, J-B., Yuan, Y-R., Meister, G., Pei, Y., Tuschl, T. and Patel, D.J. (2005). Structural basis for 5'-end-specific recognition of guide RNA by the *A. fulgidus* PIWI protein. *Nature* 434, 666-670.
- Macias, M.J., Wiesner, S. and Sudol, M. (2002). WW and SH3 domains, two different scaffolds to recognize proline-rich ligands. *FEBS Lett.* 513, 30-37.
- MacLachlan, N.J., Balasuriya, U.B., Davis, N.L., Collier, M., Johnston, R.E., Ferraro, G.L. and Guthrie, A.J. (2007). Experiences with new generation vaccines against equine viral arteritis, West Nile disease and African horse sickness. *Vaccine* 25, 5577-5582.
- Manche, L., Green, S.R., Schmedt, C. and Mathews, M.B. (1992). Interactions between double-stranded RNA regulators and the protein kinase DAI. *Mol. Cell. Biol.* 12, 5238-5248.
- Manjunath, N., Wu, H., Subramanya, S. and Shankar, P. (2009). Lentiviral delivery of short hairpin RNAs. *Adv. Drug Deliv. Rev.* 61, 732-745.
- Maree, F.F. and Huisman, H. (1997). Characterization of tubular structures composed of nonstructural protein NS1 of African horsesickness virus expressed in insect cells. *J. Gen. Virol.* 78, 1077-1082.
- Maree, S. and Paweska, J.T. (2005). Preparation of recombinant African horse sickness virus VP7 antigen via a simple method and validation of a VP7-based indirect ELISA for the detection of group-specific IgG antibodies in horse sera. *J. Virol. Methods* 125, 55-65.

- Maree, S., Durbach, S. and Huismans, H. (1998). Intracellular production of African horsesickness virus core-like particles by expression of the two major core proteins, VP3 and VP7, in insect cells. *J. Gen. Virol.* 79, 333-337.
- Marshall, J.J. and Roy, P. (1990). High level expression of the two outer capsid proteins of bluetongue virus serotype 10: Their relationship with the neutralization of virus infection. *Virus Res.* 15, 189-195.
- Marshall, O.J. (2004). PerlPrimer: Cross-platform, graphical primer design for standard, bisulphite and real-time PCR. *Bioinformatics* 20, 2471-2472.
- Martin, L.A., Meyer, A.J., O'Hara, R.S., Fu, H., Mellor, P.S., Knowles, N.J. and Mertens, P.P. (1998). Phylogenetic analysis of African horse sickness virus segment 10: Sequence variation, virulence characteristics and cell exit. *Arch. Virol.* 14, 281-293.
- Martinez-Torrecuadrada, J.L., Diaz-Laviada, M., Roy, P., Sanchez, C., Vela, C., Sanchez-Vizcaino, J.M. and Casal, J.I. (1996). Full protection against African horsesickness (AHS) in horses induced by baculovirus-derived AHS virus serotype 4 VP2, VP5 and VP7. *J. Gen. Virol.* 77, 1211-1221.
- Martinez-Torrecuadrada, J.L., Iwata, H., Venteo, A., Casal, I. and Roy, P. (1994). Expression and characterization of two outer capsid proteins of African horsesickness virus: The role of VP2 in virus neutralization. *Virol.* 202, 348-359.
- Martinez-Torrecuadrada, J.L., Langeveld, J.P.M., Meloen, R.H. and Casal, J.I. (2001). Definition of neutralizing sites on African horse sickness virus serotype 4 VP2 at the level of peptides. *J. Gen. Virol.* 82, 2415-2424.
- Martinez-Torrecuadrada, J.L., Langeveld, J.P.M., Venteo, A., Sanz, A., Dalsgaard, K., Hamilton, W.D.O., Meloen, R.H. and Casal, J.I. (1999). Antigenic profile of African horse sickness virus serotype 4 VP5 and identification of a neutralizing epitope shared with bluetongue virus and epizootic haemorrhagic disease virus. *Virol.* 257, 449-459.
- Martin-Serrano, J., Eastman, S.W., Chung, W. and Bieniasz, P.D. (2005). HECT ubiquitin ligases link viral and cellular PPXY motifs to the vacuolar protein-sorting pathway. *J. Cell Biol.* 168, 89-101.
- Martin-Serrano, J., Yarovoy, A., Perez-Caballero, D. and Bieniasz, P.D. (2003). Divergent retroviral late-budding domains recruit vacuolar protein sorting factors by using alternative adaptor proteins. *Proc. Natl. Acad. Sci. USA* 100, 12414-12419.
- Martin-Serrano, J., Zang, T. and Bieniasz, P.D. (2001). HIV-1 and Ebola virus encode small peptide motifs that recruit Tsg101 to sites of particle assembly to facilitate egress. *Nat. Med.* 7, 1313-1319.
- Maruri-Avidal, L., López, S. and Arias, C.F. (2008). Endoplasmic reticulum chaperones are involved in the morphogenesis of rotavirus infectious particles. *J. Virol.* 82, 5368-5380.
- Massagué, J. (2000). How cells read TGF- β signals. *Nature Rev. Mol. Cell. Biol.* 1, 169-178.
- Massagué, J., Seoane, J. and Wotton, D. (2005). Smad transcription factors. *Genes Dev.* 19, 2783-2810.
- McIntosh, B.M. (1958). Immunological types of horse sickness virus and their significance in immunization. *Onderstepoort J. Vet. Res.* 27, 465-538.
- McManus, M.T. and Sharpe, P.A. (2002). Gene silencing in mammals by small interfering RNAs. *Nature Rev. Genet.* 3, 737-747.

- Meiring, T.L., Huismans, H. and Van Staden V. (2009). Genome segment reassortment identifies non-structural protein NS3 as a key protein in African horsesickness virus release and alteration of membrane permeability. *Arch. Virol.* 154, 263-271.
- Meister, G. and Tuschl, T. (2004). Mechanisms of gene silencing by double-stranded RNA. *Nature* 431, 343-349.
- Meiswinkel, R and Paweska, J.T. (2003). Evidence for a new field *Culicoides* vector of African horse sickness in South Africa. *Prev. Vet. Med.* 60, 243-253.
- Mellor, P.S. (1993). African horse sickness: Transmission and epidemiology. *Vet. Res.* 24, 199-212.
- Mellor, P.S. (1994). Epizootiology and vectors of African horse sickness. *Comp. Immun. Microbiol. Infect. Dis.* 17, 287-296.
- Mellor, P.S. and Hamblin, C. (2004). African horse sickness. *Vet. Res.* 35, 445-466.
- Mellor, P.S., Boorman, J. and Jennings, M. (1975). The multiplication of African horse sickness virus in two species of *Culicoides* (Diptera: Ceratopogonidae). *Arch. Virol.* 47, 351-356.
- Mellor, P.S., Boorman, J., Wilkinson, P.J. and Martinez-Gomez, F. (1983). Potential vectors of bluetongue and African horse sickness viruses in Spain. *Vet. Rec.* 112, 229-230.
- Mertens, P.P.C. (2004). The dsRNA viruses. *Virus Res.* 101, 3-13.
- Mertens, P.P.C. and Diprose, J. (2004). The bluetongue virus core: A nano-scale transcription machine. *Virus Res.* 101, 29-43.
- Mertens, P.P.C., Attoui, H. and Mellor, P.S. (2008). Orbiviruses. In: Encyclopedia of Virology, pp. 454-465.
- Mir, K.D., Parr, R.D., Schroeder, F. and Ball, J.M. (2007). Rotavirus NSP4 interacts with both the amino- and carboxyl-termini of caveolin-1. *Virus Res.* 126, 106-115.
- Mirchamsy, H. and Hazrati, A. (1973). A review of the aetiology and pathology of African horse sickness. *Arch. Inst. Razi.* 25, 23-46.
- Mittal, V. (2004). Improving the efficiency of RNA interference in mammals. *Nature Rev. Genet.* 5, 355-365.
- Miura, S., Takeshita, T., Asao, H., Kimura, Y., Murata, K., Sasaki, Y., Hanai, J.I., Beppu, H., Tsukazaki, T., Wrana, J.L., Miyazono, K. and Sugamura, K. (2000). Hgs (Hrs), a FYVE domain protein, is involved in Smad signaling through cooperation with SARA. *Mol. Cell. Biol.* 20, 9346-9355.
- Miyagishi, M. and Taira, K. (2005). siRNA becomes smart and intelligent. *Nat. Biotechnol.* 23, 946-947.
- Mizukoshi, N., Sakamoto, K., Iwata, A., Tsuchiya, T., Ueda, S., Apiwatnakorn, B., Kamada, M. and Fukusho, A. (1993). The complete nucleotide sequence of African horsesickness virus serotype 4 (vaccine strain) segment 4, which encodes the minor core protein VP4. *Virus Res.* 28, 299-306.
- Modrof, J., Lympelopoulou, K. and Roy, P. (2005). Phosphorylation of Bluetongue virus non-structural protein 2 is essential for formation of viral inclusion bodies. *J. Virol.* 79, 10023-10031.

- Montero, H., Arias, C.F. and López, S. (2006). Rotavirus nonstructural protein NSP3 is not required for viral protein synthesis. *J. Virol.* 80, 9031-9038.
- Montgomery, M.K., Xu, S. and Fire, A. (1998). RNA as a target of double-stranded RNA-mediated genetic interference in *Caenorhabditis elegans*. *Proc. Natl. Acad. Sci. USA* 95, 15502-15507.
- Moore, C.B., Guthrie, E.H., Huang, M.T. and Taxman, D.J. (2010). Short hairpin RNA (shRNA): design, delivery, and assessment of gene knockdown. *Methods Mol. Biol.* 629, 141-158.
- Moorthamer, M. and Chaudhuri, B. (1999). Identification of ribosomal protein L34 as a novel Cdk5 inhibitor. *Biochem. Biophys. Res. Commun.* 255, 631-638.
- Mosca, J.D. and Pitha, P.M. (1986). Transcriptional and posttranscriptional regulation of exogenous human beta interferon gene in simian cells defective in interferon synthesis. *Mol. Cell. Biol.* 6, 2279-2283.
- Myers, J.W., Jones, J.T., Meyer, T. and Ferrel, J.E. (2003). Recombinant Dicer efficiently converts large dsRNA into siRNAs suitable for gene silencing. *Nature Biotech.* 21, 324-328.
- Naito, Y., Yoshimura, J., Morishita, S. and Ui-Tei, K. (2009). siDirect 2.0: Updated software for designing functional siRNA with reduced seed-dependent off-target effect. *BMC Bioinformatics* 10, 392.
- O'Hara, R.S., Meyer, A.J., Burroughs, J.N., Pullen, L., Martin, L.A. and Mertens, P.P.C. (1998). Development of a mouse model system, coding assignments and identification of the genome segments controlling virulence of African horse sickness virus serotypes 3 and 8. *Arch. Virol.* 14, 259-279.
- Oellerman, R.A. (1970). Plaque formation by African horse sickness virus and characterization of its RNA. *Onderstepoort J. Vet. Res.* 37, 137-144.
- Oellerman, R.A., Els, H.J. and Erasmus, B.J. (1970). Characterization of African horsesickness virus. *Archiv. gesammte Virusforsch.* 29, 163-174.
- Overhoff, M., Alken, M., Kretschmer-Kazemi Far, R., Lemaitre, M., Lebleu, B., Sczakiel, G. and Robbins, I. (2005). Local RNA target structure influences siRNA efficacy: A systematic global analysis. *J. Mol. Biol.* 348, 871-881.
- Owens, R.J., Limn, C. and Roy, P. (2004). Role of arbovirus nonstructural protein in cellular pathogenesis and virus release. *J. Virol.* 78, 6649-6656.
- Panagiotidis, C.A., Huang, S.C. and Canellakis, E.S. (1995). Relationship of the expression of the S20 and L34 ribosomal proteins to polyamine biosynthesis in *Escherichia coli*. *Int. J. Biol.* 27, 157-168.
- Panopoulou, E., Gillooly, D.J., Wrana, J.L., Zerial, M., Stenmark, H., Murphy, C. and Fotsis, T. (2002). Early endosomal regulation of Smad-dependent signaling in endothelial cells. *J. Biol. Chem.* 277, 18046-18052.
- Parker, J.S., Roe, S.M. and Barford, D. (2005). Structural insights into mRNA recognition from a PIWI domain-siRNA guide complex. *Nature* 434, 663-666.
- Parr, R.D., Storey, S.M., Mitchell, D.M., McIntosh, A.L., Zhou, M., Mir, K.D. and Ball, J.M. (2006). The rotavirus enterotoxin NSP4 directly interacts with the caveolar structural protein caveolin-1. *J. Virol.* 80, 2842-2854.

- Parton, R.G., Hanzal-Bayer, M., Hancock, J.F. (2006). Biogenesis of caveolae: A structural model for caveolin-induced domain formation. *J. Cell Sci.* 119, 787-796.
- Patel, R., T'wallant, N.C., Herbert, M.H., White, D., Murison, J.G. and Reid, G. (2009). The potency of siRNA-mediated growth inhibition following silencing of essential genes is dependent on siRNA design and varies with target sequence. *Oligonucleotides* 19, 317-328.
- Patnaik, A., Chau, V. and Wills, J.W. (2000). Ubiquitin is part of the retrovirus budding machinery. *Proc. Natl. Acad. Sci. USA* 97, 13069-13074.
- Penheiter, S.G., Mitchell, H., Garamszegi, N., Edens, M., Doré, J.J. and Leof, E.B. (2002). Internalization-dependent and -independent requirements for transforming growth factor β receptor signaling via the Smad pathway. *Mol. Cell. Biol.* 22, 4750-4759.
- Perez, M., Craven, R.C. and de la Torre, J.C. (2003). The small RING finger protein Z drives arenavirus budding: Implications for antiviral strategies. *Proc. Natl. Acad. Sci. USA* 100, 12978-12983.
- Pfaffl, M.W., Horgan, G.W. and Dempfle, L. (2002). Relative expression software tool (REST) for group-wise comparison and statistical analysis of relative expression results in real-time PCR. *Nucl. Acids Res.* 30, e36.
- Philpott, A., Porro, E.B., Kirschner, M.W. and Tsai, L.H. (1997). The role of cyclin-dependent kinase 5 and a novel regulatory subunit in regulating muscle differentiation and patterning. *Genes Dev.* 11, 1409-1421.
- Pierce, C.M., Balasuriya, U.B. and MacLachlan, N.J. (1998). Phylogenetic analysis of the S10 gene of field and laboratory strains of bluetongue virus from the United States. *Virus Res.* 55, 15-27.
- Piron, M., Vende, P., Cohen, J. and Poncet, D. (1998). Rotavirus RNA-binding protein NSP3 interacts with eIF4GI and evicts the poly(A) binding protein from eIF4F. *EMBO J.* 17, 5811-5821.
- Poncet, D., Lindenbaum, P., L'Haridon, R. and Cohen, J. (1997). *In vivo* and *in vitro* phosphorylation of rotavirus NSP5 correlates with its localization in viroplasm. *J. Virol.* 71, 34-41.
- Pornillos, O., Garrus, J.E. and Sundquist, W.I. (2002). Mechanisms of enveloped RNA virus budding. *Trends Cell. Biol.* 12, 569-579.
- Potgieter, A.C., Cloete, M., Pretorius, P.J. and van Dijk, A.A. (2003). A first full outer capsid protein sequence data-set in the Orbivirus genus (family *Reoviridae*): Cloning, sequencing, expression and analysis of a complete set of full-length outer capsid VP2 genes of the nine African horsesickness virus serotypes. *J. Gen. Virol.* 84, 1317-1326.
- Prasad, B.V.V., Yamaguchi, S. and Roy, P. (1992). Three-dimensional structure of single-shelled BTV. *J. Virol.* 66, 2135-2142.
- Provost, P., Dishart, D., Doucet, J., Friendewey, D., Sameulsson, B. and Radmark, O. (2002). Ribonuclease activity and RNA binding of recombinant human Dicer. *EMBO J.* 21, 5864-5874.
- Puffer, B.A., Parent, L.J., Wills, J.W. and Montelaro, R.C. (1997). Equine infectious anemia virus utilizes a YXXL motif within the late assembly domain of the Gag p9 protein. *J. Virol.* 71, 6541-6546.
- Purse, B.V., Mellor, P.S., Rogers, D.J., Samuel, A.R., Mertens, P.P. and Baylis, M. (2005). Climate change and the recent emergence of bluetongue in Europe. *Nat. Rev. Microbiol.* 3, 171-181.

- Quan, M., Van Vuuren, M., Howell, P.G., Groenewald, D. and Guthrie, A.J. (2008). Molecular epidemiology of the African horse sickness virus S10 gene. *J. Gen. Virol.* 89, 159-168.
- Rafiyi, A. (1961). Horse sickness. *Bull. Off. Int. Epizoot.* 56, 216-250.
- Raiborg, C. and Stenmark, H. (2002). Hrs and endocytic sorting of ubiquitinated membrane proteins. *Cell Struct. Funct.* 27, 403-408.
- Raiborg, C., Bache, K.G., Gillooly, D.J., Madshus, I.H., Stang, E. and Stenmark, H. (2002). Hrs sorts ubiquitinated proteins into clathrin-coated microdomains of early endosomes. *Nature Cell Biol.* 4, 394-398.
- Raiborg, C., Bremnes, B., Mehlum, A., Gillooly, D.J., D'Arrigo, A., Stang, E. and Stenmark, H. (2001). FYVE and coiled-coil domains determine the specific localisation of Hrs to early endosomes. *J. Cell Sci.* 114, 2255-22563.
- Raiborg, C., Malerod, L., Pedersen, N.M. and Stenmark, H. (2007). Differential functions of Hrs and ESCRT proteins in endocytic membrane trafficking. *Exp. Cell Res.* 314, 801-813.
- Raiborg, C., Rusten, T.E. and Stenmark, H. (2003). Protein sorting into multivesicular endosomes. *Curr. Opin. Cell Biol.* 15, 446-455.
- Ramadevi, N. and Roy, P. (1998). Bluetongue virus core protein VP4 has nucleoside triphosphate phosphohydrolase activity. *J. Gen. Virol.* 79, 2475-2480.
- Ramadevi, N., Burroughs, N.J., Mertens, P.P., Jones, I.M. and Roy, P. (1998). Capping and methylation of mRNA by purified recombinant VP4 protein of bluetongue virus. *Proc. Natl. Acad. Sci. USA* 95, 13537-13542.
- Rao, C.D., Kiuchi, A. and Roy, P. (1983). Homologous terminal sequences of the genome double-stranded RNAs of bluetongue virus. *J. Virol.* 46, 378-383.
- Raynal, P. and Pollard, H.B. (1994). Annexins: The problem of assessing the biological role for a gene family of multifunctional calcium- and phospholipid-binding proteins. *Biochim. Biophys. Acta* 1197, 63-93.
- Regenberg, B., Grotkjær, T., Winther, O., Fausbll, A., Akesson, M., Bro, C., Hansen, L.K., Brunak, S. and Nielsen, J. (2006). Growth-rate regulated genes have profound impact on interpretation of transcriptome profiling in *Saccharomyces cerevisiae*. *Genome Biol.* 7, R107.
- Reynolds, A., Leake, D., Boese, Q., Scaringe, S., Marshall, W.S. and Khvorova, A. (2004). Rational siRNA design for RNA interference. *Nature Biotechnol.* 22, 326-330.
- Roberts, A.B. and Sporn, M.B. (1993). Physiological actions and clinical applications of transforming growth factor-beta (TGF- β). *Growth Factors* 8, 1-9.
- Robishaw, J.D., Guo, Z.P. and Wang, Q. (2004). Ribozymes as tools for suppression of G protein gamma subunits. *Methods Mol. Biol.* 237, 169-180.
- Rossi, F., Charlton, C.A. and Blau, H.M. (1997). Monitoring protein-protein interactions in intact eukaryotic cells by β -galactosidase complementation. *Proc. Natl. Acad. Sci. USA* 94, 8405-8410.
- Roy, P. (1992). Bluetongue virus proteins. *J. Gen. Virol.* 73, 3051-3064.

- Roy, P. (2008). Functional mapping of bluetongue virus proteins and their interactions with host proteins during virus replication. *Cell. Biochem. Biophys.* 50, 143-157.
- Roy, P., Adachi, A., Urakawa, T., Booth, T.F. and Thomas, C.P. (1990). Identification of bluetongue virus VP6 protein as a nucleic acid-binding protein and the localization of VP6 in virus-infected vertebrate cells. *J. Virol.* 64, 1-8.
- Roy, P., Fukusho, A., Ritter, D.G. and Lyons, D. (1988). Evidence for genetic relationship between RNA and DNA viruses from the sequence homology of a putative polymerase gene of bluetongue virus with that of vaccinia virus: Conservation of RNA polymerase genes from diverse species. *Nucl. Acids Res.* 16, 11759-11767.
- Roy, P., Mertens, P.P.C. and Casal, I. (1994). African horse sickness virus structure. *Comp. Immunol. Microbiol. Infect. Dis.* 17, 243-273.
- Rual, J.F., Venkatesan, K., Hao, T., Hirozane-Kishikawa, T., Dricot, A., Li, N., Berriz, G.F., Gibbons, F.D., Dreze, M., Ayivi-Guedehoussou, N., Klitgord, N., Simon, C., Boxem, M., Milstein, S., Rosenberg, J., Goldberg, D.S., Zhang, L.V., Wong, S.L., Franklin, G., Li, S., Albala, J.S., Lim, J., Fraughton, C., Llamas, E., Cevik, S., Bex, C., Lamesch, P., Sikorski, R.S., Vandenhaute, J., Zoghbi, H.Y., Smolyar, A., Bosak, S., Sequerra, R., Doucette-Stamm, L., Cusick, M.E., Hill, D.E., Roth, F.P. and Vidal, M. (2005) Towards a proteome-scale map of the human protein-protein interaction network. *Nature* 437, 1173-1178.
- Sachse, M., Ramm, G., Strous, G. and Klumperman, J. (2002). Endosomes: Multipurpose designs for integrating housekeeping and specialized tasks. *Histochem. Cell Biol.* 117, 91-104.
- Sambrook, J., Fritsch, E.F. and Maniatis, T. (1989). Molecular cloning: A laboratory manual. Second edition. Cold Spring Harbour Laboratory Press, Cold Spring Harbor, New York.
- Sanchez-Vizcaino, J.M. (2004). Control and eradication of African horse sickness with vaccine. *Dev. Biol.* 119, 255-258.
- Sandy, P., Ventura, A. and Jacks, T. (2005). Mammalian RNAi: A practical guide. *Biotechniques* 39, 215-224.
- Sapin, C., Colard, O., Delmas, O., Tessier, C., Breton, M., Enouf, V., Chwetzoff, S., Ouanich, J., Cohen, J., Wolf, C. and Trugnan, G. (2002). Rafts promote assembly and atypical targeting of a nonenveloped virus, rotavirus, in Caco-2 cells. *J. Virol.* 76, 4591-4602.
- Scanlen, M., Paweska, J.T., Verschoor, J.A. and van Dijk, A.A. (2002). The protective efficacy of a recombinant VP2-based African horsesickness subunit vaccine candidate is determined by adjuvant. *Vaccine* 20, 1079-1088.
- Scanlon, K.J., Ohta, Y., Ishida, H., Kijima, H., Ohkawa, T., Kaminski, A., Tsai, J., Horng, G. and Kashani-Sabet, M. (1995). Oligonucleotide-mediated modulation of mammalian gene expression. *FASEB J.* 9, 1288-1296.
- Scherer, L.J., Yildiz, Y., Kim, J., Cagnon, L., Heale, B. and Rossi, J.J. (2004). Rapid assessment of anti-HIV siRNA efficacy using PCR-derived Pol III shRNA cassettes. *Mol. Ther.* 10, 597-603.
- Schmitt, A.P. and Lamb, R.A. (2005). Influenza virus assembly and budding at the viral budzone. *Adv. Virus Res.* 64, 383-416.

- Schmitt, A.P., Leser, G.P., Morita, E., Sundquist, W.I. and Lamb, R.A. (2005). Evidence for a new viral late-domain core sequence, FPIV, necessary for budding of a paramyxovirus. *J. Virol.* 79, 2988-2997.
- Schubert, S., Grünweller, A., Erdmann, V.A. and Kurreck, J. (2005). Local RNA target structure influences siRNA efficacy: Systematic analysis of intentionally designed binding regions. *J. Mol. Biol.* 348, 883-893.
- Schwarz, D.S., Hutvagner, G., Du, T., Xu, Z., Aronin, N. and Zamore, P.D. (2003). Asymmetry in the assembly of the RNAi enzyme complex. *Cell* 115, 199-208.
- Serebriiskii, I.G., Estojak, J., Berman, M. and Golemis, E.A. (2000). Approaches to detecting false positives in yeast two-hybrid systems. *Biotechniques* 28, 328-336.
- Shah, J.K., Garner, H.R., White, M.A., Shames, D.S. and Minna, J.D. (2007). siR: siRNA Information Resource, a web-based tool for siRNA sequence design and analysis and an open access siRNA database. *BMC Bioinformatics* 8, 178.
- Shao, Y., Chan, C.Y., Maliyekkel, A., Lawrence, C.E., Roninson, I.B. and Ding, Y. (2007). Effect of target secondary structure on RNAi efficiency. *RNA* 13,1631-1640.
- Simons, K. and Ikonen, E. (1997). Functional rafts in cell membranes. *Nature* 387, 569-572.
- Sledz, C.A., Holko, M., de Veer, M.J., Silverman, R.H. and Williams, B.R. (2003). Activation of the interferon system by short-interfering RNAs. *Nature Cell Biol.* 5, 834-839.
- Smith, G.A. and Enquist, L.W. (2002). Break ins and break outs: Viral interactions with the cytoskeleton of mammalian cells. *Annu. Rev. Cell Dev. Biol.* 18, 135-161.
- Sobhanifar, S. (2003). Yeast two-hybrid assay: A fishing tale. *Bio Teach J.* 1, 81-87.
- Song, J.J., Smith, S.K., Hannon, G.J. and Joshua-Tor, L. (2004). Crystal structure of Argonaute and its implications for RISC slicer activity. *Science* 305, 1434-1437.
- Sorkin, A. and von Zastrow, M. (2009). Endocytosis and signalling: Intertwining molecular networks. *Nature Rev. Mol. Cell. Biol.* 10, 609-622.
- Sorrell, D.A. and Kolb, A.F. (2005). Targeted modification of mammalian genomes. *Biotechnol Adv.* 23, 431-469.
- Stark, G.R., Kerr, I.M., Williams, B.R., Silverman, R.H. and Schreiber, R.D. (1998). How cells respond to interferons. *Annu. Rev. Biochem.* 67, 227-264.
- Stassen, L., Huismans, H. and Theron, J. (2007). Silencing of African horse sickness virus VP7 protein expression in cultured cells by RNA interference. *Virus Genes* 35, 777-783.
- Stauber, N., Martinez-Costas, J., Sutton, G., Monastyrskaya, K. and Roy, P. (1997). Bluetongue virus VP6 protein binds ATP and exhibits an RNA-dependent ATPase function and a helicase activity that catalyze the unwinding of double-stranded RNA substrates. *J. Virol.* 71, 7220-7226.
- Stenmark, H. and Aasland, R. (1999). FYVE-finger proteins - effectors of an inositol lipid. *J. Cell Sci.* 112, 4175-4183.
- Stenmark, H., Aasland, R., Toh, B.H. and D'Arrigo, A. (1996). Endosomal localization of the autoantigen EEA1 is mediated by a zinc-binding FYVE finger. *J. Biol. Chem.* 271, 24048-24054.

- Stoltz, M.A., van der Merwe, C.F., Coetzee, J. and Huismans, H. (1996). Subcellular localization of the nonstructural protein NS3 of African horsesickness virus. *Onderstepoort J. Vet. Res.* 63, 57-61.
- Stone-Marchat, M.A., Moss, S.R., Burrage, T.O., Barber, M.L. and Roy, P. (1996). Immunization with VP2 is sufficient for protection against lethal challenge with African horsesickness virus type 4. *Viol.* 220, 219-222.
- Strack, B., Calistri, A., Accola, M.A., Palu, G. and Gottlinger, H.G. (2000). A role for ubiquitin ligase recruitment in retrovirus release. *Proc. Natl. Acad. Sci. USA* 97, 13063-13068.
- Strack, B., Calistri, A., Craig, S., Popova, E. and Gottlinger, H.G. (2003). AIP1/ALIX is a binding partner for HIV-1 p6 and EIAV p9 functioning in virus budding. *Cell* 114, 689-699.
- Stram, Y. and Kuzntzova, L. (2006). Inhibition of viruses by RNA interference. *Virus Genes* 32, 299-306.
- Stuart, D.I. and Grimes, J.M. (2006). Structural studies on orbivirus proteins and particles. *Curr. Top. Microbiol. Immunol.* 309, 221-244.
- Stuart, D.I., Gouet, P., Grimes, J., Malby, R., Diprose, J., Zientara, S., Burroughs, J.N. and Mertens, P.P.C. (1998). Structural studies of orbivirus particles. *Arch. Virol.* 14, 235-250.
- Stuchell, M.D., Garrus, J.E., Muller, B., Stray, K.M., Ghaffarian, S., McKinnon, R., Krausslich, H.G., Morham, S.G. and Sundquist, W.I. (2004). The human endosomal sorting complex required for transport (ESCRT-I) and its role in HIV-1 budding. *J. Biol. Chem.* 279, 36059-36071.
- Sudol, M. (1996). Structure and function of the WW domain. *Prog. Biophys. Mol. Biol.* 65, 113-132.
- Szymkiewicz, I., Shupliakov, O. and Dikic, I. (2004). Cargo- and compartment-selective endocytic scaffold proteins. *Biochem. J.* 383, 1-11.
- Tafer, H., Ameres, S.L., Obernosterer, G., Gebeshuber, C.A., Schroeder, R., Martinez, J. and Hofacker, I.L. (2008). The impact of target site accessibility on the design of effective siRNAs. *Nature Biotechnol.* 26, 578-583.
- Tan, B-H., Nason, E., Staeuber, N., Jiang, W., Monastyrskaya, K. and Roy, P. (2001). RGD tripeptide of bluetongue virus VP7 protein is responsible for core attachment to *Culicoides* cells. *J. Virol.* 75, 3937-3947.
- Taraporewala, Z., Chen, D. and Patton, J. (2001). Multimers of the bluetongue virus non-structural protein NS2, possess nucleotidyl phosphatase activity: Similarities between NS2 and rotavirus NSP2. *Viol.* 280, 221-231.
- Taylor, M.B., van der Meyden, C.H., Erasmus, B.J., Reid, R., Labuschagne, J.H., Dreyer, L. and Prozesky, O.W. (1992). Encephalitis and chorioretinitis associated with neurotropic African horse sicknessvirus infection in laboratory workers. IV. Experimental infection of the vervet monkey *Cercopithecus pygerythrus*. *S Afr J Med Sci* 81, 462-467.
- Taylor, M.P., Burgon, T.B., Kirkegaard, K. and Jackson, W.T. (2009). Role of microtubules in extracellular release of poliovirus. *J. Virol.* 83, 6599-6609.
- Theiler, A. (1921). African horsesickness (pestis equorum). *SA Dept Agri Sci Bull* 19, 1-29.
- Theron, J. and Nel, L.H. (1997). Stable protein-RNA interaction involves the terminal domains of bluetongue virus mRNA, but not the terminally conserved sequences. *Viol.* 299, 134-142.

- Thomas, C.P., Booth, T.F. and Roy, P. (1990). Synthesis of bluetongue viral-coded phosphoprotein and formation of inclusion bodies by recombinant baculovirus in insect cells: It binds the single-stranded RNA species. *J. Gen. Virol.* 71, 2073-2083.
- Tilesi, F., Fradiani, P., Socci, V., Willems, D. and Ascenzioni, F. (2009). Design and validation of siRNAs and shRNAs. *Curr. Opin. Mol. Ther.* 11, 156-164.
- Toby, G.G. and Golemis, E.A. (2001). Using the yeast interaction trap and other two-hybrid-based approaches to study protein-protein interactions. *Methods* 24, 201-217.
- Tomari, Y. and Zamore, P.D. (2005). Perspective: machines for RNAi. *Genes Dev.* 19, 517-529.
- Torres-Vega, M.A., González, R.A., Duarte, M., Poncet, D., López, S. and Arias, C.F. (2000). The C-terminal domain of rotavirus NSP5 is essential for its multimerization, hyperphosphorylation and interaction with NSP6. *J. Gen. Virol.* 81, 821-830.
- Tsukazaki, T., Chiang, T.A., Davison, A.F., Attisano, L. and Wrana, J.L. (1998). SARA, a FYVE domain protein that recruits Smad2 to the TGF- β receptor. *Cell* 95, 779-791.
- Tucker, S.P., Thornton, C.L., Wimmer, E. and Compans, R.W. (1993). Vectorial release of poliovirus from polarized human intestinal epithelial cells. *J. Virol.* 67, 4274-4282.
- Turnbull, P.J., Cormack, S.B. and Huismans, H. (1996). Characterization of the gene encoding core protein VP6 of two African horsesickness virus serotypes. *J. Gen. Virol.* 77, 1421-1423.
- Uetz, P. and Hughes, R.E. (2000). Systematic and large-scale two-hybrid screens. *Curr. Opin. Microbiol.* 3, 303-308.
- Ui-Tei, K., Naito, Y., Takahashi, F., Haraguchi, T., Ohki-Hamazaki, H., Juni, A., Ueda, R. and Salgo, K. (2004). Guidelines for the selection of highly effective siRNA sequences for mammalian and chick RNA interference. *Nucl. Acids Res.* 32, 936-948.
- Uitenweerde, J.M., Theron, J., Stoltz, M.A. and Huismans, H. (1995). The multimeric nonstructural NS2 proteins of Bluetongue virus, African horsesickness virus, and Epizootic hemorrhagic disease virus differ in their single-stranded RNA-binding ability. *Virol.* 209, 624-632.
- Urakawa, T., Ritter, G.D. and Roy, P. (1989). Expression of largest RNA segment and synthesis of VP1 protein of bluetongue virus in insect cells by recombinant baculovirus: Association of VP1 protein with RNA polymerase activity. *Nucl. Acids Res.* 17, 7395-7401.
- Urbano, P. and Urbano, F.G. (1994). The *Reoviridae* family. *Comp. Immun. Microbiol. Infect. Dis.* 17, 151-161.
- Usami, Y., Popov, S., Popova, E. and Göttlinger, H.G. (2008). Efficient and specific rescue of human immunodeficiency virus type 1 budding defects by a Nedd4-like ubiquitin ligase. *J. Virol.* 82, 4898-4907.
- Utley, T.J., Ducharme, N.A., Varthakavi, V., Shepherd, B.E., Santangelo, P.J., Lindquist, M.E., Goldenring, J.R., Crowe, J.E. (2008). Respiratory syncytial virus uses a Vps4-independent budding mechanism controlled by Rab11-FIP2. *Proc. Natl. Acad. Sci. USA* 105, 10209-10214.
- Vaccaro, M.C. (2003). Sequencing and characterization of the *Xenopus laevis* ribosomal protein L34 cDNA. *Gene* 318, 163-167.

- Van Niekerk, M., Freeman, M., Paweska, J.T., Howell, P.G., Guthrie, A.J., Potgieter, A.C., Van Staden, V. and Huismans, H. (2003). Variation in the NS3 gene and protein in South African isolates of bluetongue and equine encephalosis viruses. *J. Gen. Virol.* 84, 581-590.
- Van Niekerk, M., Smit, C.C., Fick, W.C., Van Staden, V. and Huismans, H. (2001a). Membrane association of African horsesickness virus nonstructural protein NS3 determines its cytotoxicity. *Virology* 279, 499-508.
- Van Niekerk, M., Van Staden, V., van Dijk, A.A. and Huismans, H. (2001b). Variation of African horsesickness virus nonstructural protein NS3 in southern Africa. *J. Gen. Virol.* 82, 149-158.
- Van Rensburg, L.B.J., De Clerk, J., Groenewald, H.B. and Botha, W.S. (1981). An outbreak of African horse sickness in dogs. *J. S. Afr. Vet. Med. Assoc.* 52, 323-325.
- Van Staden, V. and Huismans, H. (1991). A comparison of the genes which encode nonstructural protein NS3 of different orbiviruses. *J. Gen. Virol.* 72, 1073-1090.
- Van Staden, V., Stoltz, M.A. and Huismans, H. (1995). Expression of nonstructural protein NS3 of African horsesickness virus (AHSV): Evidence for a cytotoxic effect of NS3 in insect cells, and characterization of the gene products in AHSV-infected Vero cells. *Arch. Virol.* 140, 289-306.
- Vasquez, K.M., Marburger, K., Intody, Z. and Wilson, J.H. (2001). Manipulating the mammalian genome by homologous recombination. *Proc. Natl. Acad. Sci. USA* 98, 8403-8410.
- Venter, G.J. and Meiswinkel, R. (1994). The virtual absence of *Culicoides imicola* (Diptera: Ceratopogonidae) in a light-trap survey of the colder, high-lying area of the eastern Orange Free State, South Africa, and implications for the transmission of arboviruses. *Onderstepoort J. Vet. Res.* 61, 327-340.
- Venter, G.J., Graham, S.D. and Hamblin, C. (2000). African horse sickness epidemiology: Vector competence of South African *Culicoides* species for virus serotypes 3, 5 and 8. *Med. Vet. Entomol.* 14, 245-250.
- Verwoerd, D.W. and Huismans, H. (1969). On the relationship between bluetongue, African horsesickness and reoviruses: Hybridization studies. *Onderstepoort J. Vet Res.* 36, 175-180.
- Verwoerd, D.W., Els, H.J., De Villiers, E.M. and Huismans, H. (1972). Structure of bluetongue virus capsid. *J. Virol.* 10, 783-794.
- Vicinanza, M., D'Angelo, G., Di Campli, A. and De Matteis, M.A. (2008). Phosphoinositides as regulators of membrane trafficking in health and disease. *Cell. Mol. Life Sci.* 65, 2833-2841.
- Vickers, T.A., Koo, S., Bennett, C.T., Crooke, S.T., Dean, N.M. and Baker, B.F. (2003). Efficient reduction of target RNAs by small interfering RNA and RNase H-dependent antisense agents. A comparative analysis. *J. Biol. Chem.* 278, 7108-7118.
- Vidalain, P.O., Boxem, M., Ge, H., Li, S. and Vidal, M. (2004). Increasing specificity in high-throughput yeast two-hybrid experiments. *Methods* 32, 363-370.
- Visintin, M., Quondam, M. and Cattaneo, A. (2004). The intracellular antibody capture technology: Towards the high-throughput selection of functional intracellular antibodies for target validation. *Methods* 34, 200-214.

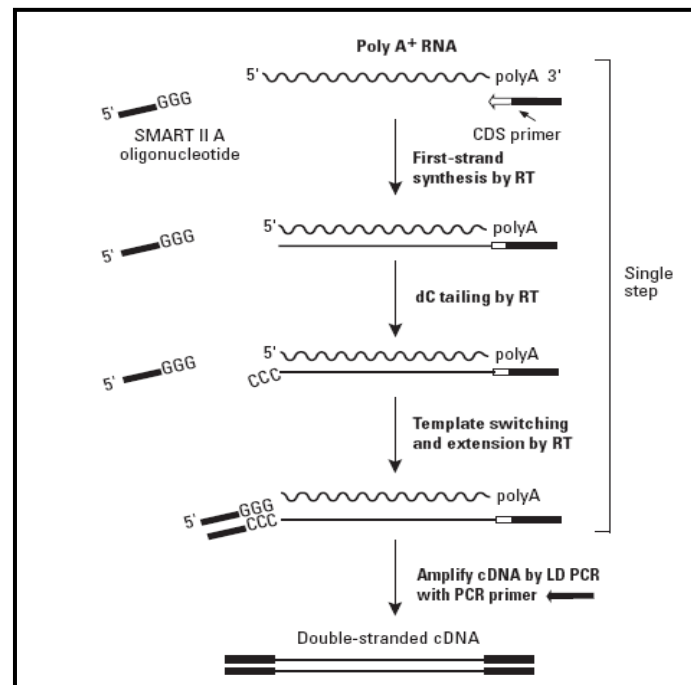
- Vitour, D., Lindenbaum, P., Vende, P., Becker, M.M. and Poncet, D. (2004). RoXaN, a novel cellular protein containing TPR, LD, and zinc finger motifs, forms a ternary complex with eukaryotic initiation factor 4G and rotavirus NSP3. *J. Virol.* 78, 3851-3862.
- Vreede, F.T. and Huismans, H. (1994). Cloning, sequencing and expression of the gene that encodes the major neutralization-specific antigen of African horsesickness virus serotype 3. *J. Gen. Virol.* 75, 3629-3633.
- Vreede, F.T. and Huismans, H. (1998). Sequence analysis of the RNA polymerase gene of African horse sickness virus. *Arch. Virol.* 143, 413-419.
- Wade-Evans, A.M., Pullen, L., Hamblin, C., O'Hara, R., Burroughs, J.N. and Mertens, P.P.C. (1997). African horsesickness virus VP7 sub-unit vaccine protects mice against a lethal, heterologous serotype challenge. *J. Gen. Virol.* 78, 1611-1616.
- Wadhwa, R., Kaul, S.C., Miyagishi, M. and Taira, K. (2004). Vectors for RNA interference. *Curr. Opin. Mol. Ther.* 6, 367-372.
- Wang, X., Wang, X., Varma, R.K., Beauchamp, L., Magdaleno, S. and Sendera, T.J. (2009). Selection of hyperfunctional siRNAs with improved potency and specificity. *Nucl. Acids Res.* 37, e152.
- Welsch, S., Müller, B. and Kräusslich, H.G. (2007). More than one door - Budding of enveloped viruses through cellular membranes. *FEBS Lett.* 581, 2089-2097.
- Wirblich, C., Bhattacharya, B. and Roy, P. (2006). Nonstructural protein 3 of Bluetongue virus assists virus release by recruiting ESCRT-I protein Tsg101. *J. Virol.* 80, 460-473.
- Wu, J., Bonsra, A.N. and Du, G. (2009). pSM155 and pSM30 vectors for miRNA and shRNA expression. *Methods Mol. Biol.* 487, 205-219.
- Wu, V., Chen, S., Iwata, H., Compas, R. and Roy, P. (1992). Multiple glycoproteins synthesized by the smallest RNA segment (S10) of bluetongue virus. *J. Virol.* 12, 7104-7112.
- Wu, W., Hodges, E., Redelius, J. and Höög, C. (2004). A novel approach for evaluating the efficiency of siRNAs on protein levels in cultured cells. *Nucl. Acids Res.* 32, e17.
- Xia, Y., Lu, L.J. and Gerstein, M. (2006). Integrated prediction of the helical membrane protein interactome in yeast. *J. Mol. Biol.* 357, 339-349.
- Xiang, Y., Cameron, C.E., Wills, J.W. and Leis, J. (1996). Fine mapping and characterization of the Rous sarcoma virus Pr76 Gag late assembly domain. *J. Virol.* 70, 5695-5700.
- Xuan, B., Qian, Z., Hong, J. and Huang, W. (2006). EsiRNAs inhibit Hepatitis B virus replication in mice model more efficiently than synthesized siRNAs. *Virus Res.* 118, 150-155.
- Yang, D., Buchholz, F., Huang, Z., Goga, A., Chen, C-Y., Brodsky, F.M. and Bishop, J.M. (2002). Short RNA duplexes produced by hydrolysis with *Escherichia coli* RNase III mediate effective RNA interference in mammalian cells. *Proc. Natl. Acad. Sci. USA* 99, 9942-9947.
- Yasuda, J. and Hunter, E. (1998). A proline-rich motif (PPPY) in the Gag polyprotein of Mason-Pfizer monkey virus plays a maturation-independent role in virion release. *J. Virol.* 72, 4095-4103.
- Yin, J., Li, G., Ren, X. and Herrler, G. (2007). Select what you need: A comparative evaluation of the advantages and limitations of frequently used expression systems for foreign genes. *J. Biotechnol.* 127, 335-347.

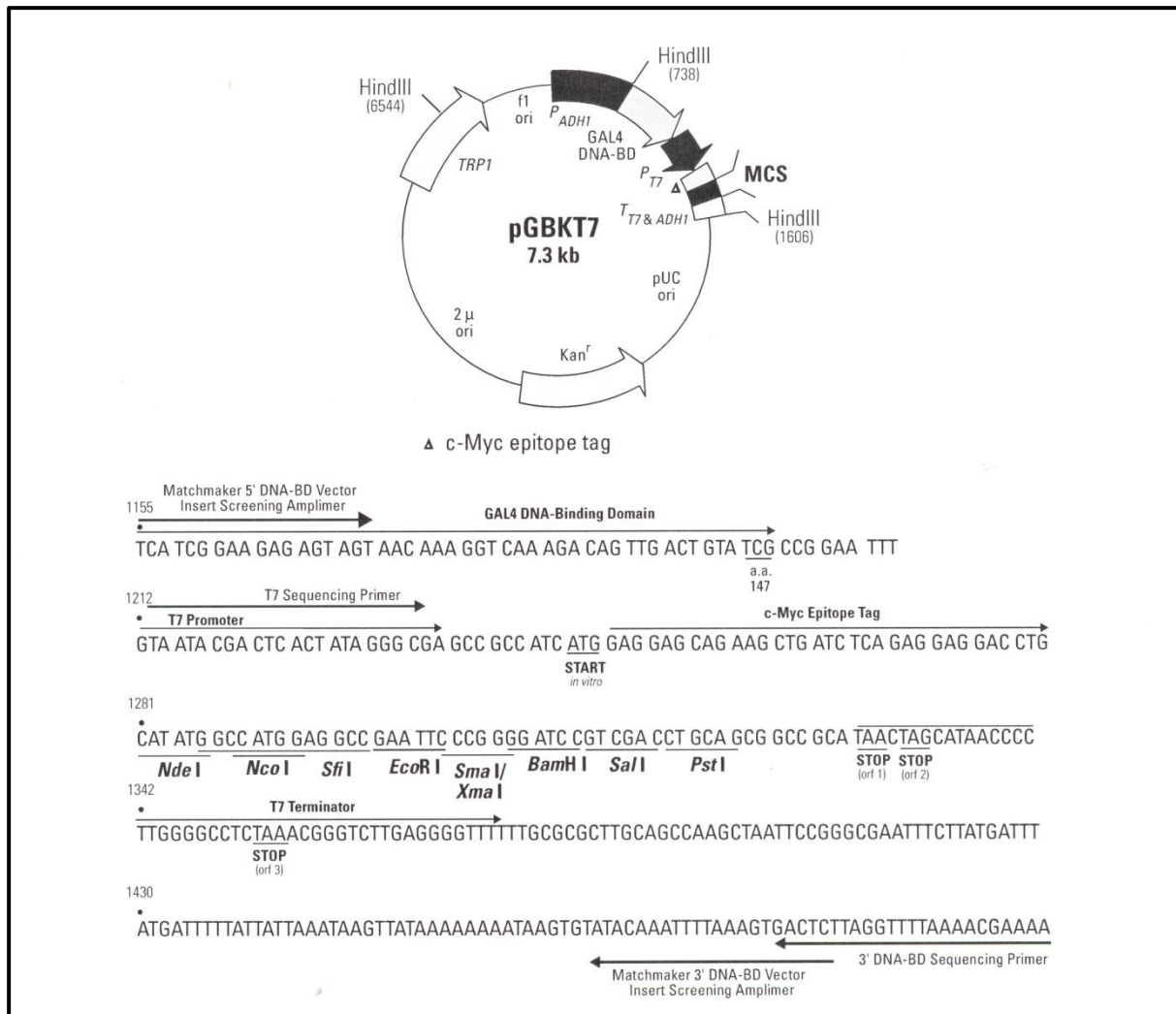
- Yokota, T., Sakamoto, N., Enomoto, N., Tanabe, Y., Miyagishi, M., Maekawa, S., Yi, L., Kurosaki, M., Taira, K., Watanabe, M. and Mizusawa, H. (2003). Inhibition of intracellular hepatitis C virus replication by synthetic and vector-derived small interfering RNAs. *EMBO Rep.* 4, 602-608.
- Young, K.H. (1998). Yeast two-hybrid: so many interactions, (in) so little time... *Biol Reprod.* 58, 302-311.
- Zambrano, J.L., Díaz, Y., Peña, F., Vizzi, E., Ruiz, M.C., Michelangeli, F., Liprandi, F. and Ludert, J.E. (2008). Silencing of rotavirus NSP4 or VP7 expression reduces alterations in Ca²⁺ homeostasis induced by infection of cultured cells. *J. Virol.* 82, 5815-5824.
- Zhang, G., Gurtu, V. and Kain, S.R. (1996). An enhanced green fluorescent protein allows sensitive detection of gene transfer in mammalian cells. *Biochem. Biophys. Res. Commun.* 227, 707-711.
- Zhang, H., Fabrice, A.K., Jaskiewicz, L., Westhof, E. and Filipowicz, W. (2004). Single processing centre models for human Dicer and bacterial RNase III. *Cell* 118, 57-68.
- Zhang, X., Boyce, M., Bhattacharya, B., Zhang, X., Schein, S., Roy, P. and Zhou, Z.H. (2010). Bluetongue virus coat protein VP2 contains sialic acid-binding domains, and VP5 resembles enveloped virus fusion proteins. *Proc. Natl. Acad. Sci. USA* 107, 6292-6297.
- Zuker, M. (2003). MFOLD web server for nucleic acid folding and hybridization prediction. *Nucl. Acids Res.* 31, 3406-3415.

APPENDIX

cDNA synthesis: SMART™ technology

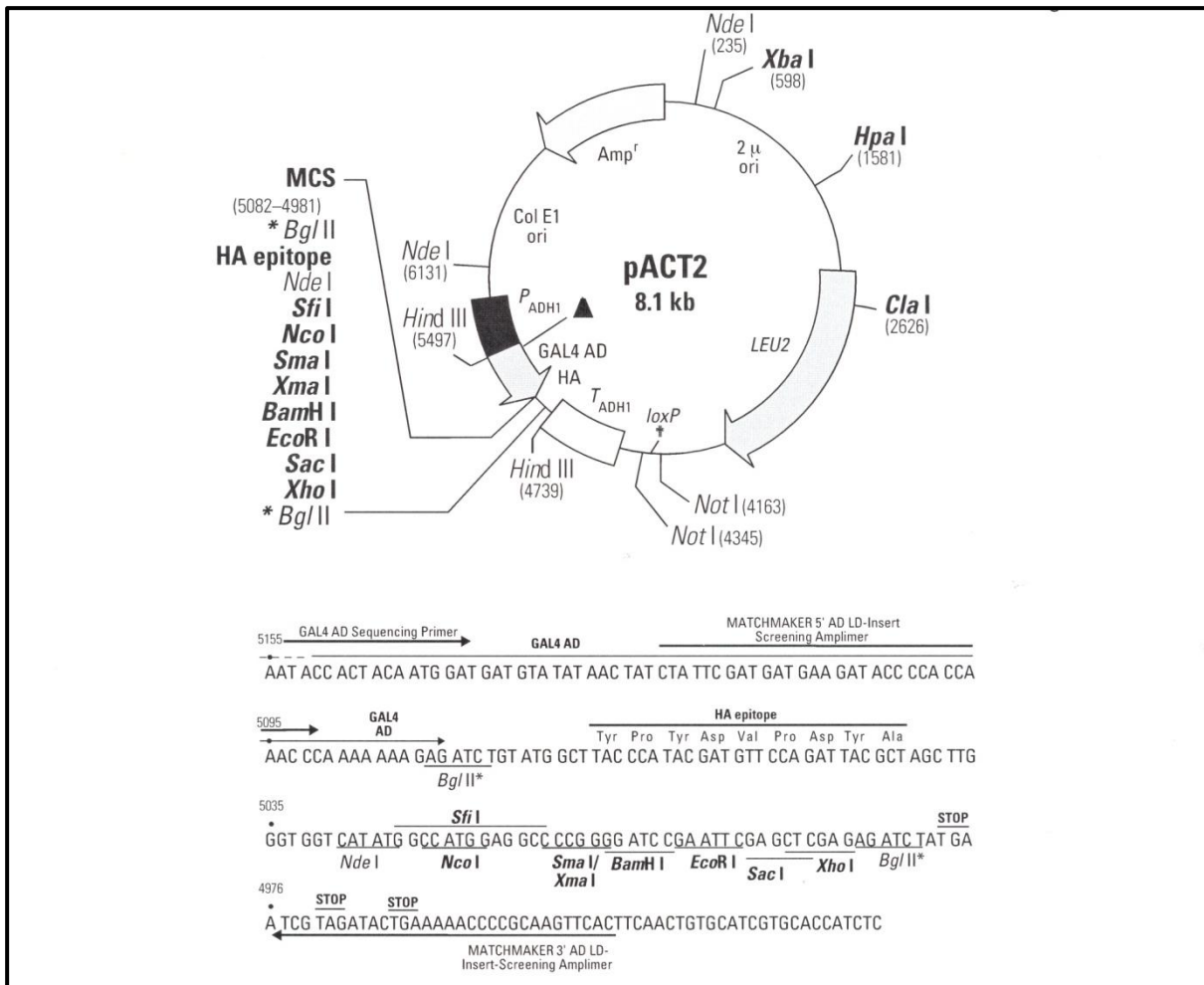
The Super SMART™ cDNA synthesis technology (Clontech Laboratories, Inc.) used during this study provides a novel PCR-based method for producing high quality cDNA from nanogram quantities of total RNA. A flow chart of the technology is presented in the figure below. A modified oligo(dT) primer, the CDS III/ 3' PCR primer, primes the first-strand cDNA reaction. When the reverse transcriptase (RT) reaches the 5' end of the mRNA, the enzyme's terminal transferase activity adds a few additional nucleotides, primarily deoxycytidine, to the 3' end of the cDNA. The SMART™ oligonucleotide, which has an oligo(dG) sequence at its 3' end, base-pairs with the deoxycytidine stretch, resulting in the formation of an extended template. The RT is then switches templates and continues replication to the end of the oligonucleotide. The single-stranded (ss) cDNA product thus contains the complete 5' end of the mRNA, as well as sequences that are complementary to the SMART™ oligonucleotide. The SMART™ anchor sequence and poly(A) sequence serve as universal priming sites for end-to-end cDNA amplification. In contrast, cDNA without these sequences, e.g. prematurely terminated cDNAs or contaminating genomic DNA, will not be exponentially amplified (Clontech Laboratories, Inc.). Since the terminal transferase activity of the RT adds a random number of deoxycytidine to the first cDNA strand, cloning and expression of these fragments are possible since various reading frames are generated randomly.





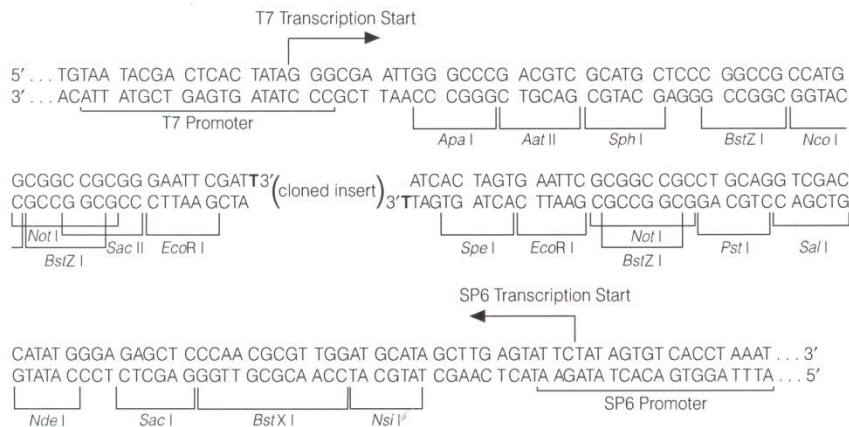
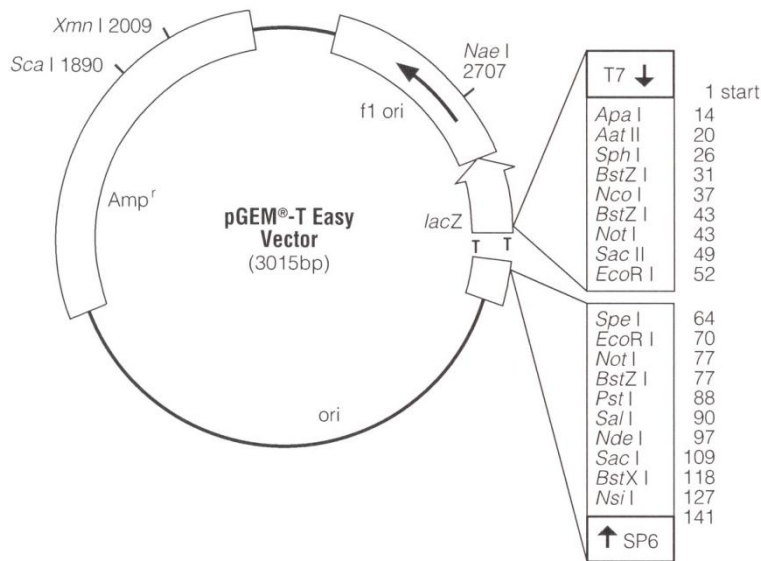
Plasmid map and multiple cloning site of the pGBKT7 DNA-BD vector.

The pGBKT7 vector expresses proteins fused to amino acids 1-147 of the GAL4 DNA binding domain (DNA-BD). In yeast, fusion proteins are expressed at high levels from the constitutive *AOHI* promoter (*P_{ADHI}*); transcription is terminated by the T7 and *ADHI* transcription termination signals (*T_{T7 & ADHI}*). pGBKT7 also contains the T7 promoter, a c-Myc epitope tag, and a multiple cloning site (shown below the plasmid map). pGBKT7 replicates autonomously in both *E. coli* and *S. cerevisiae* from the pUC and 2 μ *ori*, respectively. The vector carries the Kan^r for selection in *E. coli* and the *TRP1* nutritional marker for selection in yeast (Clontech Laboratories, Inc.).



Plasmid map and multiple cloning site of the pACT2 AD vector.

pACT2 generates a fusion of the GAL4 AD (amino acids 768-881), an HA epitope tag, and a protein of interest (or protein encoded by a cDNA in a fusion library) cloned into the multiple cloning site in the correct orientation and reading frame. The hybrid protein is expressed at high levels in yeast host cells from the constitutive ADH1 promoter (*P*); transcription is terminated at the ADH1 transcription termination signal (*T*). The protein is targeted to the yeast nucleus by the nuclear localization sequence from SV40 T-antigen, which has been cloned into the 5'-end of the GAL4 AD sequence. pACT2 is a shuttle vector that replicates autonomously in both *E. coli* and *S. cerevisiae*, and carries the *bla* gene that confers ampicillin resistance in *E. coli*. pACT2 also contains the *LEU2* nutritional gene that allows yeast auxotrophs to grow on limiting synthetic media. Transformants with AD/library plasmids can be selected by complementation by the *LEU2* gene by using an *E. coli* strain that carries a *leuB* mutation (e.g. KC8) (Clontech Laboratories, Inc.).



Plasmid map and multiple cloning site of the pGEM[®]-T Easy vector.

pGEM[®]-T Easy is a high copy number vector for the cloning of PCR products. The pGEM[®]-T Easy vector contains T7 and SP6 RNA polymerase promoters, flanking a multiple cloning region within the α -peptide coding region of the enzyme β -galactosidase. Insertional inactivation of the α -peptide allows recombinant clones to be directly identified by colour screening on X-gal - containing indicator plates. pGEM[®]-T Easy contain multiple restriction sites within the multiple cloning site and the region is flanked by recognition sites for the restriction enzymes EcoR I, BstZ I and Not I. These allow for single-enzyme digestions for release of the insert. The pGEM[®]-T Easy vector also contains the *ori* of the filamentous phage f1 for the preparation of single-stranded (ss) DNA (Promega).